UNIVERSITY OF THESSALY
School of Agricultural Sciences

N. R. Rigakis

Theoretical and Experimental Investigation of Microclimate in Screenhouses

PhD Dissertation

Volos – N. Ionia, Greece, 2015

N. R. Rigakis

Theoretical and Experimental Investigation of Microclimate in Screenhouses

This research has been co-financed by the European Union (European Social Fund – ESF) and Greek national funds through the Operational Program "Education and Lifelong Learning" of the National Strategic Reference Framework (NSRF) - Research Funding Program: Heracleitus II. Investing in knowledge society through the European Social Fund.

Theoretical and Experimental Investigation of Microclimate in Screenhouses

Advisory committee

Constantinos Kittas, Supervisor University of Thessaly	Professor Agricultural Constructions
Dr. Thierry Boulard, Member French National Institute for Agricultural Research	Director of Research Bioclimatology
Nikolaos Katsoulas, Member University of Thessaly	Assistant Professor Agricultural Constructions

Examination committee

Constantinos Kittas University of Thessaly	Professor Agricultural Constructions
Dimitrios Briassoulis Agricultural University of Athens	Professor Agricultural Constructions
Dr. Thierry Boulard French National Institute for Agricultural Research	Director of Research Bioclimatology
Anastasios Siomos Aristotle University of Thessaloniki	Professor Horticulture
Dimitrios Savvas Agricultural University of Athens	Associate Professor Horticulture
Nikolaos Katsoulas University of Thessaly	Assistant Professor Agricultural Constructions
Dr. Tomas Bartzanas Centre for Research and Technology-Hellas	Senior Researcher Agricultural Engineer

N. R. Rigakis

Theoretical and Experimental Investigation of Microclimate in Screenhouses

ISBN

Ν. Ρ. Ρηγάκης

Θεωρητική και Πειραματική Διερεύνηση του Μικροκλίματος των Διχτυοκηπίων

Η παρούσα έρευνα έχει συγχρηματοδοτηθεί από την Ευρωπαϊκή Ένωση (Ευρωπαϊκό Κοινωνικό Ταμείο - ΕΚΤ) και από εθνικούς πόρους μέσω του Επιχειρησιακού Προγράμματος «Εκπαίδευση και Δια Βίου Μάθηση» του Εθνικού Στρατηγικού Πλαισίου Αναφοράς (ΕΣΠΑ) – Ερευνητικό Χρηματοδοτούμενο Έργο: Ηράκλειτος ΙΙ. Επένδυση στην κοινωνία της γνώσης μέσω του Ευρωπαϊκού Κοινωνικού Ταμείου.

Θεωρητική και Πειραματική Διερεύνηση του Μικροκλίματος των Διχτυοκηπίων

Τριμελής Συμβουλευτική Επιτροπή

Κωνσταντίνος Κίττας, Επιβλέπων Πανεπιστήμιο Θεσσαλίας	Καθηγητής Γεωργικές Κατασκευές,
Δρ. Thierry Boulard, Μέλος French National Institute for Agricultural Research	Διευθυντής Ερευνών Βιοκλιματολογία
Νικόλαος Κατσούλας, Μέλος Πανεπιστήμιο Θεσσαλίας	Επίκουρος Καθηγητής Γεωργικές Κατασκευές,

Επταμελής Εξεταστική Επιτροπή

Κωνσταντίνος Κίττας Πανεπιστήμιο Θεσσαλίας	Καθηγητής Γεωργικές Κατασκευές,
Δημήτριος Μπριασούλης Γεωπονικό Πανεπιστήμιο Αθηνών	Καθηγητής Γεωργικές Κατασκευές
Δρ. Thierry Boulard French National Institute for Agricultural Research	Διευθυντής Ερευνών Βιοκλιματολογία
Αναστάσιος Σιώμος Αριστοτέλειο Πανεπιστήμιο Θεσσαλονίκης	Καθηγητής Λαχανοκομία
Δημήτριος Σάββας Γεωπονικό Πανεπιστήμιο Αθηνών	Αναπληρωτής Καθηγητής Λαχανοκομία
Νικόλαος Κατσούλας Πανεπιστήμιο Θεσσαλίας	Επίκουρος Καθηγητής Γεωργικές Κατασκευές,
Δρ. Θωμάς Μπαρτζάνας Εθνικό Κέντρο Έρευνας και Τεχνολογικής Ανάπτυξης	Κύριος Ερευνητής (Β') Γεωργική Μηχανική

Ν. Ρ. Ρηγάκης

Θεωρητική και Πειραματική Διερεύνηση του Μικροκλίματος των Διχτυοκηπίων

ISBN

Nikolaos R. Rigakis, 2015. Theoretical and Experimental Investigation of Microclimate in Screenhouses. PhD Dissertation, University of Thessaly, Volos – N. Ionia, Greece, Magnesia, Greece.
19 Preliminary pages, 174 pages, 39 Tables, 47 Figures, 231 Citations

Abstract

Screenhouses are steadily spreading around Mediterranean regions and especially in Israel, southern regions of Spain, Italy and Greece. Using screens to protect horticultural crops affect the microclimate, promoting crop productivity and fruit quality of the covered crops.In the present study, the influence of three different covering screens with different shading intensity and porosity on the screenhouse and crop microclimate and pepper crop performance was experimentally and theoretically investigated. The experiments were carried out from May until the end of October on two consecutive years, 2011 and 2012, in the experimental farm of the University of Thessaly in Velestino, Central Greece. Seedlings of sweet pepper plants were transplanted on May inside three screenhouses and outside. The three screenhouses (floor area 200 m^2) were covered by the following nets: (a) an anti-thrip insect proof, 50-mesh, clear net with shading intensity of about 13% (IP-13), (b) an anti-thrip insect proof, 50-mesh, white net with shading intensity of about 34% (IP-34) and (c) a green shading net with shading intensity of about 36% (S-36). The shading intensities were determined in the laboratory by means of a spectroradiometer and an integral sphere. Screens (a) and (b) had same porosity but different shading intensity, while screens (b) and (c) had similar shading intensity but different porosity (0.46 and 0.63 for IP-34 and S-36, respectively).

The following microclimatic parameters were recorded regularly inside the three screenhouses and at the open field: solar radiation, air temperature and relative humidity, crop temperature, crop transpiration rate, wind speed and direction. The reduction of solar radiation above the crop was proportional to the shading intensity of the screen as determined in the laboratory. However, an increase of *in situ* shading factor was observed as opposed to that determined in the laboratory and attributed to the diffuse component of the solar radiation (unlike the laboratory beam radiation) to the sun's inclination towards the covering screens depending on sun's azimuth and elevation (unlike the perpendicular light source of laboratory tests), to the frames of the supporting construction which reduce the overall transmittance of the construction and to the dust accumulated on screens surface. The covering screens increased the diffuse fraction of solar radiation of the enclosures with respect to their porosity and colour (brightness). The diffused radiation was greater inside IP-13 while the shade net scattered the incoming solar radiation in a lower rate (about half) as compared to the insect proof screens (IPs). Analysis of the spectral distribution of the light (direct, diffuse and total) of each treatment was conducted. The internal air temperature and vapour pressure deficit were similar to the ambient. The crop temperature under screenhouse conditions was lower than that of the open field crop. The canopy-to-air temperature difference was higher in the open field than under screenhouse conditions, with the lowest values observed under the screenhouse IP-34. In addition, the canopy-to-air vapour pressure deficit was significantly lower in the crop grown under shading than in the open field. The crop transpiration rate observed under the IP-13 and the heavy shade screenhouses (IP-34 and S-36) was lower by about 25% and 45%, respectively, than at the open field. Furthermore, the presence of the screen material decreased not only the radiative but also the advective part of crop transpiration, something that is attributed to the reduction of air velocity inside the

screenhouse. The crop stomatal conductance under screenhouse conditions was similar or higher than the values observed for the open field crop.

Another objective of this work was to study and model the ventilation rate in screenhouses. The IPs screens reduced at the same rate the inside screenhouse air velocity, since they had the same geometrical characteristics. The internal air velocity in the IPs and the shading screenhouses was about 20% and 44%, respectively, of that measured outside. The air exchange rate and its rate of increase with respect to the external wind speed, both increased with the increase of screen porosity. Also, the size of the constructions influenced their ventilation performance, as revealed by comparing their ventilation rate to the respective of large commercial screenhouses. The obtained ventilation rate data were used to calibrate a model that can be used for the prediction of ventilation rate in screenhouses, taking into account the geometrical characteristics of the screens used and of the screenhouse and the outside wind speed. The values of the dual coefficient $C_d\sqrt{C_w}$ of the screenhouses and of the wind related coefficient C_w, were also estimated and compared to the respective coefficients of large scale screenhouses that were also here estimated.

Additionally, in the present study, the effect of the three different shading and IPs screens on pepper crop performance was investigated; measurements of crop growth, development, yield and its quality, were performed along with irrigation water monitoring. Screenhouses IP-13, IP-34 and S-36 produced more fresh fruit weight, on average on both periods, by about 66%, 35% and 17%, respectively, than the open field crop. The moderate shade (≈20-25%; IP-13) increased the production by 21% (mean for both periods) as compared to the heavy shade of the IP-34 screenhouse, while the crops inside IP-34 screenhouse produced more by about 17% as compared to the S-36 screenhouse, rising a susceptibility about the effectiveness of green nets (assuming equal shade factors). The highest fruit number (77.5 fruits m^{-2}; mean of both periods) and total fruit yield (6.3 kg m^{-2}; mean of both periods) were observed under the 13% shading insect proof screen. Marketable fruit yield for all screenhouses was more than 90% of the total yield, while for the open field crop the marketable fruit production was about 60% of the total. Fruits harvested from screenhouse crops were larger (dimensions) and heavier than the open field fruits. Pepper fruit sunscald was nearly eliminated, while BER and defects from pests were significantly reduced mainly under the IPs screens. Screenhouse crops consumed from about 20-40% less water than the open field crop; the Irrigation Water Use Efficiency (IWUE) was increased by 132% and 93%, respectively, inside IPs and S-36 screenhouses of their covered crops, as compared to that of the open field crops. Crop growth (total dry matter) was enhanced inside the IPs screenhouses, unlike the S-36 screenhouse. The crop growth was simulated by means of a model that predicts the dry matter production using as input only the cumulative intercepted PAR by the crops and the radiation use efficiency (RUE) was estimated for the crop of each treatment. The IWUE and the RUE were tightly correlated to the optical characteristics of the screens i.e., to the quantity and quality of the direct and diffuse solar radiation of the enclosures.

Keywords: Screen, Shading, Insect proof, Porosity, Diffuse radiation, Canopy temperature, Canopy conductance, Transpiration, Ventilation, Discharge coefficient, Wind effect coefficient, pepper yield, yield quality, sunscald, BER, Crop growth, Water use efficiency, Radiation use efficiency.

Νικόλαος Ρ. Ρηγάκης, 2015. Θεωρητική και Πειραματική Διερεύνηση του Μικροκλίματος των Διχτυοκηπίων. Διδακτορική Διατριβή, Πανεπιστήμιο Θεσσαλίας, Βόλος.- Ν. Ιωνία, Μαγνησίας.
19 Προκαταρκτικές σελίδες, 174 σελίδες, 39 Πίνακες, 47 Σχήματα, 231 Βιβλιογραφικές παραπομπές.

Περίληψη

Τα διχτυοκήπια συνεχώς επεκτείνονται ως τεχνική καλλιέργειας σε μεσογειακές περιοχές και κυρίως στο Ισραήλ, στις νότιες περιοχές της Ισπανίας, στην Ιταλία και στην Ελλάδα. Τα δίχτυα επηρεάζουν το μικροκλίμα των διχτυοκηπίων και προάγουν την παραγωγικότητα και την ποιότητα της παραγωγής των υπό κάλυψη καλλιεργειών.

Στην παρούσα εργασία μελετάται, θεωρητικά και πειραματικά, η επίδραση τριών διαφορετικών διχτυών κάλυψης, με διαφορετικό συντελεστή σκίασης και διαφορετικό πορώδες στο μικροκλίμα των διχτυοκηπίων και στην παραγωγικότητα και την ποιότητα της παραγωγής της καλλιέργειας γλυκιάς πιπεριάς. Τα πειράματα πραγματοποιήθηκαν από τον Μάιο έως και τον Οκτώβριο, δυο διαδοχικών ετών, στο πειραματικό αγρόκτημα του Πανεπιστημίου Θεσσαλίας στο Βελεστίνο (κεντρική Ελλάδα). Σπορόφυτα γλυκιάς πιπεριάς μεταφυτεύτηκαν τον Μάιο εντός των διχτυοκηπίων αλλά και στον ανοικτό αγρό (υπαίθρια, μη προστατευμένη καλλιέργεια). Η υπαίθρια καλλιέργεια χρησιμοποιήθηκε ως μάρτυρας για στατιστικές συγκρίσεις έναντι των καλλιεργειών των διχτυοκηπίων. Τα τρία διχτυοκήπια (έκτασης 200 m^2) καλύφθηκαν με τα εξής δίχτυα: (α) εντομοστεγανό, 50-mesh, διάφανο, με συντελεστή σκίασης περίπου 13% (IP-13), (β) εντομοστεγανό, 50-mesh, λευκό, με συντελεστή σκίασης περίπου 34% (IP-34) και (γ) πράσινο δίχτυ σκίασης με συντελεστή σκίασης περίπου 36% (S-36). Οι συντελεστές σκίασης υπολογίστηκαν βάσει εργαστηριακών μετρήσεων με τη χρήση ενός φασματοφωτομέτρου και μιας σφαίρας ολοκλήρωσης. Τα δίχτυα (α) και (β) είχαν ίδιο πορώδες αλλά διαφορετικό συντελεστή σκίασης, ενώ τα δίχτυα (β) και (γ) είχαν ίδιο συντελεστή σκίασης αλλά διαφορετικό πορώδες (0,46 και 0,63 για το IP-34 και S-36, αντίστοιχα.

Κατά τη διάρκεια των πειραμάτων μετρήθηκαν οι εξής παράμετροι του μικροκλίματος, εντός των διχτυοκηπίων και στον ανοικτό αγρό: ηλιακή ακτινοβολία, θερμοκρασία και σχετική υγρασία του αέρα, θερμοκρασία καλλιέργειας, ρυθμός διαπνοής καλλιεργειών και ταχύτητα και διεύθυνση ανέμου. Η προσπίπτουσα στην καλλιέργεια ηλιακή ακτινοβολία μειώθηκε αναλογικά με τον συντελεστή σκίασης που προσδιορίστηκε εργαστηριακά. Ωστόσο, παρατηρήθηκαν διαφορές μεταξύ της περατότητας των διχτυών στο εργαστήριο και εκείνης των κατασκευών στον πειραματικό αγρό (αύξηση των *in situ* περατοτήτων) και αποδόθηκαν στην διάχυτη ηλιακή ακτινοβολία του η οποία δεν υπήρχε στο εργαστήριο, στην γωνία πρόσπτωσης της ηλιακής ακτινοβολίας η οποία οφείλεται στο αζιμούθιο και στο ύψος του ηλίου, σε αντίθεση με την κάθετη πρόσπτωση της ακτίνας της φωτεινής πηγής στο εργαστήριο, στο σκελετό των κατασκευών ο οποίος εμποδίζει μέρος της ηλιακής ακτινοβολίας να εισέλθει στο εσωτερικό τους, μειώνοντας τον συνολική περατότητα των διχτυοκηπίων και στην συσωρευτική επικάθιση σκόνης στην επιφάνεια των διχτυών. Τα υλικά κάλυψης αύξησαν την διάχυτη ηλιακή ακτινοβολία εντός των κατασκευών ανάλογα με το πορώδες τους και το χρώμα τους (φωτεινότητα). Η διάχυτη ακτινοβολία ήταν περισσότερη εντός του IP-13, ενώ εντός του S-36 ήταν περίπου η μισή εκείνης των εντομοστεγανών (IPs) διχτυοκηπίων. Επιπλέον, πραγματοποιήθηκε ανάλυση της φασματικής κατανομής της ηλιακής ακτινοβολίας (άμεση, διάχυτη κα συνολική) εντός των διχτυοκηπίων. Η θερμοκρασία και το έλλειμμα κορεσμό υδρατμών του αέρα εντός των κατασκευών ήταν παρόμοια με

εκείνα του ανοικτού αγρού. Η θερμοκρασία καλλιέργειας ήταν μικρότερη εντός των διχτυοκηπίων σε σχέση με εκείνη του ανοικτού αγρού, ενώ το έλλειμμα κορεσμού υδρατμών καλλιέργεια-αέρα, ήταν υψηλότερο στον ανοικτό αγρό. Ο ρυθμός διαπνοής εντός του IP-13 και των υψηλής σκίασης διχτυοκηπίων (IP-34 και S-36) ήταν 25% και 45% μικρότερος σε σχέση με εκείνον της καλλιέργειας του ανοικτού αγρού. Η παρουσία του διχτυού μείωσε τόσο το κλάσμα της διαπνοής που οφείλεται στην ακτινοβολία αλλά και εκείνο που οφείλεται στη μεταφορά, λόγω της μείωσης της ταχύτητας του αέρα στο εσωτερικό των διχτυοκηπίων. Η στοματική αγωγιμότητα των καλλιεργειών ήταν αυξημένη ή παρόμοια εντός των κατασκευών σε σχέση με εκείνη του ανοικτού αγρού.

Ένας άλλος στόχος της παρούσας εργασίας ήταν η μελέτη και η προσομοίωση του ρυθμού αερισμού των διχτυοκηπίων. Τα εντομοστεγανά δίχτυα μείωσαν κατά το ίδιο ποσοστό την ταχύτητα του αέρα στο εσωτερικό των κατασκευών, λόγω των ίδιων γεωμετρικών χαρακτηριστικών που είχαν. Η ταχύτητα του αέρα στο εσωτερικό των εντομοστεγανών και του διχτυοκηπίου S-36 ήταν περίπου το 20% και το 44% της ταχύτητας του εξωτερικού ανέμου. Ο ρυθμός αλλαγής του αέρα και ο ρυθμός αύξησής του σε σχέση με την ταχύτητα του εξωτερικού ανέμου, αυξάνονταν με την αύξηση του πορώδους του διχτύου. Επιπλέον, το μέγεθος των κατασκευών επηρεάζει την απόδοση του αερισμού τους, όπως αποδείχθηκε συγκρίνοντας το ρυθμό αερισμού των διχτυοκηπίων της παρούσας εργασίας με τον αντίστοιχο μεγάλων εμπορικών διχτυοκηπίων. Τα δεδομένα του ρυθμού αερισμού των διχτυοκηπίων της παρούσας εργασίας χρησιμοποιήθηκαν για την βαθμονόμηση προσομοιώματος που υπολογίζει τον ρυθμό αερισμού των κατασκευών λαμβάνοντας υπ' όψιν τα γεωμετρικά χαρακτηριστικά των διχτύων κάλυψης και την ταχύτητα του ανέμου στο εξωτερικό. Επιπλέον, υπολογίστηκαν ο διπλός συντελεστής $C_d\sqrt{C_w}$ των διχτυοκηπίων και ο συντελεστής που σχετίζεται με τον άνεμο C_w και συγκρίθηκαν με τους αντίστοιχους διχτυοκηπίων μεγάλης κλίμακας, οι οποίοι επίσης υπολογίστηκαν στην παρούσα εργασία.

Στην παρούσα εργασία μελετήθηκε (πειραματικά και θεωρητικά) και η επίδραση των τριών διαφορετικών διχτυών στην επίδοση καλλιέργειας γλυκιάς πιπεριάς και συγκρίθηκε με εκείνη του ανοικτού αγρού. Για το σκοπό αυτό πραγματοποιήθηκαν μετρήσεις αύξησης, ανάπτυξης, παραγωγικότητας και ποιότητας παραγωγής καθώς και μετρήσεις του χρησιμοποιούμενου νερού άρδευσης. Οι καλλιέργειες εντός του IP-13, IP-34 και S-36 παρήγαγαν περισσότερο νωπό βάρος καρπών κατά μέσο όρο και τις δυο χρονιές 66%, 35% και 17%, αντίστοιχα, σε σχέση με εκείνη του ανοικτού αγρού. Το μέτριας σκίασης διχτυοκήπιο (≈20-25%; IP-13) προήγαγε την αύξηση της παραγωγής κατά 21% σε σχέση με το πυκνότερης σκίασης διχτυοκήπιο IP-34, ενώ η παραγωγή στο τελευταίο ήταν αυξημένη κατά 17 % σε σχέση με το αντίστοιχης σκίασης διχτυοκήπιο S-36. Το τελευταίο, προάγει έναν σκεπτικισμό σχετικά με την αποτελεσματικότητα πράσινων διχτυών έναντι αντίστοιχης σκίασης ουδέτερου χρώματος (διάφανα ή λευκά). Η υψηλότερη παραγωγή (6.3 kg m^{-2}, κατά μέσο όρο για τις δυο περιόδους) και ο υψηλότερος αριθμός καρπών (77.5 καρποί m^{-2}, κατά μέσο όρο για τις δυο περιόδους) παρατηρήθηκε εντός του IP-13. Η εμπορεύσιμη παραγωγή εντός των διχτυοκηπίων ήταν το 90% της συνολικής παραγωγής έναντι 60% εκείνης του ανοικτού αγρού. Οι συγκομισμένοι καρποί των υπό κάλυψη καλλιεργειών ήταν μεγαλύτερων διαστάσεων και βάρους σε σχέση με εκείνους του ανοικτού αγρού. Τα ηλιακά εγκαύματα σχεδόν εξαλείφθηκαν, η εμφάνιση BER μειώθηκε σημαντικά και η προσβολές εντόμων περιορίστηκαν σε μεγάλο βαθμό κυρίως εντός των εντομοστεγανών διχτυοκηπίων. Οι καλλιέργειες εντός των διχτυοκηπίων κατανάλωσαν 20-40% λιγότερο αρδευτικό νερό

σε σχέση με εκείνες του ανοικτού αγρού, αυξάνοντας την Αποτελεσματικότητα Χρήσης Αρδευτικού Νερού (IWUE) κατά 132% και 93% εντός των εντομοστεγανών διχτυοκηπίων και του S-36, αντίστοιχα, σε σχέση με εκείνη του ανοικτού αγρού. Η αύξηση των καλλιεργειών επηρεάστηκε θετικά εντός των εντομοστεγανών διχτυοκηπίων, σε αντίθεση με την αντίστοιχη εντός του διχτυοκηπίου S-36. Επιπλέον, η αύξηση των καλλιεργειών προσομοιώθηκε με την χρήση προσομοιώματος που προβλέπει τη παραγωγή ξηράς ουσίας λαμβάνοντας υπ' όψιν αθροιστική προσλαμβάνουσα PAR από την καλλιέργεια και ταυτοχρόνως υπολογίστηκε και η Αποτελεσματικότητα Χρήσης Ακτινοβολίας από τις καλλιέργειες κάθε μεταχείρισης. Η IWUE και η RUE συσχετίστηκαν ισχυρά με τα οπτικά χαρακτηριστικά των διχτύων κάλυψης, δηλαδή με την ποσότητα και την ποιότητα (φασματική) της άμεσης και της διάχυτης ηλιακής ακτινοβολίας στο εσωτερικό των διχτυοκηπίων.

Λέξεις κλειδιά: Δίχτυ, Σκίαση, Εντομοστεγανό, Πορώδες, Διάχυτη ακτινοβολία, Θερμοκρασία καλλιέργειας, Αγωγιμότητα κόμης καλλιέργειας, Διαπνοή, Αερισμός, Συντελεστής παροχής, Συντελεστής επίδρασης ανέμου, Παραγωγή πιπεριάς, Ποιότητα παραγωγής, Ηλιακό έγκαυμα, Ξηρά σήψη κορυφής, Αύξηση, Αποτελεσματικότητα Χρήσης Νερού, Αποτελεσματικότητα Χρήσης Ακτινοβολίας.

Prologue and Acknowledgments

This dissertation would not have been possible without the guidance and the help of several individuals who in one way or another contributed and extended their valuable assistance in the preparation and completion of this study.

First and foremost, I would like to express my deep appreciation and gratitude to my supervisor, Professor Constantinos Kittas for the patient guidance and mentorship he provided to me, all the way from when I applied to the PhD program in the School of Agricultural Sciences through to completion of this degree. He passionately supported and guided me through my entire postgraduate studies, MSc and PhD degree, integrating my field of knowledge about screened horticulture. Additionally, I wish to express my sincere thanks to Professor Kittas, who as the Director of the Laboratory of Agricultural Constructions and Environmental Control of School of Agricultural Sciences of the University of Thessaly provided me with all the necessary facilities for the research. I am truly fortunate to have had the opportunity to work with him.

I would also like to thank the Researcher from the French National Institute for Agricultural Research, Dr. Thierry Boulard for his contribution and suggestions during this research project and especially for the definition of the experimental configuration and procedures prior the commence of the field trials. Moreover, I greatly appreciate the intention of Dr. Boulard to be physically present at the public support and examination of the present dissertation.

Furthermore, I would like to thank Assistant Professor Nikolaos Katsoulas for his friendly guidance, thought-provoking suggestions, and the general collegiality that he offered to me over the project years. His support and experience in getting familiar with sensor handling and microclimatic measurement techniques was extremely valuable.

It would have been an omission not to express my gratitude to Dr Thomas Bartzanas who as a Senior Researcher of the Centre for Research and Technology-Hellas (CERTH) he greatly contributed to the present research program not only through the grand of CERTH's screenhouse constructions but also with his expertise, and sincere and valuable guidance to the preparation of the experimental protocol.

I should also thank Prof. Kittas, Asst. Prof. Katsoulas and Dr Bartzanas for the determinant contribution in the writing of the proposal of the present research project for its funding.

Additively, I would like to thank Professor Demetres Briassoulis, Professor Anastasios Siomos and Associate Professor Dimitrios Savvas, for their valuable time to read and examine the present dissertation.

Moreover, I would like to greatly thank Dr Teitel for conducting the wind tunnel tests and providing the raw data for the determination of the aerodynamic properties of the screens used in this research. Also, I am grateful for the aid of Dr. Eleni. Kamoutsi, Laboratory of Materials, Dept. of Mechanical Engineering, University of Thessaly, in determining the geometrical characteristics of the screens of the present study and for the supporting of this effort by Dr Leonidas Spirou, Researcher, Grade D, CERTH - Mechatronics Institute.

Furthermore, I should mention the constructive cooperation in the experimental field as well as in the laboratory with the postgraduate students Miss Chrysa Nikolaou, Miss Anna Kandila and Mr Panagiotis Belitsiotis, for which I am thankful. The latter student, Panagiotis, greatly helped me by sharing a lot of handy work during the second experimental period. I also do not forget the valuable help in pest and disease control and in specific handy works of Mr Ilias Giannakos. Of course, I should mention the determinant crop management guidance freely and lavishly offered by the agronomists Vaios and Dimitris Argyrakis of the “Agricultural Laboratory Ltd.”.

Additionally, I would like to thank the administrators of the research program Heraclitus II at the Research Committee of University of Thessaly, Mr Apostolos Zisis, Mrs Chrysoula Kourti and Mrs Katerina Papaoikonomou for their kind support.

I also should thank Agroplast-Hatzikosti Bros. for offering the white anti-thrip nets IP-13 and IP-34 and Plantas S.A. for offering the pepper plant seedlings, especially after the determinant actions of Mr Dimitris Karelas.

I would never forget to mention the generous and untiring day by day support of my exceptional and beloved parents. I own them what I became. I would also like to mention the endless discussions and the significant support of my sister Lia and her husband George, against everyday difficulties and unanticipated obstacles that had risen before me during my research.

Finally, I would like to acknowledge the innumerable and continuous sacrifices made by my wife, Ismini, in shouldering far more than her fair share of the parenting and household burdens. Her efforts and actions, under exceptional difficult everyday life, in keeping me focused and undistracted despite of living far away from her and

our son, were determinant to the successful completion of my PhD research. There are no more words left to me to express my gratitude to you Ismini.

To my beloved wife Ismini
and our son Rigas,
who so much missed me
during this project.

Index of contents

Index of tables

Index of figures

1. Introduction

1.1. Screened enclosures

As Tanny, (2013) quoted in his review for screened covered enclosures, there are different isolation or protection levels between open field or hi-tech closed greenhouse systems, such as vertical wind breaks (Brandle et al., 2004), horizontal screen strips which cover the hedgerows only (Tanny and Cohen, 2003), horizontal screens without sidewalls (Tanny et al., 2009), complete screenhouses consisting of screened roofs and sidewalls (Dicken et al., 2013a, 2013b; Haijun et al., 2015; Möller et al., 2004a; J. Tanny et al., 2003; Tanny et al., 2010, 2006) and naturally ventilated plastic greenhouses with screened roof and/or side openings (Teitel, 2007). Growers' experience shows that, in many situations, high profits can also be achieved using intermediate-level isolation structures such as naturally ventilated greenhouses or various screen constructions. This makes these structures highly attractive in many regions of the world (Tanny, 2013). The most profitable investment in a certain region is not necessary the most expensive or the most technologically advanced (Vanthoor et al., 2011).

Screenhouses are steadily spreading around subtropical regions; semi-arid regions as Oman and Mediterranean regions, in particular in Israel, southern regions of Spain, Italy and Greece. Precise records about screenhouse covered crops are not available. Nevertheless, screenhouse covered areas are extensive in Israel been about 6000 acres (M. Teitel, personal communication), while in Greece the screen covered horticultural crops (mostly by horizontally deployed shade nets) are estimated approximately about 1000 acres (estimates by "Thrace Plastics S.A."). These low cost structures protect covered crops from environmental (wind, hail, rain storms, excessive radiative loads during hot period of the year) and biological (pests, birds, bats) pressure factors, while reduce pesticide applications (case of insect-proof screenhouses) and irrigation water applications, increasing in this way the water use efficiency (Castellano et al., 2008a; Katsoulas et al., 2012; Möller and Assouline, 2007) preventing against shortage of water resources. Using screens to protect horticultural crops improves the microclimate, promoting crop productivity and fruit quality (Ilić et al., 2014, 2012; Kittas et al., 2012; Leyva et al., 2015; Shahak, 2008). Screenhouses are passive structures, i.e., they do not contain devices for modifying crop climate, while the only means to regulate their microclimate are the shape of

their structure and the characteristics of their covering screens. Screenhouses became popular among growers because of their relative simplicity and cost effectiveness and is likely to remain in the future, since if a grower were to invest more resources in a screenhouse, he might opt for a greenhouse instead (Möller et al., 2004b).

1.2. Technical characteristics of agricultural screens/nets

Screen physical and optical properties are the main factors that affect the resulting microclimate inside an enclosure i.e., screenhouse or greenhouse with screened openings. The optical properties of screens affect the construction's transmission to solar and thermal radiation and accordingly determine their heat load (Desmarais et al., 1999; Kumar et al., 2009; Möller et al., 2010; Willits, 2001), while the physical properties of screens affect the natural ventilation performance of the enclosures (Kittas et al., 2002; Kumar et al., 2009; Miguel and Silva, 2000; Miguel et al., 2001, 1998; Möller et al., 2004b; Josef Tanny et al., 2003; Tanny, 2013), which is the only means of removing the excessive heat load in screenhouse structures, which negatively affects the productivity and quality of open field-grown crops (Möller et al., 2004b; Stanhill and Cohen, 2001).

The rapid spreading of the use of agricultural nets leaded to the globally increase in industrial production of agricultural plastic nets. Nevertheless, the design and use of the agricultural nets is more or less empirical. Thus, the necessity of the establishment of European standards is more than essential. A pre-normative research work on the examination of the mechanical behavior and properties of agricultural nets was reported by Briassoulis et al. (2007a and 2007b). Additionally to the later properties, Castellano et al. (2008a) reported the calibration efforts that they conducted in order to optimize the UNI10335, which however is the only national standard in Europe providing a methodology to evaluate nets shading factors, on the laboratory simulation of the *in situ* shading effect of all nets.

The agricultural nets are constructed by combining in a certain texture (weave or knit) plastic yarns (polyethylene (PE), polypropylene (PP)). Nets have different characteristics upon their intended use; hole size-shape, yarn dimensions-type, transmittance to solar radiation etc. To precisely describe an agricultural net in order growers/agronomists to make the best choice for their case, it is suggested to present the following characteristics:

- Thread material: ex. polyethylene (PE), polypropylene (PP) etc.
- Type of thread: monofilament or tape
- Thread diameter: mm
- Thread color: single or combined colors
- Texture: woven - knitted
- Dimensions of the open spaces (cell dimensions)
- Porosity: the ratio between open area and total area
- Mesh: number of open spaces per inch in each direction
- Discharge coefficient
- Transmittance to short and long wave
- Spectral transmittance

In Europe the respective “mesh” number stands for the number of spaces per centimeter in each direction (10×20 screen has 10 spaces/cm in one direction and 20 in the other direction). Generally the information about the characteristic of the screen/nets are insufficient presenting only few characteristics (Teitel, 2007). For instance, screens with the same length of mesh but with different thread diameters will have different resistance to airflow. On the other hand, it is possible to have screens with the same discharge coefficient and the same resistance to airflow but with different mesh sizes (Teitel, 2007).

1.2.1. Geometrical characteristics

Concerning the physical properties of screens, their geometrical characteristics strongly affect screens’ permeability to air flow. The pressure drop through screens is related to screen porosity and geometry and can be determined either by Forchheimer’s or by Bernouli’s equation (Lopez-Martínez et al., 2014; Miguel, 1998; Miguel et al., 1997a). The porosity of a woven screen that is made of a monofilament thread and that has a simple texture was determined by 2-D or 3-D geometric analysis (Cabrera et al., 2006; Pinker and Herbert, 1967) or with specifically developed software (Álvarez et al., 2012), while, for the case of screens with complex texture, the image analysis is proposed (microscope or image processing software) (Möller et al., 2010; Soni et al., 2005). Determination of the aerodynamic characteristics of screens can be done through wind tunnel measurements (Miguel et al., 1997a;

Molina-Aiz et al., 2009; Teitel et al., 2009). Pirkner et al. (2014) measured pressure drops across a woven and a knitted screen, reporting that the woven screen induces larger resistance to air flow than the knitted (Pirkner et al., 2014). The authors ascribed the differences of the pressure drop to the differences in the screen textures that probably resulted in different flow patterns through the screens and pressure distributions on the threads and hence different pressure drops.

As insect proof screens acts as a barrier to momentum and transport processes they promote the increase of air temperature and humidity inside the enclosures. Therefore, it is essential to alleviate these negative effects on the internal microclimate. One effective way, as clearly documented by Boulard et al. (2011), is by improving nets air porosity while preserving its properties for insects-exclusion. By this technique the anti-insect function is fulfilled along with the improved ventilation efficiency of the enclosures (screenhouses and greenhouses) (Boulard et al., 2011).

1.2.2. Optical characteristics

Agricultural nets influence the underneath crops by reducing and/or modifying the radiative environment under which they are growing. The influence of the screens/nets on the radiative environment is related to their optical properties; transmittance, absorbance and reflectance. The definition of the latter properties on newly developed screen/nets is of great importance for the horticultural production. The diffusive effect of the screens is another extremely important characteristic that greatly impacts on the radiative environment of the screened crops. Additionally, the texture and the color of a screen directly influence its optical properties. The color of a net influences the spectral distribution of the radiation passing through its matrix, by absorbing the complementary colors of the spectrum and emitting (transmit and reflect) light through a narrower wavelength band. The quantitative and qualitative analysis and presentation of these properties will help agronomists and growers to decide on the best type of screen according to their production goals. UNI10335 is the only national standard in Europe providing a methodology to evaluate nets shading factors (Castellano et al., 2008a).

2. Literature review of screened enclosures

2.1. Microclimate of screened enclosures

2.1.1. Radiative environment

2.1.1.1. Irradiance reduction under screens/nets

The primarily target installing a shade net is to protect the underneath crop from the supra-optimal solar radiation during the hot period of the year. Waggoner et al. (1959) and Desmarais et al. (1999) quantified the reduction of the solar radiation under different screens enclosures without crops. Several studies have been conducted on the *in situ* determination of the reduction of incident irradiance on the canopy covered crops. Several researchers conducted comparative experiments with more than one screen/net in order to quantify the influence of the covering screen/net to the covered crop. Waggoner et al. (1959) and Allen, (1975) measured the radiation incident on the canopy of covered tobacco and soybean crops. Kittas et al. (2012) measured global radiation and PAR under four different shade nets. Haijun et al. (2015) and Pirkner et al. (2014) quantified the influence of the type of screen textures (woven and knitted) on global and net radiations in order to determine the optimal choice for the protected banana plantation. Shahak et al. (2009a, 2004a, 2004b) monitored the global and PAR under colored photoselective shade nets that protected different horticultural crops.

The reduction of solar radiation by an agricultural screen/net is associated to its optical and geometrical characteristics. The determination of the impact of a screen to the radiative environment is essential prior to installation. Möller et al. (2010), successively attempted to predict screen radiative properties adequately based on screen geometry and composition which is of great importance (screen design; crop growth simulations etc.). Their mode of course should be further improved (as accurately pointed by the authors) to accurately embed the diffusive effect of the screens. The installed screens/nets are supported by frames constructed by various materials (ex. wood, steel and cables). The shape/type of these structures is also varying (ex. flat roof, arch). The materials and the type of the supporting structures are influencing (reducing) the overall transmittance of the enclosure to solar radiation. Reduction of net transmittance caused by the presence of the supporting structure was reported by Castellano et al. (2006). Moreover, the solar radiation under agricultural screens is correlated to the sun position with respect to the covering screen. Möller

and Assouline and Möller et al. (2007 and 2003) documented the negative correlation between the solar elevation angle and screen transmittance to short wave radiation; transmittance was reaching a maximal value around solar noon, while the daily average was significantly lower than the maximal value. This unimodal pattern was attributed to the thickness of the screen material itself which blocked the direct beam radiation at low elevation angles (Möller and Assouline, 2007; Möller et al., 2003).

Screens and nets create a mixture of (i) natural light (i.e., the fraction of light that freely passes through the holes) and (ii) modified light (i.e., the fraction that passes through the thread material). The modification of that light depends on the optical properties of the material. Thus, this light is differentially absorbed, transmitted and reflected by the screen threads, relatively to their optical properties. Additionally, this light could be spectrally modified relatively to thread color or to special additives embedded on the threads. Finally, this light is scattered by the threads relatively to the inherit diffusive properties of their material. The final relative composition of the mixture of light that pass through a screen is depended on screen texture (woven/knitted) and density; in particular is depended on its solidity (the surface area covered by the plastic threads divided by the total surface area of the screen/net) and type of texture; the fraction of the modified light increases with screen solidity.

Al-Helal and Abdel-Ghany (2011; 2010) extensively studied the solar radiative properties of different shade nets and their responses to global and diffuse PAR transfer. The authors documented the effect of net color and net porosity (ratio between open and total screen/net area) on its transmittance and absorbance. They quoted that the effect of color is much more than the effect of solidity/porosity. Given the same porosity, increasing the brightness of the net (ex. dark green to light green) increases the PAR transmission due to scattering. Given the same color, nets with high porosities are expected to have higher transmittances than nets with low porosities. Increasing the darkness of the net together with decreasing the net porosity significantly increased the ability of the net to absorb PAR. Net color had a significant effect on the value PAR absorbance much more than the effect of porosity. Under cloudy or overcast sky conditions nets with a high porosity showed higher values for diffused PAR transmittance than nets with a low porosity. Nets with bright colors (i.e., white, orange and beige) showed higher transmittances than those with dark

colors (i.e., black, green, blue and dark-green). Accordingly, a net with a high porosity and bright color is recommended to be used for covering agricultural structures under diffuse radiation of cloudy or overcast sky conditions (Al-Helal and Abdel-Ghany, 2010; Castellano et al., 2008a). The forward scattering of the incident radiation on the thread surfaces mainly depends on the net color (increases with net brightness and vice versa), while the un-scattered radiation (freely passes through net holes) mainly depended on the net structure (woven-knitted) and the percent of its open area (holes) (Abdel-Ghany and Al-Helal, 2011). Healey and Rickert, (1998), also studied the proportion of diffuse radiation transmitted by different screens and nets, reporting similar results as the before mentioned. The correlation between the porosity and the diffusive effect of the agricultural nets have also been supported by Oren-Shamir et al. (2001), who reported an increase by 2.5-2.9 of the diffuse light by the more densely knitted colored nets when compared to the nets with higher porosity (black net; aluminized reflective net). The dense colored nets in their experiments reached a ratio of diffuse:beam radiation of 0.46-0.53. The effect of color and texture was also studied by Romero-Gámez et al. (2012), who reported that transmittance of a screen/net increases with the porosity and the brightness of its threads (given equal porosities).

The diffusive effect of a screen/net depends on the ambient diffuse fraction of solar radiation (Allen, 1975; Healey and Rickert, 1998). Allen, (1975) showed that the scattering of the beam solar radiation by a screen increased the underneath diffuse radiation up to the threshold of 38% ambient diffuse radiation.

2.1.1.2. Optical modification of radiative environment

Agricultural screens with respect to their color can be black, neutral (transparent/clear, white,) or colored (blue, yellow, red, orange, green (light-to-dark) etc.). The colored nets absorb the complementary colors of the visible wavelength bands of the incident irradiance and reflect and transmit irradiance with a certain wavelength spectrum. Thus, the radiation under these nets is spectrally different as opposed to that above. The colored nets shift the spectrum of the reflected and transmitted irradiance towards a narrow wavelength band. Moreover, the nets could be neutral colored but. Shahak, (2008), accurately describes the influence of the color of the screen to the incident and transmitted solar radiation: "*Black nets reduce the amount of light reaching the underneath plants, but do not affect light quality, as they*

neither modify its spectral composition, nor its relative content of scattered/diffused light. Transparent nets scatter the light transmitted through them, but do not alter its spectral composition. The uniqueness of the translucent photo-selective nets is that they both spectrally-manipulate and scatter the transmitted light.". The influence of the modified radiative environment under agricultural photoselective nets on the growth and development of the covered crops is extensively quoted by (Rajapakse and Shahak, 2007). The reports of Ganelevin and Stamps, (2008 and 2009) integrate the presentation of the effects and the possible application of photoselective nets. The quality of the radiative environment under colored nets has been investigated on the determination of the optimal protection of the crops (Kittas et al., 2012; Shahak et al., 2009a, 2004a, 2004b).

2.1.2. Wind speed

The presence of a screen acts as barrier on the momentum and mass freely transfer. Therefore, agricultural screens/net greatly impact to the prevailing ambient wind, reducing the air velocity and changing (or not) its direction inside screnhouses or under netted shelters, as compared to the respective outside. Several studies have been devoted to the relationship between inside and outside air velocity in screenhouses (Allen, 1975; Desmarais et al., 1999; Mistriotis and Castellano, 2012; Möller and Assouline, 2007; Möller et al., 2010, 2004b; Waggoner et al., 1959). The air velocity inside empty enclosures (Desmarais et al., 1999) and enclosures with various crops was investigated (ex.: tobacco and cotton (Waggoner et al., 1959), soybean (Allen, 1975), pepper (Möller and Assouline, 2007; Josef Tanny et al., 2003) banana (Haijun et al., 2015; Tanny et al., 2006), banana simulated (Siqueira et al., 2011).

Tanny et al. (2009) studied the effect on the microclimate of shading screens deployed horizontally above an apple orchard and they reported that the wind speed under the screen was 9% lower than that in the uncovered plot, while the logarithmic wind speed model was approximately valid under the screens. Tanny, (2013), in his review presented a summary of literature data on the effect of screen covers and screenhouses on air velocity. The ratio between inside to outside air velocity referred was greatly ranged between 0.2 and 0.70. Additionally, Al-Mulla et al. (2011), reported, for an insect proof screenhouse (no screen details reported) in Arabic

Peninsula (Oman), that the average reduction of air velocity (as deduced by their presented figure) was about 0.75, with the internal air velocity never exceed 1.08 m s^{-1}, while ambient wing speed ranged from 1.34 to 2.14 m s^{-1} (average: 1.74 m s^{-1}). Similarly, but in a tropical greenhouse experiment, Al-Shamiry et al. (2006) reported that the highest value of average wind speed was recorded as 1.39 m s-1, while the internal air velocity was recorded on average as 0.4 m s-1, resulted on a reduction about 0.70. The influence of the screen texture to the internal air velocity was documented by Pirkner et al. (2014), who reported that under a knitted screen the horizontal mean air velocity was 18% higher than under a woven screen, which was covering a banana plantation. Furthermore, inside another banana screenhouse covered by a transparent shading screen (hole size of 3.5 × 2.5 mm), the wind speed was been reduced by more than 60% (Haijun et al., 2015).

The influence of the screenhouse on the azimuth of the prevailing wind is a very ambiguous issue, according to the reports of Tanny et al. (2010, 2006) and those of Möller et al. and J. Tanny et al. (2003 and 2003), since two different patterns of directional flow have been recorded. In a banana screenhouse Tanny et al. (2010, 2006) reported that most of the time, the azimuth of internal air flow at the center of the screenhouse was approximately similar to that of the external wind. This situation differed from the findings reported by Möller et al. and J. Tanny et al. (2003 and 2003) in a 50-mesh insect-proof screenhouse in which pepper was grown, who reported that the air flow direction at the center of the screenhouse was nearly opposite to that of the external wind. Furthermore, the latter authors demonstrated that, over the windward half of the screenhouse, the air flow direction was opposite to the external wind whereas over the leeward half, inside and outside air flow was in the same direction. The differences of the directional flows were attributed by the authors to the ambient pressure distribution induced by the wind around the screenhouse. The curvature of streamlines at the windward edge of the house induces suction at this region, which causes internal backflow that starts apparently from the leeward edge, supporting it with relevant quotations about greenhouse case studies (Lee et al., 2000; Wang and Deltour, 1999; Wang et al., 1999). The directional flows across the roof of the same screenhouse was also quoted by J. Tanny et al. (2003), reporting a counter flow across the screenhouse roof. That counter flow can induce hydrodynamic instabilities and enhance mixing in this region.

2.1.3. Air temperature and vapor pressure deficit

2.1.3.1. Mean values of air temperature and vapor pressure deficit

Agricultural screens and nets, as they significuntly reduce the incoming heat load and the internal air velocity, they strongly affect the underneath microclimate parameters; air temperature and humidity. Insect-proof screens impose a higher resistance to air flow than shading screens and thus reduce the ventilation, which may cause greater temperature increases (Tanny, 2013). Several studies were foccused on the monitoring of the air temperature and humidity as they are modified by the presense of a screen/net. As screens impede ventilation they usually inhibit the removal of water vapour from the screenhouse. Hence, in most studies reported in the literature internal humidity was larger than external (Tanny, 2013).

Tanny et al. (2009) study the effect of shading screens deployed horizontally above an apple orchard on its microclimate. The authors reported that the screens reduced air temperature during the day (maximum of 1.5°C at noon) and increased air temperature at night (maximum of 0.5°C), when compared to the uncovered plot, resulting in a daily average reduction by about 2°C. The effect of the screens on temperature increased with increasing shading percentage, as expected. The vapour pressure deficit (VPD) under the screens was lower than that in the uncovered plot during daytime, but no significant alteration of VPD was observed at night. Similar results were reported by (Tanny and Cohen, 2003) for a citrus orchard covered with aluminized shade net.

Möller et al. (2003) and Tanny et al. (2003) for the same insect-proof, 50-mesh, pepper screenhouse, located at a coastal area, observed higher air temperatures (on average < 1ºC) inside the screenhouse than in the open air, while the in-to-out difference never exceeding 2.5ºC. Furthermore, the enclosure preserved greater humidities than outdoors. Tanny et al. (2003) quoted that during most of the day the positive air temperature gradient inside the screenhouse stabilized the air and reduced the interaction with the external atmosphere. For their case study this was a negative effect because the construction prevented the sea breeze to cool down the enclosure, unlike to the continental region case study of Romacho et al. (2006) where the prevention of the warmer external temperature (lack of sea breeze) to penetrate inside the enclosure was a positive effect. Moreover, Tanny et al. (2003) documented that the upper region of the screenhouse interacted strongly with the ambient air and that interaction was greatly enhanced by the wind speed; the increase of wind speed

above 2 ms^{-1} resulted in strong mixing between the external and internal upper region began, such that the absolute humidity just below the roof of the screenhouse became almost indistinguishable from the ambient. Romacho et al. (2006) investigated the influence of two different covering screens on the internal microclimate. The authors reported that air temperature shows a slight thermal inversion at night, while during the morning, before noon, the outdoor temperature is lower than the inside. They also compared the air temperature of the two enclosures; the higher transmittive screenhouse was slightly warmer as opposed to the lower transmitive house. The authors ascribed the lower air temperature in the nethouses after noon to the evapotranspiration inside the enclosure and to the high ambient air temperature which was preserved and further increased by the extrem heat loads radiated from the bare soil to the ambient. The VPD, which was mainly influenced by the reduction of air velocity inside the screenhouses, that restricts the exit of water vapour and by the evolution of air temperature and solar radiation, was lower in the screenhouses, especially around noon. Möller and Assouline, (2007) reported for a screnhouse covered by a 30% black shade net that the internal air temperature was predominantly lower (on 67% of all measurement days) than that outside, and that the maximal inside-to-outside difference ("greenhouse effect") did not exceed 1.0 ^{o}C. The significant reduction of the solar radiation (on seasonal basis: 43%) and the relatively large holes of the net (porosity 0.7), allowed a significant ventilation rate which enabled efficient removal of warm air (Tanny, 2013). Al-Mulla et al. (2011) reported, for a screenhouse (80 micron insect-proof screen) in arid region (Oman), that the inside air was slightly warmer (+1.7°C) and more humid (+7.3%) than outside, while air temperature and relative humidity (on average 55.5%), were uniformly distributed inside the enclosure. The same authors distinguished the microclimate parameters for cooler and warmer periods of the year, reporting that the average inside temperature was warmer than outside by 0.4-3°C during January and February and colder than outside by 0.2-0.8°C during March and April. The inside vapour pressure deficit (VPD) was always lower than outside by 0.2-1 kPa. The experiments were conducted inside the same screenhouse but during different experiment (Al-Mulla et al., 2008). The air temperature inside the screenhouse in which (Haijun et al. (2015) conducted their trials was reduced by only 1% (or on average 0.2 ◦C), while the relative humidity increased by 8%.

The inherited characteristics (texture, porosity etc.) of the covering screen/net and of the supposrting structure influence the internal microcliamtae. The differential effect of the woven vs knitted nets on the internal microclimate was documented by Pirkner et al. (2014), who reported lower specific humidity (-8%) under a knitted screen as opposed to the woven screen, while no significant temperature difference were revealed. The increased of the absolute humidity under the woven screen, did not modify the average VPD under the two, which, according to the authors, suggests that most of the difference in latent energy between the two screens was due to differences in air velocity (Pirkner et al., 2014). Moreover, the increase of the construction height enhances the reduction of the air temperature and VPD of the enclosures (Tanny et al., 2008).

2.1.3.2. Profiles of air temperature and humidity

Temperature profiles were studied for the shaded and un-shaded crops by Allen, (1975) after a long dry period without rain. The author reported that the unshaded soybean temperature profiles had a strong decrease of temperature with increasing height, which indicated instability and a large sensible heat transfer from the plants and/or soil to the atmosphere above. Similarly, Tanny et al. (2009) demonstrated that during most of the day (from 08:00 until 24:00), the gradient in un-shade exposed plots of an apple orchard was negative whereas that under the shading screens was positive; and this difference was significant, while being increased with the shading level, with its maximum value under the 60% treatment (result not significant). The authors quoted that the soil surface heating by direct solar radiation could be ascribed to that negative gradient in the exposed treatment. Furthermore, between midnight and nearly 08:00, all treatments (including the control) exhibited a positive gradient, i.e., there was a stable boundary layer. This was probably due to long wave radiative cooling, which cools the soil and its adjacent air layer. Although the screens somewhat reduced the long wave radiative cooling, as compared with the control, the temperature gradient did not change its sign (Tanny, 2013).

Humidity and temperature profiles show that within the screenhouse temperature increased and absolute humidity decreased with increasing height (stabilized atmoshere) (J. Tanny et al., 2003). The stabilizing temperature gradient influenced the humidity profiles resulting to the decrease of the humidity with the increase of the height. Accordingly, the authors revealed diffrences between the crop

and below the roof levels. The humidity was higher within the foliage layer (at 0.5 m height) and decreased towards the screenhouse roof. It was suggested by the authors that this vertical gradient in humidity resulted from the great interaction between the upper and the lower atmosphere within the enclosure. Furthermore, the higher humidity at plants level was associated by the authors with the lower temperature and vice versa, demonstrating the cooling effect of the transpiring plants. The gradient of the specific humidity under two different in texture screens (woven vs knitted), at three different heights was studied by Pirkner et al. (2014), who reported similar values within the canopy (at 1.5 and 2.5 m), while, above the canopy (4.75 m) the specific humidity under the knitted screen was smaller by 8% on average than that under the woven screen. Möller et al. (2003) reported that inside an insect proof screenhouse they observed horizontal temperature differences between the center and edge; they documented that the central region was slightly warmer (and more humid) than the edge, indicating some non-uniformity of the micro-climate within the screenhouse, presumably caused by non-uniform mass exchange processes.

2.1.3.3. Crop temperature and crop-to-air vapor pressure deficit

Reduced crop temperatures and lower canopy-to-air temperature differences by about 3.5 ^{o}C were documented by Kittas et al. (2012), under a 49% black shade net covering a summer tomato crop. A more detailed approach of the influence of the covering nets on the canopy temperature was reported by Al-Mulla et al. (2011). The authors reported that the upper leaf temperature was higher than the middle and lower part of the canopy during midday (12:00 pm and 4:00 pm) whereas, lower leaf temperature exceeded the upper one during the night time of the day. Additionally, the crop-to-air temperature difference during the hottest period of the day was ranged from -2.5 ^{o}C (11:00 h, local time) to -4.5 ^{o}C (12:00-16:00 h, local time) and finally up to -7 ^{o}C (17:00 h, local time). The positive effect of the screenhouse on the reduction of the crop temperature with respect to air temperature was also documented by (Leyva et al., 2015).

The diffusive effect of the covering screens/nets alleviates the negative effect of radiative heating of the canopy of the protected crops. Beam (direct) light heats leaves more than the scattered light in the shade, and hence sunlit leaves can be several degrees warmer than shaded leaves under sunny and dry conditions (Dai et al., 2004). Diffuse light results in lower leaf or flower temperature and less photoinhibition (Li et

al., 2014; Urban et al., 2012) because of less severe local peaks in light intensity and consequently lower locally accumulated heat radiation. Sunlit leaves receive more near-infrared radiation than shaded leaves do (Gu, 2002), increasing their temperature as opposed to the shaded leaves.

The reduction of canopy temperature brings a significant reduction on the crop-to-air vapor pressure defficit, which resultes in increased stomatal conductance that positively influences the rates of photosynthesis (Cohen and Moreshet, 1997; Haijun et al., 2015; Kittas et al., 2012; Nicolás et al., 2005), with respect to the response type of the covered crops to the increase of capor pressure deficit; iso- or aniso-hydric (Tanny, 2013).

2.1.4. Ventilation

Tanny et al. (2006, 2003) studied the ventilation performance of various commercial screenhouses of different size (covered ground area ≈ 0.66 and 8 ha; Height = 3.2 m and 6 m). The air exchange rate was found to range between 7 and 33 h^{-1} for wind speed between 1.5 and 3.5 m s^{-1}. Tanny et al. (2006) who studied the volume flow rate in a banana screenhouse compared their results with those obtained by Tanny et al. (2003) in a pepper screenhouse and by Demrati et al. (2001) in a banana greenhouse. The flow rate in the banana screenhouse was much larger than those in the banana greenhouse of and the pepper screenhouse, while the reported air exchange rates were of the same order of magnitude (Tanny, 2013). Tanny et al. (2008) reported that the increase of the height of a screenhouse structure enhanced mixing and ventilation of the air near the plants.

The air exchange rate and its correlation to buoyancy and wind forces has been extensively studied in greenhouses and several models have been developed to predict greenhouse air exchange rate as a function of vent opening characteristics, vent opening area, inside to outside air temperature difference and outside air velocity (Boulard and Baille, 1995; Kittas et al., 2002, 1997; Zhang et al., 1989). The screenhouse air exchange rate could be estimated as a wind driven air flow through an opening (ASHRAE, 1993). Generalizing the latter method for both wind pressure effect and temperature difference effect and assuming the ideal condition of unidirectional flow, Desmarais et al. (1999) defined the air exchange rate of small experimental screenhouses. However, to the best of our knowledge, there is no model

available to be used for the simulation of screenhouse air exchange rate as a function of screen physical properties, screenhouse covering area and wind velocity.

2.1.5. Evapotranspiration

Screened structures reduce significantly the crop water demands, which is a profound effect that attracted great attention by researchers aiming towards improving the irrigation strategy of the screened crops. The observed lower transpiration rate of a screenhouse sweet pepper crop as compared to the simulated transpiration of a similar crop grown outside was primarily attributed by Möller et al. (2003) to the significantly reduced radiative load (40–50% in global radiation) and to a lesser extent to the higher humidity and lower wind speed below the screen as opposed to the external conditions. Möller et al. (2004) demonstrated for the first time the feasibility of using the eddy covariance (EC) technique in an insect proof screenhouse in which pepper was being grown. The authors developed a one-dimensional screenhouse model to calculate evapotranspiration of the screenhouse crop, based on a modified Penman–Monteith equation incorporating an additional boundary layer resistance. The sensitivity analysis for that model revealed that reduced radiation and wind speed and modified vapour pressure deficit were the main factors influencing transpiration. The evapotranspiration in a large banana screenhouse was also measured by an EC system by Tanny et al. (2006). Inside a 30% black shade net screenhouse the crop water requirements (ETc) were 38% lower than the estimates for an open field crop (Möller and Assouline, 2007). The latter authors applied successfully the FAO-Penman–Monteith approach based on meteorological measurements in the screenhouse which accurately predicted daily crop evapotranspiration, as verified by the close agreement with lysimeter measurements. Tanny, (2013) compared the outcome results of the EC technique (Tanny et al., 2006) as opposed to the results of the reference evapotranspiration model for external meteorological conditions (Allen et al., 1998) and to the results of the modified ET model for screenhouse conditions. Dicken et al. (2013a) used successfully the Bowen ratio energy balance technique to estimate evapotranspiration inside a large banana screenhouse and supported the application of the method for irrigation management of the covered crops. Furthermore, Siqueira et al. (2011) quoted that the overall effect of the screen resulting in water savings for the same amount of gross primary production, which profoundly enhances water use efficiency. The modification of the internal

microclimate (lower radiation and wind speed; cooler air by on average 0.2 ^{o}C (≈1%); increased relative humidity by 8%) leaded to reductions of 33% in calculated ET_o (Haijun et al. (2015).

2.2. Influence of microclimate on screened crops

2.2.1. Irradiance regime on crop performance

Under excess levels of solar radiation energy, above the saturation point the photosynthesis is inhibited i.e., supra-optimal light energy results in photoinhibition of photosynthesis. The carbon metabolism may limit the consumption of photosynthetic energy, resulting in excess photon absorption and therefore accumulation of the unutilized excitation energy, resulting in reductions in photosynthetic efficiency. Furthermore, the photosystem II (PSII) undergoes severe damages (Aro et al., 1993). Plants developed multiple mechanisms in order to alleviate the negative effects of excess light. However, they cannot completely avoid photo-damage, and have developed an effective but energy-dependent recovery system to repair the damaged PSII. During the day almost the whole PSII complex pool can be destroyed and quickly repaired, with expected energy expense for plants (Chow, W.S. and Aro, 2005). Arboree et al. (2011) documented that the maximal amount of active PSII damaged by a photon unit is not influenced by light reduction therefore, the more the absorbed photons, the more the photo-damage to be repaired, at the expense of energy/assimilates. The authors quoted that optimizing light interception by deploying a moderate shade net over an orchard does not negatively affect net carbon assimilation, but profoundly reduces carbon and energy costs for photosystems recovery. Thus, shaded plantations can accumulate more assimilates because their photosynthetic performance is not decreased by the reduced intercepted light energy and they do not waste carbon for repairing photo-damages.

The positive effect of the diffuse radiation on ecosystems performance attracted great attention by several researchers. Gu, (2002) resumed their finding for the diffuse radiation as follows: (1) diffuse radiation results in higher light use efficiencies by plant canopies; (2) diffuse radiation has much less tendency to cause canopy photosynthetic saturation; (3) the advantages of diffuse radiation over direct radiation increase with radiation level; (4) temperature as well as vapor pressure deficit can cause different responses in diffuse and direct canopy photosynthesis, indicating that their impacts on terrestrial ecosystem carbon assimilation may depend on radiation regimes and thus sky conditions. Sunlit leaves receive not only more PAR, but also more near-infrared radiation than shaded leaves do. Therefore temperatures of sunlit leaves are expected to be higher than shaded leaves. This leads to greater temperature

gradients between sunlit leaves and surrounding air (Young and Smith, 1983). Differences in leaf temperature can also result in differences in VPD at the leaf surface and thus affect stomatal conductance (Baldocchi and Harley, 1995; Baldocchi et al., 1997; Collatz et al., 1991). These differences directly or indirectly influence canopy photosynthesis. The profound effect of the diffuse radiation on the photosynthesis was studied by several authors (Brodersen and Vogelmann, 2007; Brodersen et al., 2008; Gorton et al., 2010; Gu, 2002; Hemming et al., 2008; Li et al., 2014).

As screens/nets profoundly increase the underneath diffuse radiation and the diffuse radiation enhance crop photosynthesis, screens influence indirectly the photosynthetic performance of the covered crops. Since cultivating inside screenhouses is a relative new practice there are no sufficient reports that directly quantify the influence of the diffuse radiation on the covered crops. Mostly, there are quotations that are used to support theoretically that the increased diffuse radiation inside screenhouses could explain the increase of the productivity of the covered crops. (Wright and Hammer, 1994) and (Bange, 1995), on trials with peanut and sunflower, respectively, demonstrated "theoretically" that radiation use efficiency is increasing with the increase of diffuse fraction of the available solar radiation to the crops. Healey et al. (1998) conducted experiments of different shade treatment on *Panicum maximum* cv. Petrie (green panic) and *Bothriochloa insculpta* cv. Bisset (creeping bluegrass) and documented that the increased radiation use efficiency under shade could be ascribed to the increased diffuse radiation. Dicken et al. (2013b) quoted that the increased CO_2 fixation per leaf area of a banana crop may have been ascribed to the increased fraction of diffuse radiation under the screen (as Möller et al. (2010) documented), which increases the relative amount of light reaching lower (and more shaded) leaves and thus increases their photosynthesis. The authors used the quotations of (Gu, 2002) and (Gu et al., 2003) to explain positive effect of the diffuse radiation on the enhance of photosynthesis. Shahak et al. (2004a, 2004b) investigated the diffuse radiative environment under photoselective nets and ascribed it to the enhanced performance of the covered crops.

Choosing the right covering screen/net is of great importance for the performance of the underneath crops. Shahak et al. (2004b) studied the photosynthetic performance of apple tree leaves under different nets and at the open field, reporting the profound increase of photosynthesis rate during most of the day under shade, with

respect to the net type. The favourable microclimate under shade (reflective) nets (lower light energy, canopy temperature, increased VPD) resulted in increase of CO_2 assimilation in shaded plants than in exposed/un-shaded plants (Alarcón et al., 2006; Medina et al., 2002).

2.2.2. Light spectral quality on crops

The photosynthetically active radiation (PAR; 400-700 nm) provide plants with the necessary energy for photosynthesis. The amount of the intercepted by a crop canopy PAR influences the rate of photosynthesis. In higher plants red and blue light best drive photosynthesis with the primarily photosynthetic pigment chlorophyll a and b strongly absorb light through the blue (peak near 430 nm) and the red (peak near 660 nm) spectral bands, while the have very little absorption in green region (500-600 nm). Thus, photosynthesis can be increased by increasing the amount of blue and red light that incident over a crop canopy. Greenhouse industry is aiming to increase blue and red light inside greenhouses by incorporating photoluminescent pigments in the covering materials that can transform the little used UV and green light into blue and red (Rajapakse and Shahak, 2007).

However, plants respond not only in the quantity of the intercepted PAR but also to its spectrum quality. Light quality is embeds important environmental information to a developing plant. Photomorphogenesis indicates that two main photoreceptors are mainly involved in the perception of light quality, phytochrome (*phy*) and cryptochrome (*cry*). Rajapakse and Shahak, (2007) reported a comprehensive review of light quality manipulation by horticulture industry, presenting the important spectral bands of light for plant growth and development along with the relative plant responses to light quality modifications. In the followings are presented plant responses to light quality with respect to the green wavelength band, in order to rationalize the extensive use of green shade nets on horticulture.

Recent evidence shows that green light has discrete effects on plant biology, and the mechanisms that sense this light quality are now being elucidated. Green light has been shown to affect plant processes via *cry*-dependent and *cry*-independent means. Sellaro et al. (2010) concluded that cryptochrome is a sensor of blue irradiance and blue/green ratio. The authors reported that the length of the hypocotyl of Arabidopsis (*Arabidopsis thaliana*) seedlings decreased linearly with increasing blue/green ratios of the light within the range of ratios found in natural environments and this effect

was stronger under higher irradiances (Sellaro et al., 2010). Previous research showed that blue light is qualitatively required for normal photosynthetic functioning, and quantitatively mediates leaf responses resembling those to irradiance intensity (Hogewoning et al., 2010). In other words, the photosynthetic capacity increases with the increase of percent of blue light before the threshold, and keep stable beyond the threshold (Kong et al., 2012).

Green light effects, in general, oppose those directed by light across the red and blue wavebands. The work presented by Klein, (1992) is very enlightening about the "*effects of green light on biological systems*". Folta and Maruhnich, (2007) in their review for the green light effects on plants, quoted that green light sensory systems adjust development and growth in orchestration with red and blue sensors. Klein and Klein et al. (1964 and 1965) tested the action spectrum of growth inhibition not only on early plant tissue culture but also on rapidly growing plants and found that the most deleterious light quality was green light, peaking at 550 nm. Dougher and Bugbee and Went (2001 and 1957) conducted analogous experiments by removal or supplement of green light to full spectrum and reported enhanced or inhibited plant growth, respectively. Stomatal opening exhibits two main peaks of activity in the visible range; a red peak, mediated by photosynthesis, and a blue peak, mediated by one or more blue light photoreceptors. Under certain conditions green light opposes stomatal opening (Eisinger et al., 2003; Frechilla et al., 2000, 1999; Talbott et al., 2002). As reported by several authors, green light inhibited (delayed or suppressed) flowering (Banerjee et al., 2007; Klein et al., 1965; Vince et al., 1964). Upon surveying the influence of green light on plants Folta and Maruhnich, (2007) concluded that green light tend to reverse the processes established by red and/or blue light. In this way, green light may be functioning in a manner similar to far-red light, informing the plant of photosynthetically unfavourable conditions.

2.2.3. Utilization efficiency of radiation and water (RUE and WUE)

Sinclair et al. (1992), quoted that radiation use efficiency (RUE) of field crops increased as the fraction of diffuse radiation increased and the total radiation decreased, which is valid for the greenhouse and screenhouse radiative environments. The improved microclimate under screens increases the efficiency that covered crops utilize the radiation and therefore increases their growth. Healey et al. (1998) reported that the increased (RUE) in response to a decrease in the level of incident radiation

and an increase in the proportion of diffuse radiation could probably explain the differences between shaded and un-shaded crops. The authors supported this increase this increase by several factors: (i) increased shoot to root ratio, (ii) leaf to stem ratio (iii) decreased respiration rates of whole plants (iv) increased canopy efficiency due to the better light distribution (v) lower values for the light extinction coefficient under nets. Increased RUE of tomato crops under shade nets, as opposed to the open field was also reported by Kittas et al. (2012).

The significant effect of screens is increasing the water use efficiency of shaded crops as compared to exposed ones, due to the reduction of crop irrigation demands and the simultaneous increase of crops productivity. A mobile shade net increased water use efficiency (WUE) by reducing the crop transpiration rate (Lorenzo et al., 2004, 2003). For a screenhouse sweet pepper crop the reported irrigation water use efficiency (IWUE) was between 10.70 and 13.54 kg m^{-3}, while the respective value for an open field crop was (on average) 4.75 kg m^{-3} (Möller and Assouline, 2007). Leyva et al. (2015), reported that the WUE by a cherry tomato crop inside a screenhouse was 7.03 kg m^{-3} (fresh mass), while this value decreased when a fog system was deployed. Furthermore, water use efficiency (WUE; mmol CO_2 $mmol^{-1}$ H_2O) of citrus, lemon and apricot trees was also increased under nets deployed above an open field orchard or over a greenhouse plantation (Alarcón et al., 2006; Medina et al., 2002; Nicolás et al., 2005). Siqueira et al. (2011) who simulated WUE (mmol CO_2 $mmol^{-1}$ H_2O) of a screenhouse and an open field banana crop, reported an increase of about 25% of the WUE inside the screenhouse as opposed to that of the open field.

2.2.4. Plant development under screens

The distinctive effect of the increase of plant height under shade is termed as "shade avoidance syndrome" and has been extensively investigated (Mullen et al., 2006; Zhang et al., 2011). In plant communities, when sunlight is filtered by a foliar canopy, red and blue light are selectively reduced, resulting in an enriched environment of far-red light (Zhang et al., 2011). Careful examination of the spectrum transmitted through leaves shows that along with the strong decrease in R:FR ratio, there is an overall decrease in the fluence rate and an enrichment of green wavebands relative to blue and red (Folta and Maruhnich, 2007; Franklin, 2008).

Under shade screens, the ambient light is filtered by the surface of the screen matrix resulting in the formerly mentioned "*mixture of natural + modified light*"

(2.1.1.1 above, on page 5) that is provided to the screened crops. The influence of the shade and the modified radiative environment on plant height was extensively presented by several researchers (Franklin, 2008; Rajapakse and Shahak, 2007; Rajapakse et al., 1999). Rylski and Spigelman, (1986a) reported that shaded sweet pepper plants were taller than unshaded. The elongation of Pittosporum branches grown under different colored nets was reported to be related to the modified radiative environment that the colored nets created over the crop (Oren-Shamir et al., 2001). Abdullah et al. (2008) documented that decreasing light intensity produced taller plants (*Curcuma alismatifolia*) with longer flower stalk whereas increasing the light intensity produces more compact plants with shorter flower stalks. Kittas et al. (2012) reported that unshaded plants were 25% shorter as compared to plants under shade nets. The authors ascribed the differences to the decreased values of R:FR under the screens.

2.2.5. Yield and quality of yield

Kittas et al. (2012) reported a 43% increase of the total and the doubling of the marketable yield of tomato crop under shade nets as compared to the respective of the open field, while Rylski and Spigelman, (1986) presented 12% and 60% increase of the total and marketable yield, respectively, of a sweet pepper crop under shade, as opposed to the yield of the open field crop. Increasing the intensity of shading to > 40% decreased flowering and fruit yield of tomato crop (Abdel-Mawgoud et al., 1996). Leonardi et al. (2000) reported increase in yield of shaded greenhouse tomato crop as opposed to the yield of the unshaded crop.

The marketable yield of a shaded greenhouse tomato crop was significantly higher than the respective obtained in an unshaded greenhouse (Lorenzo et al., 2003). The shade increased the marketable tomato production by about 35% compared to non-shading conditions in experiments under white, black and photoselective shade nets (Ilić et al., 2012).

According to Barber and Sharpe, (1971) symptoms of sunscald are mostly formed in areas where the number of hours of sunlight is high in the ripening period. The application of 26 – 47% shading to a pepper crop decreased the incidence of sun-scald on fruit from 36% of total production under no shading, to 3 - 4% of total production under shading (Rylski and Spigelman, 1986b). When midday air temperature was 30-32°C, apple fruit surfaces under a white shade net were on

average 5.6 °C cooler than an open field grown fruit and significantly reduced sunburn incidents (Gindaba and Wand, 2008). A mobile shade net reduced the BER (Blossom End Rot) incidence on greenhouse tomato fruits (Lorenzo et al., 2004, 2003). Peppers grown inside a greenhouse with supplemental shade, reduced the incidence of sunburned fruits (López-Marín et al., 2011). Kittas et al. (2012) documented the elimination of sunburn and a reduction trend (but not statistically significant) of BER incidence on tomato fruits for crops grown under four different shade nets. Ilić et al. (2012) reported the elimination of fruit sunburns under shade and reduction of BER by about 50%.

The influence of shade on fruits chemical characteristics have been studied by several researchers. Compared to open-air tomatoes, those grown under the screenhouse tended to have; higher contents of malic and oxalic acids, similar contents of citric and glutamic acids, slightly lower levels of sugars (glucose and fructose) and slightly lower ratios of total sugars (sucrose equivalents) with citric and glutamic acid contents. It is possible to identify accessions in which the use of screenhouses has a minor impact on fruit organoleptic quality and can be recommended to reduce the incidence of virus vectors (Cebolla-Cornejo et al., 2008). Sugar content could be a consequence of the lower light intensity produced by the screenhouse cover, as several studies report that plant shading reduced total sugar content (Davies and Hobson, 1981; Dorais et al., 2001). Soluble solids concentrations and titratable acid concentrations were not affected by the shade net (white shade net) (Gindaba and Wand, 2008). Pepper grown in an arid region under red and yellow shade nets, had a significant higher yield compared with black nets of the same shading factors, without reducing fruit size, while the export-quality fruit yield was also significantly increased under colored nets (Fallika et al., 2009). Total soluble solids (TSS) were on average 5.9 and 6.6 for ‘Romans’ and ‘Vergasa’ (Fallika et al., 2009).

2.2.6. Pest control by screens and nets

The use of screens to exclude insects from the crops is an old technique. The insects could be excluded by adjusting the size of screen holes to the size of the targeted pest (mechanical exclusion) or by hamper the “vision” (optical exclusion). The characteristics of the screens for mechanical exclusion were clearly presented in the review of Teitel, (2007); the average sizes of some of the most common pests that

attack greenhouse crops (Bethke and Paine, 1991; Bethke, 1994) the maximum sizes of the openings in a screen to exclude the insects (Bailey, 2003; Ross and Gill, 1994) are presented in Table 1.

Table 1. The average sizes of some of the most common pests that attack greenhouse crops and the maximum sizes of the openings in a screen that can exclude these insects (Bethke and Paine, 1991; Bethke, 1994) (Bailey, 2003; Ross and Gill, 1994). The same table was presented by Teitel, (2007).

Common name	Scientific name	Thorax (micrometer)	Mesh size (micrometer)
Western flower thrips	Frankliniella occidentalis	184.4 (♂) 245.5 (♀)	190
Silverleaf whitefly	Bemisia argentifolii	239	240
Greenhouse whitefly	Trialeurodes vaporariorum	288	290
Melon aphid	Aphis gossypii	355 (♀)	340
Sweet potato whitefly	Bemisia tabaci	215.8 (♂) 261.3 (♀)	462
Serpentine leaf miner	Liriomyza trifolii	562.5 (♂) 653.8 (♀)	610

Ben-Yakir et al. (2012, 2008) presented the optical exclusion of insects from crops. As the authors quoted; sucking insect pests, such as aphids, whiteflies and thrips use reflected sunlight as optical cues for host finding. Aphids and whiteflies have light receptors in the ultraviolet (UV) region with peak sensitivity at 330-340 nm and in the green-yellow region with peak sensitivity at 520-540 nm (Coombe, 1981; Döring and Chittka, 2007; Mellor et al., 1997). Thrips have light receptors in the UV region (350-360 nm), the blue region (440-450 nm) and the yellow region (540-570 nm) (Vernon and Gillespie, 1990). The response of insects to light is strongly affected by the intensity of the radiation, the shape and contrast of the radiation source and the physiological state of the insect. Ben-Yakir et al. (2012) proposed to use optical cues to divert pests away from crop plants, by repelling, attracting and camouflaging optical cues. They suggested the incorporation of optical additives into the materials of the screens/nets and supported this idea by their reported results that revealed reduced infestation levels of sucking pests and incidences of viral diseases that they transmit by 2-10 folds (Ben-Yakir et al., 2012, 2008; Shahak et al., 2009b).

Berlinger and Lebiush-Mordechai, (1995) reported the successful combination of the mechanical effect of anti-insect screens with the behavioral effect of colors.

However, although whiteflies reacted to colors, it seems that the main excluding mechanism of screens is mechanical and not behavioral, contrary to the results obtained with western flower thrips (Berlinger et al., 1993).

As insect proof screens acts as a barrier to momentum and transport processes they promote the increase of air temperature and humidity inside the enclosures. The technology can improve the mechanical exclusion without compromising the effectiveness of the transport processes of the enclosures as clearly presented by Boulard et al. (2011).

3. No data on confinement for screenhouse crop production

Despite of the elevated interest in growing horticultural crops inside screenhouses, the reported studies related to the influence of the covering screens on the performance and productivity of the covered crops do not sufficiently cover this subject matter. Furthermore, the majority of these studies have been conducted in geographical regions with different climate than this of Greece, and especially of central continental Greece. Additionally, the majority of the screens that are produced or imported in Greece are green and black, mostly due to their durability and long-lasting usage, while their impact on the underneath microclimate and crop performance have never been evaluated. Moreover, the shade intensity of the majority of the available shade nets are over 30%, which may be effective in some regions in lower latitudes but probably not suitable for Greek regions and therefore they do not contribute to the overall increase of the quantity and quality of the screened horticultural production. Thus, the necessity of the determination of suitable screens/nets for different horticultural crops in Greek regions arises in order to maximize the productivity of the crops and the quality of their yield.

4. Aim of the study

The overall objective of the current work was to investigate the modification of the ambient microclimate inside screenhouses as it is imposed by their covering screens/nets with different shade intensities, porosities and color and its influence on the covered sweet pepper crops.

More detailed, the objectives of the present research are:

i. The characterization of the screenhouse/crop microclimate.

ii. The investigation of the ventilation performance of the enclosures

iii. The development of a model for screenhouse air exchange simulation as a function of screen physical properties and outside climate variables.

iv. The investigation of the performance and productivity of crops inside screenhouses.

v. The investigation of the influence of screen properties on the Water Use Efficiency and on the Radiation Use Efficiency of the covered crops.

5. Materials and methods

5.1. Experimental facilities

The experiments were performed in three experimental flat roof screenhouses, located at the experimental farm of the University of Thessaly near Volos (Velestino: Latitude 39º 23', longitude 22º 45', altitude 79 m; Figure 1), on the continental area of Eastern Greece, from late spring until autumn of 2011 and 2012.

Figure 1. Satellite photo (Google earth) of the experimental site (screenhouses, meteorological station and control room). The photo was taken on 2010 i.e., one year before the present work.

The geometrical characteristics of the screenhouses were as follows: length of 20 m (oriented North-South, 36º declination from North), width of 10 m and height h of 3.2 m (Figure 2). The distance between two adjacent screenhouses was 8 m. Adjacently to the screenhouses complex, an open field treatment was installed as a control (hereafter, Cont) against the protected crops' performance.

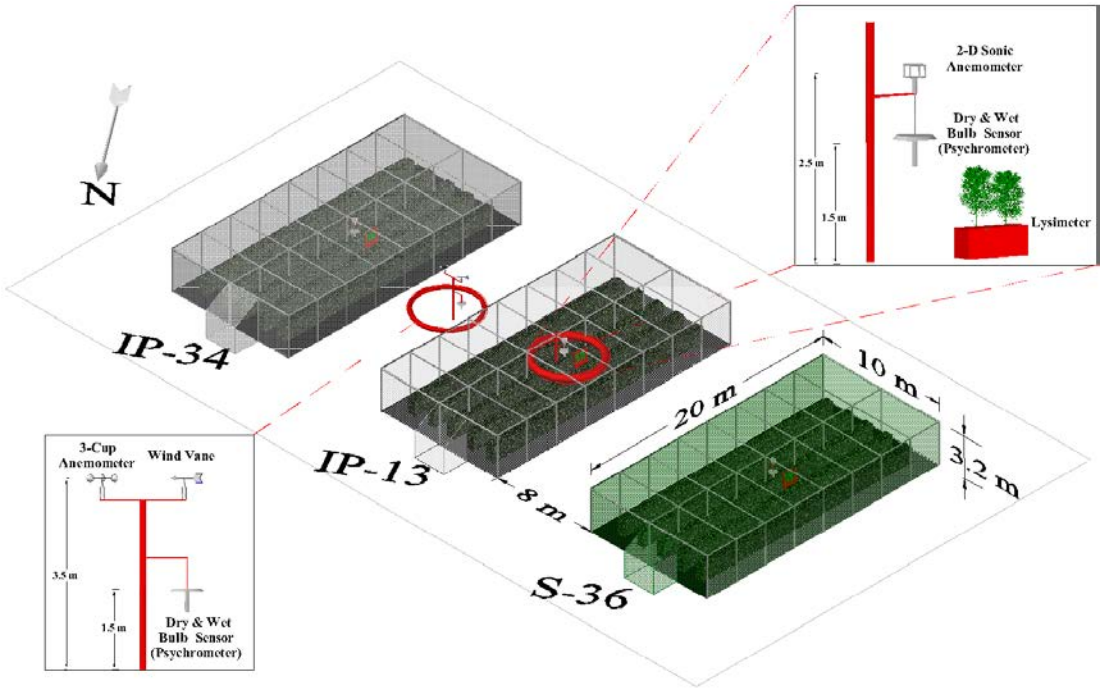

Figure 2. Configuration of experimental facilities: screenhouses constructions and sensors deployment.

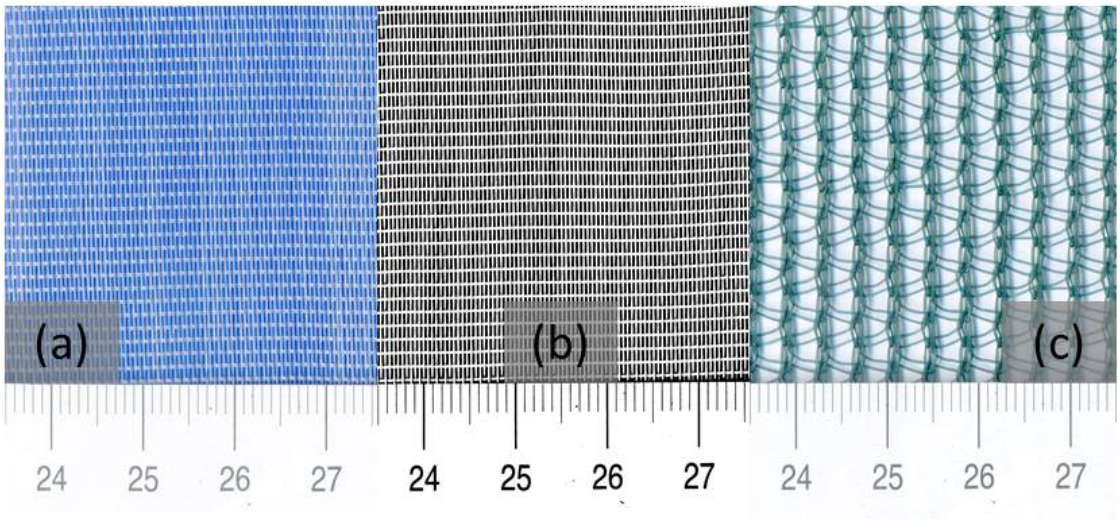

Figure 3. Screenhouse covering materials with rank indication as in the text: (a) IP-13, (b) IP-34 and (c) S-36. The ruler indicates measurement scale in cm. Background colours: (a) blue, (b) black and (c) white.

Three different screens were tested and installed on screenhouse frames (Figure 4). Two were insect-proof (IP) screens (Figure 3, a-b) manufactured by Meteor Ltd., Israel: (1) a clear 50 mesh (10/20) AntiVirus^{TM} screen with a mean light transmittance in lab measurements (350-1100 nm) of 87%, that is, a shading factor of 13% (hereafter, IP-13); and (2) a white 50 mesh (10/20) BioNet^{TM} with a mean light

transmittance of 66% (hereafter IP-34). The third one (Figure 3, c) was a green shade screen (Thrace Plastics Co. S.A. Xanthi, Greece) with a mean light transmittance of 64% (hereafter S-36). The screenhouses were named as their covering screen/net.

Figure 4. Photo of general view of the experimental facilities at the experimental farm of the University of Thessaly in Velestino. Front: IP-34; Middle: IP-13; Back: S-36.

The latter transmission values were determined together with other optical properties (spectrum: 350-1100nm; τ: transmittance; r: reflectance a: absorbance; NSF: Nominal shade factor (NSF=1-τ)) prior to installation of the screens, in the laboratory by means of a spectroradiometer (model LI-1800, LI-COR, Lincoln, NE, USA) equipped with a 10 W glass halogen lamp and an external integrating sphere (model LI-1800-12S, LI-COR, Lincoln, NE, USA), following LI-COR protocol. The optical properties of the screens used in the present research are presented in Table 2 and in Figure 5 (spectral distribution of the properties).

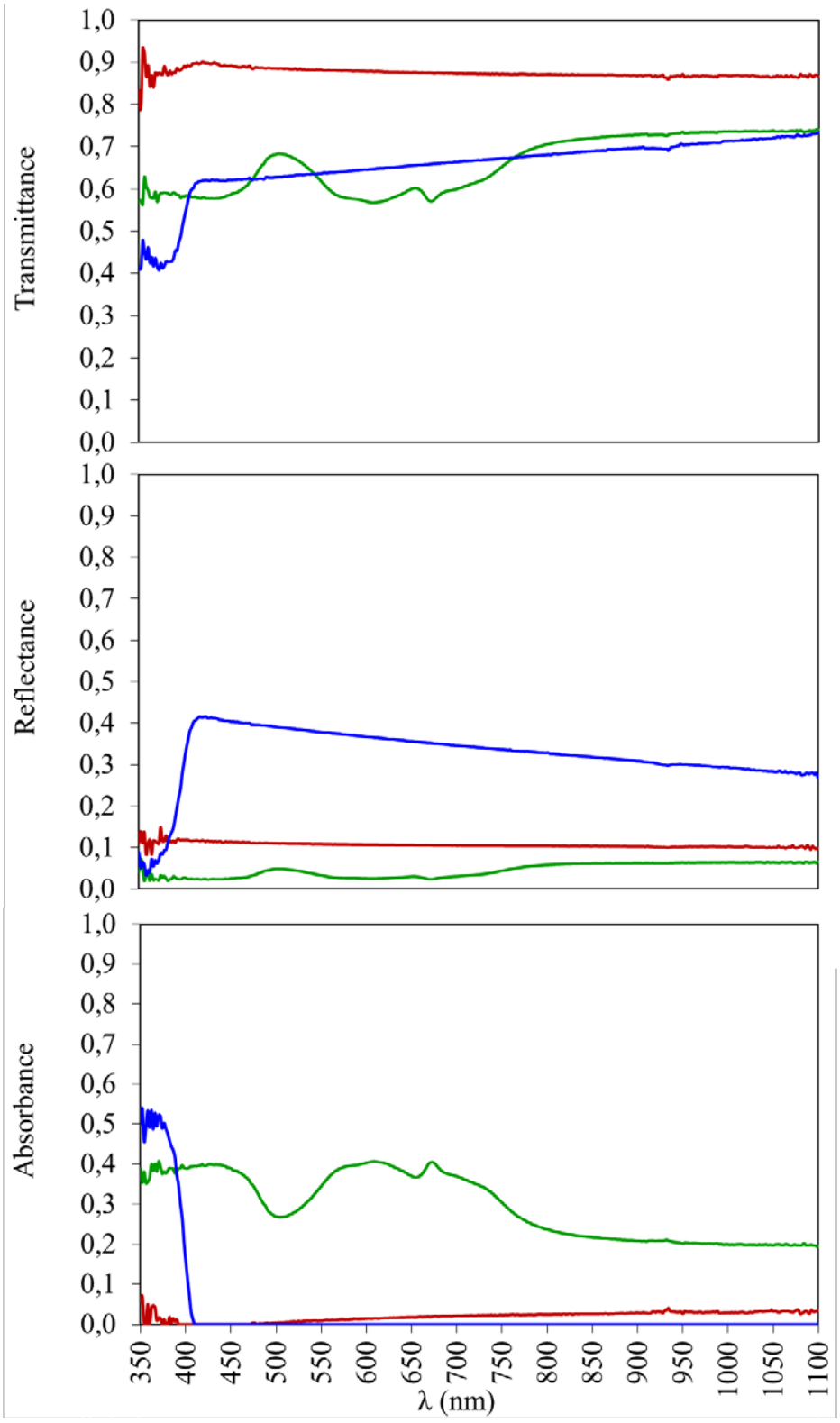

Figure 5. Optical properties (transmittance; reflectance; absorbance) of the screens IP-13 (red line), IP-34 (blue line) and of the shade net S-36 (green line), as measured in the laboratory.

Table 2. Optical properties (transmittance: τ; reflectance: r; absorbance: a) and Nominal Shade Factor (NSF) of the insect proof screens (IP-13; IP-34) and the shade net (S-36) within the spectrum of 350-110nm, as measured in the lab.

Screen	τ	r	a	NSF
IP-13	0,87	0,11	0,02	0,13
IP-34	0,66	0,34	0,00	0,34
S-36	0,64	0,04	0,32	0,36

The insect proof (Figure 3, a-b) had a regular mesh netting with a hole size of 0.75 x 0.25 mm and thread diameter of 0.24 mm, while the green shading net, due to its different knitting (Figure 3, c), presented meshes that were irregular in size and arrangement and mean thread diameter of 0.25 mm. Screens porosity (ε) was measured by image processing using an image analysis software (ImageJ). The calculated values of porosity for the screens IP-13 and IP-34 were of 0.46, as also reported by Möller et al. (2010), while the porosity of S-36 was of 0.63.

5.2. Cropping techniques

5.2.1. Experimental crops

Sweet pepper plants (*Capsicum annuum* L., cv. Dolmy) were transplanted on May 31 and on May 8 on 2011 and 2012, respectively, inside the three screenhouses and at the open field. Final harvest took place at the end of October on both years. Plants were laid out 0.5 m apart in the row, in five double rows with a distance between the double rows of 1.2 m and a distance between the two rows of a double row of 0.5 m. The planting pattern resulted in a plant population of 360 plants per treatment i.e., per 200 m^2. Thus, the planting density was considered 1.8 plants per m^2. To compare with open field conditions, plants were also transplanted and cultivated outside under open field conditions.

5.2.2. Cropping management

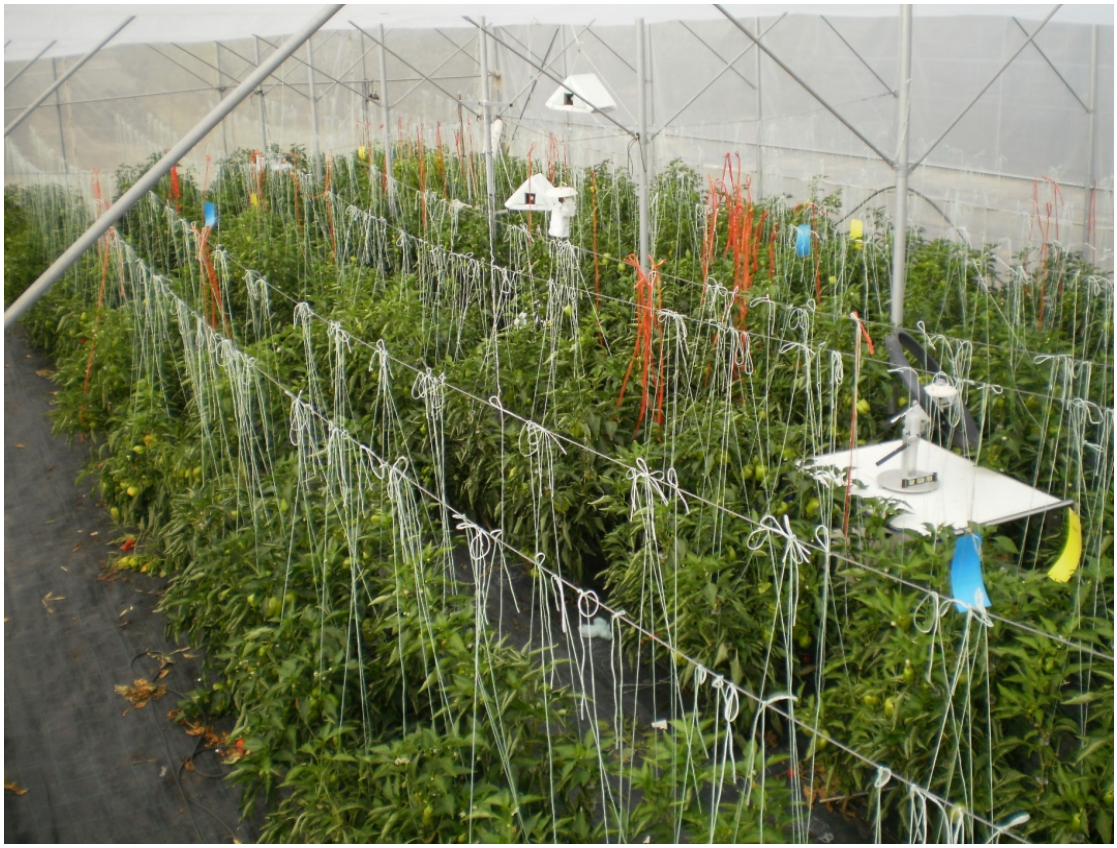

Figure 6. Photo of the interior of IP-13 screenhouse at the end of the experimental period of 2012.

Cropping techniques (fertigation, pruning, chemical treatments) were identical in all treatments. The plants were supported vertically by cords hanging from cables

attached longitudinally to the frame of the screenhouses, or on special supporting structures built for the outside crop (Figure 6). The plants were pruned in order to form 3-4 main branches. Bellow the main branches all leaves and suckers were pruned, while above the main branches intersection, plants remained unpruned.

Irrigation water was supplied through drip-laterals with one drip-line per row and one dripper per plant. The dripper flow rate was 2 l h^{-1}. In all treatments, irrigation scheduling was based on the concept of crop coefficient (Kc) as described in Katsoulas et al. (2006). The amount of water supplied, with respect to the soil mechanical and physical properties, identical for all crops, was calculated as the product of Kc and a fixed integral of outside solar radiation (21.5 MJ m^{-2}). The value of K_c was fixed (after Allen et al. (1998))at a level that ensured that the crops were fully watered during the months with the highest water demand.

The soil in the screenhouses and open field was silty clay. Analysis of physical and chemical soil properties were made at the beginning of each experimental period. Soil samples from each treatment were analyzed and no significant differences were revealed between all treatments. Furthermore, one soil sample consisted of the mixture of the samples from all treatments i.e., screenhouses and open field, was also analyzed and presented (Table 3). The latter sample (mixture of samples) didn't significantly differed from those of each treatment.

Table 3. Physicochemical soil analysis of the experimental field. Analysis of one soil sample, consisted by the mixture of the samples from all treatments (screenhouses and open field).

Parameter	Units	Values	Parameter	Units	Values
Sand	%	18.3	Mg	mg/kg d.v.	340
Silt	%	41.1	NO_3-N	mg/kg d.v.	143.6
Clay	%	40.7	P	mg/kg d.v.	14.4
ph	-	7.8	K	mg/kg d.v.	170
$CaCO_3$	%	6.7	Cu	mg/kg d.v.	2.4
Organic matter	%	1.9	Zn	mg/kg d.v.	1.01
Elec. Conductivity	mS/cm	1.76	Mn	mg/kg d.v.	15.8
			Fe	mg/kg d.v.	7.4
			B	mg/kg d.v.	0.48

The screenhouse soil surface was totally covered by black polypropylene (water permeable) mulch, primarily deployed against weeds and secondly in minimizing soil water evaporation.

During the two campaigns, the insect population was monitored and controlled to similar levels by color traps and spray application of pesticides, according to the common practice followed by the local growers.

Pollination was supported by a bumblebee heave (Koppert B.V., The Netherlands) that was alternatively installed between screenhouses after 2 continuing days of pollination.

5.3. Measurements

5.3.1. Screenhouse spectral properties

5.3.1.1. Measurements' protocol

Measurements of the spectral properties of the screenhouses were conducted during the experimental periods of 2011 and 2012, by means of the LI-1800 portable spectroradiometer (LI-COR Inc., Nebraska, USA), in the range 350-1100 nm at 1nm intervals. The spectroradiometer which was equipped with a cosine receptor (2π steradian field of view) was located at 0.8m above the ground. All measurements were made under clear sky conditions, about 60 minutes around solar noon, at an interval of 3 min, alternately in the open field and in the middle of each screenhouse construction (Figure 7). Four measurements were conducted for each screenhouse at each measuring date.

A variation of the above mentioned method was followed in order to conduct spectral analysis measurement for the total (beam+diffuse; b+d) and the diffuse (d) solar radiation inside screenhouses and at the open field, during summer 2012. The measurements were conducted during days with clear sky. Three representative days were chosen at July 25, August 14 and September 4. Measurements took place at 2 hours intervals around solar noon i.e., 9:30, 11:30, 13:30, 15:30 and 17:30, for the investigation of any potential changes in optical indices of the screens during the measurement day, due to the change of the azimuth of the sun-screenhouse system. In order to measure the diffuse component (d) of the total solar radiation, a custom made opaque square (10cm x 10cm) plate that was covered with a non-reflective black cloth was held 40 cm above the cosine receptor of the spectroradiometer in order to mask out the beam radiation. Coupled measurements at the same treatment (screenhouse or open field) were conducted for the determination of total solar radiation and its diffuse fraction i.e., initially for total solar radiation immediately followed by a measurement for its diffuse component, in order to ensure steady sky conditions and sun position. The protocol involved coupled measurements alternately in the open field and in the middle of each screenhouse construction.

Figure 7. Photos during *in situ* measurements of light quality by means of a portable spectroradiometer LI-COR 1800. Left: measurement inside the screenhouse; Right: measurement at the open field.

5.3.1.2. Calculation of spectral screenhouse transmittance

In every case of the above mentioned protocols, an average spectral distribution was calculated from all the individual energy curves for the total (b+d) and for the diffuse component (d) of the solar radiation. Additionally, the spectral distribution of the direct (beam; b) component of the solar radiation was calculated as the difference between the total minus the diffuse component at each nm across the entire spectrum. All spectral data were expressed as solar energy (W m^{-2} nm^{-1}).

Using the solar radiation spectra measured in the open-field (subscript 'o') and inside the screenhouses (subscript 'i'), broadband integrals of solar radiation (W m^{-2}) over the total (T, 350-1100 nm), the photosynthetically active radiation (P, 400-700 nm), the blue (B, 400-500 nm), the green (G, 500-570 nm), the red (R 600-700 nm), the far-red (FR, 600-700 nm) and the near infrared (N, 700-1100 nm) wavelength band and were calculated. The screenhouse vertical transmittances in the respective wavelength bands were then obtained by calculating the following ratios:

$$\text{eq. 1: } \tau T = \frac{T_i}{T_o}; \quad \text{eq. 2: } \tau P = \frac{P_i}{P_o}; \quad \text{eq. 3: } \tau B = \frac{B_i}{B_o}; \quad \text{eq. 4: } \tau G = \frac{G_i}{G_o};$$

$$\text{eq. 5: } \tau R = \frac{R_i}{R_o}; \quad \text{eq. 6: } \tau FR = \frac{FR_i}{FR_o}; \quad \text{eq. 7: } \tau N = \frac{N_i}{N_o}$$

The latter calculations were conducted for the total (b+d; τ_{b+d}) solar radiation and for its direct (b; τ_b) component.

5.3.1.3. Calculations for the diffuse and direct (beam) fractions of the solar radiation

5.3.1.3.1. *Fraction of diffuse-to-total solar radiation*

The fraction of diffuse-to-total (beam+diffuse; b+d) solar radiation (f_{dif}) was calculated using measured data of diffuse (d) and total radiation (b+d) at the open field and inside each screenhouse was determined. The calculations were conducted for each respective wavelength band; T, P, B, G, R, FR and N. In the following example is presented the calculation for through the T wavelength band, while accordingly were conducted for the rest of the bands:

eq. 8: $f - \mathrm{T_{dif,o}} = \frac{\mathrm{T_{dif,o}}}{\mathrm{T_o}}$ and

eq. 9: $f - \mathrm{T_{dif,i}} = \frac{\mathrm{T_{dif,i}}}{\mathrm{T_i}}$,

for outside and inside each screenhouse, respectively.

5.3.1.3.2. *Diffuse ratio of screenhouses*

The diffuse ratio (τ_{dif}; Cabrera et al., 2009) (or enrichment ratio of diffuse radiation after Möller et al. (2010)) of each screenhouse was calculated for each respective wavelength band; T, P, B, G, R, FR and N as:

eq. 10: $\tau_{dif} = \frac{\mathrm{T_{dif,i}}}{\mathrm{T_{dif,o}}}$

5.3.1.4. Light quality parameters

The light quality parameters were calculated after Kittas et al. (1999). The literature on plant photomorphogenesis indicates that two main photoreceptors are involved in the perception of light quality, phytochrome and cryptochrome (Casal, 2000; Franklin et al., 2005).

The most common way of characterizing the phytochrome response is through the ratio of red to far-red light, which is generally quoted as ζ. According to Kittas et al. (1999), ζ was calculated as the narrow wavelength band ratio of red (R, 655-665 nm) to far-red (FR, 725-735 nm) radiation, both R and FR being expressed in W m^{-2}. A surrogate to ζ is the broad wavelength band ratio R:FR, where R and FR are in the

wavelength bands of 600-700 nm and 700-800 nm, respectively (Kittas et al., 1999; Rajapakse et al., 1999).

The cryptochrome response is generally analyzed through the morphogenetically active radiation (MAR), defined as the amount of radiation in the broad wavelength band 400-500 nm. In this study, we used the ratios B:R and B:FR, where B corresponded to the wavelength band 400-500 nm (Kittas et al., 1999; Rajapakse and Shahak, 2007).

The effect of green light, that has been quoted by several researchers (Klein, 1992; Sellaro et al., 2010), was also studied in the present study in order to reveal any impact of the green shade net (S-36) to the crops inside the respective screenhouse. The wavelength band under study for the green light was considered the 500-570 nm (Klein, 1992; Sellaro et al., 2010).

The above mentioned calculations were conducted for the (i) total (beam+diffuse) solar radiation and its (ii) diffuse and (iii) direct components, inside and outside screenhouses.

5.3.2. Microclimate characterization

5.3.2.1. Climate Measurements

Series of climatic data were recorded in the centre of each screenhouse and outside. Air temperature and vapour pressure deficit were monitored by means of temperature and humidity sensors (HOBO H8 ProRH/ Temp.Logger., Onset, USA), placed inside a protective (heat insulated) and aspirated shield against solar radiation, 1.5 m aboveground (Figure 8).

Leaf temperature was measured by means of copper-constantan thermocouples (Cu-Co, type T, wire diameter 0.5 mm, Omega Engineering, Manchester, U.K.). The thermocouple junctions were firmly attached to the back side of leaves and the canopy temperature was calculated as the mean value of measurements on 10 healthy and mature leaves per treatment, distributed randomly along the different layers of the canopy (Figure 8).

Moreover, the wind speed and direction were also measured outside the screenhouses. Irrigation water was monitored by means of flow meters properly installed to the main tubes of irrigation supply network each treatment (Figure 8).

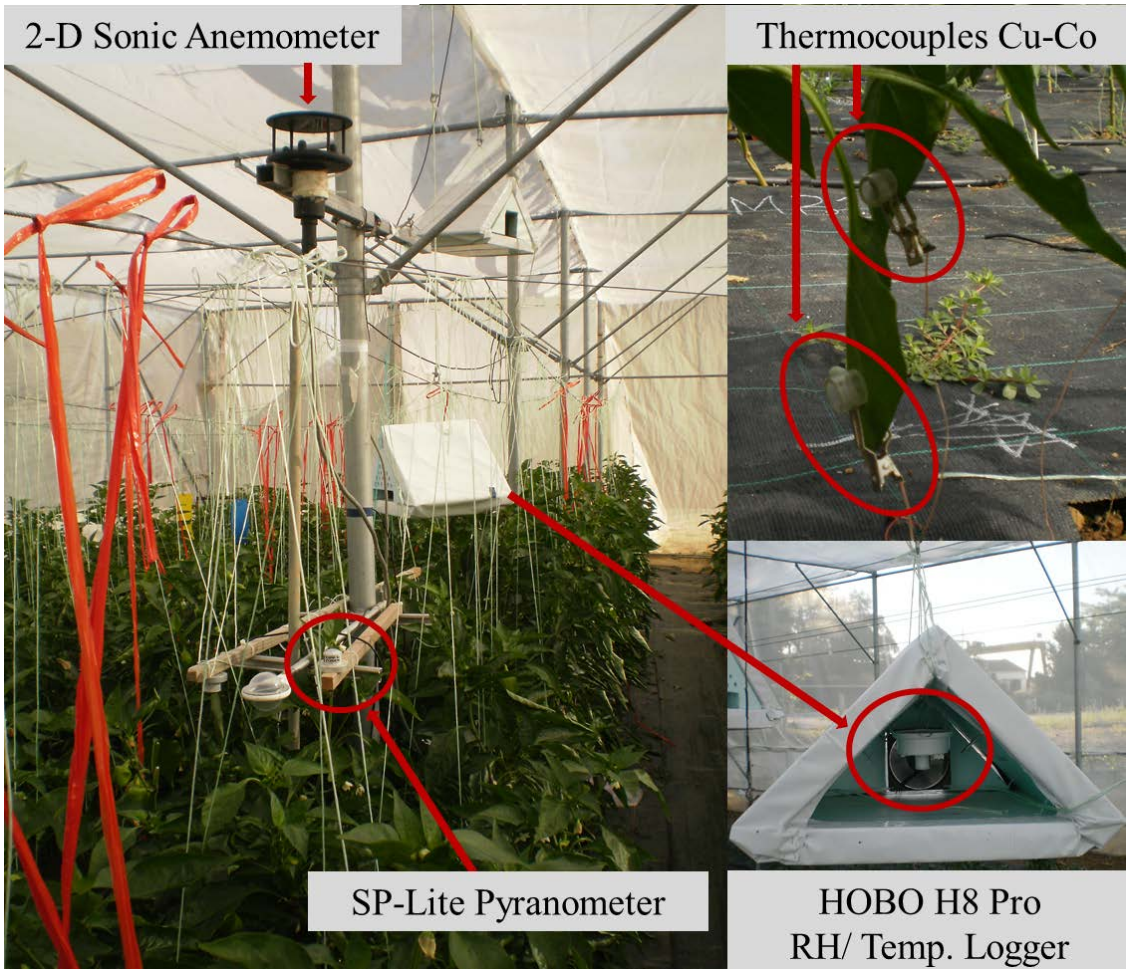

Figure 8. Monitoring system configuration for microclimatic parameter measurements

Global solar radiation ($R_{G,o}$; $R_{G,i}$) was measured, by means of pyranometers (model SP-LITE Silicon Pyranometer, Campbell Scientific, Inc., U.S.A.), placed 1.5 m aboveground, at the mid-length above central crop row of each treatment (Cont; IP-13; IP-34 and S-36). The diffuse component of global solar radiation (R_{dif-i}) was measured by means of a shadow ring (CM 121B, Kipp & Zonen B.V., Delft, The Netherlands) that shielded a pyranometer (CM11 Pyranometer, Kipp & Zonen B.V., Delft, The Netherlands) that was mounted on it from solar radiation. The shadow ring was installed in the corridor between the central and an adjacent double crop row, at a height of 1.5m above ground (Figure 9). Next to the shadow ring, a second CM11 pyranometer was installed to measure total (beam+diffuse) global solar radiation ($R_{G,i}$) simultaneously to the mounted pyranometer. The configuration of the shadow ring plus the pyranometer for the total solar radiation was transferred at 1 day intervals between the three screenhouses in order to determine the ratio of diffuse to total solar radiation in each screenhouse at about the same solar inclination.

Figure 9. Shadow ring for diffuse radiation measurements.

5.3.2.2. Data acquisition

Solar radiation (global and diffuse), leaf temperature, wind speed and direction, crop transpiration rate and irrigation water supply measurements were recorded in a data logger system (model DL3000, Delta-T Devices, Cambridge, U.K.). Measurements took place every 30 s and used to compute 10 min average values, but for the irrigation water that was cumulatively recorded at each event as the sensors of the flow meters were digital.

5.3.2.3. Calculations for the microclimate characterization

5.3.2.3.1. *Radiative environment*

5.3.2.3.1.1. Screenhouse hemispherical transmittance

The screenhouse hemispherical transmittance to global solar radiation (τ; 310-2800 nm) was calculated from the pyranometer data sets installed inside ($R_{G,i}$) and outside ($R_{G,o}$) screenhouses as:

eq. 11: $\tau_G = \frac{R_{G,i}}{R_{G,o}}$

5.3.2.3.1.2. Screenhouse fraction of diffuse-to-global solar radiation

The fraction of diffuse-to-global solar radiation ($f - R_{G;dif,i}$) inside each screenhouse was calculated using measured data of inside diffuse ($R_{G;dif-i}$) and global radiation ($R_{G,i}$) calculated as follows:

eq. 12: $f - R_{G;dif,i} = \frac{R_{G;dif,i}}{R_{G,i}}$

5.3.3. Crop transpiration rate determination

5.3.3.1. Measurements

For the determination of the transpiration of the sweet pepper crop under screenhouse conditions, measurements of the crop transpiration rate inside each screenhouse were performed during August and early September 2011. The crop transpiration rate (Tr_i) was measured every 10 min using weighing lysimeters located in a central row of each screenhouse. The device included an electronic balance (model 60000 G SCS, Presica, Dietikon, Switzerland, scale capacity = 62 kg, resolution = ±1 g) equipped with a tray carrying two plants on separate pots and an independent system of water supply and drainage (Figure 10). The soil surface of the pots was covered with the same black PP mulch as the screenhouse soil. The weight loss measured by the electronic balance was assumed to be equal to crop transpiration. Two lysimeters were available and therefore it was not possible to measure crop transpiration simultaneously in all four treatments. Thus, the lysimeters were moved in the different treatments in sequence almost per week.

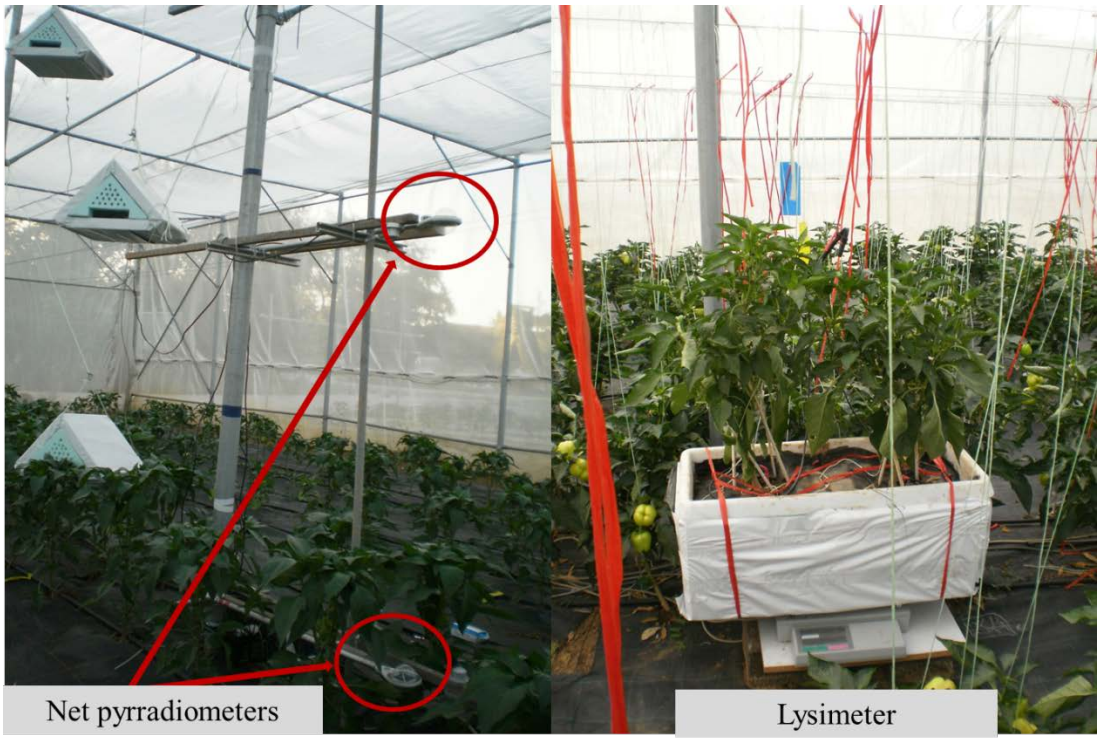

Figure 10. Left: photo of net pyrradiometer set-up above and below the crop canopy for the determination of the intercepted net radiation. Right: photo of lysimeter configuration for crop transpiration rate measurements. Electronic balance equipped with a tray carrying two plants in a container.

Additionally, incoming net radiation above and below crop canopy were measured by means of two net pyrradiometers (CN1-R Net Thermopile Pyrradiometer, Middleton Solar, Victoria, Australia) per treatment (Figure 10).

All measurements took place every 30 s and 10-minute average values were recorded in a data logger (model DL3000, Delta-T Devices, Cambridge, U.K.).

5.3.3.2. Crop Transpiration Model

The P–M equation (Monteith, 1973) has been originally developed to calculate evapotranspiration from homogeneous vegetated surfaces. When applied to greenhouse crops it may be written as:

eq. 13: $Tr_i = \lambda E = A\,R_s + B\,D$

with: $A = \frac{\delta}{\delta+\gamma(1+g_a/g_c)}$ and $B = \frac{\rho C_p g_a}{\delta+\gamma(1+g_a/g_c)}$

where Tr_i is the transpiration rate (W m^{-2}), E_c is the transpiration rate (kgm^{-2} s^{-1}), R_s (W m^{-2}) is the solar radiation measured above the level of the crop, D (kPa) is the air vapour pressure deficit, ρ and C_p are the density (kg m^{-3}) and specific heat (J kg^{-1} K^{-1}) of air, respectively, g_a and g_c are the crop aerodynamic and stomatal conductance (m s^{-1}), respectively, γ is the psychrometric constant (kPa K^{-1}) and δ is the slope of the humidity ratio (or vapour pressure) saturation curve (kPa K^{-1}). A is referred to as the 'radiation term' and B as the 'aerodynamic term' (sometimes called 'advection term'). Hence, A and B may be referred to as the 'radiation coefficient' and the 'aerodynamic coefficient'. eq. 13 may be regarded as empirical formulae, with A and B obtained by regressing measured evapotranspiration against measured R_s and D. From this point of view, A and B are often treated as constants for a given crop, or as simple functions of readily measurable quantities, such as the leaf area index (LAI). These coefficients may be corrected for changes in the environmental conditions and for water stress. Baille et al. (2006) suggested the following formulas for A and B as functions of LAI:

eq. 14: $A = \alpha f_1(LAI) = \alpha[1 - e^{-kLAI}]$

and

eq. 15: $B = \beta f_2(LAI) = \beta LAI$

where k is the extinction coefficient (k = 0.7 (Marcelis et al., 1998)). The reason for the choice of eq. 14 is that represents the classical relationship for radiation interception by a canopy. The choice of eq. 15 is straightforward as LAI can be considered as a multiplicative factor in the 'advective' term of the Penman-Monteith equation.

5.3.3.3. Aerodynamic, total and stomatal conductance calculation

The sensible heat flux H_c (W m^{-2}) exchanged between the canopy and the air was estimated from:

eq. 16: $H_c = R_{n,int} - \lambda E_c$

where $R_{n,int}$ is the intercepted net radiation (=$R_{above} - R_{below}$; W m^{-2}), λ is the latent heat of vaporization of water (Jkg^{-1}(vapour)) and E_c is the transpiration rate (kgm^{-2} (ground covered by crop) s^{-1}). The aerodynamic conductance was calculated from the relationship linking H_c to the canopy-to-air temperature difference ΔT:

eq. 17: $g_a = \frac{H_c}{\rho C_p \Delta T}$

where ρ is the air density (kg m^{-3}) and $C_p$is the specific heat of air (J kg^{-1} K^{-1}).

The total canopy conductance to water vapour transfer g_t (mm s^{-1}) was estimated from:

eq. 18: $g_t = \frac{\lambda E_c \gamma}{\rho C_p D_{c-air}}$

where γ is the psychrometric constant (kPa K^{-1}) and D_{c-air} the canopy-to-air vapour pressure deficit. The bulk conductance g_c (mm s^{-1}) was estimated from:

eq. 19: $g_c = \frac{g_a g_t}{g_a - g_t}$

5.3.4. Ventilation rate determination

5.3.4.1. Physical Measurements

The dimensions of the constructions were: (i) screenhouse covered area A_g of 200 m^2, (ii) screen cover area A_s of 392 m^2 and (iii) screenhouse volume V_{sc} of 640 m^3. The distance between two adjacent screenhouses was 8 m. Plant height was not considerably changed during the period of measurements in the different treatments varying from 0.9 m (mid of August) to 1.1 m (mid of September).

In Figure 2 (on page 29) the microclimatic monitoring systems configurations are presented. The following climatic data were recorded:

(a) wet and dry bulb temperature by means of aspirated psychrometers (Type VP1, Delta-T Devices, Cambridge, U.K.), at the center of each screenhouse (at 1.5 m height aboveground) and outside at 1.5 m height aboveground,

(b) wind speed (u_o) and direction outside the screenhouses by means of a cup anemometer (A100R Switching Anemometer, Campbell Scientific Ltd, U.K.) and a wind vane (W200P Windvane, Vector Instruments Ltd, U.K.) located at a height of 3.5 m above ground,

(c) wind speed (u_{in}) and direction at the centre of each screenhouse, 2.5 m above ground, by means of 2-D sonic anemometers (WindSonic™, Gill Instruments Ltd, U.K.) (Figure 8, on page 40). Two 2-D anemometers were available and therefore the anemometers were moved in the different screenhouses in sequence in appropriate time intervals.

(d) For the determination of the ventilation rate of each screenhouse, measurements of screenhouse and outside microclimate variables were performed during August and early September 2012. The vapour fluxes measured were used for the calculation of screenhouse ventilation rate, water vapour balance technique (Boulard and Draui, 1995; Roy et al., 2002). Finally, the calculated values of the screenhouse ventilation rate were used for the calibration of a model for screenhouse ventilation rate simulation.

Measurements took place every 30 s and 10-minute average values were recorded in a data logger (model DL3000, Delta-T Devices, Cambridge, U.K.).

5.3.4.2. Calculations for ventilation rate determination

5.3.4.2.1. *Air flow characteristics of porous screens*

Wind tunnel tests were conducted in order to determine the aerodynamic properties of the screens. The screen samples were fitted in the wind tunnel and an air flow of a vertical angle attack was forced to the samples' surface. The pressure drop (ΔP) through screens' surface was measured over a range of upstream air velocities (u). The discharge coefficient (C_{ds}) of the screens was estimated by fitting the data of ΔP and u to Bernoulli's equation (Teitel, 2001), using Marquardt's algorithm (Marquardt, 1963):

eq. 20: $\Delta P = 0.5 \frac{\rho v^2}{C_{ds}^2} = 0.5 \frac{\rho \mathrm{u}^2}{\varepsilon^2 C_{ds}^2} = 0.5 \frac{\rho \mathrm{u}^2}{C_{ds*}^2}$

where, ρ is density of air (kg m^{-3}), ε is porosity (dimensionless), C_{ds*} discharge coefficient of a screen multiplied by its porosity (dimensionless).

The permeability (K) and the inertial factor (Y) of the screens were determined by fitting the data of ΔP and u into the Forchheimer's equation (Forchheimer, 1901; Miguel, 1998; Miguel et al., 1997b; Teitel, 2001; Valera et al., 2006, 2005):

eq. 21: $(\mu/K)u + \rho\left(Y/K^{1/2}\right)|u|u = \partial P/\partial x$

where μ is the dynamic viscosity (Kg m^{-1} s^{-1}), K is the permeability of the porous material (i.e., the screen/net) (m^2), ρ is the density of air (kg m^3), Y is the inertial factor, P pressure (Pa) and x the direction of flow (m).

5.3.4.2.2. *Ventilation rate estimates applying the water vapour balance technique*

The screenhouse ventilation rate was determined using the water vapour balance technique, using the water vapour as tracer gas (Boulard and Draui, 1995; Roy et al., 2002). Assuming homogeneity of the water vapour within the air, the following relation holds:

eq. 22: $\rho\, V_{sc} \frac{dx_i}{dt} = -\rho\, Q(t)[x_i(t) - x_O(t)] + Tr_i(t)$

where: ρ is the air density (kg m^{-3}), V_{sc} is the screenhouse volume (m^3), Q is the ventilation rate (m^3 s^{-1}), $x_i(t)\ and\ x_O(t)$ are the inside and outside concentrations (air absolute humidity) of water vapour (tracer gas) (kg m^{-3}), and $Tr_i\ (t)$ is the rate of supply of water vapour within the screenhouse by means of the crop transpiration process (kg m^{-2} s^{-1}).

The air flow rate (G_{sc}; m^3 s^{-1}) of the screenhouse can be calculated as follows (Josef Tanny et al., 2003):

eq. 23: $G_{sc} = A_g \ \frac{Tr_i(t) - h\frac{d\bar{x}_i}{dt}}{(\bar{x}_i - x_o)}$

where: h is the screenhouse height (m). Then, the screenhouse air exchange rate (N, in h^{-1}) is calculated as follows:

eq. 24: $N = 3600\frac{G_{sc}}{V_{sc}}$

where V_{sc} (m^3) is the screenhouse volume.

5.3.4.2.3. *Screenhouse ventilation modelling*

Based on the application of Bernoulli's equation, G_{sc} can be also derived by taking into account the two main driving forces of natural ventilation: the wind and stack effects (Boulard and Baille, 1995; Baptista et al., 1999). However, since the air velocity in the screenhouses is relatively high and inside to outside air temperature differences are low, the stack effect could be ignored (de Jong and Bot, 1992; Kittas et al., 1996). Thus, following the modelling procedure used in greenhouse, the ventilation rate could be expressed by the following equation (Kittas et al., 1996):

eq. 25: $G_{sc} = \frac{A_T}{2}\ C_d\sqrt{C_w}\ u + \ G_{sc,o}$

where A_T is the ventilation area, C_d the discharge coefficient of the screenhouse, C_w is the wind related coefficient and $G_{sc,o}$ the ventilation rate observed at zero wind velocities. Fitting the ventilation rate calculated by eq. 23 and the wind

velocity measured to eq. 25, the dual coefficient $C_d\sqrt{C_w}$ for each screenhouse was estimated.

In greenhouses with screened vent openings, the total pressure drop coefficient indicates the pressure drop across both the inlet opening and the screen (Kittas et al., 2002; Teitel, 2007). In screenhouses, the total cover area can be considered as a screened vent opening. Therefore, it could be assumed that the total pressure drop coefficient is equal to the pressure drop coefficient across the screen, alone. Thus, the total discharge coefficient C_d of the screenhouse construction (or "vent") is considered to be equal to the discharge coefficient of the covering screen ($C_d = C_{ds^*}$).

5.3.5. Crop determinations

5.3.5.1. Plant measurements

Each treatment was divided in four equal blocks of 10m length by 5m width (four quadrants of each treatment), in order to minimize any differences due to soil variability or plant position in each experimental plot (Figure 11).

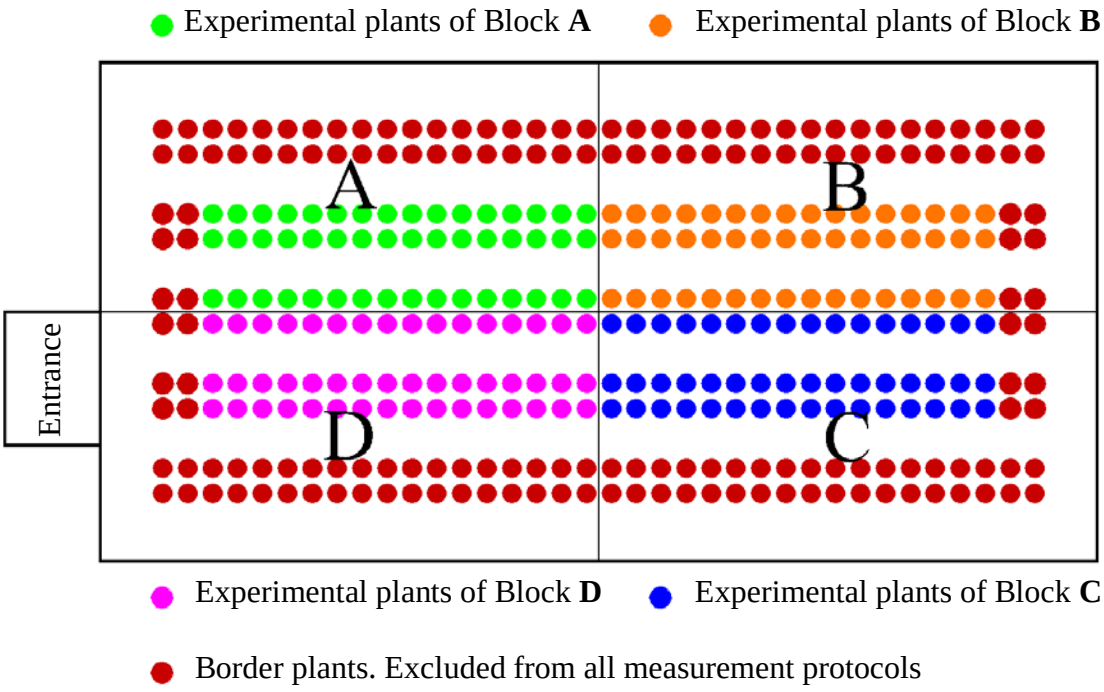

Figure 11. Configuration of the experimental plot inside each of the 4 treatments.

Destructive measurements were conducted during 2011 and 2012 cropping period at 3-week interval throughout the whole crop cycle. The respective schedule of the measurements is presented in Table 4 (on page 55). On each measurement date, 4 plants from each treatment (1 from each block) were cut off just above soil surface. Plants from the outer double rows were excluded from sampling in order to eliminate any errors associated to the alley effect. Prior to the detachment of the plants from the experimental field, their height (vertical projection of canopy's side view) was measured.

After the removal of the aerial part of the plants from the experimental field their different organs (vegetative: stems + leaves; generative: presented unripen fruits) had been separated in respective groups per plant. The number of the attached on the plants (presented) leaves and fruits were counted. The different organs (stems, leaves and fruits) were first weighted to record their fresh mass weight.

Afterwards, the leaf area (L_a) per plant was measured. All leaves of a plant were scanned and the black 'n' white pictures of each plant were processed with an image analysis software (DT-scan; DeltaT-Devices, USA) in order to determine the area of leaves of each picture. The sum of all pictures of each specific plant was the Leaf Area (L_a) of the plant. Multiplying the L_a by the plant density (1.8 plant m^{-2}) the LAI of each plant was also been calculated.

Consequently, the dry weight of the different organs of the plant were measured after been dried for 48 h at 85°C and the dry matter production and partitioning were determined. The dry matter partitioning was calculated by dividing the dry weight of each organ by the total dry matter of the respective plant, while the dry matter content of each respective organ was calculated as the ratio of its dry to fresh weight.

During the reproductive period of the plants ripened fruits were collected every week. As ripe fruits were considered those who had the characteristic marketable colour of Dolmi cultivar (medium to light green). Fruit harvesting was conducted by experience and at each collection date the ripe fruits were harvested. The fresh and dry weights of the ripened harvested fruits that were collected during the harvesting period up to the date of the destructive measurement were measured on each harvesting date and summed up on the destructive date as the total fresh and dry weight of harvested fruits. The total fresh and dry weight of harvested fruits added to the corresponding weights of the attached on the plants (present) fruits to determine the total fresh and dry weight of the fruits. The total dry matter production (hereafter, DMP) was the total aerial dry matter production and it was calculated as the sum of the dry weights of stems, leaves and the total dry weight of the fruits (presented + harvested).

5.3.5.2. Crop yield

Fruit harvest from 8 randomly selected plants per treatment (same plants from the beginning to the end of each period) at each collection date was recorded and summed up to determine the cumulative and the final total yield, expressed in fresh fruit mass per unit area (kg m^{-2}). Moreover, the number of the harvested fruits per plant was recorded and the number of fruits per ground area (# m^{-2}) was determined. The same procedure was conducted on both experimental periods (2011 and 2012).

5.3.5.3. Fruit quality

5.3.5.3.1. *Fruit shape, color and chemical characteristics*

The quality of crop yield was determined during cropping period 2011. A sample of 16 fruits per treatment (4 fruits from each block) and harvesting date was randomly collected five times during the harvesting period and used for quality measurements, which included fruit shape, color, total soluble solids, and titratable acidity of the fruit sap.

The shape of fruits was determined by calculating the ratio of the vertical (height; H; mm) to the longitudinal (width; W; mm) axis' length. The value of the longitudinal axis was the mean value of two (perpendicular to each other) measurements of the axis.

With respect to fruit color, the results were expressed by means of the L*, a*, b* (CIELAB) system. L* represents the lightness of the color i.e., gives the difference between light (where L* = 100 indicates diffuse white) and dark (where L* = 0 yields black), a* its position between red and green i.e., gives the difference between green (a* = -50) and red (a* = 50), and b* its position between yellow and blue i.e., gives the difference between yellow (b* = 50) and blue (b* = -50). The chroma (c), which indicates color saturation or intensity, was also calculated on the basis of the following equation:

eq. 26: $c = \sqrt{\left(a^{*2} + b^{*2}\right)}$

where c = chroma, which indicates color saturation or intensity (dimensionless)
a* = gives the fruit color difference between red and green (dimensionless)
b* = gives the fruit color difference between yellow and blue (dimensionless).
Higher values of c indicate a more vivid color, whereas lower values correspond to dull colors.

The free acidity in the fruit sap was measured by titration with 0.1 M NaOH to pH 8.0, while the total soluble solids were determined in the fruit sap using a manual refractometer (model ART 53000C, TR di Turoni & C. snc, Forli, Italy). Color measurements were also performed by means of a colorimeter (Miniscan XE Plus, model MSXP-4500L, Hunter Associates Laboratory, Inc., Reston, Va.) on two opposite sides of the pepper fruit surface at the equatorial region.

5.3.5.3.2. *Marketable yield and fruit defect analysis*

During the entire cropping period 2012, on each harvesting date, measurements relative to the quality (physical characteristics) of the fruits were carried out on the harvested yield. The marketable yield (fresh weight and number of fruits) was determined excluding all fruits with a defect (sunscald, BER, Thrip and Helicoverpa attacks) from total yield. The marketable number of fruits was calculated by subtraction from the total harvested number of fruits the number of fruits with any defect due to sunburn, BER, and pest attacks. The marketable yield (kg m^{-2}) was calculated by multiplying the mean fruit weight for each treatment (at each harvesting date) by the number of marketable fruits. The defect analysis was based and therefore expressed as the number of defected fruits (# m^{-2}) that were excluded from the total number of harvested fruits.

5.3.6. Water use efficiency

For each treatment the water use efficiency (WUE; kg m^{-3}) was determined as the ratio of the total fresh fruit yield (kg m^{-2}) to the total water provided (rain + irrigation; mm) to the crop, while irrigation water use efficiency (IWUE; kg m^{-3}) was determined by dividing the total fresh fruit yield to the applied irrigation water to each crop.

5.3.7. Simulating dry matter production

5.3.7.1. Interception model

In order to calculate the fraction (f_{i-I}) of the incident radiation just above the crop (I_o) that is absorbed ($I_{abs,L}$) by the underlying LAI (L; m^2 m^{-2}), the following model was adopted (Marcelis et al., 1998):

eq. 27: $f_{i-I} = I_{abs,L}/I_o = (1-\rho)\left(1-e^{-k*L}\right)$,

where: ρ is the canopy reflection and k the extinction coefficient and took default values of 0.07 and 0.7, respectively as suggested by Marcelis et al. (1998).

Daily PAR interception (PARi) was calculated from the daily values of f_{i-PAR} and the daily sum of PAR energy (MJ m^{-2}) just above the crops:

eq. 28: $\mathrm{PAR}_i = f_{i-PAR} * ((\mathrm{PAR/TOTAL})_{LICOR1800} * \Sigma R_{s,x}) = f_{i-PAR} * 0.57 * R_{s,x}$

The PAR energy just above the crops was calculated as the product of measurement of the daily sum of global solar radiation that was measured just above the crop of each treatment ($\Sigma R_{s,x}$) and a ratio PAR/TOTAL ($(\mathrm{PAR/TOTAL})_{LICOR1800}$) for each screenhouse and for the open field treatment. The latter ratios were determined by the spectrum analysis measurements that were conducted by means of a portable spectroradiometer (LICOR 1800) and were calculated about 0.57 for all screenhouse cases and for the open field.

5.3.7.2. DMP model

Daily increment of dry matter production for a given day (DDMP_i; g m^{-2}) was obtained as the product of the cumulative intercepted PAR ($\mathrm{c-PAR}_i$) until that day and the crop radiation-use efficiency (RUE) for an entire pepper crop:

eq. 29: $\mathrm{DDMP}_i = \mathrm{c-PAR}_i * \mathrm{RUE},$

RUE was estimated by fitting the data of DMP and $\mathrm{c-PAR}_i$ (measured values from throughout the calibration crop (2011period)) into eq. 29, using Marquardt's algorithm (Marquardt, 1963). DMP refers to the aboveground crop DMP i.e., stems leaves fruits (mature harvested during productive period until the day of the destructive measurement plus the presented on the plant on the day of the destructive measurement). DMP for a given day was the accumulated value up to and including that day.

5.3.8. Schedule of agronomical measurements

Table 4. Schedule of destructive agronomical measurements.

# of measurement	2011			2012		
	DATE	WAT*	DAT**	DATE	WAT*	DAT**
1	29-Jun	4	29	13-Jun	5	37
2	21-Jul	7	51	3-Jul	7	57
3	10-Aug	10	71	24-Jul	10	78
4	1-Sep	13	93	13-Aug	13	98
5	20-Sep	15	112	3-Sep	16	119
6	26-Oct	21	148	25-Sep	19	141
7				30-Oct	24	176

* WAT: Week After Transplanting; ** DAT: Days After Transplanting

Table 5. Schedule of measurements of fruit quality (fruit shape; chemical characteristics) and fruit color.

2011			2012		
Quality			Color		
DATE	WAT*	DAT**	DATE	WAT*	DAT**
18-Aug	11	79	20-Sep	15	112
1-Sep	13	93	22-Sep	16	114
20-Sep	15	112	30-Sep	17	122
30-Sep	17	122	6-Oct	18	128
12-Oct	19	134	12-Oct	19	134

* WAT: Week After Transplanting; ** DAT: Days After Transplanting

5.4. Statistical analysis

The statistical package SPSS (SPSS-14.0 for Windows standard version, 2005, SPSS BI Greece S.A.) was used for statistical analysis of the data.

5.4.1. Statistical analysis of data of crop determinations

Agronomical data (section 2.2.2.) were analysed using General Linear Model Analysis (Univariate Analysis), with the level of significance set at $P < 0.05$, and Duncan's multirange Post Hoc Tests.

5.4.2. Statistics of DMP simulation

Models that were used to predict leaf area and DMP were calibrated and validated by means of non-linear regression analysis using Marquardt's algorithm (Marquardt, 1963).

To evaluate the agreement between simulated and measured values, the following statistical indices were used: (1) the root mean square error (RMSE) and the relative error (RE) (Stöckle et al., 2004), (2) the Willmott index of agreement (d) (Willmott, 1982) and (3) the slope (m) and coefficient of determination (R^2) of the linear regression between simulated and measured values. The slope and the intercept of the linear regression equations were compared with the 1:1 line by determining simultaneous confidence intervals at $P<0.05$ (Montgomery and Peck, 1992). All statistical analyses were conducted with SPSS (SPSS-14.0 for Windows standard version, 2005, SPSS BI Greece S.A.). The performance of these indices was interpreted using the criteria developed by Stöckle et al. (2004):

$d \geq 0.95$ and $RE \leq 0.10$ very good (VG)
$d \geq 0.95$ and $0.15 \geq RE > 0.10$ good (G)
$d \geq 0.95$ and $0.20 \geq RE > 0.15$ acceptable (ACC)
$d \geq 0.95$ and $0.25 \geq RE > 0.20$ marginal (M)

Other combinations of d and RE values indicated poor performance (Stöckle et al., 2004); in addition, all combinations with $m < 0.9$ or $m > 1.1$, or with $R^2 < 0.85$ were considered poor.

6. Results

6.1. Microclimate inside screenhouses and at the open field

6.1.1. Air temperature and vapour pressure deficit

In Table 6 are presented the monthly average of daytime mean values (11-17h) and monthly average of mean daily maximum air temperature (T_{air}; ^{o}C), during 2012 period. In Table 7 are presented the respective values of the above mentioned statistical parameters for the air vapour pressure deficit ($D_{air;}$ kPa), during 2012 period. The presented microclimatic parameters were measured at a height of 1.5 m above ground, by means of sensors HOBO H8 (5.3.2 above on page 39). The interval of time period (11-17 h) was selected in order to reveal any differences between the treatments during the warmer period of the day.

Table 6. Monthly average of daytime mean (11:00-17:00 h, local hour) and monthly average mean maximum daily air temperature, during 2012 period.

	Air Temperature (°C)											
	Cont			IP-13			IP-34			S-36		
Month	Mean	*(±Stdv)*	Max	Mean	*(±Stdv)*	Max	Mean	*(±Stdv)*	Max	Mean	*(±Stdv)*	Max
June	32.6 [a]	*2.0*	32.0	33.1 [a]	*1.9*	32.5	32.6 [a]	*2.2*	32.0	31.9 [a]	*2.0*	31.5
July	34.6 [a]	*2.0*	36.3	35.2 [a]	*1.7*	36.8	34.6 [a]	*2.1*	36.2	33.6 [a]	*1.9*	35.1
August	33.2 [a]	*2.4*	35.1	33.3 [a]	*2.0*	35.2	32.9 [a]	*2.5*	34.9	32.3 [a]	*2.4*	34.2
September	27.7 [a]	*3.3*	29.5	27.8 [a]	*2.6*	29.6	27.4 [a]	*3.3*	29.2	26.9 [a]	*3.2*	28.8
October	24.6 [a]	*0.9*	25.8	24.5 [a]	*0.9*	25.7	24.2 [a]	*0.9*	25.3	24.2 [a]	*0.9*	25.0

[a]: Means with different superscript letters within the same line are statistically significantly different (a=0.05)

Table 7. Monthly mean daytime (11:00-17:00 h, local hour) and monthly mean maximum air vapour pressure deficit (kPa; Max), during 2012 period.

	Dair (kPa)											
	Cont			IP-13			IP-34			S-36		
Month	Mean	*(±Stdv)*	Max	Mean	*(±Stdv)*	Max	Mean	*(±Stdv)*	Max	Mean	*(±Stdv)*	Max
June	3.61 [a]	*0.7*	3.94	3.58 [a]	*0.7*	3.91	3.44 [a]	*0.7*	3.76	3.28 [a]	*0.6*	3.61
July	4.00 [a]	*0.7*	4.66	4.02 [a]	*0.7*	4.66	3.83 [a]	*0.6*	4.47	3.56 [a]	*0.7*	4.21
August	3.47 [a]	*0.8*	4.15	3.45 [a]	*0.8*	4.19	3.38 [a]	*0.8*	4.13	3.34 [a]	*0.9*	4.15
September	2.07 [a]	*0.8*	2.56	1.99 [a]	*0.9*	2.54	1.97 [a]	*0.9*	2.51	1.92 [a]	*0.8*	2.48
October	1.58 [a]	*0.2*	1.88	1.50 [a]	*0.2*	1.81	1.48 [a]	*0.2*	1.77	1.48 [a]	*0.1*	1.72

[a]: Means with different superscript letters within the same line are statistically significantly different (a=0.05)

The observed differences of air temperature (Table 6) and vapour pressure deficit (Table 7) were not statistically significant. As it can be seen, the screenhouse IP-13 was warmer than the open field about 0.21 ^{o}C (by on average from June to October), unlike the IP-34 and S-36 screenhouses that were cooler than the open field, by 0.23 ^{o}C and 0.78 ^{o}C, respectively. About the same values of differences between inside and outside the screenhouses were measured for the monthly average of the mean daily maximum T_{air} i.e., 0.21, -0.21 and -0.80 ^{o}C for IP-13, IP-43 and S-36, respectively. The D_{air} inside screenhouse IP-13 was about equal to the ambient D_{air} ($\delta D_{air,in\text{-}out}$ = -0.02 kPa), while lower as compared to the ambient D_{air} by 0.11 and 0.21 kPa, inside IP-43 and S-36 screenhouses, respectively. Finally, no statistically significant differences were revealed between the four treatments, for the respective parameters, for diurnal (08:00-20:00) or daily (24 h) intervals, respectively (data not shown).

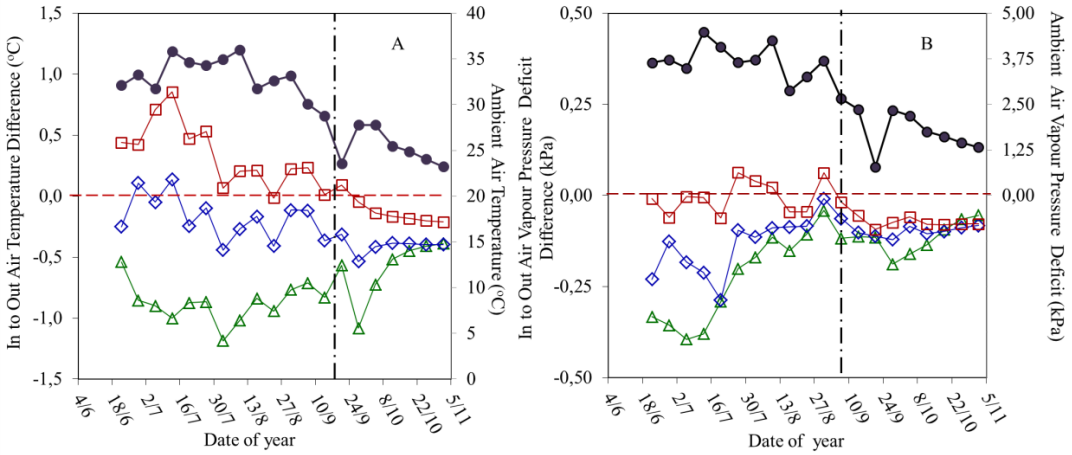

Figure 12. Evolution of inside-to-outside: air temperature differences (figure A; ^{o}C) and air vapour pressure deficit differences (figure B; kPa), for the screenhouses IP-13 (squares), IP-34 (diamonds) and S-36 (triangles), during experimental period 2012. On the left vertical axes of each figure is presented the ambient (circles) condition: (i) air temperature and (ii) vapour pressure deficit, respectively. Data points are weekly averages of mean daytime (11:00 – 17:00 h; local hour) values of air temperature and vapour pressure deficit. Dashed red lines represent the zero axes for the inside to outside air temperature and air vapour pressure deficit differences and for ambient air vapour pressure deficit.

In Figure 12 are presented the evolution of the weekly averages of daytime mean (11:00 – 17:00 h; local hour) values of the inside to outside T_{air} differences (Figure 12 A; ^{o}C) and D_{air} (Figure 12 B; ^{o}C) for the screenhouses IP-13, IP-34 and S-36. On the right vertical axes are presented the ambient air temperature and air vapour

pressure deficit in Figure 12 A and B, respectively, during experimental period 2012. The presented microclimatic parameters were measured at a height of 1.5 m above ground. The highest values of the weekly average of mean daytime (11:00-17:00 h, local hour) ambient air temperature were recorded on July 9 (35.8 ^{o}C) and on August 6 (35.9 ^{o}C), while only after September 10 the value decreased bellow 30 ^{o}C. The screenhouse enclosure seems to be cooler than the ambient in the case of the heavy shaded screenhouses (IP-34; S-36), while only after September 10 screenhouse IP-13 managed to be cooler than the ambient. Screenhouse IP-13 was warmer (0.4-0.9 ^{o}C) than the ambient from the commence of the experimental period until 23 of July (DAT 79), while IP-34 had about the same air temperature as the ambient. The air vapour pressure deficit inside the IP-34 and S-36 screenhouses was lower than the ambient during the entire experimental period, while inside IP-13 was about equal to the open field and only after mid-August became lower than the open field.

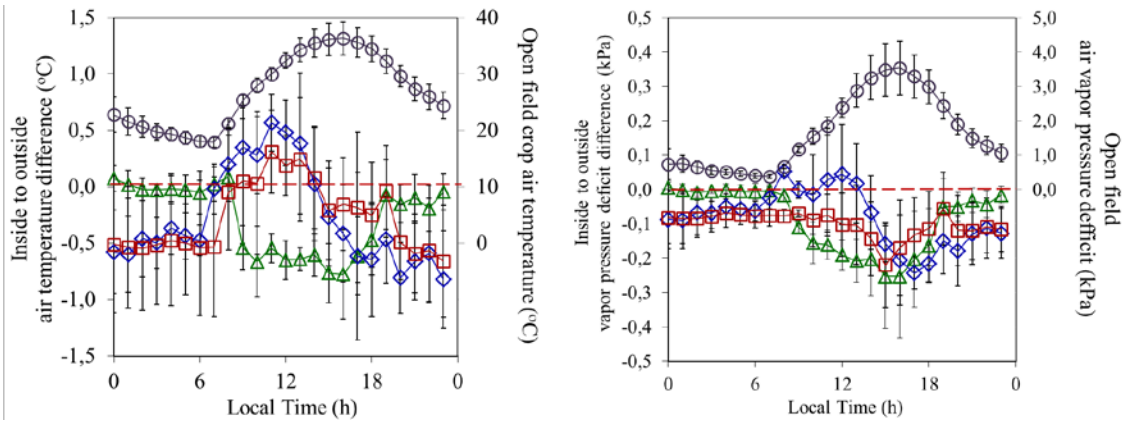

Figure 13. Daily (24 h) evolution of (i) inside to outside air temperature difference (left; δT_{air}; ^{o}C) and (ii) inside to outside vapour pressure deficit difference (right; δD_{air}; kPa) for the screenhouses (IP-13: squares; IP-34: diamonds; S-36: triangles). On the left axis are presented the ambient (Cont, circles) air temperature (left; T_{air}; ^{o}C) and vapour pressure deficit difference (right; D_{air}; kPa). Each data point is the mean of six (6) measurements (20-25 August, 2012). Vertical bars stand for the 95% confidence intervals.

In Figure 13 are presented the daily evolution of: (i) inside-to-outside air temperature difference (δT_{air}; ^{o}C) and (ii) inside-to-outside vapour pressure deficit difference (δD_{air}; kPa) for the screenhouses (IP-13: squares; IP-34: diamonds; S-36: triangles). Moreover, the air temperature (T_{air}; ^{o}C) and the vapour pressure deficit (D_{air}; kPa) at the open field treatment (Cont, circles) are also presented. The measurements had been conducted by means of aspirated psychrometers during the

measurement period for the screenhouse ventilation rate determination (5.3.4.1, on page 46). The hottest part of the latter period (20-25 August, 2012) is presented in order to investigate the microclimate of the enclosures under harsh summer conditions. Each data point is the mean of six (6) measurements.

During the daytime interval between 08:00 and 20:00 the air inside screenhouse S-36 was steadily cooler than the ambient by on average 0.49 ^{o}C. Inside the insect proof screenhouses IP-13 and IP-34, between 08:00 and 14:00 h, the air was warmer by about 0.33 ^{o}C and 0.10 ^{o}C, respectively. Only after 14:00 until 20:00 the air became cooler than the ambient by 0.20 ^{o}C and 0.54 ^{o}C, inside IP-13 and IP-34, respectively. The maximal positive δT_{air} was 0.3, 0.57 and 0.09 ^{o}C for the IP-13, IP-34 and S-36 screenhouses, respectively, recorded at 11:00 h and 08:00 h for the insect proof screenhouses and the shade screenhouse, respectively. During daytime, the greater reduction of air temperature was observed at 16:00 h inside screenhouse S-36 (-0.78 ^{o}C) and at 18:00 h inside IP-13 (0.25 ^{o}C) and IP-34 (0.64 ^{o}C) screenhouses.

Table 8. Average of daytime (11:00-17:00 h, local hour) mean and max air temperature (T_{air}; $^{\circ}$C) and vapour pressure deficit (D_{air}; kPa) over 6-day intervals.

		T_{air} (^{o}C)			D_{air} (kPa)		
Period	Treatment	Mean [1]	±Stdv	Max	Mean [1]	±Stdv	Max
(1st) 20-25 Aug. 2012	Out	34,33 a	1,87	36,38 a	3,82 a	0,55	4,55 a
	IP-13	34,37 a	1,85	36,22 a	3,63 a	0,50	4,30 a
	IP-34	34,35 a	1,27	36,08 a	3,70 a	0,54	4,34 a
	S-36	33,67 a	1,23	35,62 b	3,56 a	0,46	4,25 b
(2nd) 26-31 Aug. 2012	Out	31,85 a	2,66	33,67 a	3,26 a	0,71	3,59 a
	IP-13	31,74 a	2,60	32,68 b	3,04 a	0,66	3,33 ab
	IP-34	31,52 a	2,71	32,52 b	3,06 a	0,68	3,39 ab
	S-36	31,23 a	2,56	32,06 c	3,01 a	0,65	3,30 b
(3rd) 1-6 Sept. 2012	Out	27,46 a	0,51	31,77 a	2,06 a	0,11	3,06 a
	IP-13	27,46 a	0,47	31,68 a	1,90 a	0,09	2,83 ab
	IP-34	27,37 a	0,53	31,37 a	1,89 a	0,10	2,80 b
	S-36	27,03 a	0,51	30,98 b	1,89 a	0,10	2,79 b

[1] Mean values calculated as the average of the mean diurnal (11:00-17:00, local time) temperature and the respective standard deviations.

a, b : Means with different superscript letters within the same column are statistically significantly different (a=0.05)

In Table 8 are presented the average values of daytime (11:00-17:00 h, local hour) mean and max air temperature (T_{air}; $^{\circ}$C) and vapour pressure deficit (D_{air}; kPa) over 6-day intervals. The measurements had been conducted by means of aspirated psychrometers during the measurement period for the screenhouse ventilation rate determination (5.3.4.1, on page 46). About the same results as these presented by Table 7 are also observed in Table 8. In all period intervals, the S-36 screenhouse was slightly cooler than the ambient and the insect proof screenhouses, while the vapour pressure deficit inside the enclosure was lower than the ambient.

6.1.2. Air to crop temperature and vapour pressure deficit differences

In Figure 14 is presented the daily (24 h) evolution of: (i) air temperature (T_{air}; ^{o}C) (ii) canopy temperature (T_c; ^{o}C) and (iii) inside to outside canopy temperature differences (right; $\delta T_{c,in-out}$; ^{o}C) of the crops inside screenhouses (IP-13; IP-34; S-36) and at the open field treatment (Cont), from 20 until 25 August, 2012. As it can be seen the canopies of the protected crops are cooler as compared to the canopy of the open field crop during the daylight period (08:00-20:00 h) by on average 3.34 ^{o}C, 2.35 ^{o}C and 1.92 ^{o}C, for the crop canopy inside screenhouse IP-13, IP-34 and S-36, respectively. The lower heat loads (NIR radiation) incident on the canopy surface of the covered crops, along with their transpiration rates as compared to the respective of the open field crops should be the cause of the recorded lower canopy temperatures inside screenhouses.

Accordingly, the canopy-to-air temperature difference is significantly lower inside the screenhouses, unlike at the open field (Figure 15). The average value of $\delta T_{c\text{-}air}$ was -1.69 ^{o}C, -2.53 ^{o}C, -0.76 ^{o}C and +0.78 ^{o}C, for IP-13, IP-34, S-36 and Cont, respectively. During the period between 15:00 and 19:00 the $\delta T_{c\text{-}air}$ of S-36 was statistically significantly greater than the $\delta T_{c\text{-}air}$ of the insect proof screenhouses. The incident NIR inside IP-13 was greater (Table 10, on page 65) than the respective inside S-36 and seems like a logical expectation the recorded T_c and $T_{c\text{-}air}$ inside the S-36 would be lower than the moderate shaded enclosure of IP-13 screenhouse. But the recorded values were absolutely reversed i.e., T_c and $T_{c\text{-}air}$ for the S-36 were greater as compared to the respective values of IP-13 screenhouse. The grate values of diffused NIR inside the screenhouse (Table 12,on page 69 and Table 13, on page 70), unlike the shade screenhouse could probably ascribe to the greater decrease of the $\delta T_{c\text{-}air}$

inside the former screenhouses as compared to the respective decrease inside the shade screenhouse (S-36).

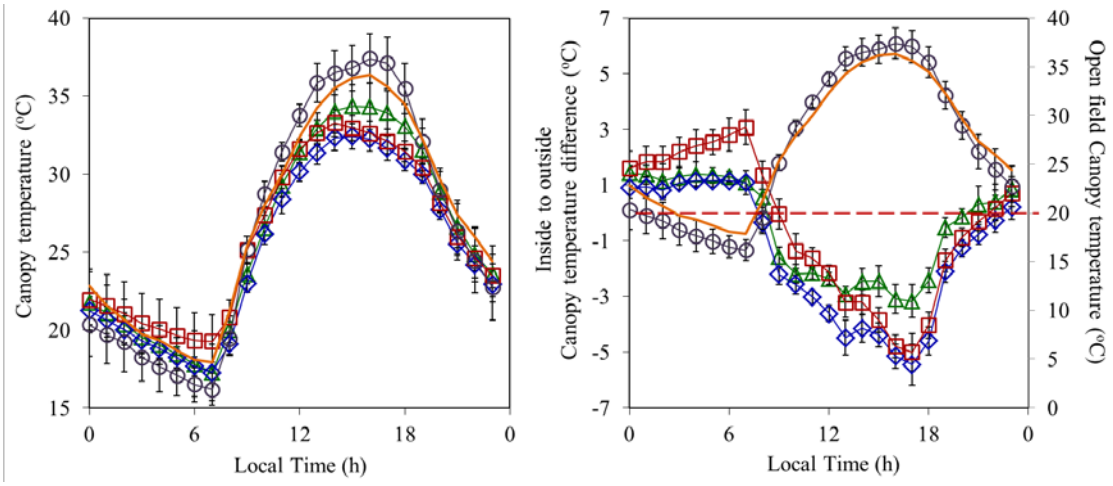

Figure 14. Daily (24 h) evolution of: (i) ambient air temperature (T_{air}; ^{o}C; left & right; orange-solid line), (ii) canopy temperature (left; T_c; ^{o}C) and (iii) inside-to-outside canopy temperature differences (right; $\delta T_{c,in-out}$; ^{o}C) of the crops inside screenhouses (IP-13: squares; IP-34: diamonds; S-36: triangles) and at the open field treatment (Cont, circles). Each data point is the mean of six (6) measurements (20-25 August, 2012). Vertical bars stand for the 95% confidence intervals.

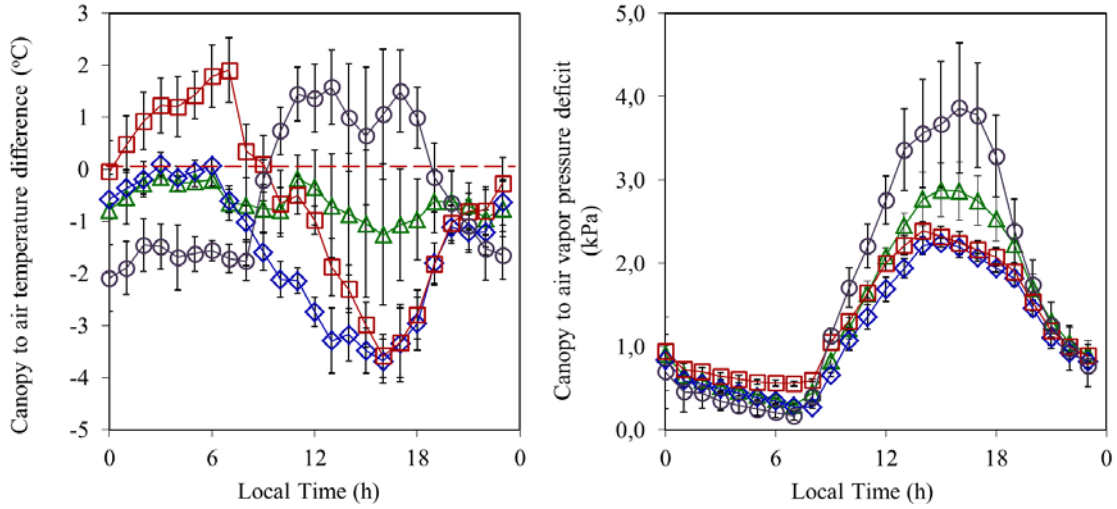

Figure 15. Daily (24 h) evolution of (i) canopy-to-air temperature difference (left; $\delta T_{c\text{-}air}$; ^{o}C) and (ii) canopy to air vapour pressure deficit (right; $D_{c\text{-}air}$; kPa) inside screenhouses (IP-13: squares; IP-34: diamonds; S-36: triangles) and at the open field treatment (Cont, circles). Each data point is the mean of six (6) measurements. Vertical bars stand for the 95% confidence intervals.

About the same rank as for the $\delta T_{c\text{-}air}$ was revealed for the canopy-to-air vapour pressure deficit ($D_{c\text{-}air}$; kPa; Figure 15), from 20 until 25 August, 2012. During daytime period between 10:00 and 18:00 the $D_{c\text{-}air}$ at the open field was on average

3.13 kPa and statistically significantly deferent than the respective values of $D_{c\text{-}air}$ inside the screenhouses (IP-13: 2.04 kPa ; IP-34: 1.60 kPa ; S-36: 2.36 kPa). Significant differences of the $D_{c\text{-}air}$ were observed between the insect proof screenhouses ($D_{c\text{-}air\text{-}IPscr}$) and the shade screenhouse ($D_{c\text{-}air\text{-}S\text{-}36}$) during the time period between 14:00 and 18:00 h; $D_{c\text{-}air\text{-}IPscr}$= 2.19 kPa and $D_{c\text{-}air\text{-}S\text{-}36}$= 2.78 kPa.

6.1.3. Irradiance regime

6.1.3.1. Total solar radiation and its diffuse component

6.1.3.1.1. *Incident solar energy above crops*

In Table 9 is presented the monthly average value of daily integrals of the incident total solar energy (MJ m^{-2} d^{-1}), together with the corresponding daily average values of diffuse fraction of the total solar radiation, during experimental period 2012. The hemispherical transmittance of the screenhouse (ratio of inside:outside daily integral of the incident total solar energy) was 0.75, 0.61 and 0.62 for screenhouse IP-13, IP-34 and S-36, respectively. Insect proof screenhouses enhanced their radiative environment with greater amounts of diffuse radiation compared to the screenhouse covered with the plain shade net. The average values of the diffuse fraction of solar radiation during July, August and September were 0.66, 0.62 and 0.40 for IP-13, IP-34 and S-36 screenhouse, respectively.

Table 9. Monthly averages of daily integral values of incident global solar radiation (R_G; MJ m^{-2} d^{-1}) inside screenhouses IP-13, IP-34 and S-36 and at the open field, during experimental period 2012. In the parenthesis are the daily average values of diffuse fraction of total solar radiation ($f - R_{G;dif,i}$).

	Cont	IP-13		IP-34		S-36	
Month	R_G (MJ m^{-2} d^{-1})	R_G (MJ m^{-2} d^{-1})		R_G (MJ m^{-2} d^{-1})		R_G (MJ m^{-2} d^{-1})	
May	19,48 [a]	14,53 [b]		11,68 [c]		12,28 [bc]	
June	28,26 [a]	21,15 [b]		16,92 [c]		17,84 [c]	
July	25,62 [a]	18,75 [b]	(0,63)	15,41 [c]	(0,58)	15,98 [c]	(0,39)
August	22,08 [a]	16,30 [b]	(0,69)	13,52 [c]	(0,65)	13,64 [c]	(0,41)
September	17,07 [a]	12,87 [b]	(0,66)	10,62 [c]	(0,63)	10,31 [c]	(0,40)
October	11,32 [a]	8,89 [b]		7,24 [c]		6,90 [c]	

In Figure 16 are presented the evolution of the total (beam+diffuse) and diffuse solar radiation energy (W m^{-2}; 310-2800 nm) inside screenhouses (IP-13, IP-34 and S-

36) and the total solar radiation (310-1100 nm) at the open field, during sequential representative summer days of experimental year 2012. Moreover, the diffuse fraction (ratio diffuse to total radiation) of total solar radiation inside screenhouses is also presented during the same period. The shape of the curves that stand for the diurnal evolution of the diffuse fraction of radiation are in agreement with the reported curves by Jones, (2014).

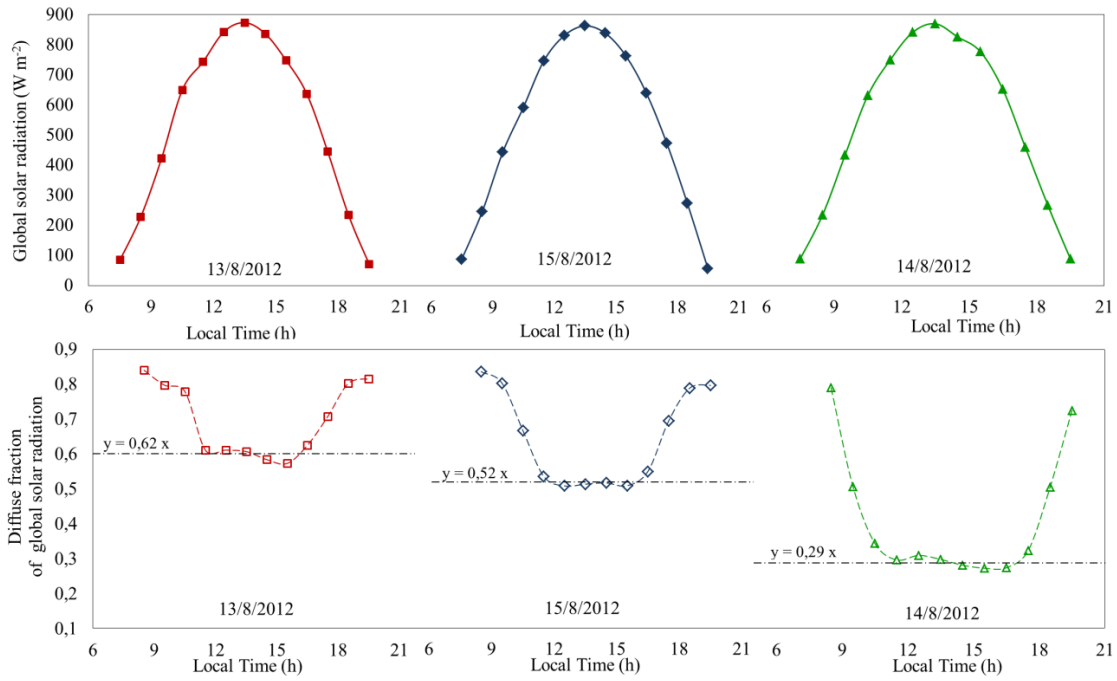

Figure 16. Upper row: Daily evolution of global solar radiation (R_G; W m^{-2}) at the open field (solid lines and solid symbols; 310-2800nm). Lower row: Daily evolution of diffuse fraction of global solar radiation (f-$R_{G,dif}$) (dashed lines and open symbols; 310-2800nm) inside screenhouses (IP-13: squares; IP-34: diamonds and S-36: triangles). The presented values are from measurements during three representative summer clear sky days of August 2012; 13th for IP-13, 14th for S-36, and 15th of August for and IP-34. Dashed-dotted lines represent the best fitted regression line for a local time period for each day between 11:30 and 16:30.

6.1.3.2. Spectrum quality of screenhouse solar radiation

6.1.3.2.1. *Screenhouse transmissions*

In Table 10 are presented the spectral transmissions of the screenhouses (IP-13, IP-34 and S-36) during the two experimental periods (2011-2012). The selected wavelength band ranges were (i) Total (350-1100nm; T), (ii) PAR (400-700nm; P), (iii) NIR (700-1100nm; N), (iv) Blue (400-500nm; B), (v) Green (500-570nm ; G), (vi) Red broad band (600-700nm; R_{br}), (vii) Red narrow band (R_{nar}, 655-665 nm), (viii) Far-Red broad band (700-800 nm; FR_{br}), (ix) far-red narrow band (FR_{nar}, 725-735 nm) and (x) near-infrared (800-1100 nm; N).

Table 10. Values of screenhouse (IP-13; IP-34 and S-36) spectral transmissions for the Total waveband (350-1100 nm; T), the PAR (400-700 nm; P), the NIR (700-1100 nm; N), the Blue (400-500 nm; B) wavebands, during period 2011 and 2012.

Year	Treatment	τT	τP	τB	τG	τR_{nar}	τFR_{nar}	τR_{br}	τFR_{br}	τN
2011	IP-13	0,82 [a]	0,80 [a]	0,78 [a]	0,81 [a]	0,82 [a]	0,83 [a]	0,82 [a]	0,84 [a]	0,84 [a]
	IP-34	0,63 [c]	0,61 [c]	0,58 [c]	0,61 [c]	0,63 [b]	0,65 [b]	0,63 [b]	0,66 [b]	0,67 [c]
	S-36	0,68 [b]	0,64 [b]	0,64 [b]	0,66 [b]	0,64 [b]	0,66 [b]	0,63 [b]	0,68 [b]	0,72 [b]
2012	IP-13	0,76 [a]	0,75 [a]	0,79 [a]	0,73 [a]	0,75 [a]	0,77 [a]	0,79 [a]	0,77 [a]	0,78 [a]
	IP-34	0,60 [b]	0,57 [b]	0,64 [b]	0,54 [c]	0,57 [c]	0,61 [b]	0,62 [b]	0,60 [b]	0,62 [c]
	S-36	0,65 [c]	0,62 [c]	0,69 [b]	0,63 [b]	0,63 [b]	0,62 [b]	0,64 [b]	0,61 [b]	0,65 [b]

[a, b, c] Values followed by a different superscript letter within the same column are statistically significantly different (a=0.05).

6.1.3.2.2. *Light quality parameters of total diffuse and direct solar radiation*

In Figure 17 are presented the spectra of: (i) total (beam+diffuse; b+d) solar radiation (Figure 17; **A**) and the respective transmittance (τ_{b+d}) of the screenhouses (Figure 17; **B**). Moreover, are presented the spectra of the diffuse and direct components of the solar radiation (Figure 17; **C** and **D**, respectively) along with the diffuse ratio (τ_{dif}) and the transmittance (Figure 17; **E**) of the direct component (τ_{b+d}) of solar radiation (Figure 17; **F**) of each screenhouse. The data are from a solar noon measurement on August 14, 2012.

Screen IP-34 and shade net S-36 presented about the same Nominal Shade Factor when determined in the lab (IP-34: 0.34; S-36: 0.36) (Table 2; on page 32). The spectra of the shade net S-36 presented a pick at 475nm, enriching the radiative environment of the enclosure with green light that was radiated from its threads (Figure 17; **A**). Dissimilarly, the anti-insect screens (IP-13 and IP-34) as neutral

colored did not present such picks that indicate spectral modification of the incident solar radiation. Moreover, they enhanced the scattering of the incident solar radiation, enriching the underneath radiative environment with greater amounts of diffused solar radiation energy per nm across the entire spectrum 350-1100 nm (IP-13) or from 497 up to 1100 nm (IP-34) (Figure 17; **C** and **D**), unlike the S-36 shade net. As it can be seen in Figure 17 (**E**), the IP-13 screenhouse presented the greatest τ_{dif} across the spectrum 350-1100 nm, followed by IP-34, while S-36 screenhouse presented the lowest τ_{dif} values. The rate of increase (slopes of regression best fit lines y=ax+b) of the τ_{dif} of the insect proof screenhouses were about the same (IP-13: 38.8 10^{-4}; IP-34: 38.5 10^{-4}) and about 77% greater than the corresponding rate of screenhouse S-36 (21.8 10^{-4}). The diffuse ratio was increasing with the increase of the wavelength, which is not in agreement with the results reported by Pearson et al. (1995) on trials with cladding greenhouses materials. The latter authors quoted that *"scattered radiation decreased with wavelength"*. Moreover, the τ_{dif} of screenhouse IP-13 was steadily higher across the entire spectrum about 0.40 when compared to the τ_{dif} of screenhouse IP-34. The shade net (S-36) decreased the diffuse fraction of the PAR across its entire spectrum by 0.26 (-26%) (shaded area on Figure 17; **E)**, while the IP-34 screen decreased diffused PAR only across 400-496 nm by 0.15 (violet and blue regions of the spectrum), unlike across the remaining PAR spectrum (497-700nm) where its diffused component was increased by 1.37 on average. Unlike τ_{dif}, the transmittance of the direct component of irradiance was steady across the entire spectrum (350-1100 nm) (Figure 17; **F**) been on average 0.47, 0.36 and 0.58 for screenhouses IP-13, IP-34 and S36, respectively.

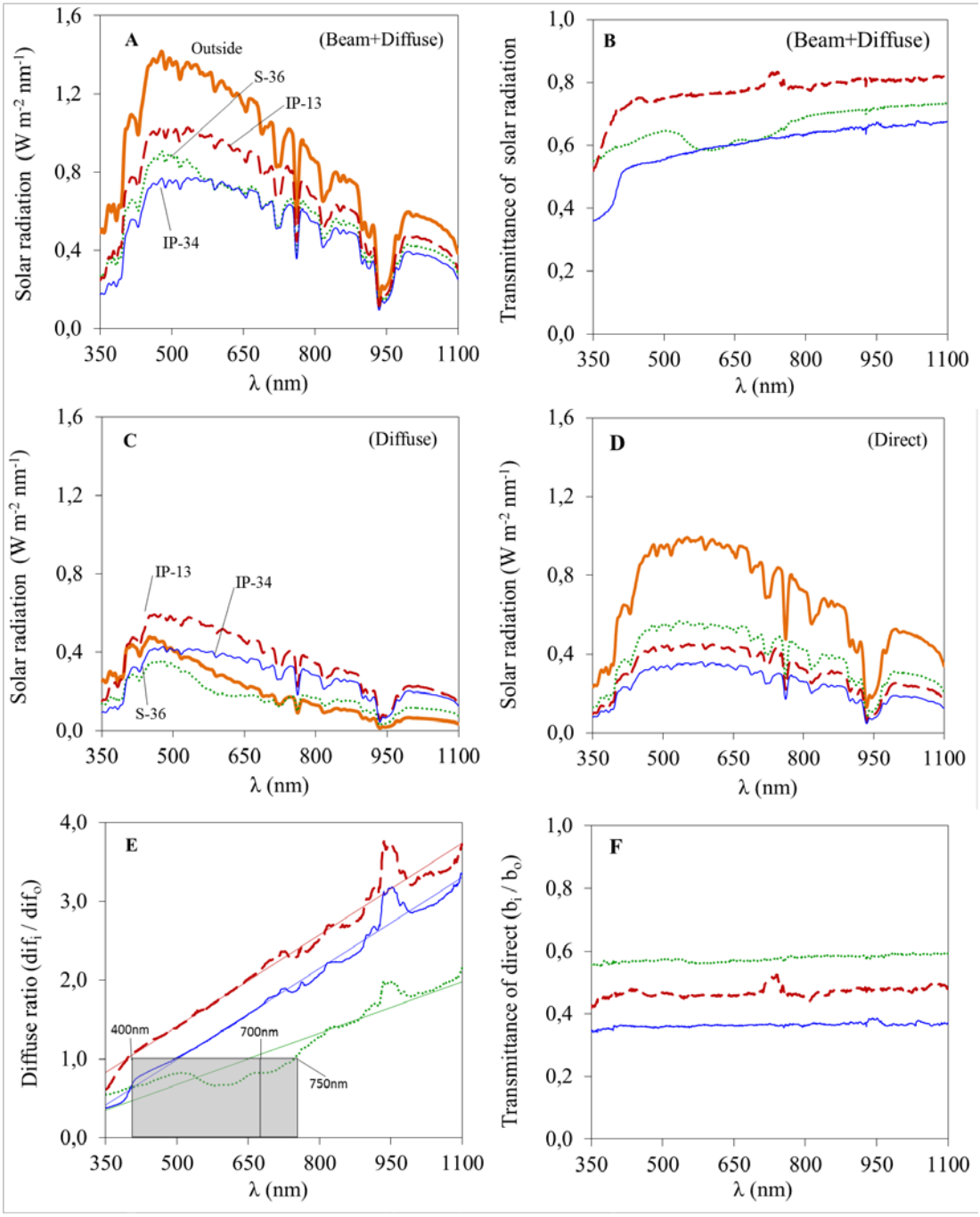

Figure 17. Spectra of: (A) total (beam+diffuse; b+d) solar radiation, (B) diffuse component of solar radiation, (C) screenhouse transmittance and (D) diffuse ratio (diffuse in : diffuse out) inside screenhouses (IP-13: red/dashed line; IP-34: blue/thin line and S-36: green/dotted line) and at the open field (Outside: orange/thick line). Measurements were conducted at around solar noon (± 30min) on representative summer day (August 14, 2012), for waveband intervals of 1nm. In figure (D) the straight lines are the best fit regression lines.

In Table 11 are presented selected quality parameters for the total (beam+diffuse; b+d) solar radiation inside screenhouses (IP-13; IP-34; S-36) and at the open field (Cont), on experimental periods 2011 and 2012. Values presented are average values of measurements around solar noon (± 30 min) during 5 and 3 representative summer days, on 2011 and 2012, respectively.

Table 11. Values of light quality parameters for the total (beam+diffuse; b+d) solar radiation inside screenhouses (IP-13; IP-34; S-36) and at the open field (Cont), on experimental periods 2011 and 2012. The presented values are average values of measurements conducted around solar noon (± 30 min).

Year	Treatment	ζ	R : FR	B : R	B : FR	P : T	P : N	G : R
2011	Cont	1,27 [a]	1,25 [a]	1,06 [b]	1,32 [a]	0,58 [a]	1,39 [a]	0,81 [b]
	IP-13	1,26 [a]	1,23 [a]	1,02 [c]	1,25 [b]	0,58 [b]	1,34 [b]	0,80 [c]
	IP-34	1,22 [b]	1,18 [b]	0,98 [d]	1,16 [c]	0,56 [c]	1,24 [c]	0,78 [d]
	S-36	1,25 [a]	1,16 [c]	1,08 [a]	1,25 [b]	0,56 [c]	1,24 [c]	0,85 [a]
2012	Cont	1,27 [a]	1,27 [a]	1,07 [b]	1,36 [a]	0,59 [a]	1,43 [a]	0,81 [b]
	IP-13	1,24 [a]	1,25 [b]	1,01 [c]	1,26 [c]	0,58 [b]	1,37 [b]	0,79 [c]
	IP-34	1,23 [a]	1,23 [c]	0,95 [d]	1,16 [d]	0,56 [c]	1,27 [c]	0,77 [d]
	S-36	1,24 [a]	1,18 [d]	1,11 [a]	1,31 [b]	0,56 [c]	1,28 [c]	0,84 [a]

[a, b, c] Values followed by a different superscript letter within the same column are statistically significantly different (a=0.05).

In Table 12 are presented the values of the ratio diffuse:(beam+diffuse) of the solar radiation across selected wavelength bands, inside the screenhouses and at the open field. The values are mean daily values of measurements during 3 representative summer days on 2012; July 25, August 14 and September 4. In each day measurements were conducted in 2 hours intervals around solar noon i.e., at 09:30, 11:30, 13:30, 15:30 and at 17:30 local hour. The diffuse component of solar radiation inside screenhouse IP-13 was significantly greater than the respective inside screenhouse IP-34, followed by that of shade screenhouse (S-36). Across the total waveband range (T; 350-1100 nm) the values for the diffuse radiation are slightly decreased (on average 6.5%) inside the insect proof screenhouses (IP-13 and IP-34) and significantly decreased (27%) inside screenhouse S-36, as compared to the values presented in Table 9 (on page 63). The values of Table 9 are from measurements conducted between 08:00 and 20:00. During the initial morning (08:00-09:00; local hour) and the last evening (19:00-20:00; local hour) hours the diffuse fraction of solar radiation at the open field and consequently inside screenhouses is extremely

increased (0.75-0.85 for all screenhouses) (Figure 16; on page 64). Measurements of diffuse solar radiation by means of the spectroradiometer during that part of the day were not available and thus not included in results presented in Table 9. The latter could be the explanation to the differences between the diffuse fraction of global and Total (350-1100nm) radiation presented in Table 9 (on page 63) and Table 12 (below). Furthermore, the different instruments (pyranometer vs spectroradiometer) deployed for each measurement procedure could be an additional factor that contributes to the decrease of the respective fraction in Table 9 (on page 63). Diffused PAR was significantly increased inside the insect proof screenhouses (IP-13: 0.62 and IP-34: 0.56) as compared to the diffused PAR at the open field (0.22), unlike inside the shade screenhouse (S-36) where it was slightly increased (0.28).

Table 12. Fraction of diffuse:(beam+diffuse) solar radiation (f_{dif}), across selected wave length bands. Data presented are mean daily values of measurements during 3 representative summer days; July 25, August 14 and September 4, on 2012 period. Values presented are mean daily values of data as measured in 2 hours intervals around solar noon i.e., at 09:30, 11:30, 13:30, 15:30 and at 17:30 local hour, on each measurement day.

	f_{dif}						
Treatment	T[1]	P[1]	B[1]	G[1]	R[2]	FR[2]	N[2]
Cont	0,17^{d}	0,22^{d}	0,30^{d}	0,21^{c}	0,14^{d}	0,12^{d}	0,10^{d}
IP-13	0,59^{a}	0,62^{a}	0,65^{a}	0,62^{a}	0,59^{a}	0,58^{a}	0,57^{a}
IP-34	0,55^{b}	0,56^{b}	0,58^{b}	0,55^{a}	0,54^{b}	0,54^{b}	0,54^{b}
S-36	0,27^{c}	0,28^{c}	0,38^{c}	0,29^{b}	0,20^{c}	0,22^{c}	0,24^{c}

[1]: T (350- 100 nm); P (400-700 nm); B (400-500 nm); G (500-570 nm)
[2]: R (600-700 nm); FR (700-800 nm); N (700-1100 nm)
[a,b,c,d]: Values followed by a different superscript letter within the same column are statistically significantly different (a=0.05).

In Table 13 are presented values of light quality parameters for the total (beam+diffuse; b+d) and the diffuse (d) component of the solar radiation inside screenhouses (IP-13; IP-34; S-36) and at the open field (Cont), during experimental period 2012. Data presented are average values of mean daily values of measurements during three representative summer days; July 25, August 14 and September 4. In the total (b+d) solar radiation, the phytochrome related ratios (ζ; R:FR) were slightly, but statistically significantly reduced under screens, with the R:FR seemed more sensitive and been more reduced inside the heavy shaded screenhouses (IP-34 and S-36). The reduction of the cryptochrome related ratios (B:R and B:FR) were also statistically

significant inside all screenhouses, except for the B:R ratio inside S-36 screenhouse that was greater compared to the ambient. The B:R ratio was found increased about 8 and 11% for 2011 and 2012, respectively, inside the green screenhouse (S-36) as it was compared to the neutral colored screenhouses IP-13 and IP-34. The P:T and P:N ratios were also significantly reduced inside screenhouses, presenting the lowest values inside the heavy shaded screenhouses (IP-34 and S-36).

Table 13. Values of screenhouse spectral transmittances (τ_{b+d}), diffuse ratio (τ_{dif}) and light quality parameters for the total (beam+diffuse; b+d) and the diffuse (d) component of solar radiation inside screenhouses (IP-13; IP-34; S-36) and at the open field (Cont), on experimental period 2012. The measurements took place at 2 hours intervals around solar noon i.e., 9:30, 11:30, 13:30, 15:30 and 17:30.

	T [1]		P [1]		B [1]		G [1]	
Treatment	τ_{b+d} [3]	τ_{dif} [4]	τ_{b+d}	τ_{dif}	τ_{b+d}	τ_{dif}	τ_{b+d}	τ_{dif}
IP-13	0,72^{a}	2,88^{a}	0,71^{a}	2,24^{a}	0,69^{a}	1,58^{a}	0,71^{a}	2,39^{a}
IP-34	0,58^{b}	2,12^{b}	0,55^{b}	1,55^{b}	0,52^{c}	1,04^{b}	0,56^{c}	1,68^{b}
S-36	0,61^{c}	1,06^{c}	0,59^{c}	0,82^{c}	0,60^{b}	0,77^{c}	0,59^{b}	0,85^{c}
	R [2]		FR [2]		N [2]			
	τ_{b+d}	τ_{dif}	τ_{b+d}	τ_{dif}	τ_{b+d}	τ_{dif}		
IP-13	0,73^{a}	3,61^{a}	0,73^{a}	4,29^{a}	0,74^{a}	5,01^{a}		
IP-34	0,58^{b}	2,62^{b}	0,60^{b}	3,27^{b}	0,62^{b}	3,99^{b}		
S-36	0,57^{b}	0,91^{c}	0,61^{b}	1,35^{c}	0,65^{b}	1,89^{c}		
	ζ		R : FR		P : T		P : N	
	(b + d)[5]	(d)[6]	(b + d)	(d)	(b + d)	(d)	(b + d)	(d)
Cont	1,27^{a}	1,43^{a}	1,25^{a}	1,50^{a}	0,58^{a}	0,76^{a}	1,40^{a}	3,21^{a}
IP-13	1,26^{a}	1,28^{b}	1,24^{b}	1,26^{b}	0,57^{b}	0,59^{b}	1,34^{b}	1,46^{b}
IP-34	1,23^{a}	1,23^{b}	1,21^{c}	1,20^{b}	0,56^{c}	0,56^{b}	1,25^{c}	1,27^{b}
S-36	1,24^{a}	1,24^{b}	1,16^{d}	1,03^{c}	0,56^{c}	0,59^{b}	1,25^{c}	1,43^{b}
	B : R		B : FR		B : P		G : R	
	(b + d)	(d)	(b + d)	(d)	(b + d)	(d)	(b + d)	(d)
Cont	1,04^{b}	2,46^{a}	1,31^{a}	3,70^{a}	0,33^{b}	0,48^{a}	0,80^{b}	1,27^{a}
IP-13	0,99^{c}	1,10^{b}	1,23^{c}	1,40^{bc}	0,32^{c}	0,34^{b}	0,78^{c}	0,82^{c}
IP-34	0,93^{d}	1,00^{b}	1,13^{d}	1,21^{c}	0,31^{d}	0,33^{b}	0,76^{d}	0,78^{d}
S-36	1,10^{a}	2,08^{a}	1,28^{b}	2,13^{b}	0,34^{a}	0,45^{a}	0,84^{a}	1,22^{b}

[1] and [2] as in Table 12. [3] τ_{b+d}: Transmittance of beam+diffuse solar radiation across a wavelength band. [4] τ_{dif} : diffuse ratio of screenhouse enclosure.
[5] (b+d): beam+diffuse radiation and [6] (d): diffuse component of the solar radiation
$^{a, b, c, d}$: Values followed by a different superscript letter within the same column are statistically significantly different (a=0.05).

In the diffuse fraction (d) of solar radiation the ζ and R:FR ratios were not significantly altered as compared to the total (beam+diffuse) radiation inside all three screenhouses, which is in agreement with the findings of Shahak et al. (2004b). The B:R ratio of the diffuse component inside S-36 was about the double as compared to the insect proof screenhouses (IP-13 and IP-34). The increase of the latter ratio inside the S-36 screenhouse could probably be ascribed to the greater energy across the green wavelength band and the simultaneous decreased energy across the red (R), as originated by the optical properties of the shade net S-36. About the same behavior was recorded for the B:FR ratio, while no significant alternations were recorded in P:T and P:N ratios of the diffuse components as compared to the total (beam+diffuse) solar radiation inside all three screenhouses.

6.2. Transpiration of sweet pepper crop under screenhouse conditions

6.2.1. Screenhouse and Outside Climate Characteristics

The data selected for analysis in this section correspond to sunny days of August and September 2011. The mean values of the daily solar radiation integral and the mean daily values of outside climate parameters (averaged over 8 – 20 h local time) during the period of August and September are given in Table 14. Furthermore, the average values of the daily solar radiation integrals in the three screenhouses during August and September are presented in Table 15 along with the mean daily values (averaged over 8 – 20 h local time) of air vapour pressure deficit in the three screenhouses.

Table 14. Daily average values (period 8 h – 20 h local time) of the outside climatic variables during August and September 2011.

	[a] $R_{s,out}$	T_{out} (°C)		D_{out} (kPa)		u_{out} (m s^{-1})	
Month	(MJ m^{-2} day^{-1})	Mean	± Stdv	Mean	± Stdv	Mean	± Stdv
August	22.43	29.1	± 1.81	2.27	± 0.42	2.37	± 0.60
September	17.46	26.3	± 3.46	1.83	± 0.72	2.13	± 0.43

[a] $R_{s,out}$, outside global radiation (MJ m^{-2} day^{-1}); T_{out}, outside air temperature (°C); D_{out} vapour pressure deficit (kPa); u_{out} outside wind speed (m s^{-1}).

Table 15. Mean values of daily solar radiation integrals (R_s) and of vapour pressure deficit (D_{air}) over 8 h - 20 h, in the three screenhouses during the period of measurements (2011).

	[a] R_s (MJ m^{-2} day^{-1})			[b] D_{air} (kPa) (Mean ± Stdv)		
Month	IP-13	IP-34	$S_{36\%}$	IP-13	IP-34	$S_{36\%}$
August	18.14	14.34	15.49	2.32± 0.41	2.25± 0.37	2.23± 0.32
September	14.02	11.17	12.07	1.90± 0.71	1.83± 0.67	1.79± 0.65

[a] R_s, screenhouse solar radiation integral (MJ m^{-2} day^{-1}); D_{air} screenhouse air vapour pressure deficit (kPa).

6.2.2. Crop Transpiration Modelling

The relation between λE and Rs measured under the three screenhouses and outside is shown in Figure 18. It can be seen that λE presented similar relation with Rs in all treatments. Linear regression of λE and Rs revealed that the slope of the regression line between the above variables was between 0.15 and 0.17 (Cont, IP-13, IP-34: $0.80<R^2<0.84$; S-36: $R^2= 0.70$).

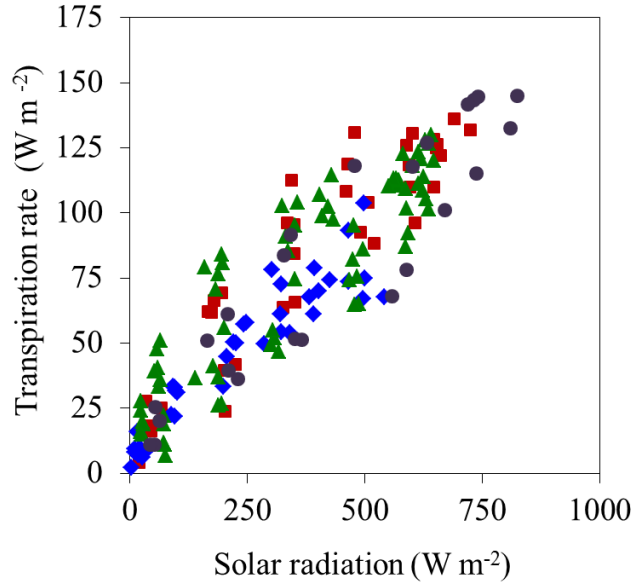

Figure 18. Covariation between transpiration rate and solar radiation observed under the three screenhouses and outside.

A statistical regression between the data (hourly average values) of pepper crop transpiration rate (W m^{-2}) and R_s, (W m^{-2}), D (kPa) and LAI was performed and gave the results presented in Table 16. It has to be noted that for the calibration of eq. 13: $Tr_i = \lambda E = A\,R_s + B\,D$ (eq. 14 and eq. 15), data of more than two days per treatment have been used.

Table 16. Values of the coefficients α and β of the simplified model of the P-M equation (eq. 14 and eq. 15).

	α (W m^{-2})		β (kPa^{-1})		
Treatment	Estimate	St.Error (±)	Estimate	St.Error (±)	[1]R^2
Cont	0.248	0.012	12.8	1.5	0.99
IP-13	0.223	0.015	3.1	0.7	0.98
IP-34	0.199	0.017	4.9	1.4	0.97
S-36	0.243	0.011	7.7	0.9	0.97

[1]R^2, coefficient of determination.

Table 16 shows that the values of radiative term α were found to be higher for the open field and the S-36screenhouse crop while the lower values were observed under the IP-13 and IP-34 screenhouses. Furthermore, the advective part of the Penman-Monteith equation was high under the open field crop (β=12.8 W m^{-2} kPa^{-1}) and the S-36screenhouse (β= 7.7 W m^{-2} kPa^{-1}) and low under the IP-13 (3.1 W m^{-2} kPa^{-1}) and IP-34 (4.9 W m^{-2} kPa^{-1}) screenhouses. The higher values of β observed under the S-36 screenhouse compared to the IP-13 and IP-34 screenhouses could be attributed to the higher values of g_a under the above treatments, since it is considered that the air velocity under the S-36 screenhouse will be higher than the IP-13 and IP-34 screenhouses due to differences in their porosity. Furthermore, it is expected that g_a will be higher under open field conditions than under the screenhouses due to the effect of the screen on air velocity reduction.

6.2.3. Model Validation

The values of the α and β parameters shown in Table 16 and the eq. 13, eq. 14 and eq. 15 were used for the estimation of λE in the three screenhouses and outside during periods different than those used for the calibration of eq. 13. Comparisons between measured and estimated values are presented in Figure 19 (on page 75). It can be seen that there is good agreement between measured and estimated values of transpiration rate for all treatments. The residuals with respect to solar radiation and air vapour pressure deficit were found to be distributed randomly (results not shown) which means that the influence of the climatic variables R_s and D was correctly taken into account by the model.

Using eq. 13 and the values of α and β shown in Table 16, it can be seen that for a crop with LAI of about 2, R_s of 500 W m^{-2} and D of 2.5 kPa λE is about 37% lower under the IP-13 and IP-34 screens than outside or about 18% lower under the S-36screen than outside and consequently, a similar reduction of crop water consumption under the above screens is expected.

The good agreement between the measured and estimated values of crop transpiration rate shows that it is possible to use the simplified Penman-Monteith formula for the irrigation scheduling of screenhouse pepper crop cultivated in Mediterranean climate conditions.

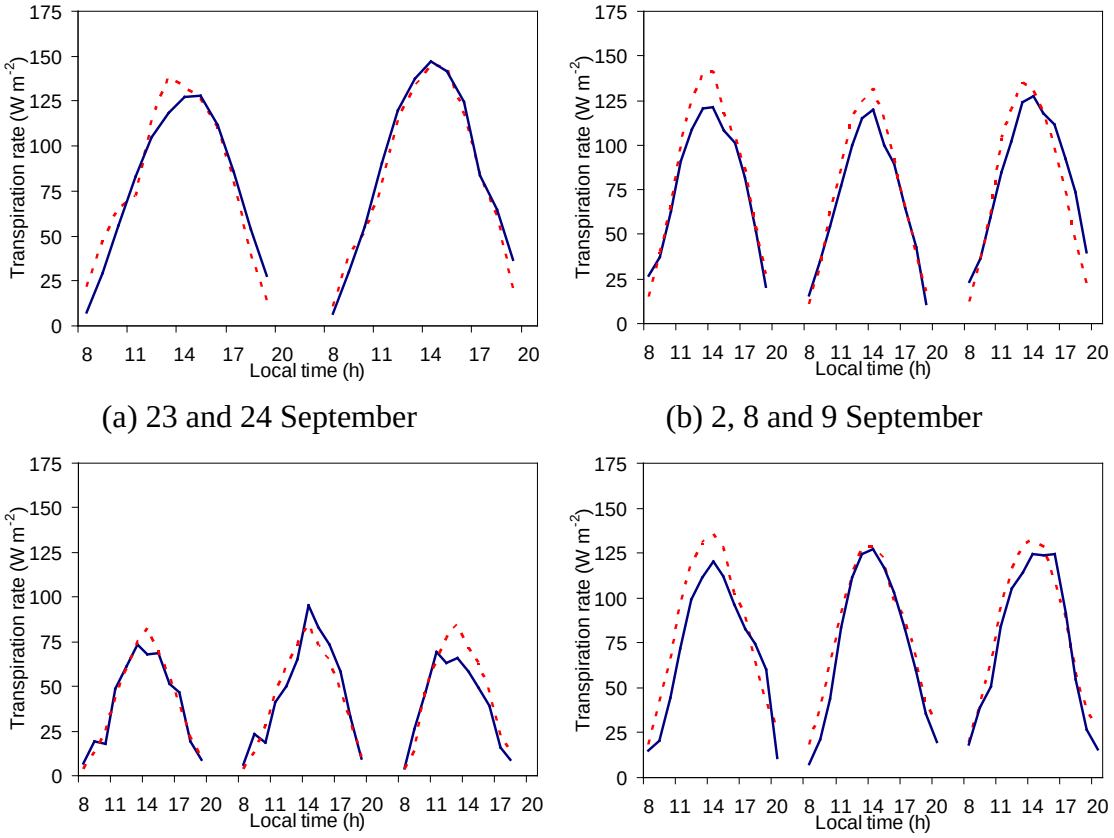

Figure 19. Comparison between measured and estimated values of crop transpiration rate under the three screenhouses and outside. (a) open field, (b) IP-13 screenhouse, (c) IP-34 screenhouse, (d) S-36 screenhouse. Continuous line: measured values, discontinuous line: estimated values.

6.2.4. Canopy conductance

The evolution of the diurnal variation of crop stomatal conductance in the three screenhouses and outside during selected days on both periods (2011 and 2012) is presented in Figure 20. For the 2011 period the selected days were 25 September for the outside treatment and 29 September for the three screenhouses. It can be seen that the crop stomatal conductance values under screenhouse conditions were similar or higher (IP-13) than the values observed for the open field crop. The mean daily values of the crop stomatal conductance observed for the period 10:00-17:00 during the selected day under the IP-13, IP-34 and S-36 screenhouses were 4.5 mm s^{-1}, 3.0 mm s^{-1}, and 2.7 mm s^{-1}, respectively, while the respective value under open field was 3.7 mm s^{-1}. It appears that although the crop temperature, and accordingly the canopy to air vapour pressure deficit, were lower under screenhouse conditions, the crop

stomatal conductance was not increased under shading indicating that the crop might still be under stress conditions even below shading.

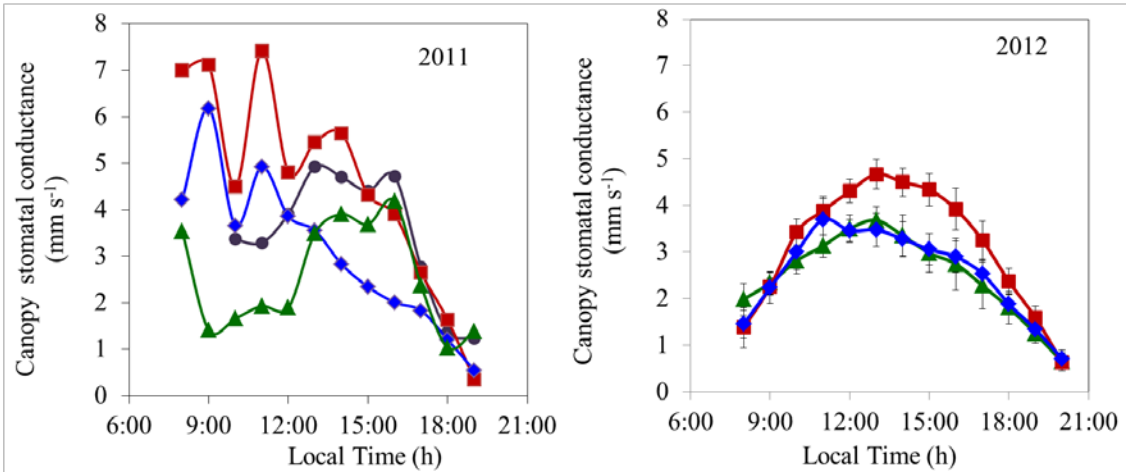

Figure 20. Diurnal evolution of canopy stomatal conductance (g_c; kPa K^{-1}) inside screenhouses (IP-13: squares; IP-34: diamonds; S-36: triangles) and at the open field (Cont: circles). Left: 2011 period (25 September for the outside treatment and 29 September for the three screenhouses) Right: 2012 period. Data points are the mean value of 12 days measurements (August 20-31, 2012). Vertical bars stand for the 95% confidence intervals.

For the 2012 period hourly averages of twelve days were calculated for each treatment. Unfortunately there was no available lysimeter for the outside treatment and therefore crop stomatal conductance was not calculated and presented in the figure. The mean diurnal values of the crop stomatal conductance observed for the period 08:00-20:00 during the selected days (20-31 August, 2012) under the IP-13, IP-34 and S-36 screenhouses were 3.12 mm s^{-1}, 2.55 mm s^{-1}, and 2.50 mm s^{-1}, respectively. The values of 2012 period were lower as opposed to that of 2011 period, which could be attributed to the different period of year that measurements had been conducted; 2011 – end of September, 2012 – twelve last days of August. Harsh summer climatic conditions had been passed for the 2011 period case and therefore, higher values of canopy stomatal conductance had been recorded, unlike the end-summer period of measurements for the case of 2012 period.

6.3. Ventilation rate determination in screenhouses

6.3.1. Air flow characteristics of porous screens

In Figure 21 are presented the pressure drop against air velocities from the wind tunnel tests. In the wind tunnel were tested samples detached from different heights of the side walls (0.5 and 1.5 m above ground) and from the roof of the screenhouses. Moreover, new (as if they were just bought from the supplier) samples of the respective screen were also tested in the wind tunnel. At the figure that presents the "pooled data" results", each data point represents the mean value of four measurements (new, roof, 0.5 and 1.5 m above ground). For comparison reasons the results from the "new" samples are also presented next to the "pooled data" figure. A slight departure from the pressure drop pattern of the new samples of IP-13 screen was observed as opposed to the IP-34 screen respective samples. However, the statistical analysis results revealed that the differences between the insect proof screens were not significantly (a=0.05) and therefore the insect proof data could be pooled without great error.

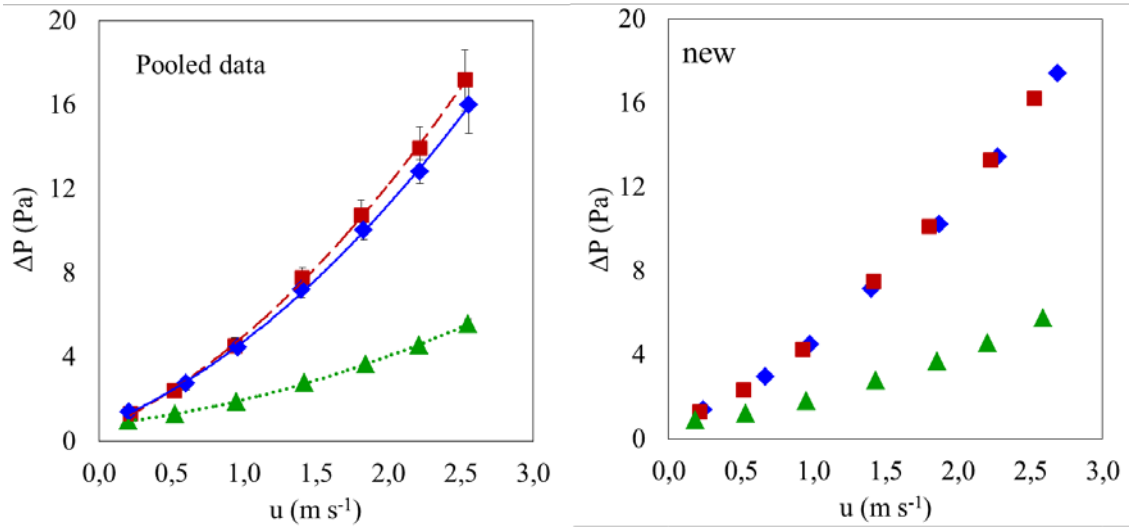

Figure 21. Pressure drop (ΔP; Pa) and upstream velocity (u; $m\,s^{-1}$) during wind tunnel tests of the insect proof screens (IP-13: squares; IP-34: diamonds) and the shade net (S-36: triangles). Left: pooled data from tested samples cut off from different locations of the screenhouse cover; each data point is the mean of four measurements; vertical bars stands for the 95% confidence intervals; curved lines represent the best fit regression lines for the insect proof screens (IP-13: dashed line; IP-34: continuous line) and the shade net (S-36: dotted line). Right: New samples of insect proof screens and shade net.

The mean estimated values of Inertial factor (Y) and permeability (K; m^2) of the covering screens that were estimated by fitting the data of ΔP and u, measured in the wind tunnel, into eq. 21 ($(\mu/K)u + \rho(Y/K^{1/2})|u|u = \partial P/\partial x$) using Marquardt's algorithm (Marquardt, 1963), are presented in Table 17.

Table 17. Estimated values (95% confidence) of the Inertial factor (Y) and permeability (K; m^2) of the covering screens.

Screen	[1]n	[2]a	[2]b	[2]c	[3]R^2	[4]K×10^{-9}	[5]Y	[6]ε	[7]Δx×10^{-4}
[8] IPs	56	1.277	3.019	0.583	0.99	2.93	0.210	0.46	4.80
S-36	28	0.444	0.742	0.787	1.00	19.8	0.065	0.63	8.00

[1]n: number of measurements; [2]a,b,c: coefficients of the best fit regression lines ($\Delta P = \alpha u^2 + bu + c$); [3]$R^2$: coefficient of determination; [4]K: permeability (m^2); [5]Y: inertial factor; [6]ε: porosity; [7]Δx: thickness of the screen / net (m); [8] IPs: Insect proof screens pooled data

In Figure 22 are presented the Pressure drop though screen/net samples against the product $0.5\rho u^2\varepsilon^{-2}$ for the insect proof screens (IPs; IP-13 and IP-34) and the shade net (S-36). Each data point represents the mean value of four measurements (new, roof, 0.5 and 1.5 m above ground). The differences in pressure drop between the insect proof screens and the shade net are very distinctive.

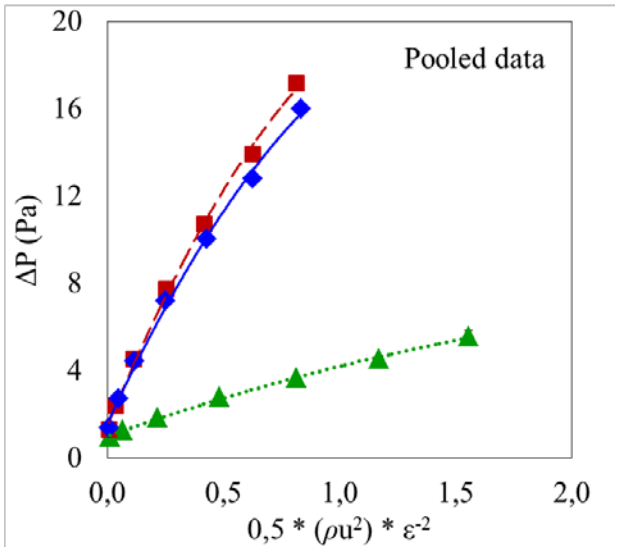

Figure 22. Pressure drop though screen/net samples against the product $0.5\rho u^2\varepsilon^{-2}$ for the insect proof screens (IP-13: squares; IP-34: diamonds) and the shade net (S-36: triangles). Pooled data: tested samples cut off from different locations of the screenhouse cover; each data point is the mean of four measurements; vertical bars stands for the 95% confidence intervals (the intervals are extremely narrow and therefore not visible); curved lines represent the best fit regression lines for the insect proof screens (IP-13: dashed line; IP-34: continuous line) and the shade net (S-36: dotted line).

The discharge coefficient C_{ds} of the screens was estimated by fitting the data of ΔP and u measured in the wind tunnel into eq. 20 ($\Delta P = 0.5\frac{\rho v^2}{C_{ds}^2} = 0.5\frac{\rho \mathrm{u}^2}{\varepsilon^2 C_{ds}^2} = 0.5\frac{\rho \mathrm{u}^2}{C_{ds^*}^2}$) using Marquardt's algorithm (Marquardt, 1963). The mean estimated values of the discharge coefficient C_{ds} from the different screen samples tested are presented in Table 18.

Table 18. Estimated values (95% confidence) of the discharge coefficient (C_{ds}) by means of eq. 20 for the insect proof (IP-13 and IP-34) and shade (S-36) screens.

Screen	Estimate	Std. Error (±)	[1]R^2	[2]df
IP-13	0.991	0.015	0.92	27
IP-34	1.035	0.017	0.91	27
IP screens (pooled data)	1.013	0.011	0.91	55
S-36	1.262	0.029	0.76	27

[1]R^2: Models coefficient of determination
[2]df: Degrees of freedom

In order to test if the C_{ds} values of the two insect proof screens were statistically different, the t-test was used (Dagnelie, 1986):

eq. 30: $t = \frac{1.03-0.99}{\sqrt{(0.017)^2+(0.015)^2}} = 1.97 < 2.00\ (t_{0.05;54})$

The t value estimated (1.97) was lower than 2.00, which is the corresponding t-value for 95% of confidence and 54 degrees of freedom (the sum of the degrees of freedom for each fit). Accordingly, the C_{ds} values estimated for the two insect proof screens were not significantly different and thus, the data were pooled and a unique value was estimated. The C_{ds} value estimated by means of eq. 20 was 1.01 (±0.011) with R^2 of 0.91.

The corresponding C_{ds^*} values were 0.465 and 0.795 for IP and S-36 screens, respectively.

6.3.2. Screenhouse microclimate during ventilation rate determinations

6.3.2.1. Air temperature and vapour pressure deficit

The average daytime (08:00-20:00, local time) mean values of the internal air temperature (Table 19) in all three screenhouses were about 0.2 ºC lower than the outside air temperature. The maximum air temperature recorded under screenhouse conditions was about 0.7 ºC lower than the corresponding outside. A similar trend was also observed for the air vapour pressure deficit values (Table 19). The maximum air vapour pressure deficit values observed in the screenhouses were about 40% higher than the mean values observed outside during the 12 h period.

Table 19. Average of daytime (08:00-20:00) mean and max air temperature (T_{air}; ^{o}C) and vapour pressure deficit ($D_{air}; kPa$) over 6-day intervals.

		T_{air} (^{o}C)			D_{air} (kPa)		
Period	Treatment	mean	stdev	max	mean	stdev	max
	Out	31.6	1.52	36.4	3.2	0.41	4.6
(1st)	IP-13	31.6	1.48	36.2	3.0	0.38	4.3
20-25 Aug.	IP-34	31.6	1.27	36.1	3.1	0.40	4.3
	S-36	31.1	1.23	35.6	2.9	0.34	4.3
	Out	29.3	2.08	33.7	2.7	0.45	3.6
(2nd)	IP-13	29.2	2.01	32.7	2.5	0.43	3.3
26-31 Aug.	IP-34	28.8	2.60	32.0	2.5	0.55	3.3
	S-36	28.9	2.06	32.0	2.5	0.43	3.3
	Out	27.5	0.51	31.8	2.1	0.11	3.1
(3rd)	IP-13	27.5	0.47	31.7	1.9	0.09	2.8
1-6 Sept.	IP-34	27.4	0.53	31.4	1.9	0.10	2.8
	S-36	27.0	0.51	30.9	1.9	0.10	2.8

The diurnal (08:00-20:00, local time) inside to outside air temperature difference (Figure 23) followed similar trends for all three screenhouses, with the minimum air temperature difference observed during noon to reach about -0.7 ºC and the minimum vapour pressure difference to reach about -0.4 kPa. The lower vapour pressure deficit values observed inside the three screenhouses could be attributed to the enrichment of screenhouse air by air vapour through crop transpiration. Comparing the three screenhouses, the lower air temperature and vapour pressure deficit values during the most part of the day were observed in the S-36 screenhouse.

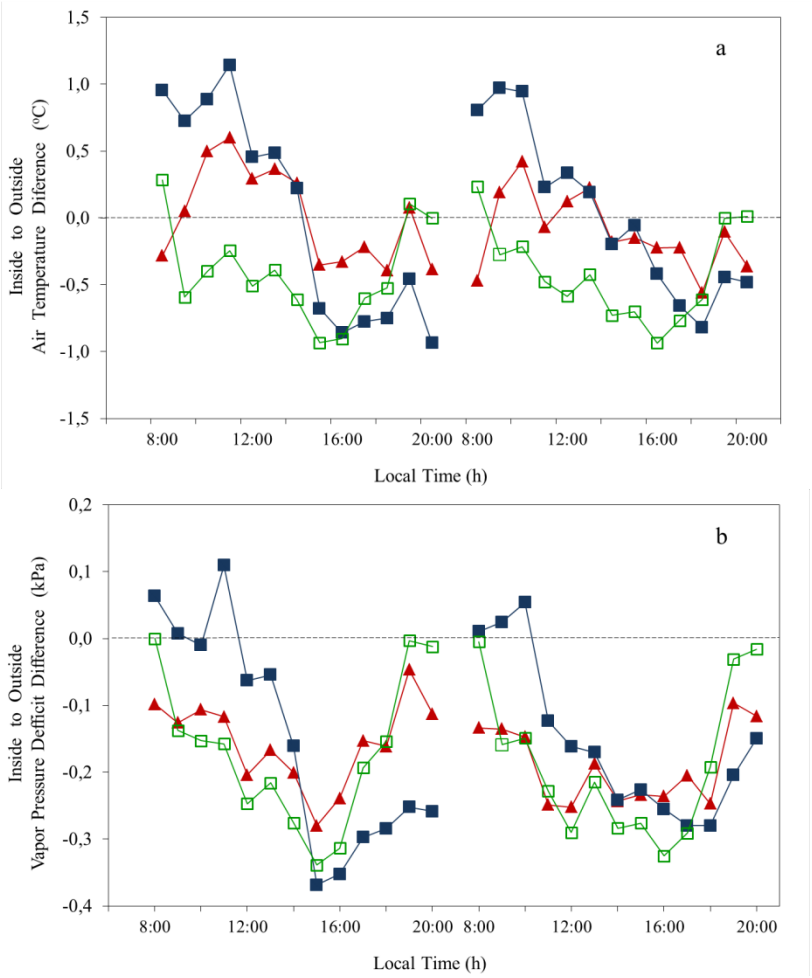

Figure 23. Diurnal (08:00 – 20:00, local time) inside to outside: (a) air temperature difference (T_{air}; ^{o}C) and (b) vapour pressure deficit (D_{air}; kPa) for screenhouses IP-13 (triangles), IP-34 (closed squares) and S-36 (open squares) during 2 consecutive days (30 & 31August, 2012).

6.3.2.2. Screenhouse air velocity and direction

The wind velocity observed inside the three screenhouses was highly correlated to that measured outside the screenhouses (Figure 24).

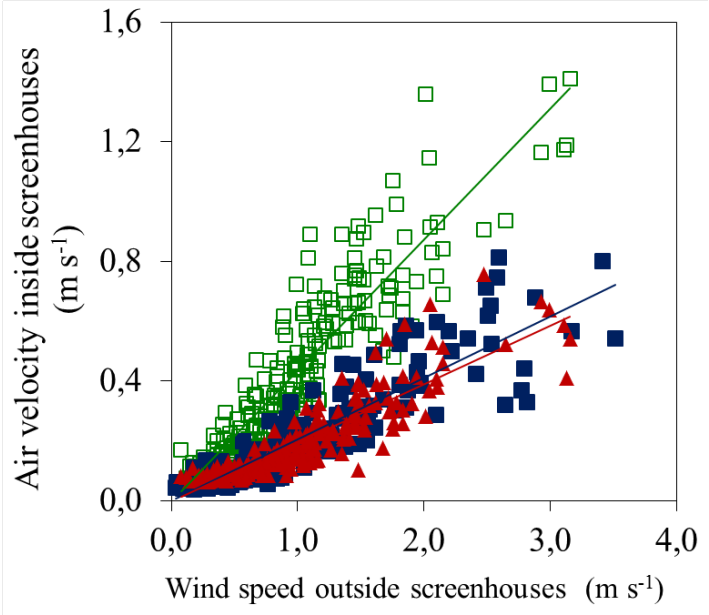

Figure 24. Air velocity inside the screenhouses as a function of the external wind speed. The figure presents data points from August 25 until 31, 2012, for screenhouses IP-13 (triangles) and S-36 (open squares). For IP-34 (closed square), data points represent measurement values from October 26 until November 5, 2012. Solid lines present the best fit regression line.

It was found that the air velocity measured inside (u_{in}) the IP screenhouses was about 50% lower than that observed under the green shading screen and about 20% of the outside (u_o). The regression lines obtained between inside and outside air velocity values for the three screenhouses were:

eq. 31: $u_{in_{IP-13}} = 0.195\ (\pm\ 0.007)\ u_o + (2.80 * 10^{-4})\ (\pm\ 0.008)$, with $R^2 = 0.80$,

eq. 32: $u_{in_{IP-34}} = 0.205\ (\pm\ 0.007)\ u_o - (1.53 * 10^{-4})(\pm\ 0.008)$, with $R^2 = 0.82$,

eq. 33: $u_{in_{S-36}} = 0.437\ (\pm\ 0.013)\ u_o + (1.04 * 10^{-4})(\pm\ 0.015)$, with $R^2 = 0.84$,

for IP-13, IP-34 and S-36, respectively. The values given in parenthesis correspond to the standard error of slope and intercept, respectively. The slope for all cases was statistically significant (a = 0.05), while the intercept was not statistically significant and could be excluded without any statistical error. A t-test was performed to compare

the slope of the correlations for IP-13, IP-34 and was found that the values were not statistically different (data not shown), and thus the data from the two screenhouses were pooled and the new correlation found between inside and outside air velocity for the insect proof (IP) screenhouses was:

eq. 34: $u_{in_{IP}} = 0.201\ (\pm 0.005)\ u_o - (7 * 10^{-4})(\pm 0.005)$, with $R^2 = 0.81$

The value of the intercept was not statistically significant and can be ignored without any statistical error.

The wind direction inside the IP-13 and S-36 screenhouses (hourly mean values) as a function of the external wind direction is presented in Figure 25.

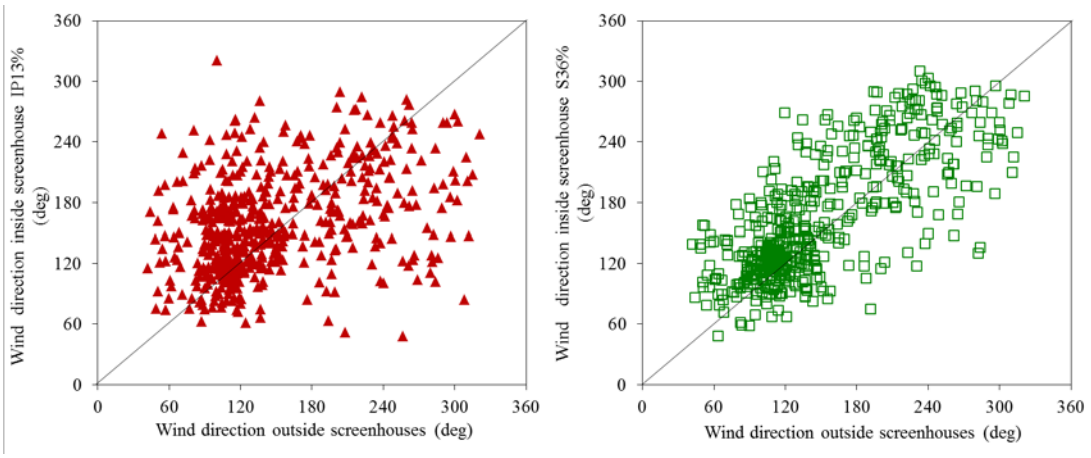

Figure 25. Wind direction inside screenhouses IP-13 (triangles) and S-36 (squares) as a function of the external wind direction. The figure presents data points from August 25 until September 15, 2012. Solid lines are 1:1 lines.

It was found that the inside wind direction was correlated with that of the outside air with data points in S-36 screenhouse uniformly distributed around the 1:1 line. The same type of distribution was less uniform in the case of IP screenhouses, something that could be attributed to the differences in the texture of the shading and insect proof screens tested. The IP screens that were denser than the shading screen seem to affect in a higher degree the wind direction, compared to the less dense shading screen. The IP screenhouses presented similar relation between the inside and outside wind direction and that is why the data from IP-34 screenhouse are not shown.

6.3.2.3. Crop transpiration

The evolution of the crop transpiration rate in the three screenhouses is shown for consecutive days (30-31 August 2012) in Figure 26. The higher values of crop transpiration rate were observed in the screenhouse with the higher transmittance to solar radiation (IP-13) while the screenhouses with the lower transmittance (IP-34 and S-36) presented similar values of crop transpiration rate.

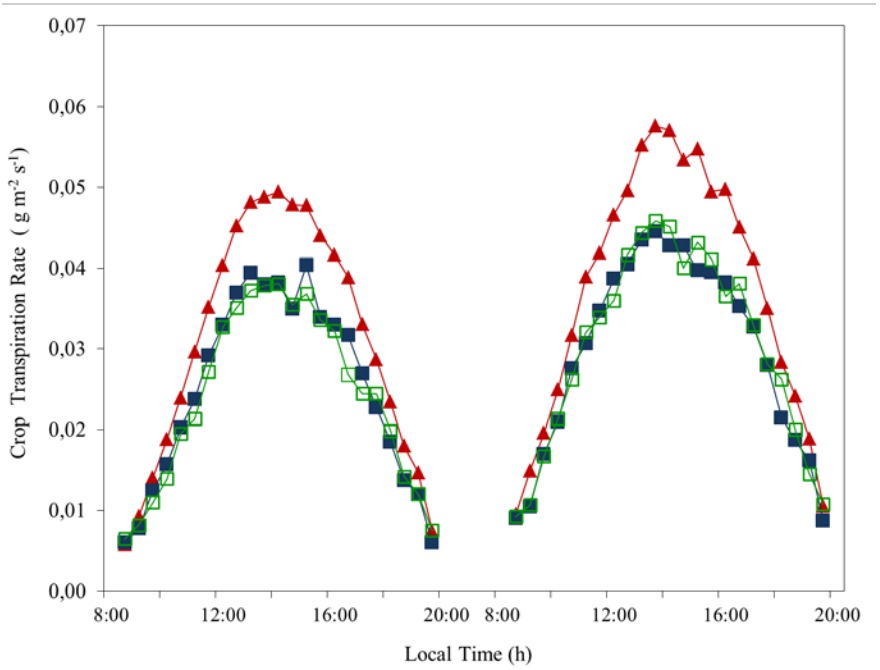

Figure 26. Diurnal (08:00-20:00, local time) crop transpiration rate (g m-2 s-1) inside screenhouse IP-13 (triangles), IP-34 (closed squares), S-36 (open squares) during 2 consecutive days (August 30 & 31, 2012).

6.3.3. Screenhouse ventilation modelling

In the results presented below, the analyzed data correspond to the main wind direction of the region (E-SE 115° ± 25°). Data from different directions were not included in the analysis. Moreover, the ventilation analysis was conducted in 30-min average climate values with stable wind direction, in order to fulfil the steady state conditions during measurements period.

The volume air flow rate observed during the period of measurements in the two IP screenhouses was similar with an average daytime value of 0.06 m^3 m^{-2} s^{-1} while the respective values observed in the S-36 screenhouse were about double (0.11 m^3 m^{-2} s^{-1}) of those observed in the IP screenhouses.

The hourly mean air exchange rate (N, h^{-1}) values observed during the period of measurements in the S-36 screenhouse and the IP screenhouses (pooled data) are shown in Figure 27, as a function of the outside air velocity.

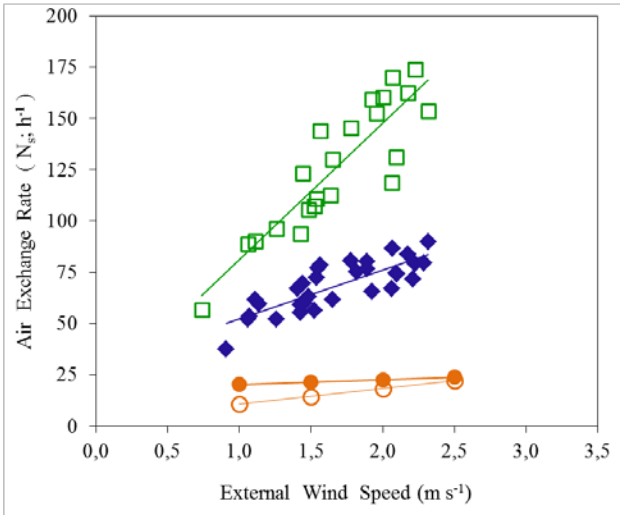

Figure 27. Screenhouse air exchange rate (h-1) as a function of measured external wind speed, during August 30 until 31, 2012. Diamond: pooled data IP-13 and IP-34, squares: S-36, closed circle: 8 ha banana screenhouse (Tanny et al. 2006) and open circle: 0.66 ha pepper screenhouse (Tanny et al. 2003). Solid lines present the best fit regression line.

The regression lines obtained between the air exchange rate and the outside air velocity for the two IP screenhouses and the S-36 screenhouse, respectively, were:

eq. 35: $N_{IP} = 23.8\ (\pm 3.2)\ u_o + 28.5\ (\pm 5.5)$, with $R^2 = 0.66$,

eq. 36: $N_{S-36} = 66.6\ (\pm 7.7)\ u_o + 14.4\ (\pm 13.4)$, with $R^2 = 0.79$

The air exchange rate was ranging between 35-80 h^{-1} and 55-180 h^{-1}, for the case of the insect-proof (IP-13 and IP-34) and the S-36 screenhouses, respectively, for wind speed values ranging between 1 m s^{-1} and 2.5 m s^{-1}. The slope of the regression line presented above for S-36 is about 2.8 times higher than that of the IP screenhouses.

Fitting the measured values of the ventilation flow rate (G_{sc}) for the two type of screenhouses to eq. 25 ($G_{sc} = \frac{A_T}{2} C_d\sqrt{C_w}\, u + G_{sc,o}$), using Marquardt's algorithm (Marquardt, 1963), allowed the estimation of model parameters ($C_d\sqrt{C_w}$ and $G_{sc,o}$) shown in Table 20. The ventilation area A_T considered in eq. 25 was the sum of the windward and leeward side walls (2 x 64 = 128 m^2) and the roof surface (20 x 10 = 200 m^2).

Table 20. Regression coefficients estimates (95% confidence) of the overall coefficient of wind efficiency on ventilation ($C_d\sqrt{C_w}$) and of the ventilation rate at zero wind velocity ($G_{sc,o}$) for groups of data (G_{sc}, A_v and u_{ext}), for screenhouses IP (Pooled data for IP-13 and IP-34) and S-36.

	$C_d\sqrt{C_w}$			$G_{sc,o}$				
Screenhouse	Estimate	Std. Error (±)	[1] Sig.	Estimate	Std. Error (±)	[1] Sig.	[2] R^2	[3] df
IP (Pooled Data IP-13 & IP-34)	0.133	0.018	0.00	5.064	0.940	0.00	0.66	30
S-36	0.371	0.043	0.00	2.532	2.385	0.30	0.79	21

[1] Sig.: Significance; If Sig < 0.05 then the parameter is significant and will have to be considered.
[2] R^2: Models coefficient of determination
[3] df: Degrees of freedom

The estimated value of the overall pressure drop and wind effect coefficient ($C_d\sqrt{C_w}$) for the insect proof screenhouses (pooled data IP-13 and IP-34) was 0.026 (±0.003), while the value estimated for the S-36 screenhouse (0.072 ±0.008) was three times higher than that of the IP screenhouses.

Assigning to eq. 25, the C_{ds^*} values estimated by means of the wind tunnel measurements (Table 18) and following the same calibration procedure (Marquardt, 1963), the C_w values estimated for the IP and S36 screenhouses were 0.003 (±0.001) and 0.008 (±0.002), respectively.

6.4. Agronomical parameters of pepper crops

6.4.1. Plant height and number of leaves

The evolution of plant height for all treatments and for 2011 and 2012 periods are presented in Figure 28. Similar trends of the evolution have been observed for all treatments in each experimental period, with the plants inside screenhouse S-36 tended to be higher compared to the plants inside insect-proof screenhouses, during the entire crop period, on 2011 and 2012.

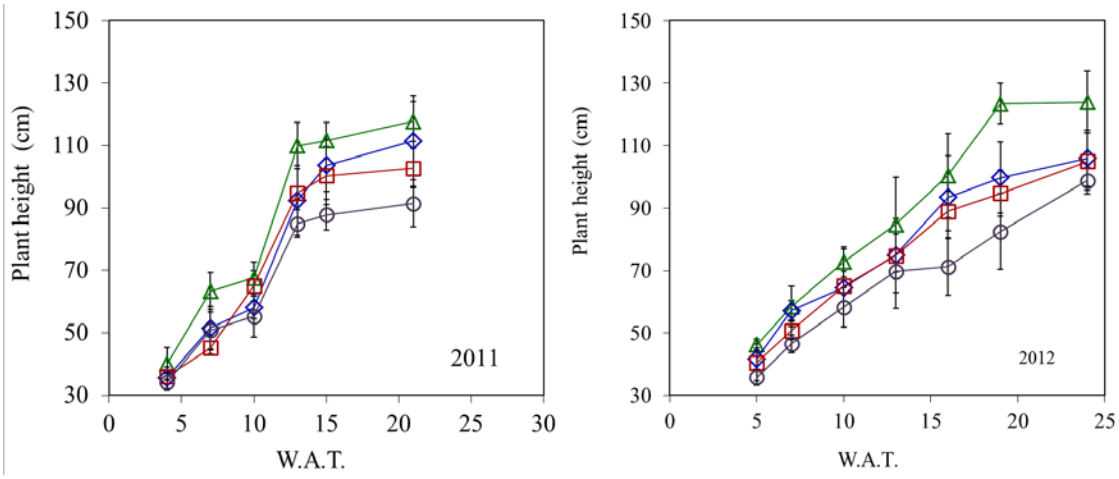

Figure 28. Evolution of plant height inside screenhouses (IP-13: squares; IP-34: diamonds; S-36: triangles) and at the open field treatment (Cont, circles), for the two experimental periods 2011 (left column) and 2012 (right column), as measured during destructive measurements program.

Table 21. Plant height and number of leaves inside screenhouses (IP-13; IP-34; S-36) and at the open field (Cont) treatment, for the two cropping periods (2011 and 2012).

	2011		2012	
	Plant Height	# of leaves	Plant Height	# of leaves
Treatment	cm	# plant^{-1}	cm	# plant^{-1}
Cont	91,5^{c}	336,8^{b}	98,8^{c}	288,5^{a}
IP-13	102,8^{bc}	480,5^{a}	105,0^{bc}	298,0^{a}
IP-34	111,5^{ab}	402,8^{ab}	106,0^{bc}	317,8^{a}
S-36	117,8^{a}	374,8^{b}	124,0^{a}	360,3^{a}

$^{a, b, c}$: Means with different superscript letters within the same column are statistically significantly different (a=0.05)

The final height per plant (vertical projection of canopy's side view) for each treatment for each experimental year is presented in. In each experimental period the height per plant presented statistically significant differences (a=0.05) between the

four treatments. The height of the plants was higher inside S-36 screenhouse as compared to the open field treatment, on both periods. Generally, the plant height is strongly related to the shade percentage that a crop is receiving, as it is been increased with the increase of the shade percentage. Consequently, it was expected that the plant height would have been increased with the increase of the shade factor. Actually, this was the case in the present study inside all treatments except in the IP-34 screenhouse, which did not differed statistically significantly compared to the IP-13 screenhouse, on neither of each experimental year.

In Figure 29 are presented the evolution of the number of leaves per plant inside the screenhouses and at the open field treatment during each experimental period (2011 and 2012). At the end of 2011 experimental period the number of leaves per plant was statistically significantly (a=0.05) greater in screenhouse IP-13 as compared to the number of leaves inside IP-34, S-36 and at the open field. No statistically significant differences were revealed for the number of leaves per plant at the end of 2012 period. The final number of leaves per plant on 2011 was greater as compared within each treatment to the corresponding numbers of the 2012 period.

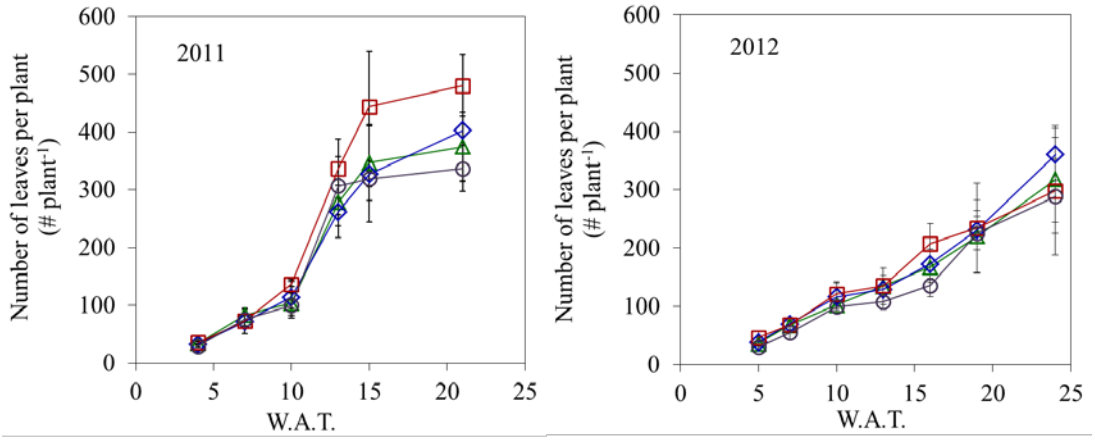

Figure 29. Evolution of number of leaves per plant inside screenhouses (IP-13: squares; IP-34: diamonds; S-36: triangles) and at the open field treatment (Cont: circles), for the two cropping periods 2011 (left column) and 2012 (right column).

6.4.2. Leaf area index

In Table 22 are presented the Leaf area index (LAI; $m^2\ m^{-2}$), area per leaf ($cm^2\ leaf^{-1}$) and the respective number of leaves per plant (# $plant^{-1}$) that were measured/scanned in order to determine the LAI. The LAI and the respective area per leaf were increased inside screenhouses on both experimental periods. The LAI of the crop inside screenhouses was on average for both periods and for all screenhouses greater by about 60% as compared to that of the open field crops. No significant differences were revealed between screenhouse treatments.

Table 22. Leaf area index (LAI; $m^2\ m^{-2}$), area per leaf ($cm^2\ leaf^{-1}$) and the respective number of leaves per plant (# $plant^{-1}$) that were measured/scanned in order to determine the LAI.

	2011			2012		
	# of leaves per plant [1]	LAI [1]	area per leaf	# of leaves per plant	LAI	area per leaf
Treatment	# $plant^{-1}$	$m^2\ m^{-2}$	$cm^2\ leaf^{-1}$	# $plant^{-1}$	$m^2\ m^{-2}$	$cm^2\ leaf^{-1}$
Cont	255,0	1,3	28,5	288,5 [a]	1,3 [b]	25,6
IP-13	367,0	2,3	34,6	298,0 [a]	1,8 [ab]	34,2
IP-34	256,0	1,8	39,2	317,8 [a]	2,2 [a]	38,8
S-36	310,0	2,4	43,6	360,3 [a]	2,0 [ab]	30,6

[a, b, c]: Means with different superscript letters are statistically significant different (a=0.05)

[1]: Only the leaves of 1 plant per treatment were scanned. Therefore, no statistical analysis presented.

6.4.3. Correlation between leaf number and leaf area

Good correlation was found between measured leaf area (L_a) and number of leaves per plant (L_n) and a model that calculates the leaf area per plant using only its number of leaves was calibrated for each treatment and each cropping period. Non-linear regression conducted for groups of pooled data of L_a and L_n for 2011 period, in order to estimate the best fit regression line:

eq. 37: $L_a = a\ L_n$

The analysis conducted for the following case studies: (i) for each treatment separately, (ii) for the “heavy shaded” screenhouses IP-34 and S-36 pooling their data

together as one treatment (Pld-35) and (iii) for all three screenhouses pooling their data together as one treatment (Pld-Scr). In Table 23 are presented the estimates for the slope of the regression line for each case. A t-test analysis (Dagnelie, 1986) for the estimates revealed that IP-34, S-36 and Pld-35 were not significantly different one each other. Moreover, the estimate of Pld-Scr case was significantly different from IP-13.

Table 23. Regression coefficients estimates (95% confidence) of the slope and intercept of the best fitted line for groups of data for L_n and L_a for screenhouses (IP-13, IP-34 and S-36), for the open field treatment and for pooled data for IP-34 and S-36 screenhouses (Pld-35).

		a			
		Estimates x 10^3	Std Error (±) x 10^3	[1]R^2	[2]df
Calibration of model via data from 2011 period	Cont	2,979[c]	0,070	0,99	13
	IP-13	3,459[b]	0,072	0,99	13
	IP-34	3,909[a]	0,094	0,97	12
	S-36	3,852[a]	0,123	0,98	13
	Pld 35	3,876[a]	0,078	0,98	26

[a, b, c] : Values with different superscript letters are statistically significantly different (a=0.05)
[1]: R^2 = coefficient of determination; [2]:df = degrees of freedom

Following the above mentioned analysis, the proposed models in the present study are different for each shading level (0%, 13% and 35%) and hold as following:

eq. 38 Cont: $L_a = (2{,}979 * 10^{-3}) * L_n$

eq. 39 IP-13: $L_a = (3.459 * 10^{-3}) * L_n$

eq. 40 Pld-35: $L_a = (3.876 * 10^{-3}) * L_n$

A validation of the proposed models (eq. 38 - eq. 40) was conducted for groups of data (L_a *and* L_n) from period 2012. The calculated values (via model for 2011) of L_a were plotted against measured values of L_a for 2012 and the slope of their best fit regression line was compared against the 1:1 line (Figure 30). As it can be seen in the Figure 30 for the Cont and S-36 cases an excellent correlation was found between calculated and measured values, while for the cases of IP-13 and IP-34 the models slightly underestimate L_a about 6% and 4%, respectively. Figure 30 also presents the

residuals ($L_{a,\ calculated}$ - $L_{a,\ measured}$) against the leaf number per plant. The randomly scatter of residuals indicate that the leaf number correctly was taken into account by the model (eq. 37: $L_a = a\ L_n$ eq. 37). Moreover, the performance of each respective model (eq. 38 - eq. 40) was evaluated using the criteria of (Stöckle et al., 2004) (Table 24).

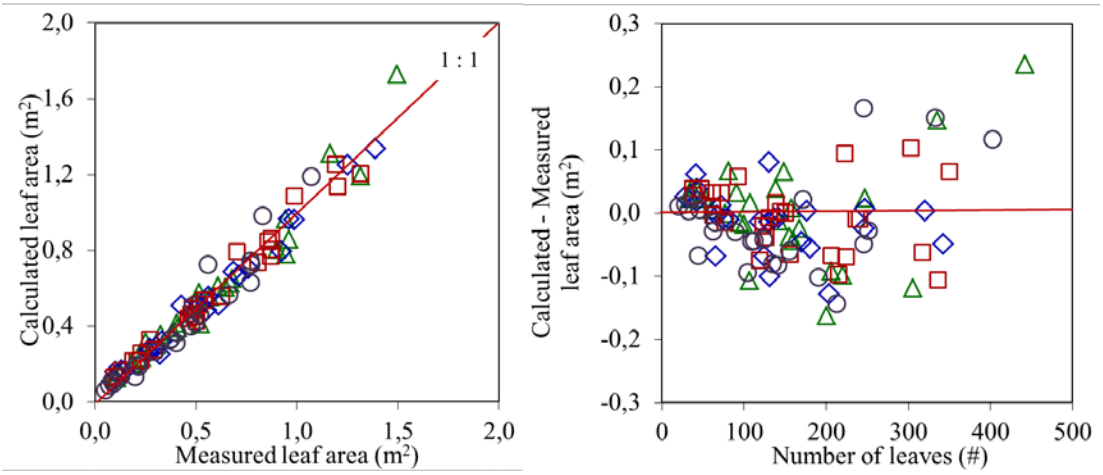

Figure 30. Left: Measured values of leaf area per plant against calculated values of leaf area per plant by fitting measured leaf number into eq. 38 - eq. 40. Right: Residuals of calculated and measured ($L_{a,\ calculated} - L_{a,\ measured}$) leaf area values against number of leaves. Top row: measured and calculated values of 2011; Bottom row: measured and calculated values of 2012. Cont: circles; IP-13: squares; IP-34: diamonds; S-36: triangles.

Table 24. Statistical indices of the validation of the model using data of 2012 period.

Treatment	[1]n	[2]RMSE	[3]RE	[4]d	[5]m	[6]R^2	[7]Performance
Cont	24	0,076	0,18	1,00	0,99	0,92	ACC
IP-13	27	0,063	0,11	1,00	1,05	0,98	G
IP-34	24	0,052	0,09	1,00	1,04	0,98	VG
S-36	27	0,079	0,14	0,99	0,99	0,96	G

[1]n n: is the number of data; [2]RMSE: root mean square error; [3]RE: relative error; [4]d: Wilmott index of agreement; [5]m and [6]R^2: slope and coefficient of determination, respectively, of the best fit regression line between simulated and measured values.

[7]Performance: VG (very good), G (good), ACC (acceptable). Performance was evaluated using the criteria of (Stöckle et al., 2004), which are described in (Giménez et al., 2012).

6.5. Productivity of pepper crops

6.5.1. Total fresh fruit yield

In Table 25 are presented the fresh weight (kg m^{-2}), the number of fruits (# m^{-2}) and the mean fruit weight (g $fruit^{-1}$) of mature fruits harvested during the entire experimental periods (2011 and 2012).

The production of fresh fruit weight, during each period, inside screenhouses was greater (in absolute values) as compared to the open field production. Though, statistically significant differences were clearly observed in 2011 period only between screenhouse IP-13 (been the most productive) and the other three treatments, whereas in 2012 period between the insect proof screenhouses (IP-13 and IP-34; been the most productive) and the shade screenhouse (S-36) and the open field (Cont) treatment. The moderate shade (≈20-25%; IP-13) enhanced the increase of the production by 21% (mean of both periods) as compared to the heavy shade of the IP-34 screenhouse, while the crops inside the heavy shaded insect proof house produced more by 17% as compared to the shade screenhouse.

Table 25. Total yield (kg m^{-2}) and total number of harvested fruits (# m^{-2}) for the crops inside screenhouses (IP-13; IP-34; S-36) and at the open field (Cont), at the end of the experimental periods 2011 and 2012.

	2011		2012	
	Fresh fruit weight	Total fruit number	Fresh fruit weight	Total fruit number
Treatment	kg m^{-2}	# m^{-2}	kg m^{-2}	# m^{-2}
Cont	3,3 ^{b}	63,9 ^{b}	4,4 ^{b}	56,3 ^{b}
IP-13	5,6 ^{a}	85,1 ^{a}	7,0 ^{a}	69,8 ^{a}
IP-34	4,4 ^{b}	58,1 ^{b}	6,0 ^{a}	58,5 ^{ab}
S-36	4,3 ^{b}	58,5 ^{b}	4,6 ^{b}	42,8 ^{c}

$^{a, b, c}$: Values followed by different superscript letter within the same column are statistically significant different (a=0.05)

Crop inside screenhouse IP-13 produced 41% and 33% more fruits (# m^{-2}) compared on average to the crops of screenhouses IP-34 and S36 and to the open field treatment. The number of fruits that were harvested inside S-36 on 2012 was lower than the corresponding number on 2011.

6.5.2. Cumulative yield

In Figure 31 are presented the evolution of the cumulative yield (fresh weight of harvested fruits; kg m^{-2}) of the crops inside screenhouses (IP-13, IP-34 and S-36) and at the open field treatment, during the entire experimental periods of 2011 and 2012.

The pattern of the evolution of the cumulative yield was the same between all treatments, within each period. Differences observed in the pattern of the evolution of the cumulative yield between the two periods. On 2011, on W.A.T. 15 a steep increase of the cumulative yield was observed for all treatments though, in a different rate; while on 2012 a linear increase was observed for all treatments.

In both periods crops inside screenhouse S-36 yielded about the same fresh fruit weight, unlike the rest of the treatments. On 2012 period, from W.A.T. 19 (around September 22) until WAT 21 the harvested yield inside S-36 screenhouse was significantly lower as compared to the IP-34 yield. That resulted to a significant "slow down" phase of the cumulative yield in the S-36 house during that period, which could ascribe to the hysteresis of the final yield of S-36 screenhouse as compared to the IP-34 yield.

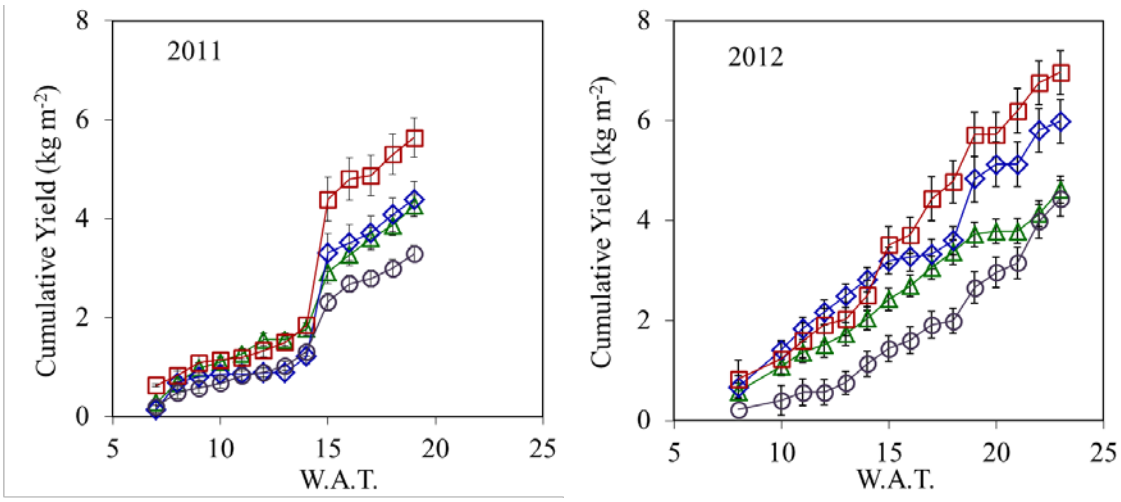

Figure 31. Cumulative yield (kg m^{-2}) during the two cropping periods 2011 (left column) and 2012 (right column). Cont (circles), IP-13 (squares), IP-34 (diamonds) and S-36 (triangles).

6.5.3. Production per harvest and time evolution

In Figure 32 are presented the evolution of the harvested fruits per week of harvest for the crops inside screenhouses (IP-13; IP-34 and S-36) and at the open field (Cont), during experimental periods of 2011 and 2012. During period 2012 strong fluctuations of the number of harvested fruits per week was recorded for all treatments. Analogous fluctuations were not observed during 2011 period.

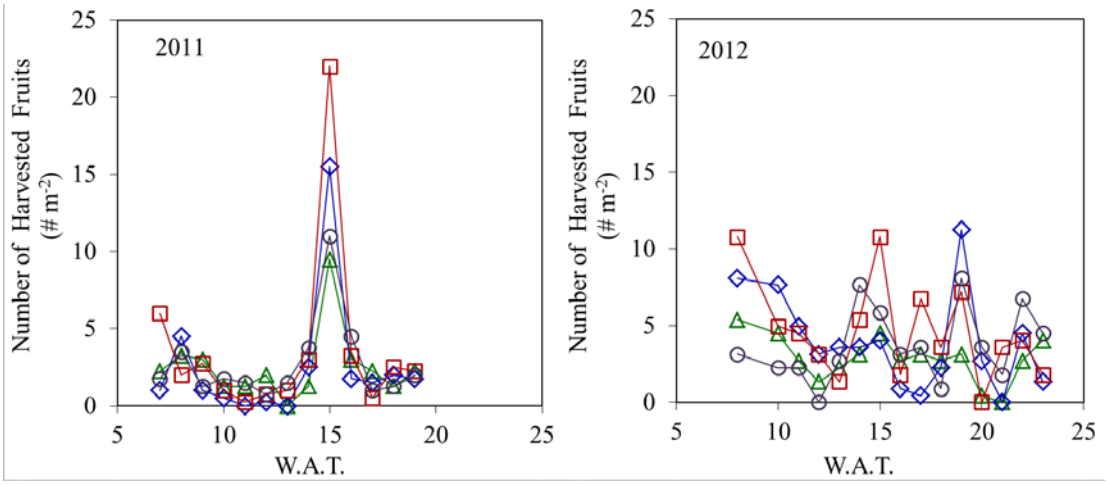

Figure 32. Evolution of the number of harvested fruits (# m^{-2}) per week for the crops inside screenhouses (IP-13; IP-34 and S-36) and at the open field (Cont), during experimental periods of 2011 and 2012.

6.5.4. Yield Quality

The yield quality analysis was conducted in two parts: i) of the fruit size and the fruits defects from biological and non-biological agents (Table 26) on 2012 period. and ii) of the shape, the color and the chemical characteristics (Table 27) on 2011 period.

6.5.4.1. Marketable and non-marketable yield

On each harvesting date, measurements relative to the quality (physical characteristics) of the fruits were carried out on the yield. In Table 26 are presented the marketable production (by excluding all defected fruits), the fruit size (g fruit^{-1}) and defectiveness analysis in terms of defected fruits from sunburn, BER, Thrip and Helicoverpa attacks of total yield of 2012 period.

Table 26. Marketable production and defection analysis (sunburn; BER; Thrip and Helicoverpa attacks) of total yield (Total Fruit number) inside screenhouses (IP-13, IP-34 and S-36) and at the open field treatment at the end of the experimental period on 2012.

	Marketable production as % fraction of		Fruit size	Defects as % fraction of Total Fruit number (# m^{-2})			
	[1]	[2]	[3]				
Treatment	T.F.F.W.	T.Fr.#	g fruit^{-1}	Sunburn	BER	Thrip	Helicoverpa
Cont	59,8^{c}	55,7^{b}	82,1^{b}	14,06^{a}	13,54^{a}	14,06^{a}	2,60^{a}
IP-13	86,9^{b}	86,0^{a}	102,0^{a}	0,80^{b}	8,00^{ab}	5,20^{b}	0,00^{b}
IP-34	90,6^{a}	89,5^{a}	104,4^{a}	1,42^{b}	6,67^{b}	2,38^{b}	0,00^{b}
S-36	89,5^{ab}	87,4^{a}	107,9^{a}	0,00^{b}	7,69^{b}	4,95^{b}	0,00^{b}

$^{a, b, c}$: Means with different superscript letters within the same column are statistically significantly different (a=0.05).

[1] : T.F.F.W. is the Total Fresh Fruit Weight (kg m^{-2}).

[2] : T.Fr.# is the Total Fruit number (# m^{-2}).

[3] : Fruit size as determined from the ratio of (total yield)/(fruit number).

The marketable yield was increased on average about 50%, while fruits were about 28% heavier inside screenhouses as compared to the open field. The fruit sunburn was nearly eliminated inside screenhouses. The defected fruits due to BER were statistically significantly reduced inside IP-34 and S-36 screenhouses. The reduction was enhanced by the increase of the shade factor of the screenhouses. Defects from thrips attacks on fruits surface were also significantly decreased inside

insect proof screenhouses as compared to the open field treatment, as it was been expected. The reduction was two-folded inside the IP-34, though not statistically significant. The UV manipulative anti-insect additives on the threads of that covering screen could be ascribed for the two-folded reduction as opposed to the IP-13 screen (no UV modification). The decreased number of defected fruits inside S-36 screenhouse cannot be ascribed to the ant-insect geometrical characteristics of the shade net that covered that screenhouse. The protection against *Helicoverpa sp.* was been absolute for the crops inside screenhouses, unlike the crop at the open field.

6.5.4.2. Fruit shape, color and chemical characteristics

In Table 27 are presented the dimensions, the color analysis and the chemical quality characteristics of the harvested fruits.

Table 27. Analysis of physical (shape and color) and chemical quality characteristics of harvested fruits from the crops inside screenhouses (IP-13; IP-34; S-36) and from the open field (Cont) during experimental period 2011.

Treatment	N [1]	H [2]	W [2]	L* [3]	a* [4]	b* [5]	c [6]	SS [7]	TA [8]	pH
Cont	80	69,1 ^{c}	63,4 ^{b}	62,5 ^{c}	-9,1 ^{c}	46,1 ^{b}	47,1 ^{b}	5,0 ^{b}	7,7 ^{a}	6,3 ^{b}
IP-13	60	78,2 ^{b}	75,2 ^{a}	60,4 ^{b}	-9,7 ^{b}	44,3 ^{a}	45,4 ^{a}	4,4 ^{a}	7,9 ^{a}	6,1 ^{a}
IP-34	60	78,8 ^{b}	75,4 ^{a}	58,7 ^{a}	-10,1 ^{a}	43,5 ^{a}	44,7 ^{a}	4,5 ^{a}	7,8 ^{a}	6,2 ^{b}
S-36	60	83,4 ^{a}	75,0 ^{a}	57,9 ^{a}	-10,0 ^{ab}	43,6 ^{a}	44,7 ^{a}	4,4 ^{a}	7,8 ^{a}	6,1 ^{a}

$^{a, b, c}$: Means with different superscript letters within the same column are statistically significantly different (a=0.05).

[1] N: number of samples,

[2] H, W: Height (length of vertical axis) and Width (length of horizontal axis)

[3] L*: gives the difference between light (L* = 100) and dark (L* = 0).

[4] a*: gives the difference between green (a* = -50) and red (a* = 50).

[5] b*: gives the difference between yellow (b* = 50) and blue (b* = -50).

[6] c: indicates color saturation or intensity as calculated by eq. 5.

[7] SS: Soluble Solids (%)

[8] TA: Titratable Acidity (meq/100 mL sap).

The ratio H:W (i.e., vertical to horizontal axis) determines the shape of the fruits. As it can be seen in the Table 27, harvested fruits were slightly elongated inside the insect proof screenhouses (IP-13: 1.04; IP-34: 1.05), while they were significantly elongated in the open field (Cont; 1.09) and inside screenhouse S-36 (1.11).

Fruits harvested inside screenhouses were statistically significantly darker (L: 57.9-60.4) as compared to those harvested from the open field treatment (L: 62.5). The darkness of the fruit color was enhanced with the increase of the shade factor of the screenhouses. Moreover, fruits from screenhouses were statistically significantly "more green" (a*= -9.9) and "less yellow" (b* = 43.8) compared to those harvested from the open field (a* = -9.1 and b* = 46.1). Furthermore, the color of fruits harvested from the open field treatment was statistically significantly more saturated compared to those harvested from the crops inside screenhouses, as can be derived from the higher c values.

The total Soluble Solids (SS) in the fruit sap were slightly reduced under screenhouse conditions, while Titratable Acidity (TA) did not present significantly differences between the four treatments.

6.6. Water Use Efficiency

The irrigation water and the precipitation accumulation during both experimental years had been monitored. Thus, the Water Use Efficiency (WUE) and the Irrigation WUE (IWUE; kg m^{-3}) of the crops inside screenhouses and at the open field were calculated. WUE is defined as the ratio of the total harvested fresh fruit weight to the total water provided to the crop by irrigation and from the precipitation, during the cropping period. IWUE is defined as the ratio of the total harvested fresh fruit weight to the total irrigation water provided to the crop during the cropping period. In Table 28 are presented the seasonal yield, irrigation water, IWUE and WUE for the open field treatment (Cont) and inside screenhouses (IP-13, IP-34 and S-36), for the two experimental periods (2011 & 2012).

Table 28. Seasonal yield, irrigation water, IWUE and WUE for the open field treatment (Cont) and inside screenhouses (IP-13, IP-34 and S-36), for the two experimental periods (2011 & 2012).

	2011				2012			
Treatment	Yield (kg m^{-2})	Seasonal Irrigation (mm)	IWUE (kg m^{-3})	WUE (kg m^{-3})	Yield (kg m^{-2})	Seasonal Irrigation (mm)	IWUE (kg m^{-3})	WUE (kg m^{-3})
Cont	3,3^{a}	496	6,6^{b}	5,2^{b}	4,4^{a}	602	7,4^{c}	6,9^{c}
IP-13	5,6^{a}	372	15,2^{a}	11,1^{a}	7,0^{b}	418	16,7^{a}	15,3^{a}
IP-34	4,4^{a}	283	15,5^{a}	10,5^{a}	6,0^{b}	341	17,5^{a}	15,8^{a}
S-36	4,3^{a}	306	13,9^{a}	9,7^{a}	4,6^{a}	350	13,2^{b}	11,9^{b}

$^{a, b, c, d}$: Means with different superscript letters are statistically significant different (a=0.05)

The statistical analysis of the results revealed that the IWUE increased significantly inside screenhouses, been on average about 2.3 and 2.1 higher compared to the IWUE at the open field on 2011 and 2012, respectively. On 2012 the IWUE inside the insect proof screenhouses was significantly higher compared to the S-36 screenhouse. This could be attributed to the statistically significant differences of the yield of these treatments on 2012. Similarly to IWUE, the WUE was significantly increased inside screenhouse, been on average about the double, on both periods, compared to the WUE of the open field treatment (Cont).

The pooled data of the cumulative yield ($Y_{c,}$; kg m^{-2}) for the two experimental periods (2011 and 2012) for each respective treatment, were plotted against the

irrigation water (W_{irr}; m^3 m^{-2}) that was provided to the crops (Figure 33). The IWUE during those experimental periods for each treatment was estimated by fitting the data of the cumulative yield and irrigation water to the following equation using Marquardt's algorithm:

eq. 41: $Y_c = IWUE * W_{irr} \pm const$

where, $const$ is the intercept implied by the non-linear regression analysis.

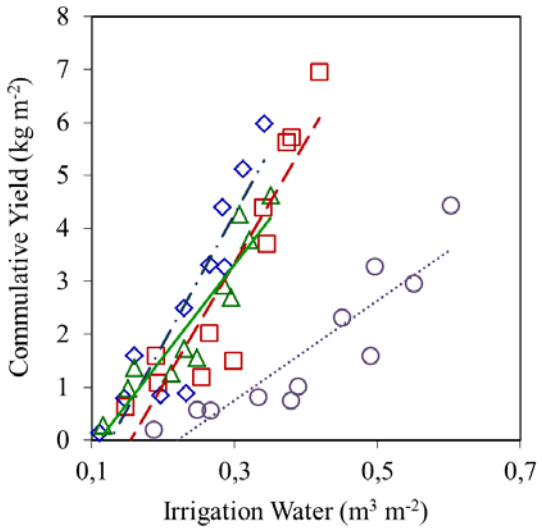

Figure 33.Cumulative yield ($Y_{c,}$; kg m^{-2}) against irrigation water (W_{irr}; m^3 m^{-2}) for the open field (Cont; circles) and the screenhouses (IP-13; squares, IP-34; diamonds and S-36; triangles) pooled for the two experimental periods (2011 & 2012). The lines represent the best fit regression line for each group of data; Cont: dotted line, IP-13: red-dashed line, IP-34: blue-dash-dotted line and S-36: green-solid line.

The equations of the best fit regression lines presented in Figure 33 were:

eq. 42: $Y_{c,Cont} = 9.5\ (\pm 1.45) * W_{irr} - 2{,}1\ (\pm 0.61)\ , with\ R^2 = 0.83$

eq. 43: $Y_{c,IP-13} = 23.3\ (\pm 3.30) * W_{irr} - 3.6\ (\pm 1.00)\ , with\ R^2 = 0.85$

eq. 44: $Y_{c,IP-34} = 24.8\ (\pm 3.71) * W_{irr} - 3.1\ (\pm 0.90)\ , with\ R^2 = 0.83$

eq. 45: $Y_{c,S-36} = 17.7\ (\pm 2.21) * W_{irr} - 2.0\ (\pm 0.56)\ , with\ R^2 = 0.88$

for Cont, IP-13, IP-34 and S-36, respectively. The values given in parenthesis correspond to the standard error of slope and intercept, respectively. The slope for all cases was statistically significant (a = 0.05). The intercept of each regression line

corresponds to the irrigation water that should be applied until the first harvest of ripened fruits. A t-test (Dagnelie, 1986) was performed to compare the slope of the best fit regression lines for all three screenhouses (eq. 43 - eq. 45) and was revealed that the values were not statistically different (data not shown). Therefore, the data from the screenhouses were pooled and the new correlation found between the cumulative yield ($Y_{c,PldSc}$) and irrigation water ($W_{irr,PldSc}$) for all screenhouses (PldSc) as following:

eq. 46: $Y_{c,PldSc} = 19.7\ (\pm 1.71) * W_{irr,PldSc} - 2.3\ (\pm 0.43)\ ,\ with\ R^2 = 0.81$

6.7. Growth analysis

6.7.1. Dry matter production

Figure 34 presents the evolution of total dry matter (aerial dry matter) production along with the dry matter distributed to different plant's organs (leaves, stems and fruits), during the two experimental periods (2011 and 2012). The rate of the increase of the total dry matter production is mainly influenced by the corresponding rate of the fruits dry matter. Total dry matter evolution is about the same for all treatments from the first destructive measurements up to about W.A.T. 15, where a significant and steep increase of the rate of the increase of the total dry matter is observed for the crop inside screenhouse IP-13, on both experimental periods (2011 and 2012). This steep increase could be attributed to the corresponding increase of the yield (Figure 31,on page 93; Figure 32, on page 94), which resulted in an analogous increase of fruit dry matter (Figure 34 - 2nd row) of the crop inside this screenhouse, compared to the other three treatments (Cont, IP-34 and S-36). During experimental period of 2011 the evolution of the total dry matter of Cont, IP-34 and S-36 presented the same pattern and the measured values did not differed statistically significant in each destructive measurement date. The dry matter allocated in the fruits that is presented in Figure 34 stands for the dry matter of the total number of fruits (Total Fruits' Dry Matter) produced on the plants ((i) the dry matter allocated to the mature harvested fruits during each experimental period + (ii) the dry matter allocated to the fruits that were attached on the plants on the day of the destructive measurement).

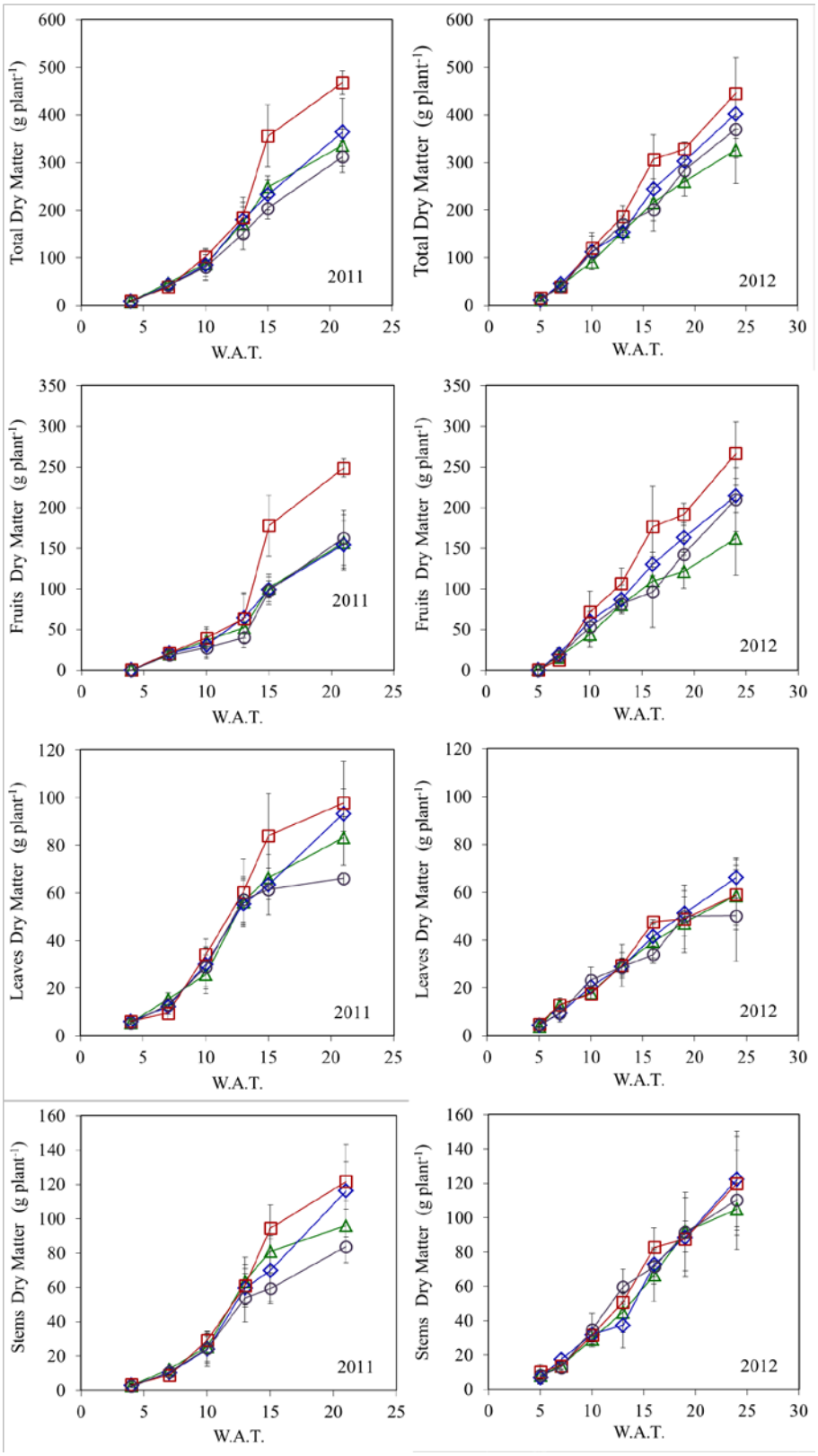

Figure 34. Evolution of total dry matter (1st row; g plant^{-1}) and dry matter (g plant^{-1}) allocated in the different plant organs (fruits (harvested+presented fruits): 2nd row; leaves: 3rd row; stems: 4th row) during the two experimental periods (2011: left column; 2012: right column). Cont (circles), IP-13 (squares), IP-34 (diamonds) and S-36 (triangles). Vertical bars stand for standard deviation (Stdv) of the respective mean values.

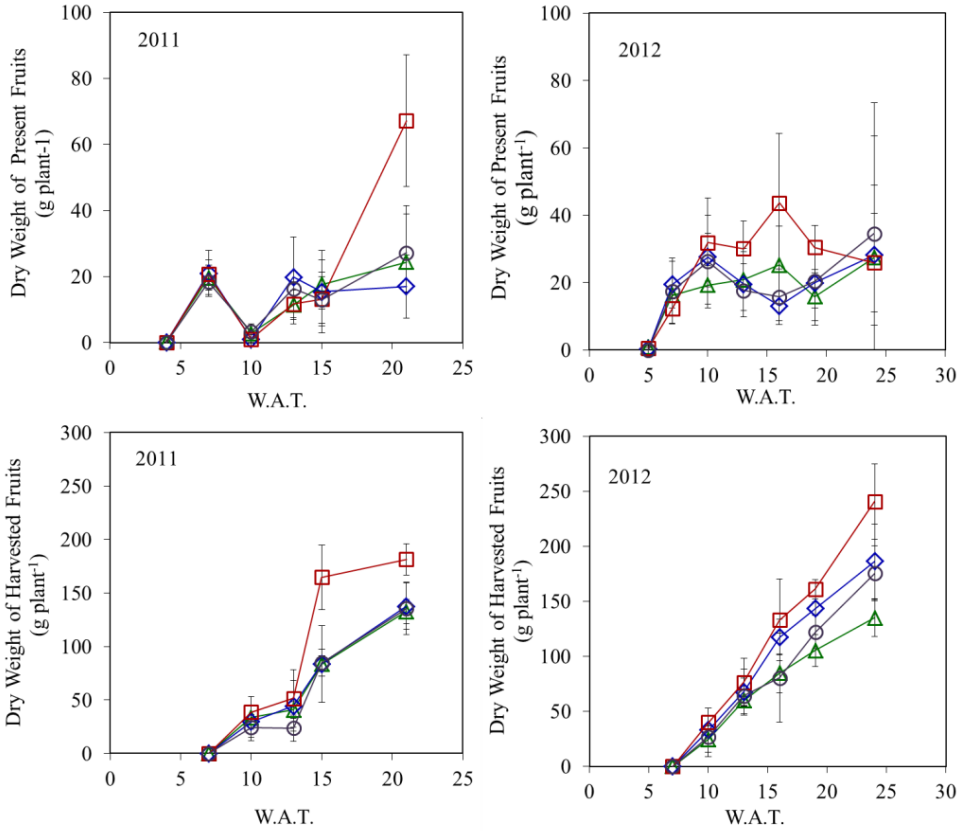

Figure 35. Evolution of fruit dry matter production per plant during the two cropping periods 2011 (left column) and 2012 (right column). 1st row: Fruits presented/attached to the plants on the day of the destructive measurement; 2nd row: harvested mature fruits during each experimental period until the day of the destructive measurement. Cont (circles), IP-13 (squares), IP-34 (diamonds) and S-36 (triangles). Vertical bars stand for standard deviation (Stdv) of the respective mean values.

In Table 29 is been presented the total dry mater production (DMP) along with the dry matter allocated in the vegetative (leaves and stems) and reproductive organs (fruits) of the plants for each treatment at the end of the two experimental periods. The latter dry matter of fruits is the sum of the dry matter allocated in the present (attached) fruits on the plant on each date of destructive measurement and the sum of the dry matter of the harvested fruits per plant until the date of the destructive measurement i.e., the date that the plant was cut off just above the soil surface. In both periods, crops inside IP-13 screenhouse produced statistically significantly greater amounts of total dry matter compared to the other three treatments (Cont, IP-34 and S-36). Moreover, the crops inside IP-34 screenhouse produced more dry matter than the S-36, but these differences were not statistically significant. Total DMP, on average for both experimental periods (2011 and 2012), of the crop inside IP-13 and IP-34 was 34% and 12%, respectively, more than the total DMP of the crop at the

open field (Cont), while total DMP, of the crop inside S-36 screenhouse was 3% less than the corresponding of the control (Cont).

Table 29. Total dry matter production and dry matter distribution to different organs (fruits, leaves and stems) per plant in the open field treatment (Cont) and inside screenhouses (IP-13, IP-34 and S-36), for 2011 and 2012.

	2011				2012			
	Total	Fruits	Leaves	Stems	Total	Fruits	Leaves	Stems
Treatment	g plant^{-1}	g plant^{-1}	g plant^{-1}	g plant^{-1}	g plant^{-1}	g plant^{-1}	g plant^{-1}	g plant^{-1}
Cont	312,6^{b}	162,7^{b}	66,0^{b}	83,9^{c}	370,5^{ab}	209,9^{ab}	50,2^{a}	110,4^{a}
IP-13	468,2^{a}	248,6^{a}	97,8^{a}	121,8^{a}	445,6^{a}	266,5^{a}	59,1^{a}	120,1^{a}
IP-34	364,3^{b}	154,7^{b}	93,3^{a}	116,3^{ab}	403,0^{ab}	214,6^{ab}	66,1^{a}	122,4^{a}
S-36	336,6^{b}	157,1^{b}	83,3^{ab}	96,3^{bc}	326,4^{b}	162,5^{b}	58,7^{a}	105,2^{a}

$^{a, b, c}$: Means with different superscript letters are statistically significantly different (a=0.05)

The final values of the dry matter allocated in fruits (harvested + presented) was greater in 2012 compared to the respective of 2011 (Table 29), something that could be attributed to the greater yield and weight per fruit observed in 2012 (Table 25, on page 92; Table 26, on page 95). The dry matter allocated in fruits was on average for both experimental periods (2011 and 2012), for the crops inside IP-13 screenhouse 38% more than the fruits' dry matter of the crops at the open field (Cont), while dry matter of the fruits produced inside S-36 screenhouse was 4% less than the corresponding of the control (Cont). Fruits dry matter of the crop inside screenhouse IP-34 was about the same compared to the fruits dry matter of the fruits of the control (Cont), on average for both experimental periods (2011 and 2012). Leaves dry matter is smaller in 2012 compared to 2011, which can be ascribed to the lesser number of leaves developed in the 2nd cropping period compared to the corresponding of the 1st period (Figure 29, on page 88).

Stems dry matter is about the same for all treatments during the entire experimental period of 2012, while in 2011, from W.A.T. 15 until the end of the period there are statistically significant differences between the four treatments (Figure 34, on page 102). At the end of the period dry matter allocated in stems inside insect-proof screenhouses was 0.75 on average of the corresponding average inside S-36 and at the open field.

6.7.2. Dry matter partitioning

In Figure 34 are presented the evolution of the dry matter partitioning (ratio of dry matter of an organ to the total dry matter of the plant) during experimental period 2012.

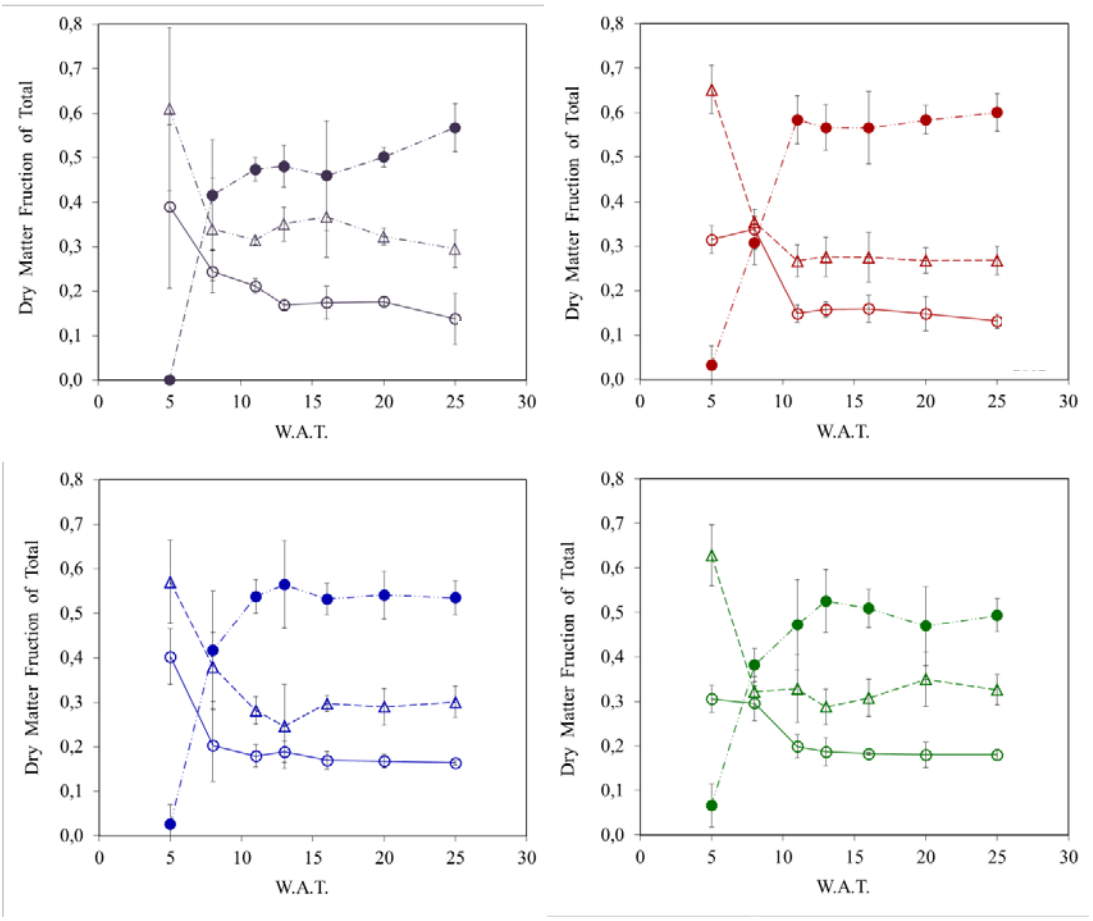

Figure 36. Dry matter partitioning per plant in the open field treatment (Cont: A) and inside screenhouses (IP-13: B; IP-34: C; S-36: D), during 2012. Fruits (closed circle); Stems (triangles); Leaves (open circles).

The fraction of dry matter of the vegetative organs (stems and leaves) is steadily decreasing and reaches a plateau from W.A.T. 11 until W.A.T. 25 (24 July until 25 30 October), while the fraction of the dry matter allocated in the fruits is steadily increasing and reaches a plateau at the same period (W.A.T. 11 – 25). At this period the dry matter allocated in the fruits is 58%, 54%, 49% and 50% of the total plant dry matter for IP-13, IP-34, S-36 and Cont respectively. In 2011, dry matter partitioning followed about the same trend, whereas the fraction of dry matter allocated into fruits at the plateau reached values of 50%, 43%, 40% and 48% for IP-13, IP-34, S-36 and Cont respectively. This difference in the dry matter partitioning between the two

experimental years could be attributed to the enhancement of vegetative growth during 2011 period by the incident precipitations, as severe flower abortion had been observed after every rainfall (data not recorded). The increased vegetative growth is mainly supported by the increased dry matter allocated in leaves (Figure 34; Table 29) due to the increased number of leaves per plant measured in 2011 on page 88).

6.7.3. Dry matter content

In Table 30 is been presented the dry matter content of vegetative (leaves and stems) and reproductive organs (harvested fruits and presented fruits at the time of the destructive measurements) for 2011 and 2012.

Table 30. Dry matter content of vegetative (leaves and stems) and reproductive organs (harvested fruits and presented fruits at the time of the destructive measurements) for 2011 and 2012.

	2011				2012			
	Stems	Leaves	Presented Fruits	Harvested Fruits	Stems	Leaves	Presented Fruits	Harvested Fruits
Treatment	%	%	%	%	%	%	%	%
Cont	22,8 [a]	16,7 [ab]	5,9 [a]	7,5 [b]	24,5 [a]	21,3 [a]	5,8 [a]	6,6 [b]
IP-13	21,4 [a]	16,7 [ab]	6,1 [a]	5,8 [a]	23,7 [a]	17,1 [a]	11,6 [a]	6,0 [a]
IP-34	23,0 [a]	17,4 [b]	6,3 [a]	5,8 [a]	23,5 [a]	16,8 [a]	8,1 [a]	5,6 [a]
S-36	21,2 [a]	15,6 [a]	6,2 [a]	5,6 [a]	23,5 [a]	18,0 [a]	7,0 [a]	5,8 [a]

[a, b, c] : Means with different superscript letters are statistically significantly different (a=0.05).

The dry matter content of harvested fruits was on average on both experimental periods 5.8% and 7.1% for the crops inside screenhouses and at the open field, respectively. The values for the crops inside screenhouses on each period were statistically significant different compared to the corresponding value of the open field treatment. The dry matter content of the fruits at the open field treatment was statistically significantly higher than the respective inside the screenhouses. No statistically significant differences in fruit DM yield were recorded between the moderate (IP-13) and the heavy shaded screenhouse treatments (IP-34 and S-36), in each period.

6.8. Modeling Dry Matter Production

6.8.1. Model calibration

An attempt to calibrate a model that predicts the dry matter production (DMP; g m^{-2}) using as input only the cumulative intercepted PAR (c-PARi; MJ m^{-2}) was done. The calibration of the model conducted by means of Marquardt (1963) algorithm (non-linear regression) for groups of data (DMP; c-PARi) measured through 2011 experimental period (Figure 37). The equation of the best fit regression line was linear $y = a\,x$, where $y = \text{DMP}$; $a = \text{RUE}$; $x = c - \text{PARi})$ and for each specific treatment holds as following:

eq. 47, Cont : $\text{DMP} = 1.05\ (\pm 0.0220\ \text{St. Error}) \times (c - \text{PARi}),$ with $R^2 = 0.99$

eq. 48, IP-13: $\text{DMP} = 1.44\ (\pm 0.0631\ \text{St. Error}) \times (c - \text{PARi}),$ with $R^2 = 0.98$

eq. 49, IP-34: $\text{DMP} = 1.41\ (\pm 0.0449\ \text{St. Error}) \times (c - \text{PARi}),$ with $R^2 = 0.99$

eq. 50, S-36: $\text{DMP} = 1.26\ (\pm 0.0128\ \text{St. Error}) \times (c - \text{PARi}),$ with $R^2 = 1.00$

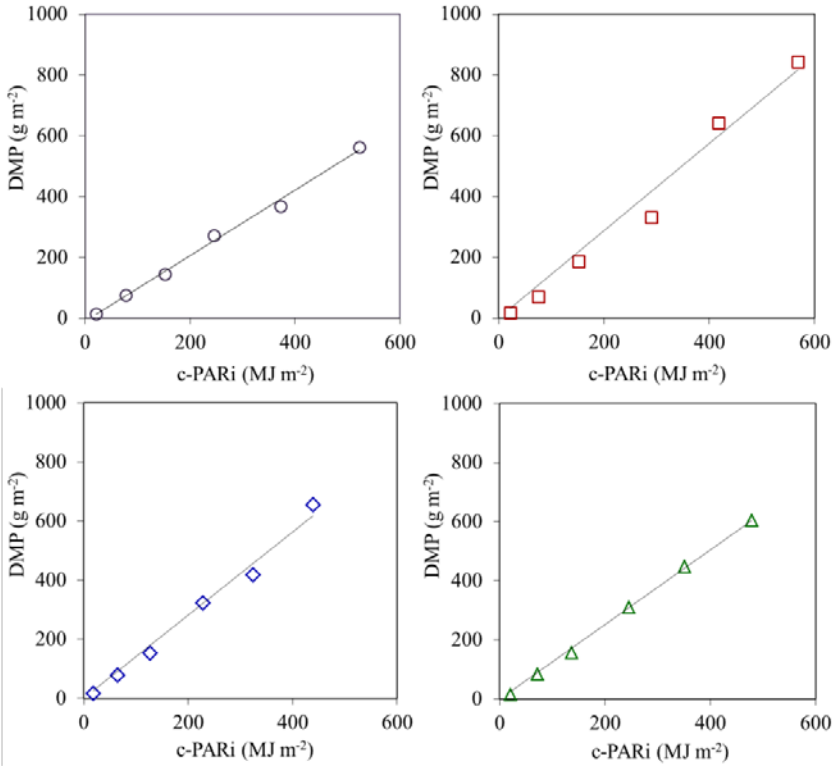

Figure 37. Dry matter production (DMP) against cumulative intercepted PAR ($c - \text{PARi}$) for the crops inside screenhouses (IP-13: squares; IP-34: diamonds; S-36: triangles) and at the open field (Cont: circles) during calibration period (2011). The straight lines stand for the best fit regression line for the group of data DMP and c-PARi of each treatment.

There was very good agreement between the simulated and measured values of DMP throughout the calibration crop (2011; Table 32; Figure 38). The model perfectly simulates the measured values for the crop inside the S-36 screenhouse, while slightly under-estimates by about 3% the DMP of the crops at the open-field and inside IP-13 and by 6% the respective value inside IP-34 screenhouse.

A t-test analysis (Dagnelie, 1986) for the estimates revealed that IP-13 and IP-34, were not significantly different one each other. Therefore, an additional calibration was conducted using pooled data (Pld-IPs) from IP-13 and IP-34 treatments. The best fit regression line for the case of Pld-IPs was:

eq. 51, Pld-IPs: $\mathrm{DMP} = 1.43\ (\pm 0.0386) * (\times\ (\mathrm{c} - \mathrm{PARi})), \quad \text{with } R^2 = 0.99$

Moreover, the respective t-test analysis revealed that the estimate for the Pld-IPs case was significantly different from the estimates for the Cont and S-36 case.

Table 31. Statistical comparison by means of t-test analysis (Dagnelie, 1986), between the estimates of eq. 47- eq. 50.

Comparison pairs	t-value	Total df	Critical t-value	Difference
Cont - IP13	5,78	10	2,23	Y
Cont - IP34	7,20	10	2,23	Y
Cont - S36	8,41	10	2,23	Y
IP13 - IP34	***0,34***	***10***	***2,23***	***N***
IP13 - S36	2,68	10	2,23	Y
IP34 - S36	3,13	10	2,23	Y
S-36 – Pld-IPs	**4,00**	**16**	**2,12**	**Y**
Cont - Pld-IPs	**8,48**	**16**	**2,12**	**Y**
IP13 - Pld-IPs	*0,13*	*16*	*2,12*	*N*
IP34 - Pld-IPs	*0,96*	*16*	*2,12*	*N*

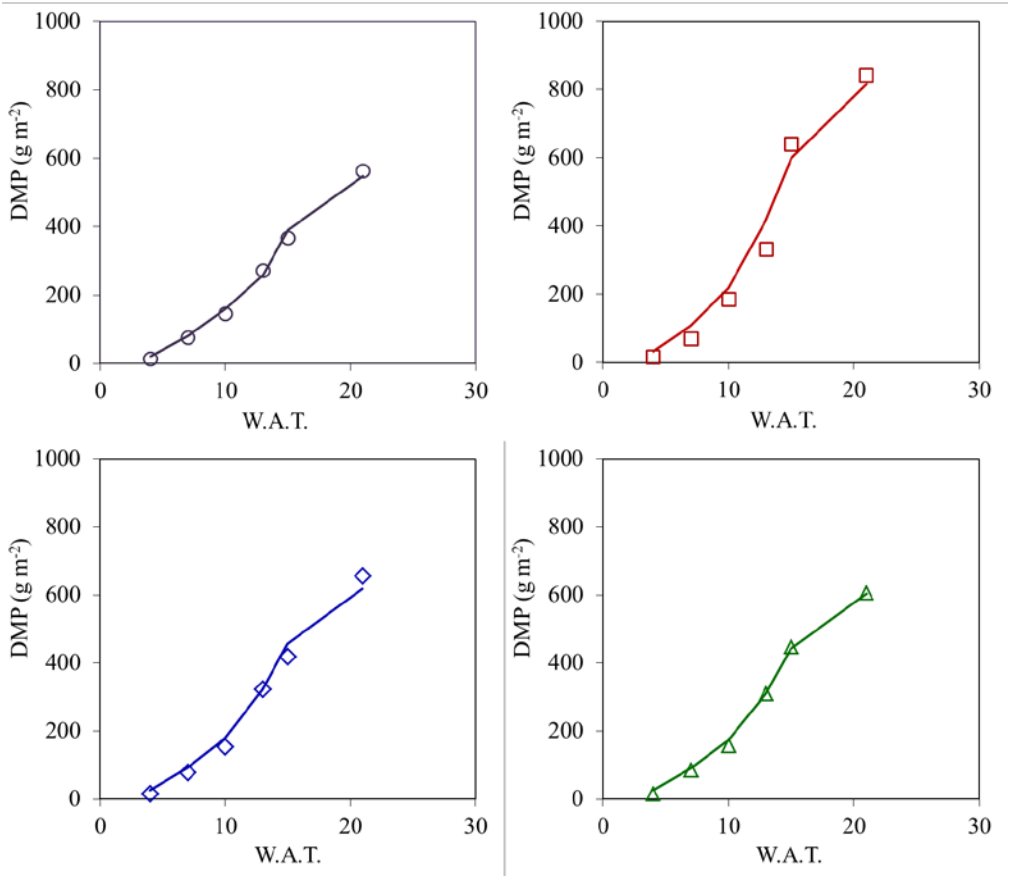

Figure 38. Evolution of measured (data points) and simulated (curves) Dry Matter Production (DMP; g m^{-2}) during the calibration period (2011). Cont (circles), IP-13 (squares), IP-34 (diamonds) and S-36 (triangles).

Table 32. For each treatment, measured and simulated values of the final dry matter production (DMP; g m^{-2}), their relative difference (RD) and the slope of the best fit regression line of calculated vs measured DMP values through the calibration period (2011). In the parenthesis are indicated the respective values calculated using the model for Pld-IPs case for IP-13 and IP-34 data.

Parameter	Cont	IP-13	IP-34	S-36
Measured	563	843	656	606
Calculated	548	816 *(811)*	619 *(626)*	604
RD	-0,03	-0,03 *(-0,04)*	-0,06 *(-0,05)*	0,00
m	1,00	0,99 *(0,98)*	1,00 *(1,01)*	1,00
R^2	0,99	0,97 *(0,97)*	0,99 *(0,99)*	1,00

[1] RD: relative difference i.e., difference of simulated minus measured as a fraction of the measured value.
[2] m and [3] R^2 are the slope and the coefficient of determination of the best fit regression line between measured and simulated values.

6.8.2. Model validation

The model for each treatment was validated for data from experimental period 2012. The measured values for 2012 period were plotted (1:1 plots) against calculated values by eq. 47 - eq. 50 (Figure 39, (A; B; C; D)).

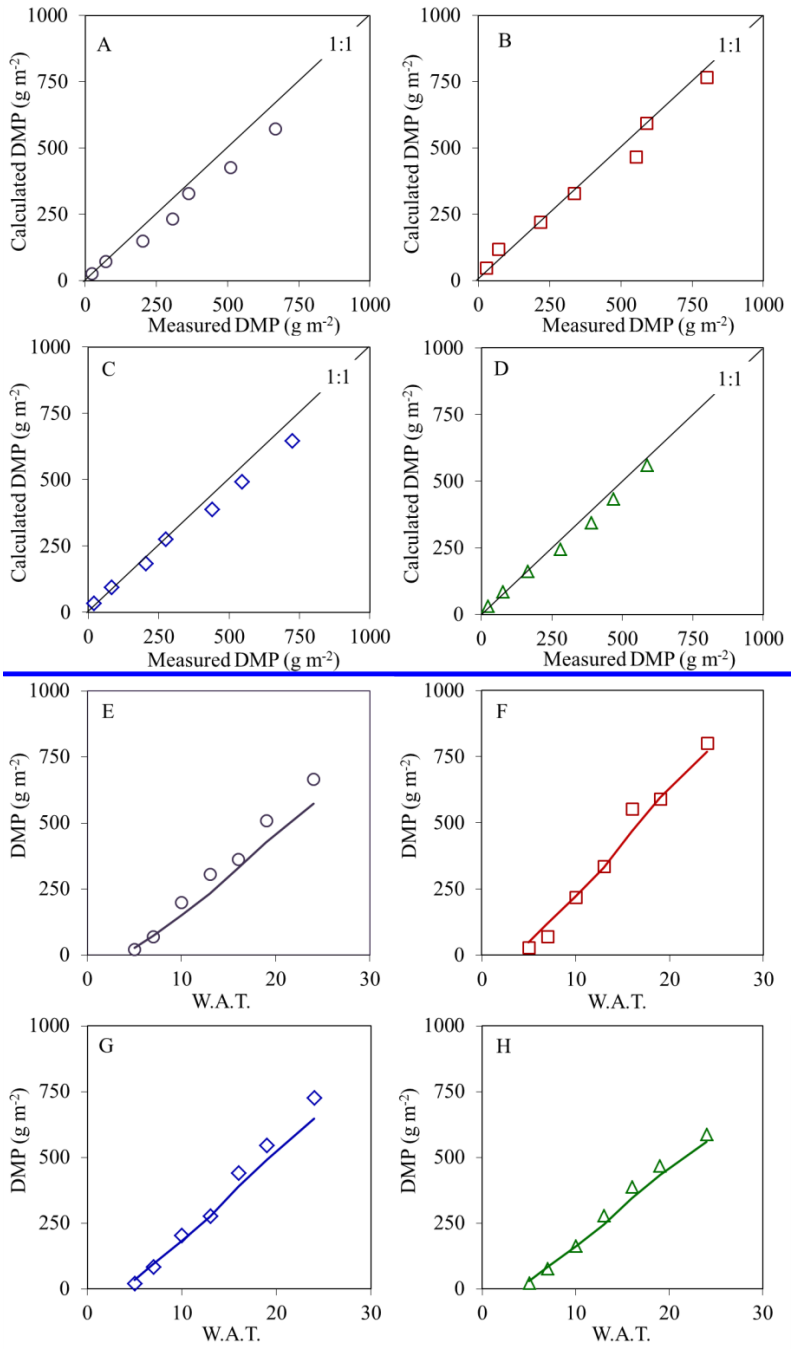

Figure 39. Upper set (A; B; C; D): Measured against simulated Dry Matter Production (DMP; g m^{-2}) during experimental period 2012. Diagonal lines are the 1:1 line. Lower set (E; F; G; H): Evolution of measured (data points) and simulated (curves) Dry Matter Production (DMP; g m^{-2}) during experimental period 2012. Cont (circles), IP-13 (squares), IP-34 (diamonds) and S-36 (triangles).

The statistical indices of the validation process that were calculated after Stöckle et al. (2004) are presented in Table 33. The performances of the models for the crops inside screenhouses were evaluated as good (eq. 48; eq. 49) and very good (eq. 50), unlike the performance of the model for the open field treatment that was graded as poor (eq. 47).

Table 33. Summary of statistical indices of the validation of the model using data of the validation period (2012). In the parenthesis are indicated the respective values calculated for the validation of the model for Pld-IPs case using data of IP-13 and IP-34 cases, separately for each case.

[1]Validation set	[2]n	[3]RMSE	[4]RE	[5]d	[6]m	[7]R^2	[8]Performance
Cont into eq. 47	7	59,481	0,19	0,98	0.84	0,99	poor
IP-13 into eq. 48	7	39,885	0,11	0,99	0.95	0,98	G
IP-13 into eq. 51 (Pld-IPs model)	*(7)*	*(41,406)*	*(0,11)*	*(0,99)*	*(0.95)*	*(0,98)*	*(G)*
IP-34 into eq. 49	7	42,117	0,13	0,99	0.91	0,99	G
IP-34 into eq. 51 (Pld-IPs model)	*(7)*	*(38,340)*	*(0,12)*	*(0,99)*	*(0.92)*	*(0,99)*	*(G)*
S-36 into eq. 50	7	27,356	0,10	0,99	0.93	1,00	VG

[1]Validation set: data set of each respective treatment fitted into the respective model, ex.; Cont data fitted into the respective model for Cont treatment is written into the table as: "Cont into eq. 47."
[2]n: is the number of data; [3]RMSE: root mean square error; [4]RE: relative error; [5]d: Wilmott index of agreement; [6]m and [7]R^2: slope and coefficient of determination, respectively, of the best fit regression line between simulated and measured values. [8]Performance: VG (very good), G (good), ACC (acceptable). Performance was evaluated using the criteria of (Stöckle et al., 2004).

The DMP of the crops inside IP-13 and S-36 screenhouse are slightly under-estimated (5% and 3%, respectively) by the respective models. The under-estimation for the DMP of the crop inside IP-34 screenhouse (9%) is relatively greater than those previously mentioned. The validation of the model that was calibrated using pooled data (Pld-IPs) measured from the crops of IP-13 and IP-34 is also presented in Table 33. The validation was conducted separately for the data of each specific case. The adoption of the Pld-IPs model slightly improved the RE and m only for the IP-34 case, unlike its general performance that was unchanged, according to the overall scheme of performance evaluation (Giménez et al., 2012).

The evolution in time (W.A.T.) of the simulated and measured values of DMP for all treatments during the validation period 2012 is presented in Figure 39 (Lower set (E; F; G; H)). There is a fairly good fit of the curves of the simulated values of DMP for the crop inside IP-13 and S-36 screenhouse. The observed deviation of the simulation curve from the measured data points of DMP by the crop inside IP-34 screenhouse is due to the underestimation of the DMP by about 12% (on average) from W.A.T. 16 until the end of the validation period (2012; W.A.T. 24). The simulated values of the DMP of the crop at the open field were systematically significantly under-estimated from W.A.T. 10 until the end of the period, as clearly presented by the deviation of the curved line (simulated values) from the marks (measured values) in Figure 39.

6.8.3. Radiation Use Efficiency

The seasonal Radiation Use Efficiency (RUE; g MJ^{-1}) of crops inside screenhouses (IP-13; IP-34; S-36) and at the open field that was estimated through the calibration period 2011 and validated for data measured through period 2012 was 1.05, 1.44, 1.41 and 1.26 for Cont, IP-13, IP-34 and S-36, respectively (section 6.8.1., eq. 47 - eq. 50). The protected crops by the highly diffusive insect screens (IP-13 and IP-34) and by the moderate diffusive shade net (S-36) utilized solar radiation by about 36% and 20%, respectively, greater efficiency as compared to the respective efficiency of the open field crop.

7. Discusion

7.1. Microclimate

7.1.1. Precipitation

In Figure 40 the precipitation rate during each experimental period is presented. On 2011 the precipitation occurrences were rather unusual for Greek summer period, as it was presented high rates at mid-June and at the beginning and end of August. On 2012 the summer was rather dry. The raining and windy weather observed during the beginning of the experimental period 2012 affected negatively the crop grown under open field conditions (optical observations).

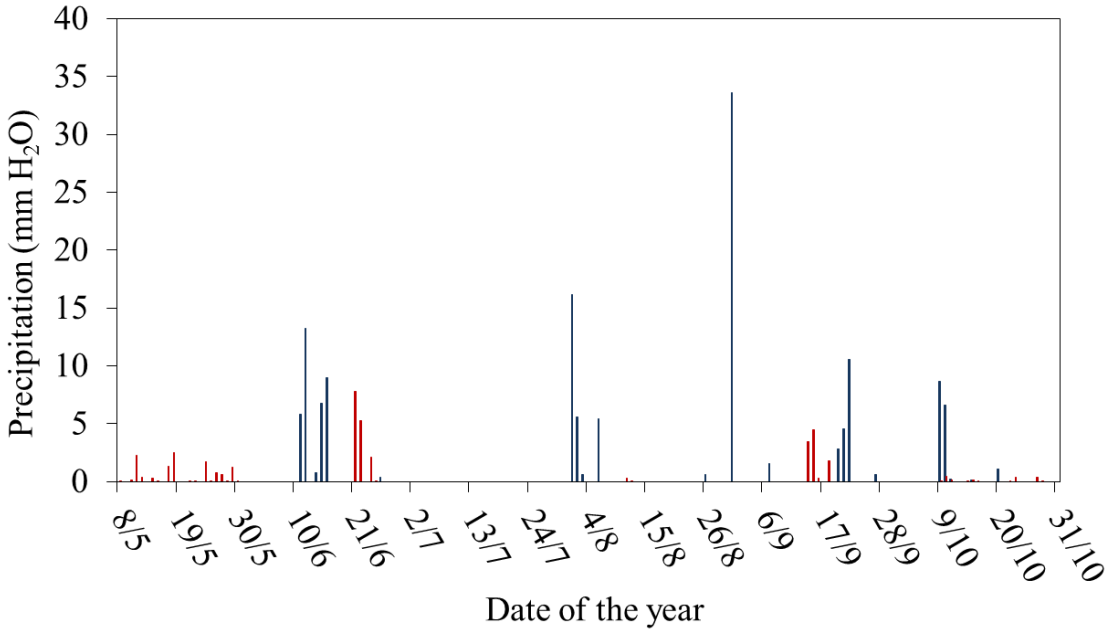

Figure 40. Precipitation rates during experimental year 2011 (blue bars) and 2012 (red bars).

7.1.2. Air temperature and vapor pressure deficit

The screenhouse enclosure seems to be cooler than the ambient in the case of the heavy shaded screenhouses (IP-34; S-36), while only after September 10 screenhouse IP-13 managed to be cooler than the ambient. Screenhouse IP-13 was warmer (0.4-0.9 ^{o}C) than the ambient from the commence of the experimental period until 23 of July (DAT 79), while IP-34 had about the same air temperature as the ambient. The screenhouse enclosure seems to be cooler than the ambient in the case of the heavy shaded screenhouses (IP-34; S-36), while only after September 10 screenhouse IP-13 managed to be cooler than the ambient. Screenhouse IP-13 was warmer (0.4-0.9 ^{o}C) than the ambient from the commence of the experimental period

until 23 of July (DAT 79), while IP-34 had about the same air temperature as the ambient. The greater air temperature inside IP-13 screenhouse as compared to the ambient could probably be ascribed to the insufficient transpirational cooling of its crop until that time. From the end of July the air temperature of the two insect proof screenhouses differed from 0.2 up to 0.4 ^{o}C, with the air inside screenhouse IP-13 been warmer and inside IP-34 cooler than the ambient. Up to that date (23 of July; DAT 79), the crop was successfully established and had developed a large canopy (about 110-120 leaves plant^{-1}; Figure 29, on page 88). The transpirational cooling effect of the well-developed canopy seemed to contribute enough to the reduction of the air temperature inside the IP-13 screenhouse. Therefore, the air temperature inside IP-13 was better regulated, been about the same as the ambient air temperature. It is very distinguishing that during the hottest period of the 2012 summer (July 6 until August 9) inside to outside air temperature difference is steadily decreasing until 0.1 ^{o}C, while during the hottest week (August 6 ±3 days; weekly mean air temperature ≈ 36.0 ^{o}C) of that summer, screenhouse IP-13 was 0.2 ^{o}C warmer and IP-34 was 0.3 ^{o}C cooler than the ambient. As both enclosure presented the same ventilation rates (Figure 27, on page 85; eq. 35eq. 36, on page 85), due to their equal porosities (0.46) the observed difference between their air temperature could be ascribed to the different heat loads form solar radiation due to their different radiation transmittance. Similarly, Romacho et al. (2006) reported that the higher transmittive screenhouse was slightly warmer as opposed to the lower transmitive house. Screenhouse S-36 seemed to be about 0.8 ^{o}C on average cooler than the insect proof screenhouses from the mid-June until mid-September. This could be ascribed to the greater air exchange rate observed in that screenhouse (Figure 27, on page 85) due to the larger size of holes of the covering shading net compared to the insect proof screens (Figure 3, on page 29). During October, where the energy of the incident global solar radiation was significantly decreased (Table 9 on page 63) the air temperature inside all screenhouses are about equal to each other and about 0.3^{o}C lower than the ambient air temperature.

The daily evolution of inside-to-outside air temperature difference air temperature (δT_{air}; ^{o}C) and inside-to-outside vapour pressure deficit difference (δD_{air}; kPa) inside screenhouses were presented in Figure 13 (on page 59). During the daytime interval between 08:00 and 20:00 the air inside screenhouse S-36 was steadily cooler than the ambient by on average 0.49 ^{o}C. Inside the insect proof

screenhouses IP-13 and IP-34, between 08:00 and 14:00 h, the air was warmer by about 0.33 ^{o}C and 0.10 ^{o}C, respectively. Only after 14:00 until 20:00 the air became cooler than the ambient by 0.20 ^{o}C and 0.54 ^{o}C, inside IP-13 and IP-34, respectively. This delayed decrease of the insect proof screenhouses could probably been attributed to the lower ventilation rates of these enclosures as compared to the S-36 screenhouse (Figure 27, on page 85).

Furthermore, screen IP-34 seems to affect the cooling process more efficiently as compared to the IP-13, since the maximal and minimal δT_{air} between 08:00 and 19:00 were +0.57 ^{o}C and -0.64 ^{o}C, respectively, whilst the mean daily δT_{air} was -0.07 ^{o}C. On the other hand, the T_{air} inside screenhouse IP-13 was about the same as the ambient T_{air}, since the daily (08:00-20:00 h) δT_{air} was -0.04 ^{o}C. Since the transpirational cooling is the only means to regulate the T_{air} of the enclosures, it seems that the greater net radiation incident to the crop inside screenhouse IP-13, as compared to the respective values in IP-34, resulted in increased transpiration rate which rapidly affected the δT_{air}, maintained its values between +0.31 ^{o}C (11:00 h) and -0.49 ^{o}C (20:00 h), respectively. Counter-wise, the transpiration rate of the crop inside screenhouse IP-34 was lower as compared to the respective in IP-13 screenhouse, thus the process of transpiration cooling was slower, resulted to a greater elevation of the T_{air} inside IP-34 screenhouse. In the progress of the daytime, the transpirational cooling effectively regulated the T_{air} resulting to a greater decrease of the T_{air}, as compare to the respective of IP-13 screenhouse.

The daily evolution of the air temperature inside the insect proof (IP) screenhouses differed significantly as compared to the respective evolution inside the shade screenhouse (Figure 13, on page 59). The observed differences could probably attributed to the reduced ventilation rate of the insect proof screenhouses as compared to the shade screenhouse. The lower ventilation rate of the insect proof screenhouses as compared to the shade screenhouse, reduced the heat exchange rate between the inside and the ambient for the IP screenhouses as opposed to the S-36 screenhouse. The incoming solar radiation increased heat accumulation from 08:00 and 14:00 h. increasing the internal air temperature of the IP screenhouses above the ambient air temperature. Obviously, during that period the crop transpirational cooling could not reduce the internal air temperature below the ambient air temperature. Only after 14:00 h the crop transpiration succeeded to reduce the air temperature of the insect proof enclosures.

The results presented by Möller and Assouline (2007), Möller et al. (2003) and Josef Tanny et al. (2003) revealed that the average internal temperature of a screenhouse is not significantly affected (±1 ^{o}C) by the structure or by the covering material (+1 ^{o}C for a 50-mesh IP screenhouse; -1 ^{o}C for a shade screenhouse), while as Romacho et al. (2006) the region (coastal or continental) where the structure is installed affect the internal temperature. In the present study no significant (statistically or arithmetically) differences were observed between the internal and the ambient air temperature.

7.1.3. Crop temperature and vapour pressure deficit

The reduction of screenhouse incoming solar radiation followed by a reduction of heat incident onto the crop canopy, resulting a reduction of canopy temperature of the covered crops unlike the respective of the open field crops. Moreover, the increased fraction of diffuse solar radiation of the enclosures further decreased the canopy temperature inside the screenhouses (Dai et al., 2004). Thus, the dual effect (decreased heat loads and increased diffuse fraction) of the screenhouses over the crop temperature could probably ascribe to the improved performance of the protected crops (less photoinhibition) (Kempkes et al., 2011,Li et al., 2014 and Urban et al., 2012). In accordance to the present results are the results presented by several authors for reduced canopy temperature under different shade regimes (Al-Mulla et al., 2011; Kittas et al., 2012; Leyva et al., 2015). Furthermore, the reduction of canopy temperature resulted in a significant reduction on the crop-to-air vapor pressure defficit (Figure 15, on page 62), which resulted in increased stomatal conductance , at least iside IP-13 screenhouse (Figure 20, on page 76), that possitively influences the rates of photosynthesis (Cohen and Moreshet, 1997; Haijun et al., 2015; Kittas et al., 2012; Nicolás et al., 2005).

7.1.4. Radiative environment

7.1.4.1. Global solar radiation

Screenhouses reduced the incoming solar radiation with respect to the transmissivity of their covering screens as measured in the laboratory. Differences in the transmittances were observed between the two experimental periods. The greater reduction was observed in screenhouse IP-13, followed by S-36 and IP-34 screenhouses. The differences between the laboratory and *in situ* tests could be ascribed

to; (i) the diffuse component of the solar radiation, which is not present in laboratory trials, (ii) the inclination of the sun towards covering screen depending on sun's azimuth and elevation, while in laboratory tests a perpendicular light source is applied (Castellano et al., 2006), (iii) the frames of the supporting construction reduce the transmittance of the overall construction (Castellano et al., 2008b), (iv) the dust accumulation (Cabrera et al., 2009; Haijun et al., 2015; Klose and Tantau, 2004; Linker et al., 2002; López-Martínez et al., 2013; Möller et al., 2010; Shahak et al., 2008b).

The IP-13 was more sensitive to dust accumulation due to its clear threads, which were drastically dimmed out as compared to the same porosity but with different colored threads IP-34. Shahak et al. (2004b) also documented the dust effect on different in texture (woven; knitted) and color nets/screens. The authors quoted that the relative dust effect might be expected to depend on the initial transmittance through the threads (the more opaque, the less dust effect), on the texture of the net and on the surface and electrostatic property of the threads. Therefore, the here studied IP-34 screen that embedded opaque white threads in its texture had been less susceptible to dust accumulation, as opposed to the clear transparent IP-13 screen. The shade net S-36, which hole size was greater than the insect screens was less affected by the dust effect since less surface was available for dust accumulation. Additionally, its less transparent threads as opposed to these of IP-13 farther contribute against dust effect.

7.1.4.2. Diffuse radiation

The fraction of the diffuse component of the total solar radiation was on average for the entire experimental period 0.64, 0.62 and 0.40 for screenhouse IP-13, IP-34 and S-36, respectively. The differences between the insect proof screenhouses (IP-13 and IP-34) and the shade screenhouse (S-36) could probably be attributed to the different geometrical characteristics of their covering screens, as the insect screens had lower porosity (ε = 0.46) compared to the shade net (ε = 0,63). As total (beam+diffuse) solar radiation passes through screen matrix, one proportion of the total solar radiation freely passes through the holes of the screen without striking onto the structure of the yarns and therefore maintains its diffuse fraction, while another proportion hits onto the surface of the screen's yarns and is been scattered, enhances the diffuse fraction of total solar radiation below the screen. Thus, the denser the

screen matrix and the smaller its hole size, the greater the part of total solar radiation that impacts the screen's yarns and consequently, the greater the diffusive effect of the screen. The latter could clearly explain the observed differences of the diffusive efficiency between the insect proof screenhouses (IP-13 and IP-34) and the shade screenhouse (S-36) (Table 9, on page 63; Figure 16, on page 64; Figure 17, on page 67). Both insect proof screens had the same geometrical characteristics therefore, the amount of the total solar radiation (i) that freely passed through the holes downward to the crop and (ii) that who had been scattered from the surface of screen's structure was equal for each anti-insect screen. The remaining part of the incident total solar radiation is been either transmitted through or absorbed by the structure of the yarns, or reflected back to the sky, proportionately to screens' optical properties (Table 2, on page 32). The transmitted part of the total solar radiation inherits a greater proportion of diffuse to beam solar radiation. The clear yarns (IP-13) contribute about 10% (0.64/0.58=1.10) more diffused radiation, as compared to the white dyed yarns (IP-34), due to the scattering of solar radiation that passes through its clear (transparent) threads. It seems that the white dye of the yarns of IP-34 screen decreased the transmittance of the screen (-21%), but also decreased the diffuse fraction of the downward radiation. The addition of the white dye at the clear threads partially blocked their diffusive capacity.

The diffuse fraction of total solar radiation was about steady from of the day, around solar noon, while in early morning and late evening hours was significantly increased. During the time period between 12 to 16 hour (local time) the freely passed proportion of the total solar radiation through the holes of the screens takes the maximum possible values and consequently the diffuse fraction of total solar radiation takes the minimum. The increased fraction during the morning (9-11; local time) and the evening (17-19 h) could be ascribed to the low incident angle of the solar radiation. As the solar-screenhouse azimuth increases the incident angle of solar radiation onto the screenhouse roof decreases. Therefore, the portion of the total solar radiation that strikes the screen's yarns increases and consequently the ratio diffuse:beam solar radiation increases inside screenhouses. The latter is in agreement with the reports of several authors who investigated the correlation of the diffuse radiation transmittance relatively to the incident angle (Al-Helal and Abdel-Ghany, 2010; Castellano et al., 2008b; Healey and Rickert, 1998; Möller et al., 2010; Oren-Shamir et al., 2001; Romero-Gámez et al., 2012). Moreover, the diffuse fraction of

total solar radiation during the morning and the evening hours is already increased before passing through the covering materials of the screenhouses, due to the increased ambient humidity at those periods of the day and the low solar elevation angle (Jones, 2014).

The effect of the screen porosity and color to their optical properties were clearly presented by several authors (Al-Helal and Abdel-Ghany, 2010; Castellano et al., 2008b; Möller et al., 2010; Oren-Shamir et al., 2001; Romero-Gámez et al., 2012). At equal porosity, the non-colored translucent screens were the most transmissive to global radiation and PAR, followed by the green screen and finally the black screens. Moreover, the global and PAR radiation transmittance lower porosity non-colored screen (20 × 10) was lower than that of the higher porosity green screen (6 × 6) (Romero-Gámez et al., 2012), which is in absolute agreement with the results presented in the present work. Al-Helal and Abdel-Ghany, (2010) demonstrated the effect of color and porosity on the transmittance, reflectance and absorbance in PAR energy values. Due to scattering, net color has a stronger effect on net transmittance than net porosity. Given the same color, nets with high porosities are expected to have higher transmittances than nets with low porosities, while given the same porosity, increasing the brightness of a net i.e., from dark green to green, increases the PAR transmission due to scattering from the net texture (yarns). Moreover, the authors reported that the forward scattering of the incident radiation on the thread surfaces mainly depended on the net color, increased with increasing net brightness and decreased with the net darkness. Similarly, (Castellano et al., 2008b) reported that nets with transparent and black threads have different values of the transmissivity for a diffuse light source. This value could be a significant parameter in the choice of the net/screen depending on the weather condition of the region and on the performance required to the netting system. In cloudy regions, they suggested the installation of nets with transparent threads as more suitable in order to maximize the transmission of diffuse radiation. In regions with many overcast periods transparent nets should be recommended for many applications (Castellano et al., 2008b). The correlation between the porosity and the diffusive effect of the agricultural nets have also been stated by Oren-Shamir et al. (2001), who reported and increase by 2.5-2.9 of the diffuse light by the more densely knitted colored nets when compared to the nets with higher porosity (black net; aluminized reflective net). This grade of enrichment of the diffuse fraction of solar radiation below the screens is in absolute agreement with

values for the insect proof screenhouses of the present study (IP-13: 2.88 and IP-34: 2.12; Table 13, on page 70). The dense colored nets in their experiments reached a ratio of diffuse:beam radiation of 0.46-0.53. The later values are in agreement with the respective value of the IP-34 screen of the present work for mean value between 11:00 and 17:00 h (0.52; Figure 16, on page 64), while they are 0.81 of the here presented mean diurnal/hemispherical value (0.62; Table 9 on page 63).

Romero-Gámez et al. (2012) measured the transmitted diffuse radiation with respect to transmitted global radiation (Di/Gi in %) for different screens tested at the various angles of incidence. The densest non-coloured screens greatly enriched diffuse radiation at all angles of incidence, followed by the more open weave non-coloured screens and for the green screen (Romero-Gámez et al., 2012). Möller et al. (2010) reported a greater enrichment in diffuse radiation below the densest screens because of the increased scattering effect of the 50 mesh screens as compared to the 25 mesh screens. Moreover, they reported t5hat that diffuse radiation below a non-black screen was much larger than that above the screens because of the contribution of scattered light by the screen threads. Similar conclusions were reported by (Castellano et al., 2008b), as the non-coloured threads maximized the transmission of ambient diffuse radiation and surplus the conversion of ambient beam into diffuse radiation, alike diffusive plastic greenhouse covering materials. The reported results of the present work are completely aligned to those reported by the latter authors.

The diffuse ratio (diffuse in : diffuse out) of the radiative environment inside screenhouses with diffused solar radiation were above presented in Table 13 (on page 70). As it was expected, the insect proof screenhouses (IP-13 and IP-34) greatly enriched the enclosure with diffuse radiation through the entire wavelength spectrum (T; 350-1100 nm) and through the PAR range (400-700 nm). The latter was significantly beneficial for the photosynthetic capacity of the covered crops, as they were illuminated with more uniformly distributed PAR thorough out the greater part of their canopy (Hemming et al., 2008; Shahak et al., 2004a, 2004b). The increased proportion of diffuse light, and observed increased rates of photosynthesis, possibly caused by more even distribution of light within the leaf canopy (Geider et al., 2001; Gu, 2002; Hollinger et al., 1994; Krakauer, 2003; Misson et al., 2005; Roderick et al., 2001; Urban et al., 2007). The differences of canopy photosynthetic responses to diffuse and direct PAR result from the differences in diffuse and direct radiative transfer regimes in plant canopies (Gu, 2002). Furthermore, the increase of the

irradiance shifts leaf photosynthesis from RuBP regeneration (electron transport) limitation to Rubisco (CO_2 diffusion) control (Farquhar et al., 1980). This leads to photosynthetic saturation and decrease in RUE under high irradiance levels. Therefore the transfer regime of direct beam radiation wastes photons by concentrating the light resource to only a fraction of all leaves, leading to a less efficient photosynthetic use of light by plant canopies. Diffuse radiation, however, effectively avoids the light saturation constraint by more evenly distributing radiation among all leaves in plant canopies, and leads to a more efficient use of light (Gu, 2002).

Additionally, the study of Brodersen and Vogelmann, (2007) showed that leaves absorb approximately 2–3% less diffuse light than collimated (direct) light. On the other hand, diffuse light distributes PAR more uniformly to all leaves within a canopy, enhancing the overall rate of photosynthesis (Gu, 2002), suggesting that direct and diffuse light affect photosynthetic processes differently. Actually, the overall differences between the direct and the diffuse light in their utilization by the photosynthetic mechanisms (Brodersen et al., 2008) consist in the spectral distribution of the available light and not to the difference of the absorbance between direct and diffuse visible light (Gorton et al., 2010). Measurements conducted by the latter authors revealed that the transmittance difference spectrum (direct minus diffuse) of shows a peak in the green region of the spectrum, which however is not strongly absorbed by leaf mass as red or blue light (Brodersen and Vogelmann, 2010; Vogelmann and Evans, 2002).

Moreover, remarkably interesting was the rate of the enrichment in the NIR range (N; 700-1100 nm), which actually is responsible for the heat of the bodies receiving the incident energy of that waveband. The corresponding indices were 5.0, 4.0 and 1.9 for the IP-13, IP-34 and S-36 screenhouses. Thus, the heating energy was greatly scattered inside the insect proof screenhouses i.e., the quantities of solar beams that directly stroke onto the surface of crop canopy were redirected in various directions. That prevented crops from receiving extreme heat loads concentrated on the particularly small area of the outer part of the canopy, uniformly heating it in depth and consequently maintaining negative crop to air temperature differences (Figure 14; on page 28). The positive effect of the diffuse radiation was also quoted by Dai et al. (2004) how supported that *"beam (direct) light heats leaves more than the scattered light in the shade, and hence sunlit leaves can be several degrees warmer than shaded leaves under sunny and dry conditions"*.

7.2. Transpiration of a sweet pepper crop under screenhouse conditions

The presence of the screen material decreases the advective part of crop transpiration, something that is attributed to the reduction of air velocity inside the screenhouse. Furthermore, the results showed that screenhouse crops had from about 20 to 40% lower transpiration rate than the open field crop and accordingly that consumed from about 20-40% less water than the open field crop. Similarly, Möller and Assouline (2007), Möller et al. (2004b) and Siqueira et al. (2011) reported decreased crop transpiration rates and water consumption inside screenhouses, as compared to the open field.

7.3. Screenhouse ventilation regime

7.3.1. Air velocity reduction

The screens used for screenhouse covering created a barrier between the screenhouse environment and the outside environment and significantly reduced screenhouse air velocity (Figure 24, on page 82 and eq. 31 to eq. 34, on page 83). This result is in general agreement with the wind tunnel measurements of lower pressure drops across the shade net as compared to the insect proof screens (Figure 21, on page 77). Tanny, (2013), using data from Desmarais et al. (1999) who reported wind measurements inside and outside several types of screenhouses, elaborated a rough linear regression between the inside and outside air velocity as following:

eq. 52: $u_{in} = 0.2(u_o - 1.16)$

This relationship is similar to the one found in the present study for the insect proof screenhouses. Furthermore, Möller and Assouline, (2007), for a 30% black knitted shade screen found a relationship between inside and outside air velocity as following (as shown by Tanny, (2013)):

eq. 53: $u_{in} = 0.5016(u_o - 0.119)$

that is in agreement with the presented reduction rate of S-36 screenhouse found in the present study.

7.3.2. Effect of screens' and screenhouse size on ventilation

Harmanto et al. (2006) presented values for the discharge coefficient (C_{ds^*}) of different anti-insect screens. A 52-mesh (anti-whiteflies and larger pests; hole size: 0.80 mm x 0.25 mm; d: 0.31; ε: 0.38) and a 40-mesh (Econet M®, anti-leaf miners and larger pests; hole size: 0.44 mm x 0.39 mm; d: 0.25; ε: 0.41) had C_d values of 0.28 and 0.31, respectively. For the IP-13 and IP-34 screenhouses, the C_{ds^*} values observed in the case of the present study were higher, something that could be attributed to the higher porosity and the different yarn and hole dimensions of the IP screens of the present study.

Teitel, (2001) reported that for a woven/knitted 22% shading screen (tape threaded; ε: 0.49) the discharge coefficient observed was 0.73 which is close to the C_{ds^*} value observed in the present study for the S-36 screen (C_{ds} * ε = 1.262 * 0.63 = 0.795).

Wind tunnel measurements of the present work were fitted into the Forchheimmer equation to estimate the permeability (K) and the inertial factor (Y) of the screens that were used, following the procedure presented by several authors (Miguel, 1998; Miguel et al., 1997b; Teitel, 2001; Valera et al., 2006, 2005). The estimated K values were 2.93 x 10^{-9} and 1.98 x 10^{-8}, while Y values were 0.120 and 0.065 for IP and S-36 screenhouse, respectively (Table 17; on page 78).

Knowing the geometrical characteristics (ε; Δx) of a screen it could be possible to calculate (i) its aerodynamic characteristics (K and Y), (ii) the resulting pressure drop through its matrix (using Forchheimmer equation) and consequently (iii) the discharge coefficient (C_{ds^*}) of the screen (Molina-Aiz et al., 2009; Teitel, 2001). Finally, using the calculated C_{ds^*}, the ventilation rate of a screenhouse could be estimated using eq. 25. Several authors have reported equations relating the aerodynamic properties with their porosity (Miguel, 1998; Teitel, 2001; Valera et al., 2006, 2005). Calculating the K and Y of the screens of the present work using the equations reported by Valera et al. (2006, 2005) resulted in a good agreement between the calculated values of C_{ds^*} coefficients (IP: 0.401; S36: 0.838) and those estimated using the wind tunnel measurements (IP: 0.465; S36: 0.795).

However, using the equations proposed by Miguel, (1998) we did not find an agreement between the calculated values (IP: K= 9.93 x 10^{-10} & Y= 0.225; S-36: K= 1.64 x 10^{-10} & Y= 0.115) and the estimated values from the wind tunnel tests. Similar results were also found by Teitel, (2001) who also did not found a good agreement using the values calculated after Miguel, (1998).

The ventilation rate values observed in the experimental screenhouses of the present study (IP-13, IP-34, and S-36) were much higher than the ventilation rate values observed in large scale (≈ 0.66 ha pepper screenhouse and ≈ 8 ha banana screenhouse) commercial screenhouses (Fig. 7), as those reported by Tanny et al. (2006, 2003).

Tanny et al. (2006), comparing the ventilation performance of a greenhouse against a screenhouse, stated that for a large enough naturally ventilated structure with

a well-developed dense canopy, the air exchange rate in the middle of the structure is less dependent on its size and vent area, since the latter represents only a small percentage of the total covered area. In the present work the size of the screenhouses seems that strongly influenced their air exchange rate. Comparing the ventilation performance of small scale screenhouses (200 m^2) against that of two large commercial constructions (≈ 8 ha and 0.66 ha) presented by Tanny et al. (2006, 2003), it can be seen that the air exchange rates of the large screenhouses (≈ 7.4 - 33.3 h^{-1} for a pepper screenhouse and 10 - 45 h^{-1} for a banana screenhouse) were much lower than the small scale screenhouses (≈ 35-160 h^{-1}) of the present work.

7.3.3. Comparison between screenhouses and greenhouses

In the present work, apart from the C_{ds^*} values of the screens, the values of the dual coefficient ($C_d\sqrt{C_w}$) of the screenhouses and of the wind related coefficient C_w, were also estimated. To the best of our knowledge, there are no previous works reporting the $C_d\sqrt{C_w}$ or the C_w coefficients in screenhouses and that is why the observed values will be compared to those observed in greenhouses.

Teitel, (2007) reported that the presence of an insect screen in the vent openings of a greenhouse reduces the $C_d\sqrt{C_w}$ coefficient by about 50%, depending the porosity of the screen used, resulting in reduction of greenhouse ventilation rate. Katsoulas et al. (Katsoulas et al., 2006a) reported values of the $C_d\sqrt{C_w}$ coefficient of 0.078 for a small greenhouse (ground covered area of 160 m^2) without screens in the side vents and of 0.096 for the same greenhouse with screened side + roof vents. These values are close to the $C_d\sqrt{C_w}$ values estimated for the S-36 screenhouse of the present work (0.072). The same authors reported a value for the dual coefficient for screened roof vent which is about the same with the estimate of the $C_d\sqrt{C_w}$ coefficient of the insect proof screens of the present work (0.026). Kittas et al. (2002) measured the ventilation rate of a small greenhouse ($A_g = 200$ m^2) with only a roof vent and estimated the $C_d\sqrt{C_w}$ to be about 0.132 for a screened vent opening, which is about double of the corresponding value for the S-36 screenhouse. A $C_d\sqrt{C_w}$ value of 0.14 was reported for a large Canarian-type greenhouse, for wind directions perpendicular to the side openings (Fatnassi et al., 2002). Pérez Parra et al. (2004) estimated the dual coefficient for a Paral-type greenhouse and for the case of rolling roof + side walls

vents reported a value of 0.025 which is similar to the $C_d\sqrt{C_w}$ value of the insect proof screenhouses presented in this work (0.026).

Considering that C_w is related to the pressure distribution around the structure, and taking into account that the IP-34 screenhouse could be considered as windward and the S-36 as leeward screenhouse, the lower values of the parameter in the case of IP screenhouses could be explained by the differences in the created pressure profile along the wind direction blowing the screenhouses. The so called 'side wall effect' (Boulard and Baille, 1995; Fernandez and Bailey, 1992) induces an inflow in the leeward side of the screenhouses' complex, something that could explain the higher values of C_w observed in the leeward screenhouse (S-36). Fatnassi et al. (2006) reported, for a 922 m^2 screened greenhouse a C_w value of 0.0009, which is one order of magnitude lower than the values estimated for the screenhouses of the present work. The C_w values of the screenhouse constructions estimated in the present study are at least on order of magnitude lower than the corresponding values reported for greenhouses (Kittas et al., 1997; Molina-Aiz et al., 2009; Pérez-Parra et al., 2006; Roy et al., 2002). Screenhouses are constructions covered with highly permeable materials unlike greenhouses which are perfectly closed constructions. Consequently, screenhouses may not disturb the wind profile as the perfectly the greenhouses do, which promotes a different pressure distribution pattern around a screenhouse construction. Thus, the lower values of the C_w coefficient estimated for the screenhouses of the present study (IP: 0.003; S-36: 0.008) compared to those reported for greenhouses may be the result of lower pressure differences between the leeward and windward sides of the screenhouse construction.

Based on previously published data for other screenhouses, an effort was made to estimate the $C_d\sqrt{C_w}$ for the pepper and the banana screenhouses reported by Tanny et al. (2006, 2003). Furthermore, knowing the characteristics of the screens, their C_d values were also estimated (Bionet: C_{ds^*}= 0.465; Crystal Shade Net: C_{ds^*}= 0.616) as described in section 4.2. Then the C_w of the constructions referred in Tanny et al. (2006, 2003) were also estimated and found equal to 0.0001 for the pepper screenhouse of 0.68 ha and 0.0002 for the banana screenhouse of 8 ha. In an effort to generalize the results and estimate the C_w values for different constructions and based on the C_w values of the present study and those estimated for Tanny et al. (Josef

Tanny et al., 2003; Tanny et al., 2006), the following relationship was found between the C_w and the screenhouse volume:

eq. 54: $C_w = 0.166\ V_{sc}^{-0.59}$,

with a value for the determination coefficient R^2 of 0.78.

Thus, based on eq. 54 that correlates a geometrical parameter of the screenhouse construction with the C_w, on the C_d coefficient of the screen, which is related to its geometrical characteristics, and using the ventilation model proposed in this study eq. 25 (on page 48), it could be possible to calculate the ventilation performance of any flat roof screenhouse.

7.4. Crop performance inside screenhouses

7.4.1. Plant height and leaves number

Plant height was significantly different among screens and open-field; the screenhouses imposed to the covered plants the "*shade avoidance syndrome*" (Mullen et al., 2006; Zhang et al., 2011). The lowest and highest values were observed for the open field crop and under the green screen respectively, whereas intermediary and similar values were observed under the two insect proof screenhouses. The increase of plant height inside screenhouses could be ascribed to the decreased values of R:FR under the screens (1.20; on average for both years and for the three screenhouses) as compared to the respective value at the open field (1.26) (Table 11, on page 68). Similarly increase in height with increasing shade was reported by Kittas et al. (2012) for tomato crops under four different shade nets. The differences in plant height between the heave shaded screenhouses IP-34 and S-36 could also been attributed to the different R:FR ratio of the irradiance inside the respective enclosure; IP-34 = 1.21 and S-36 = 1.17. The green coloured S-36 shade net strongly absorbed the incident ambient solar radiation through the red wavelength band (reducing R:FR), while significantly enriched the green band increasing G:R. The green net is acting as supplementing green to background white light, or as a plant canopy that transmits solar radiation to understorey. Both cases enhances the "*shade avoidance syndrome*" (Folta and Maruhnich, 2007; Franklin, 2008; Zhang et al., 2011).

The final number of leaves per plant on 2011 was greater as compared within each treatment to the corresponding numbers of the 2012 period (Table 21on page 87). This increased number of leaves could probably been ascribed to the increased volumes of precipitation of 2011 (unlike the respective volumes of 2012; Figure 40, on page 113), which probably enhanced the vegetative growth and development. The latter is further supported by the decreased yield on 2011, as compared to the yield on 2012 (Figure 31, on page 93).

Heuvelink and Buiskool, (1995) investigated the influence of the sink-source ratio as determined by fruit and truss pruning on dry matter production and partitioning in tomato. The dry matter production was not influenced, whereas dry matter partitioning was greatly influenced favoring the vegetative growth. They also reported that the development rate (number of leaves) of tomato plants was not influenced by the low sink-source ratio. However, in their experiments all side-shoots

were removed weekly, similar to commercial practice and their plants could not increase sink source by producing side-shoots, which of course restricted the vegetative development by lateral shooting. Similarly, fruit pruning (removal) favored vegetative (leaves + stems) growth in cucumber (Marcelis, 1991).

The role of the already developed vegetative sources (leaves) is to supply assimilates mainly toward the newly developed generative and vegetative organs plus new lateral shoots. Upon the absence of newly developed generative organs due to removal after heavy rainfall, assimilates from the sources were probably distributed toward the present sinks that succeeded to remain attached to the plants i.e., already well grown fruits and newly developed laterals. These newly developed laterals upon their growth would shift from sinks to sources that would supply assimilates to their neighboring sinks (buds, flowers and fruits). Should there a new heavy rainfall occurred, those assimilates would redistributed to the already present sinks that succeeded to remain attached to the plants. This scheme of influence of the rainfall to the sink:source ratio that promoted the vegetative growth and development was observed during experimental period 2011, where heavy summer precipitations were distributed uniformly across summer months. The removal of flowers and small fruits (newly fertigated flowers toward just formed fruitlets) after heavy summer night rainfalls was severe in period 2011. This removal of the young generative sinks promoted the vegetative growth (dry matter production) and development (number of leaves) during summer months (June-August). Consequently, the greater number of leaves per plant that recorded during 2011 period as compared to the respective number recorded on 2012 period could probably be ascribed to the influence of heavy summer precipitation to the sink:source ratio of the pepper plants. The fact that our pepper plants were remained unpruned (unlike the work of Heuvelink and Buiskool, (1995)) allowed a freely developed canopy. The combined effect of the freely developed canopy and the rain regulated sink:source ratio resulted in more “bushy/vegetative” formed plants i.e., plants with greater number of leaves as compared to the plants of 2012 period (Table 21on page 87,).

The increase of the LAI under shade conditions is another typical phenotype. Kittas et al. (2012) reported that shading of an open field tomato crop increased its LAI by approximately 42%, as compared to that of the open field crop. Smith et al. (1984) reported that tomato plants adapted under different shade conditions by increasing their leaf area, among other phenotypes. This increase was proportional to

the shade intensity of the covering screen. Similar results reported by several authors (Charles-Edwards and Ludwig, (1975); El-Gizawy et.al., (1992); Abdel-Mawgoud et al. (1996)). The increased LAI of the screened crops, as compared to that of the open field crop, greatly contributed to the transpirational cooling of the enclosures (Katsoulas et al., 2002), inducing about similar internal air temperatures as the ambient, although the reduced transport processes that were imposed by the covering screens.

7.5. Productivity of crops inside screenhouses

7.5.1. Yield

In general, the protected crops produced greater yields of fresh fruits as compared to the open field crop; a deviation from this observation was recorded for the S-36 screenhouse on 2012 period. The statistical analysis did not revealed significant differences among all specific treatments. Nevertheless, the rank of the crops with respect to the higher yield was: IP-13 > IP-34 > S-36 > open field. The robustness of this rank could be strongly supported by the results of period 2012 of yield harvested from each respective entire treatment i.e., harvests from all plants (216 plant, excluded the border plants) inside each treatment (Rigakis et al., 2014). The latter rank was: IP-13 (7.3 kg m^{-2}) > IP-34 (5.3 kg m^{-2}) > S-36 (4.4 kg m^{-2}) > open field (4.1 kg m^{-2}). The here presented beneficial effects of the shading to the total are aligned to the findings of other authors for various horticultural crops and shading technics and technologies (El-Aidy and El-Afry, 1983; El-Gizawy et al., 1992; Gent, 2008, 2007; Shahak et al., 2008a, 2004b).

Differences were observed between the respective yields of the two periods. These difference could probably been ascribed to the different lengths (23 days) of the cropping periods, as also been reported by Möller and Assouline, (2007) and Romacho et al. (2006) for screenhouse crops and by (Hodges et al., 1995) for open field crops. These differences demonstrate the necessity of early planting, before the commence of the harsh summer conditions, that probably induce heat stress of the crops at early (thus vulnerable) developmental stage (Wahid et al., 2007). Similarly, Leyva et al. (2015) quoted that the differences in yield between the two experimental period, could be due to a later sowing date (8th June and 24th May, for the 1st and 2nd period, respectively) when the development stage and plant processes are the most sensitive to heat stress.

Furthermore, the cumulative yield during experimental period 2011 presented a significant steep increase on W.A.T. 15. This increase could probably be ascribed to the simultaneous growth of increased number of fruits that had been developed after the last rainfall at the beginning of August. Due to the frequent precipitation incidents during 2011 (Figure 40, on page 113) a significant flower abortion was observed, but unfortunately not measured. Nevertheless, the abortion incidents changed temporarily the sink to source ratio in favor of the vegetative development and growth, which

obviously expressed by the significant increase of the number of leaves and lateral shoots and their respective dry matter ((Heuvelink and Buiskool, 1995; Marcelis, 1991); (Figure 29, on page 88 and Table 29, on page 104)) Assimilates produced from the increased leaf area of the crops 2011 enhanced the further development of lateral shoots that increased number of flowers that successfully fertilized and became fruits. Analogous steep increase of the cumulative yield was not observed on 2012, where no significant precipitation incidents recorded and the development process was not altered in favour of the vegetative or the reproductive organs. The "more" vegetative 2011 crop finally yielded less than the "more" generative 2012 crop.

The crops inside the insect proof screenhouses produced on average for both screenhouses on both periods 5.75 kg m^{-2} fresh fruit yield (Table 25, on page 92). Thus, yielded about 30% more fresh fruit weight as compared to the respective of the crop inside the S-36 screenhouse (4.45 kg m^{-2} on average for both periods).

Screenhouses IP-34 and S-36 imposed about the same amount of shade over their respective crops (Table 10, on page 65); in particular screenhouse S-36 transmitted about 5 % more solar radiation ($T \approx 5\%$ and $P \approx 4$ %; on average for both periods) toward its covered crop. Thus, the observed differences in their yield could not been attributed to the difference on the availability of the PAR. Probably the observed differences of the crops yield between the heavy shaded screenhouses (IP-34 and S-36) could be ascribed to the differences in light quality (spectrum and diffuse component of the incident light) incident in the covered crops (Table 11, on page 68, Table 12,on page 69 and Table 13, on page 69). Accordingly, a possible explanation of the decreased crop productivity inside screenhouse S-36 could be the negative effect of the green light emitted by the net surface over the underneath. The green light probably negatively influenced plant growth (Dougher and Bugbee, 2001; Klein, 1964; Klein et al., 1965; Went, 1957) resulting in decreased yield on 2012 experimental periods, as compared to the yield of the crops of screenhouse IP-34. Another reported negative effect of green light over plants is the flowering inhibition (Banerjee et al., 2007; Klein et al., 1965; Vince et al., 1964). In the present study no measurement relevant to flowers had been conducted. Nevertheless, observing the final harvested fruit number an insight of the flowers that became harvested fruits could be outdrawn. Inside screenhouse S-36 a significant reduction in number of harvested fruits was recorded on 2012 period, but not in 2011 period. Thus, no secure conclusion could be drawn on the effect of green light on crop flowering.

Additionally, the microclimate inside the IP-34 screenhouse was more improved as compared to the respective inside S-36 screenhouse; the canopy to air temperature difference and the canopy to air vapor pressure deficit (Figure 15, on page 62). The latter improved microclimatic parameters probably increased stomatal conductance and therefore enhanced photosynthesis rate (Cohen and Moreshet, 1997; Haijun et al., 2015; Kittas et al., 2012; Nicolás et al., 2005).

The differences between the white (IP-34) and the green (S-36) screenhouses of the present study are not aligned with the results reported by Romacho et al. (2006), how compared the influence of two 15-mesh screens, one green and one clear (black and white woven threads), on cherry tomatoes where they did not observed any significant differences between the two houses. The different findings between the two works could be ascribed to the different textures of the screens used in the two studies. Probably, the screens used by Romacho et al. (2006) scattered the incident solar radiation in a similar trend due to their same texture. The clear threads have the inherited property to scatter the incident light in a significantly greater proportion than the darker green threads, while black threads only absorb the incident solar radiation. The combination of the black and white threads in the same weave probably significantly reduced (by 50%) the diffusive effect of the clear screen. The scattering effect due to screen texture was the probably same, as both screens were 15-mesh. Therefore, the scattering due to screen texture probably could not compensate the reduction of the diffuse radiation due to the green colored threads and the two enclosures probably presented about the same diffused solar radiation, thus there beneficial effect of diffused solar radiation was about the same on both enclosures. Differently, the available solar radiation to the crop (thus, also the PAR) inside the clear house was 4% greater as been compared to the green screenhouse. Combining the above written; since the effect of diffuse radiation was equal on both enclosures, the greater amounts of available PAR to the crops inside the green nethouse probably compensated for the negative effect of the green light enrichment on the crop productivity, leading to equal fruit yields between the green and the clear houses. Adversely, in the present study, in the S-36 screenhouse the low diffuse fraction of solar radiation (as compared to the IP-34 fraction; Table 12, on page 69; Figure 16, on page 64; Figure 17, on page 67) probably could not be enough to compensate for the negative effect of the green light enrichment, thus produced lower yields as compared to the IP-34 screenhouse.

The results of the present study corroborate with results previously reported by several researchers. Kittas et al. (2012) reported significant increase of tomato total yield under shading nets by about 43% as compared to that of the open field. The authors attributed this increase to the improved microclimate (radiative, $\delta T_{c\text{-}air}$ and $D_{c\text{-}air}$) of the protected crops, which resulted in better physiological performance of shaded crops.

Möller and Assouline, (2007), reported yields for sweet pepper crops of 5.93 and 9.26 kg m^{-2} on two consecutive summer periods on 2004 and 2005, respectively. Their sweet pepper crops were grown inside a shade-net (30%; black) covered screenhouse, under Israeli climatic conditions for 21 and 26 weeks on 2004 and 2005 periods, respectively. The resulted crop yields inside the insect proof screenhouses of the present work are about 17% and 30% lower from the latter mentioned yields for 2004 and 2005 period, respectively. The different (i) cultivars of sweet pepper plants (Dolmy vs Selica; present study vs Möller and Assouline, (2007)), (ii) climatic parameters of the experimental fields, could probably explain the differences between the fresh fruit yields of the present study and the study of Möller and Assouline, (2007). As Silber et al. (2009) quoted, a commercial summer season cultivation (21 weeks duration) of sweet pepper of Selica cv, produces fruits that could be weighted between 145 and 185 g and the total number of harvested fruits could be about 50-55 m^{-2}, resulting in an average fresh fruit yield of about 8.6 kg m^{-2}. Consequently, the different types of fruits (Dolmy vs Selica; 100g vs 145-185g per fruit) between the present work and the work of Möller and Assouline, (2007), could probably explain the differences between the total yields on both periods (late summer planting 2004 vs 2011; regular spring planting 2005 vs 2012).

The open field productivity of the present study is compared to the respective yields previously reported by other authors. Möller and Assouline, (2007) quoted fresh fruit yields for open field pepper crops of about 3.9 kg m^{-2} (on average) as reported by other researchers (Doorenbos and Kassam, 1979; Hartz et al., 1996; Hodges et al., 1995; Posalski, 2006; Rilsky and Adamati, 1989; Sezen et al., 2006), which is not very different than the yield reported for the open field in the present study. Despite of the different experimental treatments and cultivation practices among the latter mentioned crop, that were clearly remarked by Möller and Assouline, (2007), their low productivity highlights the necessity of the cultivation inside screenhouses. The benefits of the shade protection of an open field crop were also

demonstrated by Kittas et al. (2012) who studied the effect of various shade nets, with different shading intensities and colors, on a tomato crop grown under Mediterranean Summer. The authors reported an increase of the productivity (43% on average for all shaded treatments) of the shaded crops unlike the open field.

The number of harvested fruits (# m^{-2}) per week presented strong fluctuations during experimental period 2012, unlike period 2011. That fluctuation pattern is typical of pepper crops and it is well documented by several authors (González-Real et al., 2009; Shahak et al., 2008; Marcelis and Baan Hofman-Eijer, 1997; Heuvelink and Körner, 2001; Hall, 1977; Bakker, 1989). Pepper crops shows a cyclic growth pattern where periods of high fruit set and slow fruit growth alternate with periods of low fruit set and rapid fruit growth (Marcelis et al., 2004). The fluctuations can be explained due to the great sink strength of the pepper fruits. Fruits are highly competitive organs to their nearby sinks (new leaves and other fruits) in terms of assimilates (González-Real et al., 2008). Due to this competition pepper plants are susceptible to bud, flower and fruitlets abscission and therefore present cyclic fluctuations through the entire reproductive stage (Bakker, 1989; Hall, 1977). The abortions and thus the characteristic fluctuating pattern can be ascribed to microclimatic parameters (heat stress, rain etc.) (Aloni et al., 1997; Turner and Wien, 1994) and to the number of the existing fruits how act as strong sinks (Heuvelink and Korner, 2001; Marcelis and Baan Hofman-Eijer, 1997). The sink strength of the fruits is decreasing upon their maturity, allowing the initiation of a new generative cycle by the formation of new fruits (González-Real et al., 2009).

During experimental period 2011 these fluctuations were dimmed out probably due to the increased abortion of flowers and fruitlets occurred after every heavy precipitation incident especially in mid-June and early August. The fruits that were already well formatted continued to grow and finally harvested, but their number was reduced compared to the number of fruits that could have been harvested under "regular/typical" summer conditions. Due to the excess abortion the vegetative development and growth was enhanced and the plants presented a significant greater number of leaves when compared to the corresponding number of the 2012 period. Thus, a very steep pick presented on W.A.T. 15 (mid-September), where a great number of ripened fruits were harvested from the crops of all treatments. After early August 2011, a balance between vegetative and generative development and growth seems been established and the final number of harvested mature fruits from the crops

did not differed significantly from the respective of 2012 period (Table 25,on page 92).

7.5.2. Quality of yield

The 50% increase of the marketable yield of crops inside the screenhouses as compared to the open field marketable yield corroborates the results previously reported by several authors. The increased marketable yield inside the screenhouses primarily can be attributed to the significant decrease of the sunburned fruits in the respective treatments and secondarily to the significant reduction of pest defected fruits. The reduction of BER influenced in a lesser extend the increase of the marketable yield inside screenhouses. The beneficial effects of the shading to the marketable production in the present study are aligned to the findings of other authors for various horticultural crops and shading technics and technologies (El-Aidy and El-Afry, 1983; El-Gizawy et al., 1992; Gent, 2008, 2007; Shahak et al., 2008a, 2004b). Kittas et al. (2012) reported a doubling of the marketable yield of tomato crop under shade nets as compared to the respective of the open field, while Rylski and Spigelman, (1986) presented an increase about 60% of marketable yield of a sweet pepper crop under shade, as opposed to the yield of the open field crop. The shade increased the marketable tomato production by about 35% compared to non-shading conditions in experiments under white, black and photoselective shade nets (Ilić et al., 2012). Additively, the marketable yield of a shaded greenhouse tomato crop was significantly higher than the respective obtained in an unshaded greenhouse (Lorenzo et al., 2003).

The reduction of the sunscald was remarkably significant, demonstrating the protection of the yield against the combined effects of supra-optimal irradiance and high air temperature (Adegoroye and Jolliffe, 1987). The reduced NIR (Table 10, on page 65) (and net) radiation inside the enclosures alleviated the harsh conditions imposed by the excess summer solar radiation upon crops, resulted to lower leaf and presumably fruit surface temperature. Moreover, the increased diffuse solar radiation inside screenhouses protected fruits against sunburns, as the diffuse radiation acted on fruits surface in the same way as in leaf surface; diffuse light results in lower leaf temperature (Li et al., 2014; Urban et al., 2012) because of less severe local peaks in light intensity and consequently lower locally accumulated heat radiation. Sunlit fruits at the open field received more near-infrared radiation than shaded fruits and therefore

presented extensive sunscald. The significant reduction of sunscald inside screenhouses is aligned with the reports for shade crops by several authors (El-Aidy and El-Afry, 1983; El-Gizawy et al., 1992; Gent, 2008, 2007; Gindaba and Wand, 2008; Kittas et al., 2012; López-Marín et al., 2011; Rylski and Spigelman, 1986b; Shahak et al., 2008a, 2004b).

Moreover, in the present study was observed a significant reduction of BER occurrences on the fruits harvested was inside screenhouses as opposed to those harvested at the open field. This decrease could probably be attributed due to the improved microclimate inside the screenhouses (lower values of $\delta T_{c\text{-}air}$ and $D_{c\text{-}air}$). The lower $\delta T_{c\text{-}air}$ and $D_{c\text{-}air}$ induced a better water status in the plant and to their fruits via regulating their transpiration, unlike the highly transpiring plants and fruits at the open field crop due to their exposure at high $D_{c\text{-}air}$ values (Bertin et al., 2000; Guichard et al., 2001; Ilić et al., 2014; Kittas et al., 2012; Cherubino Leonardi et al., 2000; Leyva, R. et al., 2013; Lorenzo et al., 2004). The observed differences between the moderate shaded (≈25%; IP-13) and the heavy shaded screenhouses (≈35%; IP-34 and S-36), even though they were not statistically significant, could probably be ascribed to the lower transpiration rate of crops inside the latter enclosures (Figure 26, on page 84). High BER incidence is related with an unbalance between the cell expansion rate and the calcium requirement of the fruit during the rapid growth period (Guichard et al., 2001; Lorenzo et al., 2004). The lower water content of fruits (Table 30, on page 106) could indicate lesser influx of xylem sap to the fruit and thus calcium (Lorenzo et al., 2004).

Rylski and Spigelman, (1986) quoted that the highest yield of high-quality fruits was obtained with 12-26% shade, which is in agreement with the findings of the present work. The screenhouse crops increased their fruit size (greater horizontal and vertical dimensions) (Table 27, on page 96) as well as the weight per fruit (Table 26, on page 95), which corroborates the finding reported by the latter authors. Moreover, there seems to be a correlation between the shade factor (and/or the diffuse radiation) with the shape (elongation; H:W) of the fruits. The ratio H:W is decreasing with increase of the shade up an upper limit of shade beyond which the ratio is increasing. The results presented by Rylski and Spigelman, (1986) also imply a congener correlation between shade factor and shape of the sweet peppers they used in their experiments. The elongation (H:W) of their fruits was: 0% shade factor (SF) = 1.09; 12% SF= 1.08; 26% SF = 1.06 and 47% SF = 1.11.

The analysis of fruits' chemical characteristics revealed that Titratable Acidity (TA) did not present significantly differences between the open field and the covered crops, similarly to the findings reported by Ilić et al. (2014). Adversely, SS were decreased under all screenhouses by on average 12%, as compared to the SS of the fruit from the open field crop (Table 27, on page 96). Similarly, Ilić et al. (2014) reported also a decrease of SS (12% on average) of tomato fruits from crops grown inside screenhouses (with photoselective shade nets) as compared to the respective values for the fruits from an open field treatment. The reduced VPD causes a significant increase in fruit fresh weight and fruit water content and a decrease in soluble solids (Bertin et al., 2000; Guichard et al., 2001; Ilić et al., 2014; Cherubino Leonardi et al., 2000; Leyva, R. et al., 2013; Lorenzo et al., 2004). The D_{air} was not improved inside screenhouses in the present study. However, the significant reduction of the $\delta T_{c\text{-}air}$ and $D_{c\text{-}air}$ could probably be ascribed to the significant increase in fruit fresh weight and fruit water content and to the decrease in SS. Additionally, the fruits dry weight was not affected at the open field and inside the insect proof screenhouses, as also quoted by the above mentioned authors.

7.6. Water use efficiency

7.6.1. WUE of screenhouse crops

The here presented profound effect of screenhouses is increasing the water use efficiency of the covered crops as compared to that of the open field (Table 28, on page 98), is in accordance with results reported for various screened/shaded crops by several researchers (Alarcón et al., 2006; Medina et al., 2002; Nicolás et al., 2005; Siqueira et al., 2011) (Lorenzo et al., 2004, 2003). Leyva et al. (2015), reported that the WUE by a cherry tomato crop inside an insect proof screenhouse was 7.03 kg m^{-3} (fresh mass).

Möller and Assouline, (2007) reported, for a screenhouse sweet pepper crop, that the irrigation WUE ranged between 10.70 and 13.54 kg m^{-3}, while the respective value for an open field crop was (on average) 4.75 kg m^{-3}. These values were on average (11.8 kg m^{-3}) 0.87 and 0.73 of the corresponding average (2011 and 2012 periods) value of the shade screenhouse (S-36; 13.6 kg m^{-3}) and of the insect proof screenhouses (IP-13 and IP-34; 16.2 kg m^{-3}) of the present work, respectively. Their case study could probably be more close to the S-36 case of 2012 (non-rainy summer) the present study, as both are screenhouses covered by shade nets, which do not (black net) or partially (S-36 net) enrich the enclosure with diffuse radiation. As IWUE is an index that reflects the positive effect of the structures on the utilization of the irrigation water by the covered crops there should not be neglected the differences in the applied irrigation water and in the total fresh yield between the present study and the study of Möller and Assouline (2007). In their case, the fresh fruit yield was 5.9 and 9.3 kg m^{-2} and applied irrigation water 554 and 673 mm on 2004 and 2005, respectively. These values are significantly greater than those of the present work, unlike the IWUE that were significantly lower. Those differences could probably be ascribed to the different optical properties (shade factor, no diffuse enrichment due to black color) of their screen as compared to the here presented insect proof screens, which enhanced the diffuse radiation of the enclosures, promoting the production of a unit of fresh weight with the consumption of lesser units of irrigation water.

Moreover, Möller and Assouline (2007) carefully (because of several limiting differences between their crop system and those of the open field crops) presented data of yield, applied irrigation water and IWUE for open field pepper crops, as previously been reported by several researchers (Hodges et al., 1995; Posalski, 2006;

Rilsky and Adamati, 1989). Average values of yield, applied irrigation water and IWUE for of the latter reported cases of open field pepper crops were 4.05 kg m^{-2}, 713 mm and 5.1 kg m^{-3}, respectively. The fresh fruit yield was not very different than the yield reported in the present work (on average for both periods; 3.85 kg m^{-2}), unlike irrigation water and IWUE, which were +30% and -27% of the respective values of the present work (549 mm and 7.0 kg m^{-3}; average values for 2011 and 2012 periods). Sezen et al. (2006) reported for an open field peper crop under various irrigation management, IWUE about 5.7 kg m^{-3} on average for all their treatments, which is 6% lower compared to the average value for both periods of the present study. Moreover, Dağdelen et al., 2004 determined WUE and IWUE values for open field grown pepper crops in the Aegean region of Turkey varying between 3.1 and 5.1 kg m^{-3} and between 4.1 to 6.7 kg m^{-3}, respectively, while Karam et al. (2009) reported value of WUE as 5.9 kg m^{-3}. After comparing our results for the open field crops (2011 and 2012) with the results reported by the formerly presented researchers, it could be assumed that the irrigation water in the present study was utilized by the open field crops more efficiently than the latter cases.

7.6.2. WUE and screen characteristics

An attempt to correlate the optical characteristics of the screens with the values of the IWUE by the crops of the present study. Non-linear regression analysis (using Marquardt, (1963) algorithm) was conducted for groups of data of IWUE-Diffuse fraction (f_{dif}) solar radiation and IWUE-Total (T; 350-1100 nm) (Figure 41, **A**). Furthermore, the diffused radiation was "decomposed" to its spectral components (P; B; G; R; FR; N) which were also correlated to the IWUE (Figure 41, **B**).

A tight correlation was revealed by the statistical analysis between the IWUE and the f_{dif} of the solar radiation (global and T) and also between the IWUE and the selected spectral bands of the diffuse irradiance:

eq. 55, $f\mathrm{R}_{\mathrm{G;dif}}$: $\mathrm{IWUE} = 29.18 * f\mathrm{R}_{\mathrm{G;dif}} + 5.49, \quad with\ R^2 = 0.97$

eq. 56, $f\mathrm{T}_{\mathrm{dif}}$: $\mathrm{IWUE} = 30.88 * f\mathrm{T}_{\mathrm{dif}} + 6.60, \quad with\ R^2 = 0.88$

eq. 57, $f\mathrm{P}_{\mathrm{dif}}$: $\mathrm{IWUE} = 32.01 * f\mathrm{P}_{\mathrm{dif}} + 5.42, \quad with\ R^2 = 0.83$

eq. 58, $f\mathrm{B}_{\mathrm{dif}}$: $\mathrm{IWUE} = 38.59 * f\mathrm{B}_{\mathrm{dif}} + 0.37, \quad with\ R^2 = 0.83$

eq. 59, $f\mathrm{G}_{\mathrm{dif}}$: $\mathrm{IWUE} = 32.32 * f\mathrm{G}_{\mathrm{dif}} + 0.37, \quad with\ R^2 = 0.83$

eq. 60, $f\mathrm{R}_{\mathrm{dif}}$: $\mathrm{IWUE} = 27.48 * f\mathrm{R}_{\mathrm{dif}} + 8.72$, $with\ R^2 = 0.82$

eq. 61, $f\mathrm{FR}_{\mathrm{dif}}$: $\mathrm{IWUE} = 28.49 * f\mathrm{FR}_{\mathrm{dif}} + 8.41$, $with\ R^2 = 0.88$

eq. 62, $f\mathrm{N}_{\mathrm{dif}}$: $\mathrm{IWUE} = 29.09 * f\mathrm{N}_{\mathrm{dif}} + 8.20$, $with\ R^2 = 0.92$

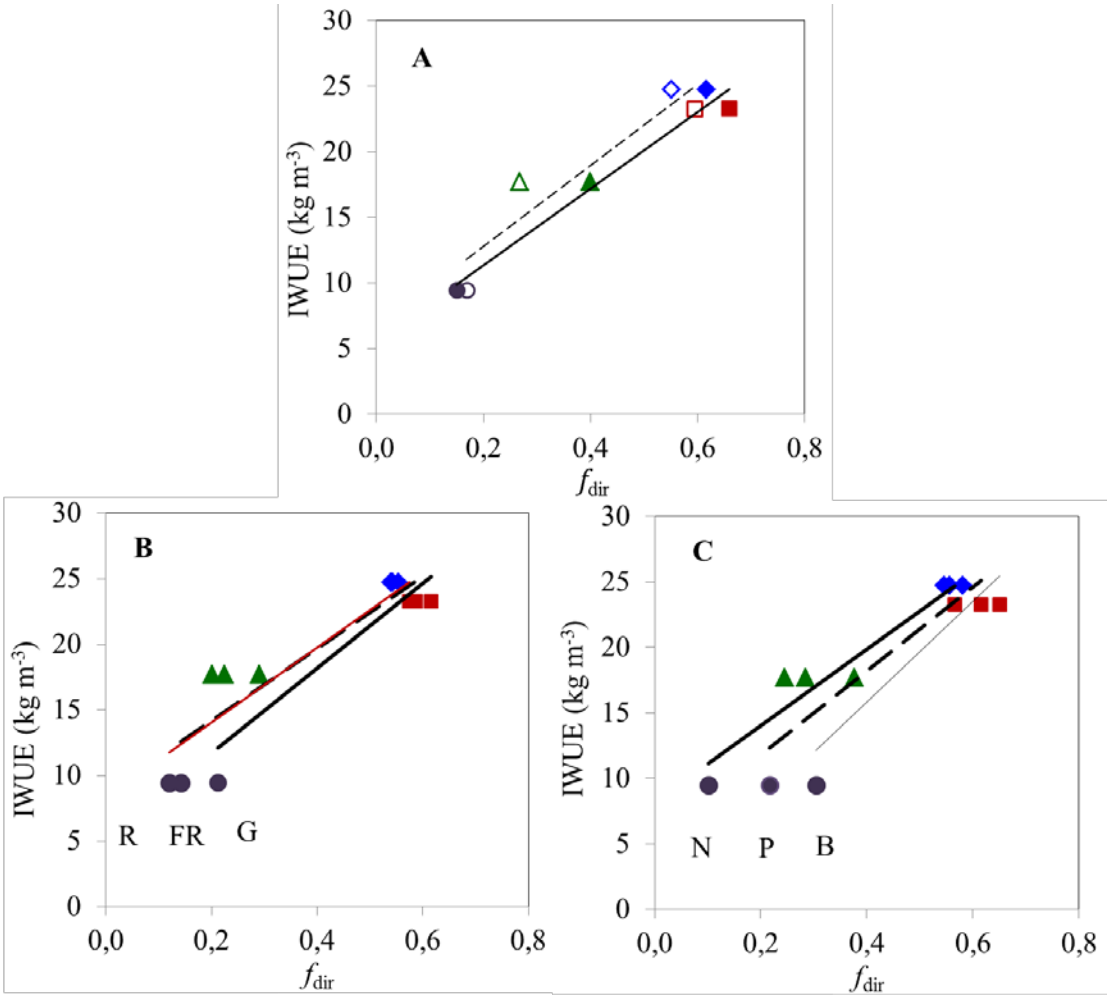

Figure 41. Irrigation Water Use Efficiency (IWUE; kg m^{-3}) against the diffuse fraction (f_{dif}) of solar radiation of the: **A**) global (closed symbols) and T (350-1100 nm; open symbols), **B**) through the R (600-700 nm; R), the FR (700-800 nm;) and G (500-570 nm) and **C**) through the N (700-1100 nm), the P (400-700 nm) and the B (400-500 nm), wavelength bands, for each treatment (Cont; circles, IP-13; squares, IP-34; diamonds and S-36; triangles) for the 2012 experimental. Straight lines represent the best fit regression line for the corresponding groups of data; **A**) global-thick line and Total-dashed line, **B**) R-dashed line, FR-thin red line and G-thick line and **C**) N-thick line, P-dashed line and B-thin line.

The reduction of the radiative load and air velocity in the enclosures resulted in lower crop transpiration rate than the open field and accordingly that protected crops consumed about 25-40% less irrigation water than the open field crop (Table 28, on page 98). Additionally, the increased diffuse radiation in the enclosures enhanced the productivity of the covered crops. The combined effect of the global solar radiation and its diffuse fraction on the increased but less irrigated productivity is clearly presented by the equations eq. 55 - eq. 62. The extremely high coefficient of determination suggests the strong positive correlation between the IWUE and the diffuse solar radiation (global and Total; eq. 55 and eq. 56). These strong correlation is also valid through each specific band (eq. 57- eq. 62) through the entire wavelength band (T).

Moreover, non-linear regression analysis was conducted for groups of data of IWUE and light quality parameters (B:R; B:FR; G:R and G:R), in order to be investigated any correlation between them. The data of the respective groups were plotted against each other and the best fit regression line for each group of data was fitted, as presented in Figure 42. The correlation between the IWUE and the light components was also significantly tight as been derived by the following equations of the best fit regression line for each case (Table 34).

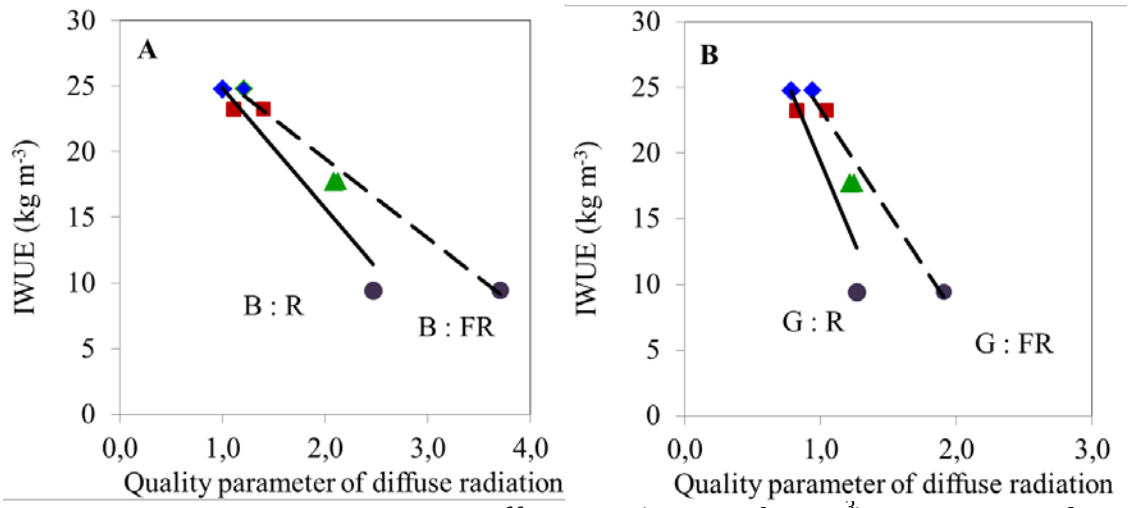

Figure 42. Irrigation Water Use Efficiency (IWUE; kg m^{-3}) against quality parameters of the diffuse solar radiation in each treatment (Cont; circles, IP-13; squares, IP-34; diamonds and S-36; triangles); **A**) B : R, B : FR and **B)** G : R, G : FR). Straight lines represent the best fit regression line for the corresponding groups of data for each wavelength band.

Table 34. Regression analysis results (slope of the best fit regression line; R^2) of groups of data of IWUE and spectra quality components of the diffuse irradiance as were determined for each respective treatment.

Spectral quality component	[1]a	[2]R^2
G : B	52.15	0.93
G : R	-24.71	0.83
G : FR	-15.76	0.98
G : T	-333.37	0.94
B : R	-9.19	0.92
B : FR	-6.08	0.99
P : N	-6.95	0.84
G : N	-28.85	0.86

[1]a: slope of regression line; [2]R^2: Coefficient of determination

As it can be seen by the presented coefficients of determination in Table 34 the quality of the diffused radiative environment is also tightly correlated to the IWUE of the crops. Interestingly, the quality parameters relevant to the green light further support the negative effect of the green light on the productivity of the crop inside the green-shaded S-36 screenhouse (Dougher and Bugbee, 2001; Klein, 1964; Klein et al., 1965; Went, 1957). No significant correlation was revealed neither for ζ nor for R:FR parameters. Therefore, it can be supported that the profound positive effect of the here presented screens/net on the IWUE was probably cryptochrome related.

Finally, the negative impact of the harsh summer radiative environment to the crops is characteristically represented by the plot of the IWUE against the transmittance of the screenhouses to the direct component τ_b of the solar radiation and fully expressed by the extremely tight negative correlation between the latter parameters, that was revealed by the statistical analysis (Figure 43 and Table 35). As τ_b was stable across the entire T wavelength band (Figure 17, on page 67), the equations of the best fit regression line for each selected spectral band were about the same (Table 35) and therefore only one case (T; 350-1100 nm) is presented.

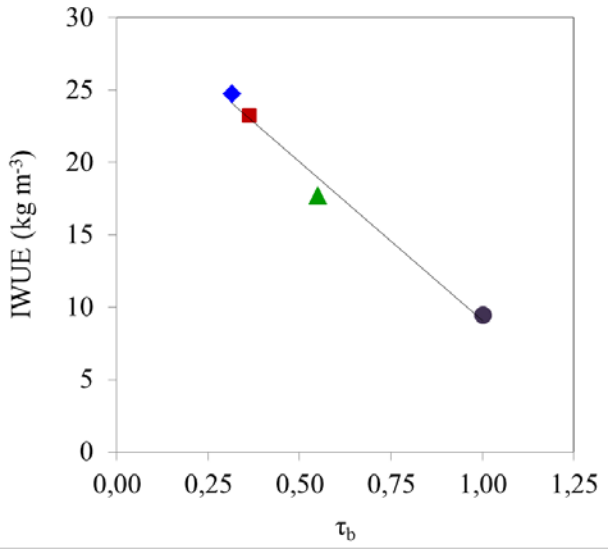

Figure 43. Irrigation Water Use Efficiency (IWUE; kg m^{-3}) against transmittance to the direct component (τ_b) of solar radiation through T (350-1100 nm) wavelength band as were determined for each respective treatment (Cont; circles, IP-13; squares, IP-34; diamonds and S-36; triangles). Straight line represent the best fit regression line for the respective group of data (RUE; τ_b).

Table 35. Regression analysis results (slope of the best fit regression line; R^2) of groups of data of IWUE and transmittance to the direct component (τ_b) of solar radiation through selected wavelength bands as were determined for each respective treatment.

Wavelength band	[1]a	[2]R^2
T	-21.73	0.98
P	-21.76	0.98
B	-21.73	0.98
G	-21.75	0.98
R	-21.78	0.98
FR	-21.90	0.98
N	-21.98	0.99

[1]a: slope of regression line; [2]R^2: Coefficient of determination

7.7. Crop growth inside screenhouses

7.7.1. Dry matter production

Cultivating inside screenhouses enhanced crop growth. The significant increase of total dry matter under the anti-insect screen could possibly be ascribed to the alleviation of the negative effects of excess light on photosynthetic performance. The protected crops probably spend less energy (assimilates) for PSII repair unlike the highly energy expense occurred in the crops at the open field (Arboree et al., 2011). Thus, the protected crops instead of wasting assimilates for recovery from photo-damage they stored them as dry matter in their organs, which cumulatively promoted the increased DMP, unlike the case of open field crops.

The differences in total dry matter production between the two consecutive experimental years could primarily be ascribed to the differences on the dry matter allocated to fruits. As an overall remark, it can be stated that light to moderate (≈18-25%) shade (IP-13) promotes dry matter allocation in fruits as compared to no shade (Cont) or heavy shade (IP-34 and S-36) (Table 29, on page 104).

Crop inside screenhouse IP-13 was the most productive with respect in total dry matter and fruit dry matter of all screenhouses. This superiority could be attributed to the greater available PAR energy due to the greatest transmittance in PAR (beam+diffuse) spectral band and to the greatest diffuse ratio (τ_{dif}; 2.24), as compared to IP-34 and S-36 screenhouses (Table 10, on page 65; Table 12, on page 69; Table 13, on page 70).

The difference between IP-34 and S-36 in dry matter of the fruits as well as in total dry matter could probably be ascribed to the quality of the radiative environment. Firstly, the profound effect of diffuse radiation on the photosynthesis was greatly weaken for the case of S-36 screenhouse, since its τ_{dif} across PAR band was extremely decreased (0.82), as compared to the respective value for the IP-34 screenhouse (1.55). That was also presented graphically as the “grey area” in Figure 17, **E** (on page 67). The practical meaning of the value 0.82 for τ_{dif} is that the S-36 net reduced the ambient diffused PAR and thus provided lower diffused energy for photosynthesis to the underneath crop, as compared to the open field. As the respective value for the screenhouse IP-34 was 1.55, it can be deduced that the screen IP-34 provided about the double diffused PAR to its underneath crop, as opposed to the S-36 screenhouse. Thus, the quantitative difference between the diffused radiative

environment of IP-34 and S-36 screenhouses differentially influenced photosynthesis and consequently the total dry matter production (Brodersen and Vogelmann, 2007; Brodersen et al., 2008; Gorton et al., 2010; Gu, 2002; Hemming et al., 2008; Kong et al., 2012; Li et al., 2014; Shahak et al., 2008b). Secondly, the quality of the diffused radiative environment of screenhouse S-36 probably negatively influenced its crop growth. The S-36 enclosure was enriched with green light (direct and diffuse), due to the color its covering shade net. The green light presumably inhibited crop growth (Dougher and Bugbee, 2001; Klein, 1964; Klein et al., 1965; Went, 1957) inside green screenhouse S-36, resulting in decreased total and fruit dry matter, as compared to the yield of the crops of screenhouse IP-34 on both experimental periods.

The increase in total fresh fruit yield under shading may be due to the greater amount of water accumulated in fruits, induced by the lower canopy-to-air VPD (Figure 15, on page 62), which improved the water status of leaves and promoted water movement to the fruit (Bertin et al., 2000). The greater water containment in fruits diluted the dry matter inside the fruits, resulting in a decreased dry matter content in the fruits harvested inside screenhouses (Table 30, on page 106).

7.7.2. Dry matter production correlations with screen optical properties

A profound effect of screens/nets is the increase of the diffuse radiation underneath them, (Abdel-Ghany and Al-Helal, 2011; Al-Helal and Abdel-Ghany, 2011, 2010; Healey and Rickert, 1998; Oren-Shamir et al., 2001; Romero-Gámez et al., 2012; Shahak et al., 2004b), which is documented that enhances photosynthesis of lower, shaded leaves due to the improved light distribution over crops canopies (Li et al., 2014), resulting in an overall increase of photosynthetic performance (Alarcón et al., 2006; Arboree et al., 2011; Medina et al., 2002; Shahak et al., 2004b) and thus increase growth of underneath crops and therefore the radiation use efficiency of shaded canopies as compared to unshaded canopies (Healey et al., 1998). As Tanny, (2013) quoted in his review paper, the "*quantification of this effect of diffuse radiation in a variety of crops and screenhouse types is a challenge for future research*".

In the present study an attempt was made to correlate the diffusive effect of the covering screens/net to the productivity of the covered crops. In the following analysis it was considered that the properties of the radiative environment of the enclosures and at the open field were constant on both experimental periods, since

detailed measurements of the diffuse component of the solar radiation were not available on 2011 period. It is presumed that this assumption would not bring a significant error to the final results.

In Figure 44 is presented the total dry matter per plant (DM; g plant^{-1}) against the diffuse ratio (τ_{dif}) through PAR (P) and green (G) wavelength bands for the screenhouses and for the open field treatment, on both experimental periods (2011 and 2012). A significantly tight correlation between the total dry matter and the diffuse ratio (τ_{dif}) of the screens was revealed by the statistical analysis (Table 36, on page 148). The τ_{dif} across P and G bands was tightly correlated to the total dry matter per plant. The different slope of the best fit regression line for each respective period could probably be ascribed to the differences of the total DM produced on each period (2011 and 20102). These strong correlation was also valid through each specific band of the entire wavelength band (T) (Table 36). For each respective band the increase of the diffuse ratio enhanced the production of dry matter per plant.

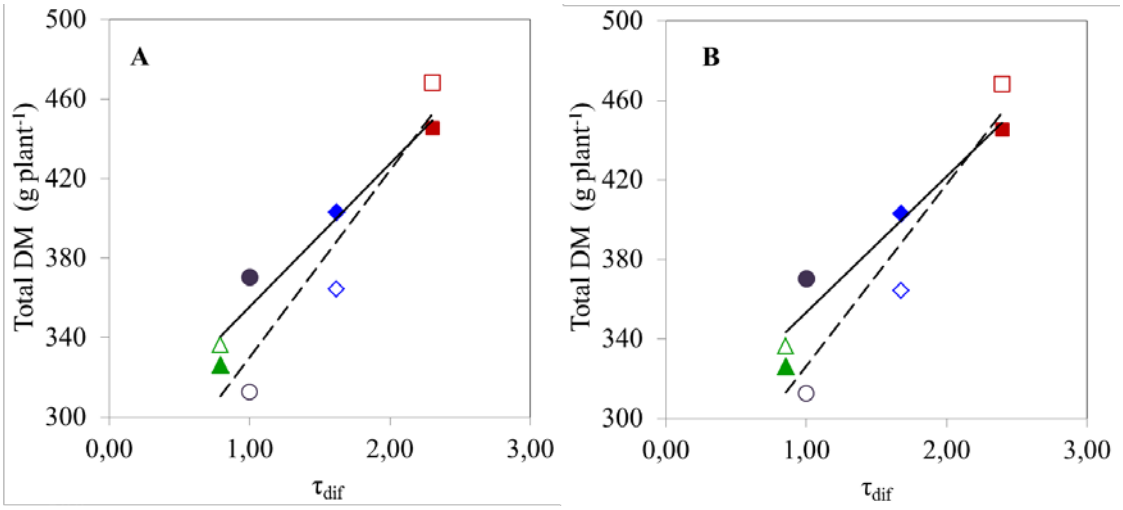

Figure 44. Total dry matter (DM) per plant against diffuse ratio (τ_{dif}) of each screenhouse (IP-13: squares; IP-34: diamonds; S-36: triangles) and of the open field (Cont: circles), through the PAR (P; fig **A**) and green (G; fig **B**) wavelength bands of solar radiation, on experimental periods 2011 (open marks/symbols and dashed line) and 2012 (closed marks/symbols). Lines stand for the best fit regression line for 2011 (dashed line) and 2012 (continuous line) data.

Table 36. Regression analysis results (slope of the best fit regression line; R^2) of groups of data of total dry matter per plant and diffuse ratio (τ_{dif}) of selected wavelength bands as measured in each respective treatment on both experimental periods (2011 and 2012).

	[1]a		[2]R^2	
Wavelength band	2011	2012	2011	2012
T: 350-1100 nm	66	49	0.87	0.86
P: 400-700 nm	94	72	0.87	0.94
B: 400-500 nm	172	135	0.82	0.92
G: 500-570 nm	91	68	0.89	0.92
R: 600-700 nm	45	34	0.83	0.89
FR: 700-800 nm	37	28	0.83	0.80
N: 800-1100 nm	31	22	0.81	0.71

[1]a: slope of regression line; [2]R^2: Coefficient of determination

7.8. Radiation use efficiency inside screenhouses

7.8.1. Simulating crop growth

The values of RUE of the crops of the Cont (1.05) were lower by about 0.35 and 0.52 the values reported by Vieira et al. (2009) (1.6 g MJ^{-1} PAR), Karam et al. (2009) (2.2 g MJ^{-1} PAR), respectively, for open field pepper crops in southern Portugal and in a Mediterranean climate. In their study, Karam et al. (2009) calculated the intercepted Photosyntheticaly Active Radiation (PARi) using the formula of Lambert-Beer (Shibles and Weber, 1965): $PAR_I = (PAR/PPD) * \left(1 - e^{-kLAI}\right)$, where PPD is the plant population density (plants m^{-2}), k is the extinction coefficient and LAI is the leaf area index (m^2 m^{-2}). The plant density in their work was 3.5 plants m^{-2} and they considered k-value for bell pepper to be 0.35 (Jovanovic and Annandale, 2000). Should we use the same interception model for the data of the present work (PPD = 1.8 plants m^{-2}; k = 0.35) the RUE would have been increased by 1.9 times as compared to the RUE evaluated in the present study (Table 37). Additionally, the plant density (PPD) also affects the RUE; increasing PPD the fi-PAR is reducing thus, the c-PARi is also reducing and therefore the RUE is increasing. The plant density in the present study was about 0.5 of the respective in Karam et al. (2009) study. By doubling the plant density on the model used by Karam et al. (2009) the c-PARi is reduced in half and (assuming that DMP remains unaffected by the increase of the PPD) the deduced RUE is therefore doubling. The latter analysis exhibits: (i) the importance of the interception model in use to calculate the PARi from the crop under study and (ii) the influence of the plant density on the c-PARi. The latter remarks (i, ii) could also explain the differences of the RUE between the present study and the study of Vieira et al. (2009).

Healey et al. (1998) reported that RUE (g MJ^{-1}) was 1.28, 1.49 and 1.89 for the crops (green panic and creeping bluegrass) at the open field and under a birdguard and a solarweave, respectively. The positive effect of the shade nets on the increase of the RUE by the underneath grown crops was documented by Kittas et al. (2012), who reported that RUE by shaded tomato crops was between 2.04 g MJ^{-1} and 2.62 g MJ^{-1}, while the respective of an open field crop was 0.94 g MJ^{-1}. Their values were relatively close to those given by Radin et al. (2003) for open field and greenhouse-grown tomatoes.

Table 37. DMP (g m^{-2}), cumulative intercepted PAR (c-PARi) as calculated by means of the interception model reported by Marcelis et al. (1998) and Karam et al. (2009), and the respective values of RUE, for the crops inside screenhouses (IP-13; IP-34; S-36) and at the open field (Cont). RUE values we

	DMP (g m^{-2})	c-PARi (MJ m^{-2})			**RUE (g MJ^{-1})		
Treatement		* M	[1] K	[2] K	* M	[1] K	[2] K
Cont	522	563	183	311	1,08	3,07 (1,9)	1,81 (0,7)
IP-13	569	843	221	339	1,48	3,82 (1,6)	2,49 (0,7)
IP-34	439	656	165	262	1,49	3,96 (1,7)	2,51 (0,7)
S-36	478	606	181	285	1,27	3,34 (1,6)	2,12 (0,7)

* M: interception model as reported by Marcelis et al. (1998).

**RUE was calculated using the values of DMP and c-PARi at the end of the period, which slightly increased the respective values calculated by eq. 47 - eq. 50.

[1] K: interception model as reported by Karam et al. (2009), where (PPD = 1.8 plants m^{-2}; k = 0.35 as reported by (Jovanovic and Annandale, 2000)).

[2] K: interception model as reported by Karam et al. (2009), where (PPD = 1.8 plants m^{-2}; k = 0.70 as suggested by Marcelis et al. (1998)).

A crop growth model was developed by Giménez et al. (2012) for pepper crops grown inside plastic greenhouses in Mediterranean regions. They reported a RUE of 4.01 g MJ^{-1} PARi, which is about 2.93 greater than the RUE calculated in the present study (on average for all screenhouses; 1.37 g MJ^{-1} PARi). The monthly mean values of integrals of daily solar radiation (MJ m^{-2} d^{-1}) reported by Giménez et al. (2012) during July, August and September (2005 and 2006) were about 0.52, while the October values were about 0.77 of the respective values of the present study for 2012 period at the open field (Cont), allowing the assumption (without significant error) that the greenhouse used by Giménez et al. (2012) were shaded (or blanched) during summer and early autumn. Thus, the RUE reported by the latter authors (4.01 g MJ^{-1} PAR) should be compared to the respective values for the screenhouse crops of the present study (Table 37). The crops were transplanted (in PPD of 2.0 plants m^{-2}) on July 21 and 20 on 2005 and 2006 period during the experiments conducted by Giménez et al. (2012). The DMP that they reported was about 1100 g m^{-2} at the end of the cropping periods, been about 1.4 of the DMP of the crops in the present study (703 g m^{-2}; average values for 3 screenhouses, for 2 periods). In their study the cumulative global solar radiation was 1729 MJ m^{-2} and the cumulative PAR was 743 MJ m^{-2} ($PAR=0.43*R_{s,global}$). Since DMP at harvest was 1193 g m^{-2} and RUE was

4.02 g MJ^{-1}, the mean seasonal fi-PAR was 0.40. In the present work, the mean seasonal fi-PAR was also 0.40 for the screenhouse cases. If it would have been used in the present study as a conversion coefficient of global solar radiation into PAR the value 0.43 instead of the 0.57 that was actually used (measured), the new RUE would have been 1.87 for the screenhouses (overall average). Thus, the improved RUE is about 0.5 of the respective value that Giménez et al. (2012) reported. As the PPD was about the same it did not affected the RUE. Thus, it is easily concluded that the lower integrals of available PAR due to the summer to winter crop season and the improved microclimate of the greenhouse enclosure during that period of year, greatly increased the RUE of the crop, unlike the screenhouse cases of the present study.

Comparison between protected (greenhouse) and open field crops was conducted by Baille, (1999), who quoted that the high RUE values in greenhouses are a consequence of the more favourable climatic conditions. Moreover, "Radiation Use Efficiency increases when the diffuse component of incident radiation is enhanced under shade", as Healey et al. (1998) clearly presented. The latter is not only valid for the plastic greenhouses but also for the screenhouses. In the present study was clearly presented the influence: (i) of the rate of the enrichment of the radiative environment with diffuse radiation and (ii) of the quality of the diffuse radiation on the productivity (total dry matter; Figure 44, on page 147;) and on the RUE (Figure 45, on page 152; Figure 46, on page 154) by the crops inside screenhouses The diffuse radiation distributed more uniformly the PAR energy upon the canopy surface enabled plants to utilize diffuse light better than direct light (Hemming et al., 2008). As more PAR reached the middle and lower layers of a crop canopy, plant CO_2 assimilation per unit of intercepted radiation is increasing, resulting in higher RUE (Healey et al., 1998).

7.8.2. RUE and screen characteristics

The differences between the RUE of the crops inside the insect proof screenhouses and the shade screenhouse S-36 could probably be ascribed to the differences in their radiative environment (beam+diffuse, diffuse and beam components), similarly to the respective observed differences of WUE and crop growth (total dry matter). In particular, it is essential to distinguish the source of the increased RUE of the crops inside screenhouse IP-34 as compared to the crops inside screenhouse S-36, although they presented about the same transmittance across the T and PAR wavelength band. Therefore, an attempt was made to correlate the optical properties of the covering screens to the RUE by the covered crops.

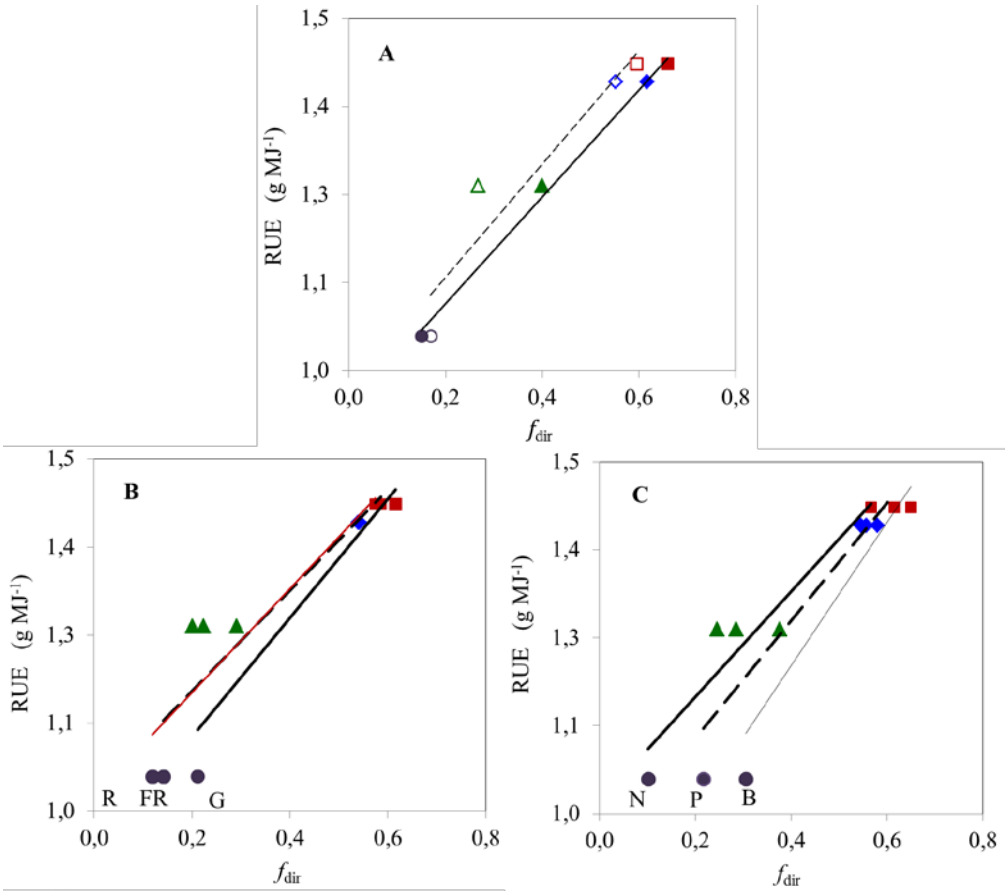

Figure 45. Radiation Use Efficiency (RUE; g MJ^{-1}) against the diffuse fraction (f_{dif}) of solar radiation of the: **A**) global and T (350-1100 nm), **B**) through the R (600-700 nm; R), the FR (700-800 nm;) and G (500-570 nm) and **C**) through the N (700-1100 nm), the P (400-700 nm) and the B (400-500 nm), wavelength bands, for each treatment (Cont; circles, IP-13; squares, IP-34; diamonds and S-36; triangles) for the 2012 experimental. Straight lines represent the best fit regression line for the corresponding groups of data; **A**) global-thick line and Total-dashed line, **B**) R-dashed line, FR-thin red line and G-thick line and **C**) N-thick line, P-dashed line and B-thin line.

For this purpose, the slope (RUE) of the eq. 47 - eq. 50 was plotted against: (i) the diffuse fraction (f_{dif}) of global (R_G) and Total solar radiation (T; 350-1100 nm) (Figure 45, **A**), (ii) against the diffuse fraction of solar radiation through the PAR (400-700 nm; P), the Blue (400-500 nm; B), the G (500-570 nm), the R (600-700 nm), the FR (700-800 nm) and the NIR (700-1100 nm; N) wavelength bands, for each treatment (Figure 45). The respective best fit regression lines were fitted and their respective equations were statistically estimated conducting a non-linear regression analysis using Marquardt, (1963) algorithm. As it can be seen in Figure 45 and in eq. 63 - eq. 70 the RUE of each treatment was tightly correlated to the f_{dif} of solar radiation, with the best fit regression line obtained for each respective group of data been as follow:

eq. 63, $f\mathrm{R}_{\mathrm{G;dif}}$: $\mathrm{RUE} = 0.76\, f\mathrm{R}_{\mathrm{G;dif}} + 0.94$, with $\mathrm{R}^2 = 1.00$

eq. 64, fT_{dif} : $\mathrm{RUE} = 0.80\, fT_{\mathrm{dif}} + 0.97$, with $\mathrm{R}^2 = 0.90$

eq. 65, fP_{dif} : $\mathrm{RUE} = 0.84\, fP_{\mathrm{dif}} + 0.94$, with $\mathrm{R}^2 = 0.86$

eq. 66, fB_{dif} : $\mathrm{RUE} = 1.02\, fB_{\mathrm{dif}} + 0.80$, with $\mathrm{R}^2 = 0.88$

eq. 67, fG_{dif} : $\mathrm{RUE} = 0.85\, fG_{\mathrm{dif}} + 0.94$, with $\mathrm{R}^2 = 0.88$

eq. 68, fR_{dif} : $\mathrm{RUE} = 0.71\, fR_{\mathrm{dif}} + 1.03$, with $\mathrm{R}^2 = 0.84$

eq. 69, fFR_{dif} : $\mathrm{RUE} = 0.74\, fFR_{\mathrm{dif}} + 1.02$, with $\mathrm{R}^2 = 0.90$

eq. 70, fN_{dif} : $\mathrm{RUE} = 0.75\, fN_{\mathrm{dif}} + 1.02$, with $\mathrm{R}^2 = 0.94$

The extremely high coefficient of determination of the above equations clearly supports the profound positive effect of the diffused radiative environment over the utilization of the radiation by the crops. The positive effect of the diffuse radiation upon the RUE was also documented by Healey et al. (1998), but unfortunately, for comparison reasons, non-statistically supported i.e., no regression equation was reported by the authors.

Moreover, the spectra quality of the diffuse solar radiation that was been available to the crops of each treatment was also strongly correlated to their RUE (Figure 46 and Table 38). The slope and the coefficient of determination of best fit regression line revealed by the statistical analysis for each respective group of data (RUE; quality parameter of diffuse solar radiation) are presented in Table 38.

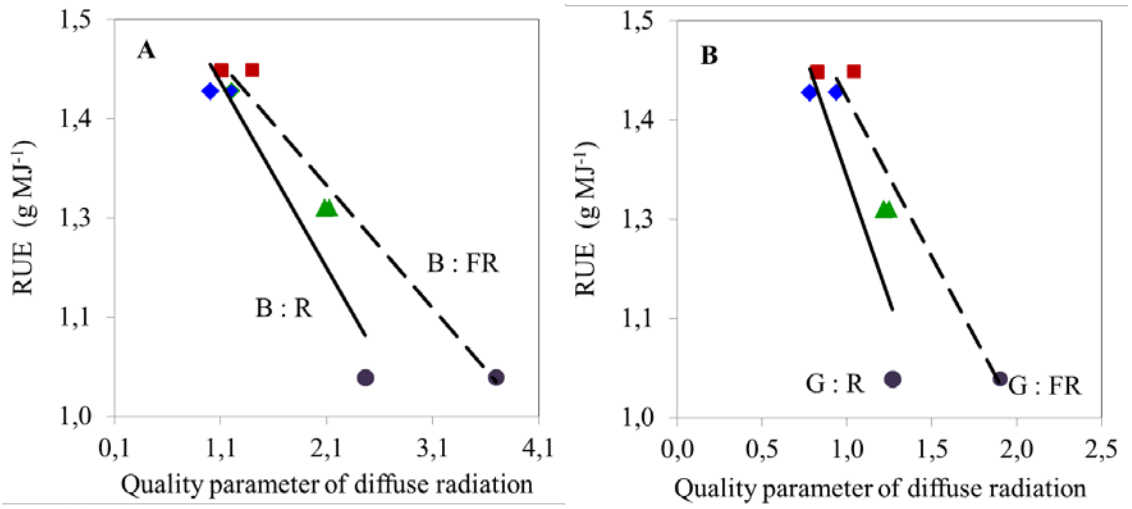

Figure 46. Radiation Use Efficiency (RUE; g MJ^{-1}) against the quality parameters of the diffuse solar radiation in each treatment (Cont; circles, IP-13; squares, IP-34; diamonds and S-36; triangles); **A**) B : R, B : FR and **B)** G : R, G : FR). Straight lines represent the best fit regression line for the corresponding groups of data for each wavelength band.

Table 38. Regression analysis results (slope of the best fit regression line; R^2) of groups of data of RUE and spectra quality components of the diffuse irradiance as were determined for each respective treatment.

Spectral quality component	[1]a	[2]R^2
G : B	1.32	0.90
G : R	-0.63	0.81
G : FR	-0.40	0.95
G : T	-8.33	0.89
B : R	-0.23	0.90
B : FR	-0.15	0.98
P : N	-0.18	0.82
G : N	-0.73	0.85

[1]a: slope of regression line; [2]R^2: Coefficient of determination

The correlations were significantly tight for the cryptochrome related ratios (B:R and B:FR). Interestingly, the correlation was also tight for quality parameters which embedded green wavelength band; G : B, G : R,; G : FR, G : T and G : N. As in the IWUE correlations, the RUE correlations with the quality parameters relevant to the green light further support the negative effect of the green light on the productivity of the crops, due to the inhibition of the crop growth i.e., the decrease of the total dry matter production, as documented by several authors (Dougher and Bugbee, 2001; Klein, 1964; Klein et al., 1965; Went, 1957). The grade of the latter negative correlations is supported by the higher absolute values of the slopes of the respective

regression lines as compared to the slopes of the lines of the non-green light embedded parameters, ex. the cryptochrome related parameters; G:R 0.63 > B:R 0.23 and G:N 0.40 > B:FR 0.15.

The RUE of the crops was also strongly correlated to the diffuse ratio of the screenhouses (τ_{dif}), with the correlation for the NIR ($\tau_{\mathrm{dif}} - N$) band been quite interesting:

eq. 71, $\tau_{\mathrm{dif}} - N$: $\mathrm{RUE} = 0.09\,\tau_{\mathrm{dif}} - N \quad + 1.02$, with $\mathrm{R}^2 = 0.88$

This tight correlation could be ascribed to the more uniform distribution of the NIR radiation over the canopy surface, as opposed to the open field treatment, that resulted to the reduction of the canopy temperature of the crop inside screenhouses, unlike the crop at the open field (Dai et al., 2004). This probably occurs because the heat load (NIR) transmitted by the diffuse light upon the crop canopy is spread/distributed over a greater area rather than been concentrated in a smaller one, which is the case of the NIR transmitted by direct light. That resulted in a reduction of the canopy temperature and consequently in canopy-to-air vapor pressure deficit reduction (Gu, 2002; Li et al., 2014; Urban et al., 2012). The synergistic effect of the later improved microclimatic parameters and the overall microclimatic improvement of the enclosures enhanced the photosynthetic performance of the covered crops (Cohen and Moreshet, 1997; Haijun et al., 2015; Kittas et al., 2012; Nicolás et al., 2005), resulting to increased productivity (DMP) inside screenhouses, as opposed to that of the open field.

Another interesting correlation of the RUE was statistically revealed for the direct component of the solar radiation in each treatment. The transmittance (τ_{b}) of the direct light was highly correlated to the RUE of the crops. As τ_{b} was stable across the entire T wavelength band (Figure 17, on page 67), the equations of the best fi regression line for each selected spectral band were about the same (Table 39) and therefore only one case band is graphically presented (Figure 47). The negative correlation of the RUE and the transmittance of the direct component of the solar radiation that incident upon the crops clearly documents the lower utilization of direct radiation by the crops.

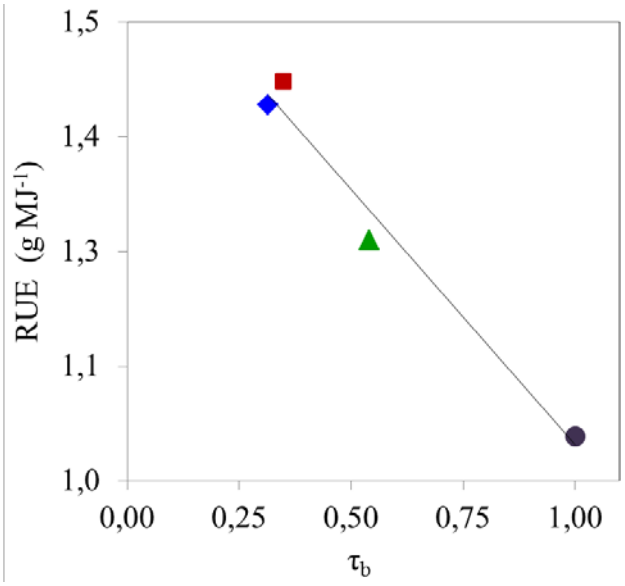

Figure 47. RUE against transmittance to the direct component (τ_b) of solar radiation through G (500-570 nm) wavelength band as were determined for each respective treatment (Cont; circles, IP-13; squares, IP-34; diamonds and S-36; triangles). Straight line represent the best fit regression line for the respective group of data (RUE; τ_b).

Table 39. Regression analysis results (slope of the best fit regression line; R^2) of groups of data of RUE and transmittance to the direct component of solar radiation through selected wavelength bands as were determined for each respective treatment.

Wavelength band	[1]a	[2]R^2
T	-0.55	0.97
P	-0.56	0.97
B	-0.55	0.97
G	-0.56	0.97
R	-0.56	0.97
FR	-0.56	0.97
N	-0.56	0.97

[1]a: slope of regression line; [2]R^2: Coefficient of determination

8. Conclusions

The high solar radiation levels observed under open field conditions were reduced under screenhouse conditions. The three different screens used resulted in a reduction of solar radiation above the crop from 22% - 38%, depending on the optical properties of the screen. Differences between the laboratory screen tests and the in situ screenhouse transmittance were observed; the *in situ* transmittance was decreased as opposed to that determined in the laboratory. Screens increased the diffuse fraction of solar radiation inside the enclosures, with respect to their color (brightness) and geometrical characteristics (porosity). Differences in the quality of the radiative environment were revealed inside screenhouses after a spectrum distribution analysis of their solar radiation (beam, diffuse and total), imposed by their colour.

The presence of the screen, although it reduced the incoming heat energy and the air exchange rate, did not affect negatively the screenhouse air temperature which was similar under screenhouse and open field conditions. Thus, the screenhouse microclimate created under Mediterranean summer conditions was favourable for pepper crop production, since the high solar radiation levels observed outside were reduced under screenhouse conditions and the crop performed better, as indicated by the lower values of canopy-to-air temperature difference and canopy-to-air vapour pressure deficit observed under screenhouse conditions that in the open field.

Crop transpiration rate was decreased inside screenhouses by 20% and 40%, resulting in proportionately reduced irrigation water consumption. It was found that the presence of the screen material decreases the advective part of crop transpiration, something that is attributed to the reduction of air velocity inside the screenhouse.

A good correlation was observed between the inside and outside air velocity measurements in the three screenhouses. The reduction of air velocity was higher in the case of insect proof screenhouses compared to the screenhouse covered by the shading screen, something that was in agreement with the differences in the porosity and permeability of the screens. The internal air velocity in the insect proof and the shading screenhouses was about 20% and 44%, respectively, of that measured outside. The discharge coefficient C_{ds^*} of the screens was estimated by means of wind tunnel experiments and was found to be 0.465 and 0.795, for the insect proof and shading screen, respectively.

A good correlation was found between the air exchange rate values calculated using the tracer gas method and the air velocity measured outside the screenhouses. The data were used to calibrate a model for the prediction of screenhouse ventilation rate related to the discharge C_d and the wind effect C_w coefficients. The value of the overall pressure drop and wind effect coefficient ($C_d\sqrt{C_w}$) coefficient observed for the insect proof screenhouses was 0.026 while the respective value estimated for the shaded screenhouse was 0.072. Finally, it was found that the ventilation rate observed in the experimental, small scale screenhouses was much higher to that observed in commercial, large scale screenhouses. A generalization of the results was attained and a method for estimating the ventilation performance for screenhouses with different volume and screens was proposed.

The total yield was significantly increased under screenhouse conditions (up to 66%) compared to open field fruit yield. Fruit yield quality was also improved under screenhouse conditions, not only due to the reduction of physiological disorders and pest defects but also due to the higher fruit size and weight. The most favourable shade intensity was the moderate shade (≈20-25%; IP-13) as compared to the heavy shade (≈34-38%; IP-34), assuming color similarity (neutral color; clear vs white color); IP-13 increased the production by 21% (mean for both periods) as opposed to that of IP-34. The most favourable screen color was the neutral white as opposed to the green, at equal shade intensities; crops inside IP-34 produced more by about 17% as compared to that of S-36.

Irrigation Water Use Efficiency (IWUE) was increased by 93%-132% as screenhouse crops consumed from about 20-40% less water in order to produce more fresh fruit weight than the open field crop.

The quantity of the diffused solar radiation that is available to the crops and its spectral quality influences their growth; the increased diffuse radiation inside the insect proof screenhouses, unlike the shade screenhouse and the negative effect of the green light enriched solar radiation inside S-36, as opposed to the insect proof screenhouses, resulted in an enhanced crop growth inside the insect proof screenhouses. The crop growth was successfully simulated by means of a model that predicts the dry matter production using as input only the cumulative intercepted PAR by the crops and the Radiation Use Efficiency (RUE) was estimated for the crop of each treatment. The RUE was increased under screenhouse conditions.

The quantity and quality of the direct and diffuse solar radiation of the enclosures directly influences the IWUE and the RUE of the crops.

9. Future perspectives for research

Cultivating inside screenhouses is a very challenging practice and therefore research should be extended at different horticultural crops and especially highly value added, such as cherry or purple tomatoes or even exclusively special cultivars. Another possible subject matter that could probably be investigated is the integration of a screenhouse construction by a hydroponic crop. The economic effectiveness of this integration should be studied. Moreover, an effort could possibly be made in order to investigate the effectiveness of bio-aggressors as been influenced by the modification of the internal microclimate.

The study of the ventilation performance of the structures should be continued toward the complete simulation of the transport processes inside the constructions in order to thoroughly investigate the occurring phenomena, using additively different screen and construction types.

Although screenhouses passively regulate their internal microclimate, yet they are very sensitive in external impacts of the ambient microclimate and therefore very complex systems. The numerical simulation of the microclimatic performance by means of CFD methodology is very challenging. In the present research work an attempt to investigate the microclimate distribution was done by conducting spatial measurements of air temperature and humidity and wind speed and direction. The process of these measurements could revealed interesting findings about the internal microclimate configuration as been imposed by the ambient conditions and the covering screen properties.

10. References

Abdel-Ghany, A. M., Al-Helal, I.M., 2011. Analysis of solar radiation transfer: A method to estimate the porosity of a plastic shading net. Energy Conversion and Management 52, 1755–1762.

Abdel-Mawgoud, A.M.R., El-Abd, S.O., Singer, S.M., Abouhadid, A.F., Hsiao, T.C., 1996. Effect of shade on the growth and yield of tomato plants. Acta Horticulturae 434, 313–320.

Abdullah, T.L., Ramlan, M.F., Chin, F.L.S., 2008. Physiological changes, growth and flowering responses of curcuma alismatifolia “Chiangmai Pink” to shading. Acta Horticulturae 769, 467–470.

Adegoroye, A.S., Jolliffe, P.A., 1987. Some inhibitory efects of radiation stress on tomato fruit ripening. Journal of the Science of Food and Agriculture. 39, 297–302.

Alarcón, J.J., Ortuño, M.F., Nicolás, E., Navarro, A., Torrecillas, A., 2006. Improving water use efficiency of young lemon trees by shading with aluminised plastic nets. Agricultural Water Management 82, 387–398.

Al-Helal, I.M., Abdel-Ghany, A. M., 2010. Responses of plastic shading nets to global and diffuse PAR transfer: Optical properties and evaluation. NJAS - Wageningen Journal of Life Sciences 57, 125–132.

Al-Helal, I.M., Abdel-Ghany, A. M., 2011. Measuring and evaluating solar radiative properties of plastic shading nets. Solar Energy Materials and Solar Cells 95, 677–683.

Allen, L.H., 1975. Shade-cloth microclimate of soybeans. Agronomy Journal 67, 175–181.

Allen, R.G., Pereira, L.S., Raes, D., Smith, M., Ab, W., 1998. Crop evapotranspiration - Guidelines for computing crop water requirements - FAO Irrigation and drainage paper 56, Rome.

Al-Mulla, Y.A., Al-Balushi, M., Al-Rawahy, M., Al-Makhmary, S., Al-Raisy, F., 2011. Evaluation of microclimatological parameters inside a screenhouse used in arid regions. Acta Horticulturae. 893, 509–516.

Al-Mulla, Y.A., Al-Balushi, M., Al-Rawahy, M., Al-Raisy, F., Al-Makhmary, S., 2008. Screenhouse microclimate effects on cucumber production planted in soilless culture (open system). Acta Horticulturae 801, 637–644.

Aloni, B., Karni, L., Zaidman, Z., Schaffer, A.A., 1997. The relationship between sucrose supply, sucrose-cleaving enzymes and flower abortion in pepper. Annals of Botany 79, 601–605.

Al-Shamiry, F.M.S., Sharif, A.R.M., Kamaruddin, R., Ahmad, D., Janius, R., Mohamad, M.Y., 2006. Microclimate inside tunnel-roof and jack-roof tropical greenhouse structures. Acta Horticulturae 710, 179–184.

Álvarez, A.J., Oliva, R.M., Valera, D.L., 2012. Software for the geometric characterisation of insect-proof screens. Computers and Electronics in Agriculture 82, 134–144.

Arboree, C., Losciale, P., Zibordi, M., Manfrini, L., Morandi, B., Corelli-Grappadelli, L., 2011. Effect of moderate light reduction on absorbed energy management, water use, photoprotection and photo-damage in peach. Acta Horticulturae 907, 169–174.

Aro, E.M., Virgin, I., Andersson, B., 1993. Photoinhibition of photosystem II. Inactivation, protein damage and turnover. Biochimica et Biophysica Acta - Bioenergetics 1143, 113–134.

ASHRAE, 1993. Handbook of Fundamentals. American Society of Heating, Refrigerating and Air-Conditioning Engineers, Atlanta, USA.

Bailey, B.J., 2003. Screens stop insects but slow airflow. Fruit Veg. Tech. 3, 6–8.

Baille, A., 1999. Energy cycle. In: Stanhill, G., Enoch, H.Z. (Eds.), Greenhouse Ecosystems.Ecosystems of the World 20. Elselvier, Amsterdam, The Netherlands, pp. 265–286.

Baille, M., Baille, A. and Delmon, D., 1994. Microclimate and transpiration of greenhouse rose crops. Agr. For. Meteorol. 71: 83-97.

Bakker, J.C., 1989. The effects of temperature on flowering, fruit set and fruit development of glasshouse sweet pepper (Capsicum annuum L). J. Hortic. Sci 64, 313–320.

Baldocchi, D.D., Harley, P.C., 1995. Scaling carbon dioxide and water vapour exchange from leaf to canopy in a deciduous forest. II. Model testing and application. Plant, Cell and Environment 18, 1157–1173.

Baldocchi, D.D., Vogel, C. A., Hall, B., 1997. Seasonal variation of carbon dioxide exchange rates above and below a boreal jack pine forest. Agricultural and Forest Meteorology 83, 147–170.

Banerjee, R., Schleicher, E., Meier, S., Viana, R.M., Pokorny, R., Ahmad, M., Bittl, R., Batschauer, A., 2007. The signaling state of Arabidopsis cryptochrome 2 contains flavin semiquinone. Journal of Biological Chemistry 282, 14916–14922.

Bange, M.P., 1995. Environmental control of potential yield of sunflower in a sub-tropical environment. PhD Thesis, University of Queensland, Australia.

Baptista, F.J., Bailey, B.J., Randall, J.M., Meneses, J.F., 1999. Greenhouse ventilation rate: Theory and measurement with tracer gas techniques. Journal of Agricultural Engineering Research 72, 363–374.

Barber, H.., Sharpe, P.J.., 1971. Genetics and physiology of sunscald of fruits. Agricultural Meteorology 8, 175–191.

Ben-Yakir, D., Antignus, Y., Shahak, Y., Offir, Y., 2012. Optical manipulations of insect pests for protecting agricultural crops. Acta Horticulturae 956, 609–616.

Ben-Yakir, D., Hadar, M.D., Offir, Y., Chen, M., Tregerman, M., 2008. Protecting crops from pests using Optinet® screens and Chromatinet® shading nets. Acta Horticulturae 770, 205–212.

Berlinger, M.J., Lebiush-Mordechai, S., 1995. Physical methods for the control of Bemisia. In: Gerling, D., Mayer, R.T. (Eds.), Bemisia 1995: Taxonomy, Biology, Damage, Control and Management. Intercept Ltd., Andover, UK. 617–634.

Berlinger, M.J., Lebiush-Mordechai, S., Fridja, D., Mor, N., 1993. The effect of types of greenhouse screens on the presence of western flower thrips. IOBC/WPRS Bull. 16, 13–16.

Bertin, N., Guichard, S., Leonardi, C., Longuenesse, J.J., Langlois, D., Navez, B., 2000. Seasonal evolution of the quality of fresh glasshouse tomatoes under Mediterranean conditions, as affected by air vapour pressure deficit and plant fruit load. Annals of Botany 85, 741–750.

Bethke, J.A., 1994. Considering installing screening? This is what you need to know. Greenhouse Manager 34–36.

Bethke, J.A., Paine, T.D., 1991. Screen hole size and barriers for exclusion of insect pests of glasshouse crop. Journal of Entomological Science. 26, 169–177.

Boulard, T., Baille, A., 1995. Modelling of air exchange rate in a greenhouse equipped with continuous roof vents. Journal of Agricultural Engineering Research 61, 37–48.

Boulard, T., Draui, B., 1995. Natural ventilation of a greenhouse with continuous roof vents: measurements and data analysis. Journal of Agricultural Engineering Research 61, 27–36.

Boulard, T., Fargues, J., Roy, J.C., Pizzol, J., 2011. Improving air transfer through insect proof screens. Acta Horticulturae 289–296.

Brandle, J.R., Hodges, L., Zhou, H.X., 2004. Windbreaks in North American Agricultural Systems. Agroforestry Systems 61, 65–78.

Briassoulis, D., Mistriotis, A., Eleftherakis, D., 2007a. Mechanical behaviour and properties of agricultural nets—Part I: Testing methods for agricultural nets. Polymer Testing 26, 822–832.

Briassoulis, D., Mistriotis, A., Eleftherakis, D., 2007b. Mechanical behaviour and properties of agricultural nets. Part II: Analysis of the performance of the main categories of agricultural nets. Polymer Testing 26, 970–984.

Brodersen, C.R., Vogelmann, T.C., 2007. Do epidermal lens cells facilitate the absorptance of diffuse light? American Journal of Botany 94, 1061–1066.

Brodersen, C.R., Vogelmann, T.C., 2010. Do changes in light direction affect absorption profiles in leaves? Functional Plant Biology 37, 403–412.

Brodersen, C.R., Vogelmann, T.C., Williams, W.E., Gorton, H.L., 2008. A new paradigm in leaf-level photosynthesis: Direct and diffuse lights are not equal. Plant, Cell and Environment 31, 159–164.

Cabrera, F.J., Baille, A., López, J.C., González-Real, M.M., Pérez-Parra, J., 2009. Effects of cover diffusive properties on the components of greenhouse solar radiation. Biosystems Engineering 103, 344–356.

Cabrera, F.J., Lopez, J.C., Baeza, E.J., Perez-Parra, J., 2006. Efficiency of anti-insect screens placed in the vents of Almeria greenhouses. Acta Horticulturae 719, 605–614.

Casal, J.J., 2000. Phytochromes, cryptochromes, phototropin: photoreceptor interactions in plants. Photochemistry and Photobiology 71, 1–11.

Castellano, S., Candura, A., Mugnozza, G.S., 2008a. Relationship between solidity ratio, colour and shading effect of agricultural nets. Acta Horticulturae 801, 253–258.

Castellano, S., Hemming, S., Russo, G., 2008b. The influence of colour on radiometric performances of agricultural nets. Acta Horticulturae 801, 227–236.

Castellano, S., Russo, G., Scarascia Mugnozza, G., 2006. The influence of construction parameters on radiometric performances of agricultural nets. Acta Horticulturae 718, 283–290.

Cebolla-Cornejo, J., Roselló, S., Nuez, F., 2008. Influence of protected cultivation on accumulation of taste intensity components in traditional spanish tomato varieties. Acta Horticulturae 181–188.

Charles-Edwards, D.A., Ludwig, L.J., 1975. The basis of expansion of leaf photosynthetic activities. Environmental and Biological Control of Photosynthesis (ed. R. Marcelle) Dr W. Junk, The Hague, pp. 37-44. Tomato Crop, pp. 144.

Chow, W.S.,Aro, E.M., 2005. Photoinactivation and mechanisms of recovery. In: T. Wydrzynski and K. Satoh (eds.), Photosystem II: The Light Driven Water/Plastoquinone Oxido Reductase, Springer, The Nederlands. p.627– 648.

Cohen, S.,,Moreshet, S., 1997. Response of citrus trees to modified radiation regime in semi-arid conditions. Journal of Experimental Botany 48, 35–44.

Collatz, G.J., Ball, J.T., Grivet, C., Berry, J. a, 1991. Physiological and environmental regulation of stomatal conductance, photosynthesis and transpiration: a model that includes a laminar boundary layer. Agricultural and Forest Meteorology 54, 107–136.

Coombe, P.E., 1981. Wavelength specific behaviour of the whitefly Trialewodes vaporariorum (Homoptera: Aleyrodidae). Journal of Comparative Physiology ??? A 144, 83–90.

Dağdelen, N., Yılmaz, E., Sezgin, F., Gürbüz, T., 2004. Effects of water stress at different growth stages on processing pepper (Capsicum annum Cv. Kapija) yield, water use and quality characteristics. Pakistan Journal of Biological Science, 7, 12, 2167-2172.

Dagnelie, P., 1986. Théorie et méthodes statistiques: Applications agronomiques. Tome II. Gembloux, Belgium: Presses Agronomiques.

Dai, Y., Dickinson, R.E., Wang, Y.P., 2004. A two-big-leaf model for canopy temperature, photosynthesis, and stomatal conductance. Journal of Climate 17, 2281–2299.

Davies, J.N.,,Hobson, G.E., 1981. The constituents of tomato fruit-the influence of environment, nutrition, and genotype. Critical Reviews in Food Science and Nutrition 15, 205–280.

De Jong, T., Bot, G.P.A., 1992. Flow characteristics of one-side-mounted windows. Energy and Buildings 19, 105–112.

Demrati, H., Boulard, T., Bekkaoui, A., Bouirden, L., 2001. Natural ventilation and microclimatic performance of a large-scale banana greenhouse. Journal of Agricultural Engineering Research 80, 261–271.

Desmarais, G., Ratti, C., Raghavan, G.S.V., 1999. Heat transfer modelling of screenhouses. Solar Energy 65, 271–284.

Dicken, U., Cohen, S., Tanny, J., 2013a. Examination of the Bowen ratio energy balance technique for evapotranspiration estimates in screenhouses. Biosystems Engineering 114, 397–405.

Dicken, U., Cohen, S., Tanny, J., 2013b. Effect of plant development on turbulent fluxes of a screenhouse banana plantation. Irrigation Science 31, 701–713.

Doorenbos, J., Kassam, A.H., 1979. Yield response to water. FAO irrigation and drainage paper no. 33. UN-FAO, Rome, Italy.

Dorais, M., Papadopulus, A.P., Gosselin, A., 2001. Greenhouse tomato fruit quality. Horticultural Reviews 26, 239–319.

Döring, T.F., Chittka, L., 2007. Visual ecology of aphids—a critical review on the role of colours in host finding. Arthropod-Plant Interactions 1, 3–16.

Dougher, T.A., Bugbee, B., 2001. Evidence for yellow light suppression of lettuce growth. Photochemistry and Photobiology 73, 208–212.

Eisinger, W.R., Bogomolni, R.A., Taiz, L., 2003. Interactions between a blue-green reversible photoreceptor and a separate UV-B receptor in stomatal guard cells. American Journal of Botany 90, 1560–1566.

El-Aidy, F., El-Afry, M., 1983. Influence of shade on growth and yield of tomatoes cultivated during the summer season in Egyptian Plasticulture 47, 2 – 6.

El-Gizawy, A.M., Abdallah, M.M.F., Gomaa, H.M., Mohamed, S.S., 1992. Effect of different shading levels on tomato plants 2. Yield and fruit quality. Acta Horticulturae 323, 349–354.

Fallika, F.E., Alkalai-Tuvia, S., Parselan, Y., Aharon, Z., Elmann, A., Matan, E., Yehezkel, H., Offir, Y., Ratner, K., Zur, N., Shahak, Y., 2009. Can colored shade nets maintain sweet pepper quality during storage and marketing? Acta Horticulturae 830, 37–44.

Farquhar, G.D., von Caemmerer, S., Berry, J.A., 1980. A biochemical model of photosynthetic CO2 assimilation in leaves of C3 species. Planta 90, 78–90.

Fatnassi, H., Boulard, T., Demrati, H., Bouirden, L., Sappe, G., 2002. Ventilation performance of a large canarian-type greenhouse equipped with Insect-proof nets. Biosystems Engineering 82, 97–105.

Fatnassi, H., Boulard, T., Poncet, C., Chave, M., 2006. Optimisation of greenhouse insect screening with computational fluid dynamics. Biosystems Engineering 93, 301–312.

Fernandez, J.E.I., Bailey, B.J., 1992. Measurement and prediction of greenhouse ventilation rates. Agricultural and Forest Meteorology 58, 229–245.

Folta, K.M., and Maruhnich, S., 2007. Green light: a signal to slow down or stop. Journal of Experimental Botany 58, 3099–3111.

Forchheimer, P., 1901. Wasserbewegung durch boden. Z. Ver. Dtsch. Ing., 45, 1736–1741, 1781–1788.

Franklin, K. A, 2008. Shade avoidance. The New Phytologist 179, 930–44.

Franklin, K. A., Larner, V.S., Whitelam, C.C., 2005. The signal transducing photoreceptors of plants. International Journal of Developmental Biology 49, 653–664.

Frechilla, S., Talbott, L.D., Bogomolni, R. A, Zeiger, E., 2000. Reversal of blue light-stimulated stomatal opening by green light. Plant & Cell Physiology 41, 171–6.

Frechilla, S., Zhu, J., Talbott, L.D., Zeiger, E., 1999. Stomata from npq1, a zeaxanthin-less Arabidopsis mutant, lack a specific response to blue light. Plant & Cell Physiology 40, 949–954.

Ganelevin, R., 2008. World-wide commercial applications of colored shade nets technology. Acta Horticulturae 770, 199-204

Geider, R.J., Delucia, E.H., Falkowski, P.G., Finzi, A. C., Grime, J.P., Grace, J., Kana, T.M., La Roche, J., Long, S.P., Osborne, B. a, Platt, T., Prentice, I.C., Raven, J. a, Schlesinger, W.H., Smetacek, V., Stuart, V., Sathyendranath, S., Thomas, R.B., Vogelmann, T.C., Williams, P., Woodward, F.I., 2001. Primary productivity of planet earth: biological determinants and physical constraints in terrestrial and aquatic habitats. Global Change Biology 7, 849–882.

Gent, M., 2008. Density and duration of shade affect water and nutrient use in greenhouse tomato. Journal of the American Society for Horticultural Science. 133, 619–627.

Gent, M.P.N., 2007. Effect of degree and duration of shade on quality of greenhouse tomato. HortScience 42, 514–520.

Giménez, C., Gallardo, M., Martínez-Gaitán, C., Stöckle, C.O., Thompson, R.B., Granados, M.R., 2012. VegSyst, a simulation model of daily crop growth, nitrogen uptake and evapotranspiration for pepper crops for use in an on-farm decision support system. Irrigation Science 31, 465–477.

Gindaba, J., Wand, S.J.E., 2008. Comparison of climate ameliorating measures to control sunburn on “Fuji” apples. Acta Horticulturae 772, 59–64.

González-Real, M.M., Baille, A., Liu, H.Q., 2008. Influence of fruit load on dry matter and N-distribution in sweet pepper plants. Scientia Horticulturae 117, 307–315.

González-Real, M.M., Liu, H.Q., Baille, A., 2009. Influence of fruit sink strength on the distribution of leaf photosynthetic traits in fruit-bearing shoots of pepper plants (Capsicum annuum L.). Environmental and Experimental Botany 66, 195–202.

Gorton, H.L., Brodersen, C.R., Williams, W.E., Vogelmann, T.C., 2010. Measurement of the optical properties of leaves under diffuse light. Photochemistry and Photobiology 86, 1076–1083.

Gu, L., 2002. Advantages of diffuse radiation for terrestrial ecosystem productivity. Journal of Geophysical Research 107.

Gu, L., Baldocchi, D.D., Wofsy, S.C., Munger, J.W., Michalsky, J.J., Urbanski, S.P., Boden, T.A., 2003. Response of a deciduous forest to the Mount Pinatubo eruption: enhanced photosynthesis. Science, New Series, 299, 2035–2038.

Guichard, S., Bertin, N., Leonardi, C., Gary, C., 2001. Tomato fruit quality in relation to water and carbon fluxes. Agronomie 21, 385–392.

Haijun, L., Cohen, S., Lemcoff, J.H., Israeli, Y., Tanny, J., 2015. Sap flow, canopy conductance and microclimate in a banana screenhouse. Agricultural and Forest Meteorology 201, 165–175.

Hall, A., 1977. Assimilate source-sink relationships in Capsicum annuum L. I. The dynamics of growth in fruiting and deflorated plants. Australian Journal of Plant Physiology 4, 623–636.

Harmanto, Tantau, H.J., Salokhe, V.M., 2006. Microclimate and air exchange rates in greenhouses covered with different nets in the Humid Tropics. Biosystems Engineering 94, 239–253.

Hartz, T.K., Costa, F.J., Schrader, W.L., 1996. Suitability of composted green waste for horticultural uses. HortScience 31, 961–964.

Healey, K.D., Hammer, G.L., Rickert, K.G., Bange, M.P., 1998. Radiation use efficiency increases when the diffuse component of incident radiation is enhanced under shade. Australian Journal of Agricultural Research 49, 665.

Healey, K.D., Rickert, K.G., 1998. Shading material changes the proportion of diffuse radiation in transmitted radiation. Australian Journal of Experimental Agriculture 38, 95-100.

Hemming, S., Dueck, T., Janse, J., Van Noort, F., 2008. The effect of diffuse light on crops. Acta Horticulturae 801 part 2, 1293–1300.

Heuvelink, E., Buiskool, R.P.M., 1995. Influence of Sink-Source Interaction on Dry Matter Production in Tomato. Annals of Botany, 75, 381-389

Heuvelink, E., Korner, O., 2001. Parthenocarpic fruit growth reduces yield fluctuation and blossom-end rot in sweet pepper. Annals of Botany 88, 69–74.

Hodges, L., Sanders, D.C., Perry, K.B., Eskridge, K.M., Batal, K.M., Granbeerry, D.M., McLaurin, W.J., Decoteau, D., Dufault, R.J., Garrett, J.T., Nagata, R., 1995. Adaptability and reliability of yield for four bell pepper cultivars across three southeastern States. HortScience 30, 1205–1210.

Hogewoning, S.W., Trouwborst, G., Maljaars, H., Poorter, H., van Ieperen, W., Harbinson, J., 2010. Blue light dose-responses of leaf photosynthesis, morphology, and chemical composition of Cucumis sativus grown under different combinations of red and blue light. Journal of Experimental Botany 61, 3107–3117.

Hollinger, A.D.Y., Kelliher, F.M., Byers, J.N., Hunt, J.E., McSeveny, T.M., Weir, P.L., 1994. Atmosphere Linked references are available on JSTOR for this article: carbon dioxide exchange between an undisturbed old-growth temperate forest and the atmosphere. Ecology 75, 134–150.

Ilić, Z.S., Milenković, L., Stanojević, L., Cvetković, D., Fallik, E., 2012. Effects of the modification of light intensity by color shade nets on yield and quality of tomato fruits. Scientia Horticulturae 139, 90–95.

Ilić, Z.S., Milenković, L., Šunić, L., Fallik, E., 2014. Effect of coloured shade-nets on plant leaf parameters and tomato fruit quality. Journal of the Science of Food and Agriculture.

Jones, H.G., 2014. Plants and microclimate. A quantitative approach to environmental plant physiology. Cambridge University Press, 3rd Edition pp 23.

Jovanovic, N.Z., Annandale, J.G., 2000. Crop growth model parameters of 19 summer vegetable cultivars for use in mechanistic irrigation scheduling models. Water SA 26, 67–74.

Karam, F., Masaad, R., Bachour, R., Rhayem, C., Rouphael, Y., 2009. Water and radiation use efficiencies in drip-irrigated pepper (Capsicum annuum L.): Response to full and deficit irrigation regimes. European Journal of Horticultural Science 74, 1611–4426.

Katsoulas, N., Baille, A., Kittas, C., 2002. Influence of leaf area index on canopy energy partitioning and greenhouse cooling requirements. Biosystems Engineering 83, 349–359.

Katsoulas, N., Bartzanas, T., Boulard, T., Mermier, M., Kittas, C., 2006a. Effect of vent openings and insect screens on greenhouse ventilation. Biosystems Engineering 93, 427–436.

Katsoulas, N., Kittas, C., Dimokas, G., Lykas, C., 2006b. Effect of irrigation frequency on rose flower production and quality. Biosystems Engineering 93, 237–244.

Katsoulas, N., Rigakis, N., Kitta, E., Baille, A., 2012. Transpiration of a sweet pepper crop under screenhouse conditions. Acta Horticulturae 957, 91–97.

Kittas, C., Baille, A., Giaglaras, P., 1999. Influence of covering material and shading on the spectral distribution of light in greenhouses. Journal of Agricultural Engineering Research 73, 341–351.

Kittas, C., Boulard, T., Bartzanas, T., Katsoulas, N., Mermier, M., 2002. Influence of an insect screen on greenhouse ventilation. Transaction of the ASAE 45, 1083–1090.

Kittas, C., Boulard, T., Mermier, M., Papadakis, G., 1996. Wind induced air exchange rates in a greenhouse tunnel with continuous side openings. Journal of Agricultural Engineering Research 65, 37–49.

Kittas, C., Boulard, T., Papadakis, G., 1997. Natural ventilation of a greenhouse with ridge and side openings: sensitivity to temperature and wind effect. Transaction of the ASAE 40, 415–425.

Kittas, C., Katsoulas, N., Rigakis, N., Bartzanas, T., Kitta, E., 2012. Effects on microclimate, crop production and quality of a tomato crop grown under shade nets. Journal of Horticultural Science and Biotechnology 87, 7–12.

Klein, R.M., 1964. Repression of tissue culture growth by visible and near visible radiation. Plant Physiology 39, 536–539.

Klein, R.M., 1992. Effects of green light on biological systems. Biological reviews of the Cambridge Philosophical Society 67, 199–284.

Klein, R.M., Edsall, P.C., Gentile, A.C., 1965. Effects of Near Ultraviolet and Green Radiations on Plant Growth. Plant physiology 40, 903–6.

Klose, F., Tantau, H.J., 2004. Test of insect screens: measurement and evaluation of the air permeability and light transmission. European Journal of Horticultural Science 69, 235–243.

Kong, Y., Avraham, L., Ratner, K., Shahak, Y., 2012. Response of photosynthetic parameters of sweet pepper leaves to light quality manipulation by photoselective shade nets. Acta Horticulturae 956, 501–506.

Krakauer, N.Y., 2003. Do volcanic eruptions enhance or diminish net primary production? Evidence from tree rings. Global Biogeochemical Cycles 17.

Kumar, K.S., Tiwari, K.N., Jha, M.K., 2009. Design and technology for greenhouse cooling in tropical and subtropical regions: A review. Energy and Buildings 41, 1269–1275.

Lee, I., Okushima, L., Ikeguchi, A., Sase, S., Short, T., 2000. Prediction of natural ventilation of multi-span greenhouses using CFD techniques and its verification with wind tunnel test. Paper No. 00-5003, ASAE Meeting, Milwaukee, WI, USA.

Leonardi, C., Baille, A., Guichard, S., 2000. Predicting transpiration of shaded and non-shaded tomato fruits under greenhouse environments. Scientia Horticulturae 84, 297–307.

Leonardi, C., Guichard, S., Bertin, N., 2000. High vapour pressure deficit influences growth, transpiration and quality of tomato fruits. Scientia Horticulturae 84, 285–296.

Leyva, R., Constán-Aguilar, C., Sánchez-Rodríguez, E., Romero-Gámez, M., Soriano, T., 2015. Cooling systems in screenhouses: effect on microclimate, productivity and plant response in a tomato crop. Biosystems Engineering 129, 100–111.

Leyva, R., Constán-Aguilar, C., Blasco, B., Sánchez-Rodríguez, E., Soriano, T., Ruíz, J.M., 2013. A fogging system improves antioxidative defense responses and productivity in tomato. Journal of American Society of Horticultural Sciences 138, 267–276.

Li, T., Heuvelink, E., Dueck, T. A., Janse, J., Gort, G., Marcelis, L.F.M., 2014. Enhancement of crop photosynthesis by diffuse light: Quantifying the contributing factors. Annals of Botany 114, 145–156.

Linker, R., Tarnopolsky, M., Seginer, I., 2002. Increased resistance to flow and temperature rise resulting from dust accumulation on greenhouse insect proof screens. ASAE Ann Int Meeting, Chicago (USA), July 28-31. Paper 024040.

López-Marín, J., González, A., Gálvez, A., 2011. Effect of shade on quality of greenhouse peppers. Acta Horticulturae 893, 895–900.

Lopez-Martínez, A., Valera-Martínez, D.L., Molina-Aiz, F., Peña-Fernández, A., Marin-Membrive, P., 2014. Microclimate evaluation of a new design of insect-proof screens in a Mediterranean greenhouse. Spanish Journal of Agricultural Research 12, 338–352.

López-Martínez, A., Valera-Martínez, D.L., Molina-Aiz, F.D., Peña-Fernández, A.A., Marín-Membrive, P., 2013. Field analysis of the deterioration after some years of use of four insect-proof screens utilized in Mediterranean greenhouses. Spanish Journal of Agricultural Research 11, 958–967.

Lorenzo, P., Sánchez-Guerrero, M.C., Medrano, E., García, M.L., Caparrós, I., Coelho, G., Giménez, M., 2004. Climate control in the summer season: a comparative study of external mobile shading and fog system. Acta Horticulturae 659, 189–194.

Lorenzo, P., Sánchez-Guerrero, M.C., Medrano, E., García, M.L., Caparrós, I., Giménez, M., 2003. External greenhouse mobile shading: effect on microclimate, water use efficiency and yield of a tomato crop grown under different salinity levels of the nutrient solution. Acta Horticulturae 609, 181–186.

Marcelis, L.F.M., 1991. Effects of sink demand on photosynthesis in cucumber. Journal of Experimental Botany 42, 1387–1392.

Marcelis, L.F.M., Baan Hofman-Eijer, L.R., 1997. Effects of seed number on competition and dominance among fruits in Capsicum annuum L. Annals of Botany 79, 687–693.

Marcelis, L.F.M., Heuvelink, E., Baan Hofman-Eijer, L.R., Den Bakker, J., Xue, L.B., 2004. Flower and fruit abortion in sweet pepper in relation to source and sink strength. Journal of Experimental Botany 55, 2261–2268.

Marcelis, L.F.M., Heuvelink, E., Goudriaan, J., 1998. Modelling biomass production and yield of horticultural crops: A review. Scientia Horticulturae 74, 83–111.

Marquardt, D.W., 1963. An algorithm for least–squares estimation of non–linear parameters. Journal of Society of Applied Mathematics 2, 432–441.

Medina, C.L., Souza, R.P., Machado, E.C., Ribeiro, R. V, Silva, J. a. ., 2002. Photosynthetic response of citrus grown under reflective aluminized polypropylene shading nets. Scientia Horticulturae 96, 115–125.

Mellor, H.E., Bellingham, J., Anderson, M., 1997. Spectral efficiency of the glasshouse whitefly Trialeurodes vaporariorum and Encarsia formosa its hymenopteran parasitoid. Entomologia Experimentalis et Applicata 83, 11–20.

Miguel, A.F., 1998. Airflow through porous screens: From theory to practical considerations. Energy and Buildings 28, 63–69.

Miguel, A.F., Silva, A.M., 2000. Porous materials to control climate behaviour of enclosures: an application to the study of screened greenhouses. Energy and Buildings 31, 195–209.

Miguel, A.F., van de Braak, N.J., Bot, G.P., 1997a. Analysis of the airflow characteristics of greenhouse screening materials. Journal of Agricultural Engineering Research 67, 105–112.

Miguel, A.F., van de Braak, N.J., Bot, G.P.A., 1997b. Analysis of the airflow characteristics of greenhouse screening materials. Journal of Agricultural Engineering Research 67, 105–112.

Miguel, A.F., van de Braak, N.J., Silva, A.M., Bot, G.P.A., 1998. Physical modelling of natural ventilation through screens and windows in greenhouses. Journal of Agricultural Engineering Research 70, 165–176.

Miguel, A.F., van de Braak, N.J., Silva, A.M., Bot, G.P.A., 2001. Wind-induced airflow through permeable materials, Part II: air infiltration in enclosures. Journal of Wind Engineering and Industrial Aerodynamics 89, 59–72.

Misson, L., Lunden, M., McKay, M., Goldstein, A.H., 2005. Atmospheric aerosol light scattering and surface wetness influence the diurnal pattern of net ecosystem exchange in a semi-arid ponderosa pine plantation. Agricultural and Forest Meteorology 129, 69–83.

Mistriotis, A., Castellano, S., 2012. Airflow through net covered tunnel structures at high wind speeds. Biosystems Engineering 113, 308–317.

Molina-Aiz, F.D., Valera, D.L., Peña, A.A., Gil, J.A., López, A., 2009. A study of natural ventilation in an Almeria-type greenhouse with insect screens by means of tri-sonic anemometry. Biosystems Engineering 104, 224–242.

Möller, M., Assouline, S., 2007. Effects of a shading screen on microclimate and crop water requirements. Irrigation Science 25, 171–181.

Möller, M., Cohen, S., Pirkner, M., Israeli, Y., Tanny, J., 2010. Transmission of short-wave radiation by agricultural screens. Biosystems Engineering 107, 317–327.

Möller, M., Tanny, J., Cohen, S., Li, Y., Grava, A., Teitel, M., 2004a. Water consumption of pepper grown in an insect proof screenhouse. Acta Horticulturae 659, 569–575.

Möller, M., Tanny, J., Cohen, S., Teitel, M., 2003. Micrometeorological characterisation in a screenhouse. Acta Horticulturae 614, 445–452.

Möller, M., Tanny, J., Li, Y., Cohen, S., 2004b. Measuring and predicting evapotranspiration in an insect-proof screenhouse. Agricultural and Forest Meteorology 127, 35–51.

Monteith, J.L., 1973. Principles of environmental Physics. Contemporary Biology, Edward Arnold, London, UK, 241 pp.

Montgomery, D., Peck, E.A., 1992. Introduction to linear regression analysis., 2nd ed. A Wiley-Interscience Publication, New York.

Mullen, J.L., Weinig, C., Hangarter, R.P., 2006. Shade avoidance and the regulation of leaf inclination in Arabidopsis. Plant, Cell and Environment 29, 1099–1106.

Nicolás, E., Torrecillas, A., Dell Amico, J., Alarcón, J.J., 2005. Sap flow, gas exchange, and hydraulic conductance of young apricot trees growing under a shading net and different water supplies. Journal of Plant Physiology 162, 439–447.

Oren-Shamir, M., Gussakovsky, E.E., Shpiegel, E., Nissim-Levi, A., Ratner, K., Ovadia, R., Giller, Y.E., Shahak, Y., 2001. Coloured shade nets can improve the yield and quality of green decorative branches of Pittosporum variegatum. Journal of Horticultural Sience and Biotechnology 76, 353–361.

Pearson, S., Wheldon, A.E., Hadley, P., 1995. Radiation transmission and fluorescence of clading materials. Journal of Agricultural Engineering Research 62, 61–70.

Pérez Parra, J.J., Baeza, E., Montero, J.I., Bailey, B.J., 2004. Natural ventilation of parral greenhouses. Biosystems Engineering 87, 355–366.

Pérez-Parra, J.J., Montero, J.I., Baeza, E.J., López-Hernández, J.C., 2006. Determination of global wind coefficients for the development of Simple Ventilation Rate Calculation Models for a Parral Multispan Greenhouse. Acta Horticulturae 710, 143–150.

Pinker, R.A., Herbert, M.V., 1967. Pressure-loss associated with compressible flow through square-mesh wire gauzes. Journal of Mechanical Engineering Science 9, 11–23.

Pirkner, M., Tanny, J., Shapira, O., Teitel, M., Cohen, S., Shahak, Y., Israeli, Y., 2014. The effect of screen type on crop micro-climate, reference evapotranspiration and yield of a screenhouse banana plantation. Scientia Horticulturae 180, 32–39.

Posalski, I., 2006. Möller's personal communication, in: Möller, M. and Assouline, S., 2007. Effects of a shading screen on microclimate and crop water requirements. Irrigation Science 25, 171–181.

Radin, B., Bergamaschi, H., Reisser, C., Barni, N.A., Matzenauer, R., Didoné, I.A., 2003. Eficiência de uso da radiação fotossinteticamente ativa pela cultura do tomateiro em diferentes ambientes. Pesquisa Agropecuária Brasileira 38, 1017–1023.

Rajapakse, N.C., Shahak, Y., 2007. Light quality manipulation by horticulture industry. In: Light and Plant Development, G. Whitelam and K. Halliday (eds.), Blackwell Publishing, UK. p.290-312.

Rajapakse, N.C., Young, R.E., Mcmahon, M.J., Oi, R., 1999. Plant height control by photoselective filters: current status and future prospects. HortTechnology 9, 618–624.

Rigakis, N., Katsoulas, N., Belitsiotis, P., Kittas, C., 2014. Pepper crop production under shading and insect proof screenhouses. Acta Horticulturae 1037, 599–604.

Rilsky, A., Adamati, A., 1989. Pepper (in Hebrew). 5, 260–291.

Roderick, M.L., Farquhar, G.D., Berry, S.L., Noble, I.R., 2001. On the direct effect of clouds and atmospheric particles on the productivity and structure of vegetation. Oecologia 129, 21–30.

Romacho, I., Hita, O., Soriano, T., Morales, M.I., Escobar, I., Suarez-Rey, E.M., Hernández, J., Castilla, N., 2006. The growth and yield of cherry tomatoes in net covered. Acta Horticulturae 719, 529–534.

Romero-Gámez, M., Suárez-Rey, E.M., Castilla, N., Soriano, T., 2012. Evaluation of global, photosynthetically active radiation and diffuse radiation transmission of agricultural screens. Spanish Journal of Agricultural Research 10, 306–313.

Ross, D.S. and Gill, S.A. 1994. Insect screening for greenhouses. Agricult. Engin. Information Facts. FACTS 186. University of Maryland, College Park.

Roy, J.C., Boulard, T., Kittas, C., Wang, S., 2002. Convective and ventilation transfers in greenhouses, part 1: the greenhouse considered as a perfectly stirred tank. Biosystems Engineering 83, 1–20.

Rylski, I., Spigelman, M., 1986a. Use of shading to control the time of harvest of red-ripe pepper fruits during the winter season in a high-radiation desert climate. Scientia Horticulturae 29, 37–45.

Rylski, I., Spigelman, M., 1986b. Effect of shading on plant development, yield and fruit quality of sweet pepper grown under conditions of high temperature and radiation. Scientia Horticulturae 29, 31–35.

Sellaro, R., Crepy, M., Trupkin, S.A., Karayekov, E., Buchovsky, A.S., Rossi, C., Casal, J.J., 2010. Cryptochrome as a sensor of the blue/green ratio of natural radiation in Arabidopsis. Plant physiology 154, 401–409.

Sezen, S.M., Yazar, A., Eker, S., 2006. Effect of drip irrigation regimes on yield and quality of field grown bell pepper. Agricultural Water Management 81, 115–131.

Shahak, Y., 2008. Photo-Selective netting for improved performance of horticultural crops . A Review of ornamental and vegetable studies carried out in Israel. Acta Horticulturae 770, 161–168.

Shahak, Y., Ben-yakir, D., Offir, Y., Yehezkel, H., Goren, A., Fallik, E., 2009a. Photoselective shade netting for improving vegetable productivity , pre- and post harvest quality and pest control. ASHS Annual Conference 25-28 July, St. Louis, Missouri.

Shahak, Y., Gal, E., Offir, Y., Ben-Yakir, D., 2008a. Photoselective shade netting integrated with greenhouse technologies for improved performance of vegetable and ornamental crops. Acta Horticulturae 797, 75–80.

Shahak, Y., Gussakovsky, E.E., Cohen, Y., Lurie, S., Stern, R., Kfir, S., Naor, A., Atzmon, I., Doron, I., Greenblat-Avron, Y., 2004a. ColorNets : A new approach for light manipulation in fruit trees. Acta Horticulturae 636, 609–616.

Shahak, Y., Gussakovsky, E.E., Gal, E., Ganelevin, R., 2004b. ColorNets: Crop protection and light-quality manipulation in one technology. Acta Horticulturae 659, 143–151.

Shahak, Y., Ratner, K., Giller, Y.E., Zur, N., Or, E., Gussakovsky, E.E., Stern, R., Sarig, P., Raban, E., Harcavi, E., Doron, I., Greenblat-Avron, Y., 2008b. Improving solar energy utilization, productivity and fruit quality in orchards and vineyards by photoselective netting. Acta Horticulturae 772, 65–72.

Shahak, Y., Ratner, K., Zur, N., Offir, Y., Matan, E., Yehezkel, H., Messika, Y., Posalski, I., Ben-Yakir, D., 2009b. Photoselective netting: an emerging approach in protected agriculture. Acta Horticulturae 807, 79–84.

Shibles, R.M., Weber, C.R., 1965. Leaf area, solar radiation interception and dry matter production by soybeans. Crop Science 5, 575–577.

Silber, A., Bar-Tal, A., Levkovitch, I., Bruner, M., Yehezkel, H., Shmuel, D., Cohen, S., Matan, E., Karni, L., Aktas, H., Turhan, E., Aloni, B., 2009. Manganese nutrition of pepper (Capsicum annuum L.): Growth, Mn uptake and fruit disorder incidence. Scientia Horticulturae 123, 197–203.

Sinclair, T.R., Shiraiwa, T., Hammer, G.L., 1992. Variation in crop radiation use efficiency with increased diffuse radiation. Crop Science 32, 1281–1284.

Siqueira, M.B., Katul, G.G., Tanny, J., 2011. The effect of the screen on the mass, momentum, and energy exchange rates of a uniform crop situated in an extensive screenhouse. Boundary-Layer Meteorology 142, 339–363.

Smith, I.E., Savage, M.J., Mills, P., 1984. Shading effects on greenhouse tomatoes and cucumbers. Acta Hortic. 148, 229-237.

Soni, P., Salokhe, V.M., Tantau, H.J., 2005. Effect of screen mesh size on vertical temperature distribution in naturally ventilated tropical greenhouses. Biosystems Engineering 92, 469–482.

Stamps, R.H., 2009. Use of colored shade netting in horticulture. HortScience : a publication of the American Society for Horticultural Science 44, 239–241.

Stanhill, G., Cohen, S., 2001. Global dimming : a review of the evidence for a widespread and significant reduction in global radiation with discussion of its probable causes and possible agricultural consequences. Agricultural and Forest Meteorology 107, 255–278.

Stöckle, C.O., Kjelgaard, J., Bellocchi, G., 2004. Evaluation of estimated weather data for calculating Penman-Monteith reference crop evapotranspiration. Irrigation Science 23, 39–46.

Talbott, L.D., Nikolova, G., Ortiz, A., Shmayevich, I., Zeiger, E., 2002. Light reversal of blue-light-stimulated stomatal opening is found in a diversity of plant species. American Journal of Botany 89, 366–368.

Tanny, J., 2013. Microclimate and evapotranspiration of crops covered by agricultural screens: A review. Biosystems Engineering 114, 26–43.

Tanny, J., Cohen, S., 2003. The effect of a small shade net on the properties of wind and selected boundary layer parameters above and within a citrus orchard. Biosystems Engineering 84, 57–67.

Tanny, J., Cohen, S., Grava, A., Naor, A., Lukyanov, V., 2009. The effect of shading screens on microclimate of apple orchards. Acta Horticulturae 807, 103–108.

Tanny, J., Cohen, S., Teitel, M., 2003. Screenhouse microclimate and ventilation: an experimental study. Biosystems Engineering 84, 331–341.

Tanny, J., Cohen, S., Teitel, M., 2003. Screenhouse Microclimate and Ventilation: an Experimental Study. Biosystems Engineering 84, 331–341.

Tanny, J., Dicken, U., Cohen, S., 2010. Vertical variation in turbulence statistics and energy balance in a banana screenhouse. Biosystems Engineering 106, 175–187.

Tanny, J., Haijun, L., Cohen, S., 2006. Airflow characteristics, energy balance and eddy covariance measurements in a banana screenhouse. Agricultural and Forest Meteorology 139, 105–118.

Tanny, J., Teitel, M., Barak, M., Esquira, Y., Amir, R., 2008. The effect of height on screenhouse microclimate. Acta Horticulturae 801, 107–114.

Teitel, M., 2001. The effect of insect-proof screens in roof openings on greenhouse microclimate. Agricultural and Forest Meteorology 110, 13–25.

Teitel, M., 2007. The effect of screened openings on greenhouse microclimate. Agricultural and Forest Meteorology 143, 159–175.

Teitel, M., Dvorkin, D., Haim, Y., Tanny, J., Seginer, I., 2009. Comparison of measured and simulated flow through screens: Effects of screen inclination and porosity. Biosystems Engineering 104, 404–416.

Turner, A.D., Wien, H.C., 1994. Dry Matter Assimilation and Partitioning in Pepper Cultivars Differing in Susceptibility to Stress-induced Bud and Flower Abscission. Ann. Bot. 73, 617–622.

Urban, O., Janouš, D., Acosta, M., Czerny, R., Markova, I., Navratil, M., Pavelka, M., Pokorny, R., Šprtova, M., Zhang, R., Špunda, V., Grace, J., Marek, M.V., 2007. Ecophysiological controls over the net ecosystem exchange of mountain spruce stand. Comparison of the response in direct vs. diffuse solar radiation. Global Change Biology 13, 157–168.

Urban, O., Klem, K., Ač, A., Havránková, K., Holišová, P., Navrátil, M., Zitová, M., Kozlová, K., Pokorný, R., Šprtová, M., Tomášková, I., Špunda, V., Grace, J., 2012. Impact of clear and cloudy sky conditions on the vertical distribution of photosynthetic CO2 uptake within a spruce canopy. Functional Ecology 26, 46–55.

Valera, D.L., Álvarez, A.J., Molina, F.D., 2006. Aerodynamic analysis of several insect-proof screens used in greenhouses. Spanish Journal of Agricultural Research 4, 273–279.

Valera, D.L., Molina, F.D., Álvarez, A.J., López, J.A., 2005. Contribution to characterisation of insect-proof Screens: experimental measurements in wind tunnel and CFD simulation. Acta Horticulturae 691, 441–448.

Vanthoor, B.H.E., Stanghellini, C., van Henten, E.J., de Visser, P.H.B., 2011. A methodology for model-based greenhouse design: Part 1, a greenhouse climate model for a broad range of designs and climates. Biosystems Engineering 110, 363–377.

Vernon, R.S., Gillespie, D.R., 1990. Spectral responsiveness of Frankliniella occidentalis (Thysanoptera: Thripidae) determined by trap catches in greenhouses. Environmental Entomology 19, 1229–1241.

Vieira, M.I., de Melo-Abreu, J.P., Ferreira, M.E., Monteiro, A.A., 2009. Dry matter and area partitioning, radiation interception and radiation-use efficiency in open-field bell pepper. Scientia Horticulturae 121, 404–409.

Vince, D., Blake, J., Spencer, R., 1964. Some effects of wave-length of the supplementary light on the photoperiodic behaviour of the long-day plants, carnation and lettuce. Physiologia Plantarum 17, 119–126.

Vogelmann, T.C., Evans, J.R., 2002. Profiles of light absorption and chlorophyll within spinach leaces from chlorophyll fluorescence. Plant, Cell & Environment 25, 1313–1323.

Waggoner, P., Pack, A., Reifsnyder, W., 1959. The climate of shade. A tobacco tent and a forest stand compared to open fields. The Connecticut Agricultural Experiment Station, Bulletin 626.

Wahid, A., Gelani, S., Ashraf, M., Foolad, M.R., 2007. Heat tolerance in plants: An overview. Environmental and Experimental Botany 61, 199–223.

Wang, S., Boulard, T., Haxaire, R., 1999. Air speed profiles in a naturally ventilated greenhouse with a tomato crop. Agricultural and Forest Meteorology 96, 181–188.

Wang, S., Deltour, J., 1999. Lee-side ventilation-induced air movement in a large-scale multi-span greenhouse. Journal of Agricultural Engineering Research 74, 103–110.

Went, F.W., 1957. The experimental control of plant growth. Waltham, MA: Chronica Botanica.

Willits, D.H., 2001. The effect of cloth characteristics on the cooling performance of external shade cloths for greenhouses. Journal of Agricultural Engineering Research 79, 331–340.

Willmott, C., 1982. Some comments on the evaluation of model performance. Bulletin of the American Meteorological Society 63, 1309–1313.

Wright, G.C., Hammer, G.L., 1994. Distribution of nitrogen and radiation use efficiency in peanut canopies. Australian Journal of Agricultural Research 45, 565– 74.

Young, D.R., Smith, W.K., 1983. Effect of cloudcover on photosynthesis and transpiration in the subalpine understory species Arnica Latifolia. Ecology 64, 681–687.

Zhang, J.S., Janni, K.A., Jacobson, L.D., 1989. Modeling natural ventilation induced by combined thermal buoyancy and wind. Transaction of the ASAE 32, 2165–2174.

Zhang, T., Maruhnich, S.A., Folta, K.M., 2011. Green light induces shade avoidance symptoms. Plant Physiology 157, 1528–1536.

Η παρούσα έρευνα έχει συγχρηματοδοτηθεί από την Ευρωπαϊκή Ένωση (Ευρωπαϊκό Κοινωνικό Ταμείο - ΕΚΤ) και από εθνικούς πόρους μέσω του Επιχειρησιακού Προγράμματος «Εκπαίδευση και Δια Βίου Μάθηση» του Εθνικού Στρατηγικού Πλαισίου Αναφοράς (ΕΣΠΑ) – Ερευνητικό Χρηματοδοτούμενο Έργο: Ηράκλειτος ΙΙ. Επένδυση στην κοινωνία της γνώσης μέσω του Ευρωπαϊκού Κοινωνικού Ταμείου.

This research has been co-financed by the European Union (European Social Fund – ESF) and Greek national funds through the Operational Program "Education and Lifelong Learning" of the National Strategic Reference Framework (NSRF) - Research Funding Program: Heracleitus II. Investing in knowledge society through the European Social Fund.